UNIVERSITY OF MINES AND TECHNOLOGY

TARKWA

FACULTY OF COMPUTING AND MATHEMATICAL SCIENCES

DEPARTMENT OF MATHEMATICAL SCIENCES

HARMONIC EXTENSIONS OF GOMPERTZ, FRÉCHET AND BURR XII DISTRIBUTIONS WITH APPLICATIONS TO LIFETIME DATA

SELASI KWAKU OCLOO

2023

UNIVERSITY OF MINES AND TECHNOLOGY

TARKWA

FACULTY OF COMPUTING AND MATHEMATICAL SCIENCES

DEPARTMENT OF MATHEMATICAL SCIENCES

A THESIS REPORT ENTITLED

HARMONIC EXTENSIONS OF GOMPERTZ, FRÉCHET AND BURR XII DISTRIBUTIONS WITH APPLICATIONS TO LIFETIME DATA

BY

SELASI KWAKU OCLOO

A THESIS SUBMITTED IN FULFILMENT OF THE REQUIREMENT FOR THE AWARD OF THE DEGREE OF DOCTOR OF PHILOSOPHY IN MATHEMATICS

THESIS SUPERVISORS

....

PROF LEWIS BREW

....

PROF SULEMAN NASIRU

....

DR BENJAMIN ODOI

TARKWA, GHANA

OCTOBER, 2023

DECLARATION

I declare that this thesis is my own work. It is being submitted for the degree of Doctor of Philosophy in Mathematics in the University of Mines and Technology (UMaT), Tarkwa. It has not been submitted for any degree or examination in any other University.

. . . .

. . . . day of . . . . (year). . . . .

ABSTRACT

This thesis aims to enhance the modelling capabilities of the Gompertz, Fréchet, and Burr XII distributions using the harmonic mixture G family. These classical distributions are widely used in various fields to represent different types of data, but they often face limitations in capturing complex data characteristics such as skewness and heavy tails.To achieve this objective, the research utilises the harmonic mixture G family as generator to modify the Gompertz, Fréchet, and Burr XII distributions. The modified distributions are then evaluated using the maximum likelihood estimation, ordinary least squares, weighted least squares, Cramér-von Mises, and Anderson Darling estimation methods to estimate their parameters. Monte Carlo simulation experiments were performed to identify the best estimation methods for the parameters. The maximum likelihood estimation method was adjudged the best estimator for the models developed. Additionally, parametric regression models were developed based on two of these modified distributions, providing a framework for analysing relationships between variables.The findings of this research demonstrate that integrating the harmonic mixture G family significantly enhances the modelling capabilities of the Gompertz, Fréchet, and Burr XII distributions. The modifications enable these distributions to better capture skewness and heavy tails, leading to more accurate representation of real-world data patterns. The developed parametric regression models further enhance the flexibility and versatility of these modified distributions, facilitating improved analysis of complex relationships.The practical implications of this research are extensive, benefiting various fields such as finance, economics, environmental sciences, engineering, and risk analysis. Researchers and practitioners can leverage the modified distributions and parametric regression models to more effectively model and analyse complex data patterns, enabling improved decision-making, risk assessment, and predictive modelling.

DEDICATION

To my father Percy Ocloo, my wife Augusta Ocloo and my son Deladem Ocloo

ACKNOWLEDGEMENT

The name of the Almighty God be praised for favour and mercies throughout this work. I want to sincerely thank Prof Lewis Brew, my supervisor and the Head of the Mathematical Sciences Department at UMaT, for unwavering support during this work. I have come this far because of your desire for me to be successful in this work. A deep thank you once more to Prof Suleman Nasiru, my external co-supervisor and Head of the Statistics and Actuarial Science Department at the C.K. Tedam University of Technology and Applied Sciences, Navrongo, for his love, care, guidance, and friendship during this work. There is no way to measure how much you have contributed to this work. A special one to Dr Benjamin Odoi, my co-supervisor for his love, concern and help throughout my period of study. Your words of encouragement and determination to see this project through to its conclusion were unparalleled.

A Special thanks goes to Dr Abdulzeid Yen Anafo for his kind heart, friendship and technical support throughout this work. A big thank you to the University of Mines and Technology, in particular the Mathematical Sciences Department in the Faculty of Engineering, for giving me the continual assistance I needed to complete my work. Thanks to the hardworking department administrator Elvis for all of your assistance, even at ungodly hours.

My wife Augusta Ocloo, my son Deladem Ocloo, my father Percy Ocloo, my mother Getrude Amevor, as well as my siblings Millicent, Elikplim, and Emefa Ocloo, deserve my deepest thanks for their emotional support during this endeavour, especially during the challenging moments.

TABLE OF CONTENTS

LIST OF TABLES

LIST OF FIGURES

LIST OF ABBREVIATIONS

A	Anderson-Darling Test
AB	Average Bias
AD	Anderson-Darling Estimation
AIC	Akaike Information Criterion
AICC	Consistent Akaike Information Criterion
BIC	Bayesian Information Criterion
CDF	Cumulative Distribution Function
CK	coefficient of kurtosis
CS	coefficient of skewness
CV	coefficient of variation
CVM	Cramér-von Mises Estimation
FRF	failure rate function
HMBRXII	Harmonic Mixture Burr XII
HMFR	Harmonic Mixture Fréchet
HMG	Harmonic Mixture-G
HMGOM	Harmonic Mixture Gompertz
KS	Kolmogorov-Smirnov Test
LHMBXII	Log-Harmonic Mixture Burr XII
MLE	Maximum Likelihood Estimation
MSE	Mean Square Error
OLSS	Ordinary Least Squares
PDF	probability density function
SF	survival function
TTT	Total Time on Test
W	Cramér-von Mises Test
WLSS	Weighted Least Squares

CHAPTER 1

INTRODUCTION

1.1 Background of Study

Over the years, the motivation for introducing new type of distributions is to provide more flexibility in fitting real data sets comparative to the well-known classical distributions. The introduction of additional location, scale or shape parameters to existing distributions are aimed at generalising these distributions. The areas in real life where classical distributions are being applied are not static, hence there is the need to introduce different types of distributions to meet the dynamic nature of these real life situations. In recent times, modifying classical distributions require the use of generators. Generators serve as the engine block that transforms the given baseline distribution into a modified distribution. Many generators in literature have improved the goodness-of-fit of the distributions they modified (Badr *et al.*, 2020; Marganpoor *et al.*, 2020; Bhat *et al.*, 2018; Bello *et al.*, 2021).

The increasingly heterogeneous nature of real data sets has made the use of mixture models popular in the last one or two decades. A mixture distribution is preferred when a particular distribution has parameters that vary in part or whole according to some other probability distribution usually referred to as a mixing distribution. Using single parametric or non-parametric distributions to handle heterogeneous data comes with its own challenges, hence the increasingly switch of most researchers to mixture distributions. The flexibility of mixture models has made them useful in various fields in the sciences. Mixture distribution families may easily be used when the data set have other sub-components with different individual properties that could be best modelled individually. They are widely useful in fields such as reliability theory, finance, economics, agriculture, medicine, survival analysis, etc. Several researchers have obtained in literature the properties and characteristics of various mixtures distributions. Karim *et al.* (2011) proposed the Rayleigh mixture, Al-Moisheer (2021) proposed the Mixture of Lindley and Lognormal Distributions, Alotaibi *et al.* (2021) studied a mixture of the Marshall–Olkin extended Weibull distribution to efficiently model failure, survival, and COVID-19 data using the classical and Bayesian approaches, the arithmetic mixture distribution was proposed by Behboodian (1972), the geometric mixture distribution or generalised escort distribution by Bercher (2012), power mean mixture or α - mixture distribution by Van Erven and Harremos (2014), Yamaguchi *et al.* (2010) estimated the parameters of a mixture of Erlang distribution using the Variational Bayesian Approach, Bhat *et al.* (2018) obtained the Mixture of Exponential and Weighted Exponential Distribution using the Maximum Likelihood Estimation technique.

The Harmonic Mixture-G (HMG) family, proposed by Kharazmi *et al.* (2022), is a new family of mixture distributions. This family combines two survival functions using weighted harmonic means. They obtained the estimates of the parameters using both the classical and Bayesian approaches. The Weibull distribution was used as a parent distribution to assess the new mixture distribution family.

In this study, three (3) new hybrid families of continuous distributions are constructed from the HMG family using the Gompertz, Fréchet and Burr XII distributions as baseline distributions.

1.2 Problem Statement

The research problem addressed in this thesis revolves around the modification and enhancement of three widely used probability distributions - the Gompertz, Fréchet, and Burr XII distributions - using the HMG family. These classical distributions have been extensively employed in various fields to model diverse types of data . However, they may exhibit limitations in capturing complex features such as skewness, heavy tails, and boundedness, which are frequently encountered in real-world datasets (Missov and Lenart, 2011; Pollard and Valkovics, 1992; Afify and Mead, 2017; Ul Haq *et al.*, 2017; Ramos *et al.*, 2020; Bhatti *et al.*, 2021). In data modelling, choosing an appropriate distribution model is a major hurdle. Finding the appropriate model classes or families serve as springboards for statisticians to derive and propose models that provide lots of flexibility (Makubate *et al.*, 2021). Existing probability distributions someday may not be able to come up with a good fit for some real data sets. In some cases, there would be the need to introduce an additional one or two parameter(s) to handle this drawbacks but in other cases a whole new method need to be adopted to fit the data sets appropriately (Nasiru, 2018).

By harnessing the flexibility and versatility offered by the HMG family, which incorporates a shape parameter and a scale parameter, we aim to enhance the modelling capabilities of the Gompertz, Fréchet, and Burr XII distributions. Subsequently, the research will focus on the following key aspects:

i. Enhancement of the Gompertz Distribution: The Gompertz distribution is commonly employed in survival analysis and demography to model mortality rates and other life-related variables. Nevertheless, it may have limitations in accurately capturing bounded data and complex skewness patterns (Abubakari *et al.*, 2021; El-Gohary *et al.*, 2013). The research will explore how the integration of the HMG family can improve the Gompertz Distribution's ability to handle asymmetric datasets, leading to more precise modelling of mortality rates and related phenomena.

ii. Modification of the Fréchet Distribution: The Fréchet distribution is widely used to model extreme events and phenomena. However, it may struggle to adequately represent skewness and heavy-tailed behaviour (Hussein *et al.*, 2021a; Pillai and Moolath, 2019). The research will justify how incorporating the HMG family can enhance the Fréchet distribution's ability to capture these characteristics, enabling more accurate modelling of extreme events in various domains.

iii. Refinement of the Burr XII Distribution: The Burr XII Distribution is widely used to model a variety of data types, including income distributions, hydrological data, and reliability analysis. However, it may struggle to accurately represent heavy-tailed behaviour and capture extreme observations (Cordeiro *et al.*, 2017; Bhatti *et al.*, 2020). The research will investigate how incorporating the HMG family can enhance the Burr XII Distribution, enabling better representation of heavy tails, extreme values, and other complex features present in diverse data sets

1.3 General Objectives

The main objective of the study is to develop harmonic extensions of the Gompertz, Fréchet and Burr XII distributions and demonstrate their applications using lifetime data.

1.4 Specific Objectives

The specific objectives of the study are:

i. To develop the harmonic mixture Gompertz distribution.

ii. To develop the harmonic mixture Fréchet distribution.

iii. To develop the harmonic mixture Burr XII distribution.

iv. To develop parametric regression models for the modified Gompertz and Burr XII distributions.

v. To illustrate the applications of the developed distributions using lifetime data.

1.5 Thesis Outline

The thesis comprises six distinct chapters, each addressing specific components of the research topic. The first chapter provides an introduction to the study, presenting the background and outlining the research problem, research questions, and objectives. In the second chapter, a comprehensive literature review is conducted, focusing on the existing extensions of the Gompertz, Fréchet, and Burr XII distributions. The third chapter provides an overview of the essential concepts and methodologies used throughout the study. Moving on to the fourth chapter, the theoretical outcomes derived from the research are presented. The fifth chapter is dedicated to simulations and practical applications, showcasing how the proposed distributions perform in real-world scenarios. Lastly, the sixth chapter concludes the thesis by summarising the main findings and offering recommendations based on the study's results.

CHAPTER 2

LITERATURE REVIEW

2.1 Introduction

New distribution families are being introduced day by day. The development of new models with much flexibility are needed to convey the true characteristic of the data sets being analysed (Eghwerido *et al.*, 2021a). The desire to get more flexible families of distributions from the classical distributions have led to the introduction of various extensions of the Gompertz, Fréchet and Burr XII distributions. This chapter discusses the modifications of these classical distributions.

2.2 Modifications of the Gompertz Distribution

According to Eghwerido *et al.* (2021a), a modification to the Gompertz distribution called the alpha power Gompertz distribution was proposed. This modification involved the addition of an extra shape parameter to address the issues of skewness and kurtosis. The resulting distribution was characterised as left-skewed and decreasing, exhibiting an upside-down bathtub shape in its probability density function (PDF). Moreover, the failure rate function of the alpha power Gompertz distribution displayed a bathtub-shaped pattern.

The transmuted power Gompertz distribution introduced by Eraikhuemen *et al.* (2021) added an extra shape parameter to the power Gompertz distribution called the transmuted parameter, which increased its flexibility. The PDF is positively skewed and takes several shapes depending on the values of the parameter while the failure rate function (FRF) is increasing.

The exponentiated generalised Weibull-Gompertz distribution was applied to the life time data of 50 devices by El-Bassiouny *et al.* (2017) and was more flexible than the classical Gompertz and other classical distributions.

Kuje *et al.* (2019) introduced the odd Lindley Gompertz distribution. They recommended that the model would be appropriate for positively skewed and large sample data sets. They also averred that based on the behaviour of the FRF, the model will fit better for data sets that are time or age dependent.

Kuje *et al.* (2020) presented a theoretical analysis of an extension of the odd Lindley Gompertz distribution proposed by Kuje *et al.* (2019). The new model can assume various shapes depending on the values of the parameter used which includes negatively skewed with high level of kurtosis.

The unit Gompertz distribution was proposed by Mazucheli *et al.* (2019) with the motivation of introducing a new distribution that has the ability to model constant, increasing, uni-modal and also bathtub shaped failure rates.

Eghwerido *et al.* (2021b) presented a new class of distribution whose PDF is bathtub, increasing, decreasing and skewed shaped and was called the Marshall-Olkin Gompertz distribution.

Kazemi *et al.* (2021) introduced a four-parameter modification of the generalised Gompertz distribution using the extended Weibull distribution. The new distribution was found to have increasing, decreasing, uni-modal or bathtub shaped FRF depending on the parameters used.

The exponentiated Gompertz distribution as proposed by Abu-Zinadah and Aloufi (2014) generalises the classical Gompertz distribution by introducing an additional shape parameter, hence resulted in a more flexible density function and FRF.

The bi-variate Gompertz distribution was derived and used by Al-Khedhairi and El-Gohary (2008) to model heterogeneous lifetime data sets. The new distribution was found to generalise the Marshall-Olkin bi-variate exponential distribution and other modified distributions in literature.

Bakouch *et al.* (2017) proposed a new weighted Gompertz distribution as part of the developments in the weighted family of distributions. They discovered that the proposed distribution could be regarded as a dual component of the log-Lindley-X family.

The bi-variate exponentiated generalised Weibull-Gompertz distribution was developed using the Marshall-Olkin method by El-Bassiouny *et al.* (2016a). They assessed the efficiency of the new model using a 1986 bi-variate data from the American national football league and found the model to provide an effective fitting.

Recently, Taniş and Saraçoğlu (2022) introduced the cubic rank transmuted generalised Gompertz distribution following the cubic rank transmutation map proposed by Granzotto *et al.* (2017).The FRF exhibited increasing, decreasing and bathtub shapes.

The inverse Gompertz distribution was derived and studied by Eliwa *et al.* (2019) using the inverse distribution method. They adopted a five estimation method to estimate with the aim of getting the best parameter values for fitting real life data.

The cubic transmuted Gompertz distribution was developed by Ogunde *et al.* (2020a) using the cubic transmuted family distribution developed by Rahman *et al.* (2018).They averred that the cubic transmuted Gompertz distribution could be used to analyse several forms of data including those with bimodal failure rates.

A three parameter Gamma-Gompertz distribution was developed from the gamma-X family by Shama *et al.* (2022).The shape of the PDF of the distribution obtained could be decreasing, unimodal or decreasing-increasing-decreasing whereas the failure rate function exhibit increasing and unimodal shapes.

Nzei *et al.* (2020) transformed the cumulative distribution function of the Gompertz random variable using the Topp-Leone as generator to obtain an extension of the Gompertz distribution called the Topp-Leone Gompertz distribution. The PDF can either be unimodal, right skewed or decreasing while the FRF exhibit bathtub, concave or convex increasing shapes.

The transmuted Gompertz distribution was obtained by Khan *et al.* (2017) using the quadratic rank transmutation map scheme proposed by Shaw and Buckley (2007). Assessing different parameter choices, they suggested that the failure rate function has an increasing pattern.

Marshall-Olkin exponential Gompertz distribution was proposed by Khaleel *et al.* (2020) and is suitable for modelling either symmetric or heavily skewed data sets.

A mixture of two exponentiated generalised Weibull-Gompertz distribution was proposed by El-Bassiouny *et al.* (2016b) and was found to be useful in modelling causes of system failure concurrently.

The Nadarajah-Haghighi Gompertz distribution was obtained by Ogunde *et al.* (2020b) using the Nadarajah-Haghighi generator. The model obtained was found to be more flexible and provided a better representation of real life data than the classical Gompertz distribution and some other distributions considered.

The weighted exponential Gompertz distribution whose failure rate could be increasing or bathtub was obtained by Ahmad *et al.* (2019).The new model was obtained by generating the integral transform of the PDF of the weighted exponential distribution.

Abdelhady and Amer (2021) introduced a three parameter inverse power Gompertz distribution.The inverse power Gompertz distribution was obtained from the inverse Gompertz distribution using a transformation that raise the random variable X to an extra shape parameter.

Rayleigh Gamma Gompertz distribution was obtained as a special case of the Rayleigh-G family by Al-Noor and Assi (2021).

The modified Beta Gompertz distribution was obtained by Elbatal *et al.* (2019b) using the modified beta generator proposed by Nadarajah *et al.* (2014) and the Gompertz distribution. They observed that the PDF and FRF of the new distribution can take various forms depending on the values of the parameters, which shows an increasing flexibility.

The wrapped generalised Gompertz distribution was derived from the class of wrapped distributions by Roy and Adnan (2012). They concluded that the distribution derived provides a better fit than some existing circular symmetric and non-symmetric distributions.

2.3 Modifications of the Fréchet Distribution

The cubic transmuted Fréchet distribution proposed by Shalabi (2020) extended the work of the cubic transmuted families of distributions using the Fréchet distribution. The new distribution increased the flexibility of the transmuted distribution and could be used to model more complex data in wealth distribution.

Yousof *et al.* (2018) proposed an extension of the Fré chet distribution using a log location-scale regression model. The new model provided a better fit than other regression models compared to it.

Nadarajah and Kotz (2003) derived the exponentiated Fréchet distribution by adding an additional shape parameter to the classical Fréchet distribution to improve its flexibility.

Badr (2019) proposed a six parameter beta generalised exponentiated Fréchet and demonstrated its advantages using lifetime data sets. The generalised family of the distribution was generated by applying the Cumulative Distribution Function (CDF) of the generalised exponentiated Fréchet to the beta distribution random variable. The FRF of the new distribution using different parameter values was decreasing.

The extended Weibull–Fréchet distribution was introduced by Hussein *et al.* (2021b). They estimated the parameters using several frequentist estimation approaches. The FRF of the extended Weibull-Fréchet distribution exhibited decreasing, increasing and also an upside-down bathtub shape while the corresponding PDF was symmetric, asymmetric, reversed-J and J shaped.

Badr and Shawky (2014) discussed the finite mixture of two components following the exponentiated Fréchet distribution. They found the Bayes approach more flexible in estimating the parameters.

A new five parameter Fréchet model was proposed by Ul Haq *et al.* (2017) to model extreme values. The modification of the Fréchet distribution was obtain using the Weibull-Fréchet distribution and the transmuted-G family of distributions. The estimates of the parameters were obtained using the maximum likelihood estimation approach.

Hassan *et al.* (2019) introduced a new four-parameter distribution and named it the truncated Weibull Fréchet distribution. They derived the new model from the truncated Weibull-G family and found that the PDF and failure rate of the new distribution take different forms that depends on values of parameters.

The extended Poisson Fréchet distribution was investigated by Khalil and Rezk (2019). The PDF of the new model was found to be right and left skewed and unimodal while its FRF was bathtub, unimodal-bathtub, increasing and decreasing.

Ibrahim (2019) introduced a modification of the Fréchet distribution using the Burr XII-G family. The new model's PDF was right skewed and unimodal while its FRF unimodal and decreasing shaped.

The Burr X Fréchet model was proposed by Jahanshahi *et al.* (2019) to model extreme values. The versatility of the developed model was practically ascertained using two real data sets one of which is the clinical trial of the relief time (hours) of 50 arthritic patients.

A four parameter Fréchet distribution was derived and studied by Hamed *et al.* (2020) using the odd Lomax-G family. The PDF indicates a reversed-J shape, left or right skewed whereas the failure rate function indicate an increasing, decreasing or unimodal shape.

Roy and Rahman (2021) mixed the Poisson distribution and the Fréchet distribution to obtain what is referred to as the Poisson-Fréchet distribution. The new distribution was applied to a 57 years rainfall data and its performance was compared with other distributions and was found to be more flexible.

The gamma extended Fréchet distribution, a new four parameter model was introduced by da Silva *et al.* (2013). They obtained the model by inserting the CDF of the extended Fréchet distribution into the CDF of the gamma-G distribution. The model was found to be more competitive than the exponentiated Weibull distribution and provides a superior fit as against the other models used for the comparison.

The Fréchet distribution was generalised by Pillai and Moolath (2019) using the T-transmuted X family proposed by Moolath and Jayakumar (2017). The FRF was initially increasing and then decreasing.

Fréchet-Weibull distribution was generated using the T-X family method by Teamah *et al.* (2020b). The FRF of the model was an upside down bathtub function of one of the shape parameters.

The new exponential-X Fréchet distribution proposed by Alzeley *et al.* (2021) was derived and studied to provide a more superior versatility for some classical reliability models that have a non-monotonic FRF.

A modified Fréchet-Rayleigh distribution was introduced by Al-Noor and Assi (2021) to overcome the inadequacies of the Rayleigh model. The new model introduced provided various shapes for the FRF, an indication of its flexibility.

A three-parameter model for modelling lifetime data was proposed by Abouelmagd *et al.* (2018b) called the Burr X Fréchet distribution using the Burr X generator. They argued that due to the flexibility of the model obtained, the model can accommodate various shapes of FRF.

The two-parameter X gamma Fréchet distribution was proposed by Yousof *et al.* (2020) and provides a better fit for repair-time data. The model was obtained using the CDF of the X gamma-G family. They observed that the FRF of the X gamma Fréchet model could be upside down bathtub, decreasing or reversed J, increasing and increasing or J shaped.

The right truncated Fréchet-Weibull distribution is derived and studied by Teamah *et al.* (2020c). Depending on the values of the parameter the FRF of the model can be unimodal, decreasing or increasing.

Iqbal *et al.* (2019) modified the transmuted Fréchet model using the double function technique. The model derived provided flexible estimates on skewed real life data sets.

Lehman Type II Fréchet Poisson distribution, a new generalisation of the Fréchet was proposed by Ogunde *et al.* (2021) using the Lehman type II distribution which is a hybrid of the generalised exponentiated distributions proposed by Cordeiro *et al.*

(2013). They observed and concluded that the model derived can be a suitable model to fit unimodal and right skewed data.

Two bivariate Fréchet distribution were derived from the univariate Fréchet and studied by Almetwally and Muhammed (2020) using the Farlie-Gumbel-Morgen-Stern (FGM) and the Ali-Mikhail-Haq (AMH) copulas.

The Fréchet - Weibull mixture distribution was introduced and studied by Teamah *et al.* (2020a) by mixing a re-parameterised Fréchet - Weibull distribution and the exponential distribution. The resulting failure rate was decreasing or upside down bathtub shaped.

The Marshall-Olkin Fréchet distribution was obtained by Krishna *et al.* (2013a) through the survival function of the Marshall-Olkin family of distributions. The PDF of the derived model is unimodal while the FRF exhibited an upside-down bathtub shape. Krishna *et al.* (2013b), then applied the model to a real life data set on failure times of air-conditioning systems in jet planes and the results revealed that the model could be applied in various areas including clinical trials used in comparing the efficacy of a medicine over another.

The modified Kies-Fréchet distribution, an extension of the Fréchet was introduced by Al Sobhi (2021). The new model could provide left-skewed, symmetric, right-skewed, J-shaped and reversed J- shaped probability densities.

A mixture of two Fréchet distribution was derived by Ahmed *et al.* (2021) and the new function was applied to number of cancer cases in Iraq. The parameters estimates were obtained from the maximum likelihood estimation method.

The quadratic transmutation map was used to generate an extension of the Fréchet distribution by Mahmoud and Mandouh (2013) and was referred to as the transmuted Fréchet distribution with the purpose of modifying the skewness and kurtosis of Fréchet distribution.

Deka *et al.* (2021) derived and studied some properties on Fréchet-Weibull distribution using the T-X family. They suggested that modified forms of the Fréchet and Weibull distributions are more flexible in modelling experimental data.

A three-parameter modified Fréchet distribution was obtained using the Lambert function and some of its statistical properties were obtained by Tablada and Cordeiro (2017). The FRF can be decreasing, unimodal and bathtub shaped while the PDF is unimodal.

Eghwerido (2020) proposed the alpha power Weibull Fréchet distribution and estimated its statistical properties using the maximum likelihood method. The resulting PDF's shape was inverted-bathtub or decreasing.

Reyad *et al.* (2021) introduced the Fréchet Topp-Leone-G family of distribution using the Fréchet distribution and the Topp-Leone-G family. The sub-models derived from the new distributions exhibited the ability to model monotonic decreasing, increasing, bathtub, upside down bathtub and reversed J FRF.

Mansour *et al.* (2018) proposed a five-parameter distribution named the Kumaraswamy exponentiated Fréchet distribution by adding two additional shape parameters to the CDF of the exponentiated Fréchet distribution to give it greater flexibility. The PDF and FRF can assume various shapes depending on the values of the parameters.

2.4 Modifications of the Burr XII Distribution

Makubate *et al.* (2021) derived and explored the Lindley-Burr XII power series distribution. They illustrated the usefulness of the new distribution by applying it to some real data sets and concluded that the new distribution is more flexible than some non-nested models.

The exponentiated Burr XII Poisson distribution was proposed by da Silva *et al.* (2015). The new lifetime model obtained demonstrates that it provides a better fit than the other distributions used for comparison.

Elbatal *et al.* (2019a) proposed the generalised Burr XII power series distribution by compounding the generalised Burr XII and the power series distributions. They derived special models such as the geometric, Poisson, binomial and logarithmic from the new family and they exhibited more flexibility.

The Gompertz-modified Burr XII distribution was developed and studied by Abubakari *et al.* (2021) using the modified Burr XII distribution as the parent distribution. The PDF of the new lifetime model could assume right and left-skewed shapes, decreasing and nearly symmetric shapes.

The Kumaraswamy exponentiated Burr XII distribution was proposed by Afify and Mead (2017) by adding two shape parameters to the PDF of the exponentiated Burr XII distribution. They revealed that the two additional shape parameters provides a greater control over the weights in the tails and centre of the model developed.

The Burr XII distribution was modified by Okasha and Shrahili (2017) using the quadratic transmutation map approach. They estimated the parameters of the new model using the maximum likelihood estimation method.

An additional shape parameter was introduced into the PDF of the Burr XII distribution using the Odd Lindley-G family of distribution by Abouelmagd *et al.* (2018a). The FRF of the new four-parameter model could assume constant, increasing, decreasing, unimodal or bathtub shape.

Daniyal and Aleem (2014) derived and discussed the classical properties of the mixture of the Burr XII and Weibull distributions. The PDF of the model derived can exhibit various shapes depending of the values of the parameters.

The Burr XII distribution is modified by replacing the PDF and CDF of the random variable X in the exponentiated T-X family with that of Burr XII. The derived distribution known as the exponentiated exponential Burr XII as discussed by Badr and Ijaz (2021) exhibited monotonic and non-monotonic failure rate.

Nasir *et al.* (2018) obtained the Burr XII uniform distribution. The developed model had a FRF with decreasing, increasing and bathtub shapes.

Using the generalised log Pearson differential equation, the generalised log Burr XII distribution was derived and studied by Bhatti *et al.* (2018a). They proposed the new model to handle positively skewed and heavy tailed data sets and also provide better fits for survival data compared to other competing models.

The modified Burr XII -inverse Weibull distribution was developed using the T-X family technique by Bhatti *et al.* (2018b). The FRF of the new distribution could accommodate various shapes as the values of the parameters are varied.

The Weibull generalised Burr XII distribution can be used to model bimodal data sets as derived and reported by Raya and Butt (2019). The PDF of the model was unimodal and right skewed while the FRF could exhibit bathtub, constant, unimodal, decreasing or increasing shapes.

A four-parameter model known as the Burr XII gamma distribution was derived from the T-X family method and linking the exponential and gamma random variables. The FRF of the new distribution can accommodate several shapes including increasing, decreasing, decreasing-increasing, increasing-decreasing-increasing, bathtub and modified bathtub as proposed by Bhatti *et al.* (2021).

The weighted distribution concept which incorporates a function called the length biased was introduced and studied by Mahdy *et al.* (2021) and a new distribution referred to as the length biased Burr XII distribution was obtained.

Anafo *et al.* (2021) derived a three-parameter equilibrium renewal Burr XII distribution using the equilibrium renewal method. The new distribution gave several shapes of the PDF and FRF including increasing, decreasing, unimodal, upside down bathtub, among others.

The generalisation of the Lindley and Burr XII distributions was obtained by multiplying the survival function of the Lindley with the Burr XII distributions through the competing risk model. The new model obtained had a FRF that was increasing, decreasing and bathtub as introduced and reported by Makubate *et al.* (2021).

Hassan *et al.* (2018) used the Bayesian analysis to obtain a mixture of the Burr XII and Burr X distributions. The Bayesian estimators for the unknown parameters had good statistical properties.

A new lifetime distribution was obtained by compounding the Burr XII distribution and the geometric distribution. The new distribution known as the Burr XII geometric distribution as obtained by Korkmaz and Erisoglu (2014) had FRF that is decreasing and unimodal.

An extension of the Burr XII distribution was derived and studied by Ghosh and Bourguinon (2017) with application in survival analysis was obtained using the general type I half logistic family of distributions proposed by Cordeiro *et al.* (2016). The parameter estimates were obtained from the maximum likelihood estimation method. The Topp-Leone Burr XII distribution was proposed by Reyad and Othman (2017) and was obtained by replacing the CDF in the Topp-Leone generated family with the CDF of the Burr XII distribution. The PDF assumes different shapes when different values of the parameters are used.

CHAPTER 3

METHODOLOGY

3.1 Introduction

Chapter Three of the thesis introduces several key definitions and concepts related to the methods, distributions, and data sets used in the study. The purpose of this chapter is to provide a foundational understanding of the methodologies and frameworks employed to achieve the research objectives. The topics discussed include the PDF, CDF, FRF and quantile functions of the Gompertz, Fréchet and Burr XII distributions. Some statistical techniques used which include Maximum Likelihood Estimation (MLE) method, Ordinary Least Squares (OLSS), Weighted Least Squares (WLSS), Cramér-von Mises Estimation (CVM) and Anderson-Darling Estimation (AD), and Total Time on Test (TTT) transform are also presented.

3.2 Gompertz Distribution

The Gompertz distribution was proposed by Benjamin Gompertz in 1825 and was connected to analysing human mortality and generating actuarial tables. The Gompertz distribution is a modification of the exponential distribution and have received a lot of attention in recent times in analysing medical and actuarial data sets.

The Gompertz distribution is both left and right skewed with its FRF monotonically increasing (Eraikhuemen *et al.*, 2021). Undeniably, in real life, there could be scenarios with data sets having non-monotonically increasing FRF or some having heavy-tailed characteristics (Eghwerido, 2020).

The CDF and the corresponding PDF of the Gompertz distribution are given by Equations (3.1) and (3.2) respectively.

$$F_G(x; f, g) = 1 - exp\left[-\frac{g}{f}\left(e^{fx} - 1\right)\right], x > 0, f > 0, g > 0, \tag{3.1}$$

and

$$f_G(x;f,g) = ge^{fx}exp\left[-\frac{g}{f}\left(e^{fx}-1\right)\right], x>0, f>0, g>0, \tag{3.2}$$

where f is a scale parameter and g is a shape parameter.

The survival function (SF) of the Gompertz distribution can be expressed as Equation (3.3).

$$S_G(x;f,g) = exp\left[-\frac{g}{f}\left(e^{fx}-1\right)\right], x>0, f>0, g>0, \tag{3.3}$$

and the FRF is given by Equation (3.4).

$$h_G(x;f,g) = \frac{f_G(x)}{S_G(x)} = ge^{fx}, x>0, f>0, g>0. \tag{3.4}$$

The quantile function of the Gompertz distribution for $p \in (0,1)$ by definition is given as

$$Q_G(p) = \mathbf{P}(X \leq x_p) = p.$$

Hence,

$$p = 1 - \exp\left[\frac{g}{f}(1-e^{fx_p})\right]. \tag{3.5}$$

By solving equation (3.5) and substituting $x_p = Q_G(p)$, we obtain the quantile function of the Gompertz distribution given as Equation (3.6).

$$Q_G(p) = \frac{1}{f}\left[1 - \frac{f}{g}\log(1-p)\right], f>0, g>0. \tag{3.6}$$

3.3 Fréchet Distribution

The Fréchet distribution, which belongs to the group of commonly used extreme value distributions (EVD). It finds application in modelling extreme events such as annual rainfall, earthquakes, floods, and more. When considering the PDF of the Fréchet distribution, it can take on two possible shapes: unimodal or decreasing. The specific shape is determined by the value of the shape parameter associated with the distribution. However, regardless of the shape parameter, the FRF of the Fréchet distribution consistently exhibits a unimodal shape (Hussein *et al.*, 2021b). There is therefore the need to extend the Fréchet distribution to model the variety of the data sets in many of the applied fields like engineering, geology, medicine, among others.

The PDF and the corresponding CDF of a two-parameter Fréchet distribution can be expressed as Equations (3.7) and (3.8) respectively.

$$f_{Fr}(x; d, g) = dg^d x^{-d-1} e^{-\left(\frac{g}{x}\right)^d}, x > 0, d > 0, g > 0, \tag{3.7}$$

and

$$F_{Fr}(x; d, g) = exp\left(-\left(\frac{g}{x}\right)^d\right), x > 0, \tag{3.8}$$

where d and $g > 0$ are shape and scale parameters respectively.

The SF of the Fréchet distribution can be expressed as Equation (3.9).

$$S_{Fr}(x; d, g) = 1 - exp\left(-\left(\frac{g}{x}\right)^d\right), x > 0, d > 0, g > 0, \tag{3.9}$$

and the FRF is given by Equation (3.10).

$$h_{Fr}(x; d, g) = \frac{f_{Fr}(x; d, g)}{S_{Fr}(x; d, g)} = \frac{dg^d x^{-d-1} e^{-\left(\frac{g}{x}\right)^d}}{1 - exp\left(-\left(\frac{g}{x}\right)^d\right)}, x > 0, d > 0, g > 0. \tag{3.10}$$

The Fréchet distribution's quantile function for $q \in (0, 1)$ by definition can be expressed as

$$Q_{Fr}(q) = \mathbf{P}(X \leq x_q) = q.$$

Hence,

$$q = \exp\left(-x^{-d} g^d\right). \tag{3.11}$$

By solving equation (3.11) and substituting $x_q = Q_{Fr}(q)$, we obtain the quantile function of the Fréchet distribution given as Equation (3.12).

$$Q_{Fr}(q) = g(-\log q)^{-\frac{1}{d}}, d > 0, g > 0. \tag{3.12}$$

3.4 Burr XII Distribution

Introduced by Burr (1942), the Burr XII distribution has gained substantial attention and recognition in several fields. This two-parameter distribution has been widely employed in a range of fields including actuarial sciences, reliability analysis, modelling income distributions, and several branches of physics. Its flexibility and versatility make it a valuable tool for modelling a wide range of data types encountered in these domains. Researchers and practitioners have extensively used the Burr XII distribution to analyse and interpret complex phenomena, making it an important distribution in various disciplines.

The Burr XII distribution has been used in different field as a result of its flexibility in fitting data sets with heavy tails and monotone failure rates, however, it does not provide a better fit for non-monotone failure rates (Nasir *et al.*, 2018). This limitation have resulted in the increasing development of more models that in the end increase its versatility.

The CDF of the Burr XII can be expressed as Equation (3.13).

$$F_{Br}(x;d,w) = 1-\left(1+x^{d}\right)^{-w}, x>0, d>0, w>0, \tag{3.13}$$

and the PDF is given as Equation (3.14).

$$f_{Br}(x;d,w) = dwx^{d-1}\left(1+x^{d}\right)^{-w-1}, x>0, d>0, w>0, \tag{3.14}$$

where both d and w are shape parameters.

The SF of the Burr XII distribution is given as Equation (3.15).

$$S_{Br}(x;d,w) = \left(1+x^{d}\right)^{-w}, x>0, d>0, w>0, \tag{3.15}$$

and the FRF is given by Equation (3.16).

$$h_{Br}(x;d,w) = \frac{f_{Br}(x;d,w)}{S_{Br}(x;d,w)} = dwx^{d-1}\left(1+x^{d}\right)^{-1}, x>0, c>0, k>0. \tag{3.16}$$

The quantile function of the Burr XII distribution for $q \in (0,1)$ by definition can expressed as

$$Q_{Br}(q) = \mathbf{P}(X \leq x_q) = q.$$

Hence,

$$q = 1 - \left(1 + (x_q)^{d}\right)^{-w}. \tag{3.17}$$

By solving equation (3.17) and substituting $x_q = Q_{Br}(q)$, we obtain the quantile function of the Burr XII distribution given as Equation (3.18).

$$Q_{Br}(q) = \left[(1-q)^{-\frac{1}{w}} - 1\right]^{\frac{1}{d}}, d, w > 0. \tag{3.18}$$

3.5 Harmonic Mixture Family of Distributions

Kharazmi *et al.* (2022) developed a new mixture distribution family by applying the weighted harmonic means of two SFs. This was referred to as the Harmonic Mixture-G (HMG) family. Based on the work of Kharazmi *et al.* (2022), the SF of the HMG family can be expressed as (3.19).

$$\bar{S}_{Hm}(x) = \frac{1}{\frac{\rho}{\bar{F}(x)} + \frac{1-\rho}{\bar{F}^{\alpha}(x)}} = \frac{\bar{F}^{\alpha}(x)}{1-\rho\left(1-\bar{F}^{\alpha-1}(x)\right)}, \tag{3.19}$$

$x \in R$, $\alpha \geq 0$, $0 \leq \rho \leq 1$,

where $\bar{F}(x)$ is the SF of the baseline distribution, $\bar{F}^{\alpha}(x)$ is the SF for the proportional hazard (PH) model relative to the SF of the baseline distribution $\bar{F}(x)$ and ρ, the weight of the function.

The corresponding CDF and PDF respectively can be expressed as Equations (3.20) and (3.21).

$$F_{Hm}(x) = 1 - \frac{\bar{F}^{\alpha}(x)}{1 - \rho\left(1 - \bar{F}^{\alpha-1}(x)\right)}, \tag{3.20}$$

and

$$f_{Hm}(x) = f(x)\bar{F}^{\alpha-1}(x)\frac{\alpha\left(1-\rho\right) + \rho\bar{F}^{\alpha-1}(x)}{\left[1 - \rho\left(1 - \bar{F}^{\alpha-1}(x)\right)\right]^2}. \tag{3.21}$$

The FRF of the HMG family is given by Equation (3.22).

$$h_{Hm}(x) = \frac{f(x)}{\bar{F}(x)}\frac{\alpha\left(1-\rho\right) + \rho\bar{F}^{\alpha-1}(x)}{1 - \rho\left(1 - \bar{F}^{\alpha-1}(x)\right)}. \tag{3.22}$$

The quantile function of the HMG family for $p \in (0,1)$ by definition can be expressed as

$$Q_{Hm}(p) = \mathbf{P}(X \leq x_p) = p.$$

Hence,

$$1 - \frac{\bar{F}^{\alpha}(x_p)}{1 - \rho\left[1 - \bar{F}^{\alpha-1}(x_p)\right]} = p. \tag{3.23}$$

By solving equation (3.23) and substituting $x_q = Q_{Hm}(q)$, we obtain the quantile function of the HMG family given as Equation (3.24).

$$\bar{F}^{\alpha}(Q_{Hm}(q)) = (1-q)\left[1 - \rho + \rho\bar{F}^{\alpha}(Q_{Hm}(q))\bar{F}^{-1}(Q_{Hm}(q))\right]. \tag{3.24}$$

The availability of a closed-form inverse for the quantile function of the HMG family, as expressed in equation (3.24), depends on the specific baseline distribution chosen.

3.6 Parameter Estimation Methods

Parameter estimation is a study area that provides tools that helps to efficiently use data and intend aid in statistical modelling of real life events (Zhang, 1997). In point estimation,the popular methods for estimating parameters include method of moments, maximum likelihood estimation, least square estimation and Bayesian estimation. In this study we discuss the maximum likelihood estimation, the ordinary least square estimation, the weighted least square estimation, the Cramér-Von Mises estimation, the Anderson-Darling estimation and the total time on test transform.

3.6.1 Maximum Likelihood Estimation

The MLE is a point estimation of an unknown parameter as it gives a single value for estimating the unknown parameter. The MLE was introduced in 1912 by an English statistician called R.A. Fisher. The MLE method is widely used and applied to various real life problems. For large sample values, the method provides an excellent estimator for the unknown parameter, say φ (Miura, 2011).

Given that $x_1, x_2, ..., x_n$ are independently and identically distributed random observations sampled from a given distribution with PDF $P(x|\varphi)$ which satisfies $P(X \leq r|\varphi) = \int_{-\infty}^{r} P(x|\varphi)\mathrm{d}x$, and joint density function

$$P(x_1, x_2, ..., x_n|\varphi) = P(x_1|\varphi)P(x_2|\varphi)...P(x_n|\varphi) = \prod_{a=1}^{n} P(x_a|\varphi), \tag{3.25}$$

equation (3.25) will then be the likelihood function which depends on the unknown parameter, φ, which can be denoted as $L(\varphi)$.

Even though the MLE method maximises the likelihood function $L(\varphi)$ with respect to φ, the log of the likelihood function, which is called the log likelihood function is easier to maximise than the likelihood function. The log likelihood function, $l(\varphi)$ is given as Equation (3.26).

$$\ell(\varphi) = \log L(\varphi) = \log \prod_{a=1}^{n} P(x_a|\varphi) = \sum_{a=1}^{n} \log P(x_a|\varphi). \tag{3.26}$$

The MLE estimate, $\hat{\varphi}$ is derived by taking the derivative of the log likelihood function with respect to the parameter and setting it to zero thus $l'(\varphi) = 0$. In situations where φ is a vector of parameters, the initial partial derivatives of log likelihood function are taken with respect to the various parameters $(\varphi_1, \varphi_2, ..., \varphi_n)$ and set to zero to obtain the MLE estimates $\hat{\varphi}_1, \hat{\varphi}_2, ..., \hat{\varphi}_n$ thus $\partial\ell/\partial\varphi_a = 0$, where $a = 1, 2, ..., n$.

3.6.2 Ordinary Least Squares

In this section, we discuss the OLSS estimation of unknown parameters. This regression based estimation method of unknown parameters was proposed by Swain *et al.* (1988) when they estimated the parameters of the beta distribution.

Suppose $t_1, t_2, ..., t_n$ is a random sample of size n from a distribution function $G(\cdot)$ and $t_{(1)} < t_{(2)} < ... < t_{(n)}$ represents the order statistics of the observed sample. For the sample of size n, we have the expectation, the variance and the covariance respectively as,

$$E\left[G\left(t_{(b)}|\varphi\right)\right] = \frac{b}{n+1}, \tag{3.27}$$

$$V\left[G\left(t_{(b)}\right)|\varphi\right] = \frac{b(n-b+1)}{(n+1)^2(n+2)}, \tag{3.28}$$

and

$$Cov\left[\left(G\left(t_{(b)}\right)|\varphi\right), \left(G\left(t_{(k)}\right)|\varphi\right)\right] = \frac{b(n-k+1)}{(n+1)^2(n+2)}; b < k, \tag{3.29}$$

where $b = 1, 2, ..., n$.

The OLSS estimator(s) can then be obtained by minimising Equation (3.30)

$$LS(\varphi) = \sum_{b=1}^{n}\left\{\left(G\left(t_{(b)}\right)|\varphi\right) - \frac{b}{n+1}\right\}^2, \tag{3.30}$$

with respect to the unknown parameter. The function $G\left(t_{(b)}\right)$ need not be necessarily a linear function of the order statistics. The OLS estimate, $\hat{\varphi}$ is derived by taking the derivative of the OLS function and setting it to zero thus $LS'(\varphi) = 0$. In situations where φ is a vector of parameters, the initial partial derivatives of OLS function are taken with respect to the various parameters $(\varphi_1, \varphi_2, ..., \varphi_n)$ and set to zero to obtain the OLS estimates $\hat{\varphi}_1, \hat{\varphi}_2, ..., \hat{\varphi}_n$ thus $\partial LS/\partial\varphi_b = 0$, where $b = 1, 2, ..., n$.

3.6.3 Weighted Least Squares

In this section, we discuss the WLSS of unknown parameters. In this method, the weights are computed as the inverse of the approximate variance of the function of an order statistics.

Suppose $t_1, t_2, ..., t_n$ is a random sample of size n from a distribution function $G(\cdot)$ and $t_{(1)} < t_{(2)} < ... < t_{(n)}$ represents the order statistics of the observed sample, then the expectation and the variance respectively are given as,

$$E\left[G\left(t_{(b)}|\varphi\right)\right] = \frac{b}{n+1}, \tag{3.31}$$

and

$$V\left[G\left(t_{(b)}\right)|\varphi\right] = \frac{b(n-b+1)}{(n+1)^2(n+2)}. \tag{3.32}$$

The WLS estimator(s) can then be obtained by minimising Equation (3.33).

$$WLS(\varphi) = \sum_{b=1}^{n} w_b \left\{ \left(G\left(t_{(b)}\right)|\varphi\right) - \frac{b}{n+1} \right\}^2, \tag{3.33}$$

with respect to the unknown parameter, where $w_b = \frac{1}{V\left(G\left(t_{(b)}\right)\right)} = \frac{(n+1)^2(n+2)}{b(n-b+1)}$ and $b = 1, 2, ..., n$. The function $G\left(t_{(b)}\right)$ need not be necessarily a linear function of the order statistics. The WLSS estimate, $\hat{\varphi}$ is derived by taking the derivative of the WLSS function and setting it to zero thus $WLS'(\varphi) = 0$. In situations where φ is a vector of parameters, the initial partial derivatives of WLSS function are taken with respect to the various parameters $(\varphi_1, \varphi_2, ..., \varphi_n)$ and set to zero to obtain the WLSS estimates $\hat{\varphi}_1, \hat{\varphi}_2, ..., \hat{\varphi}_n$ thus $\partial WLS/\partial\varphi_b = 0$, where $b = 1, 2, ..., n$.

3.6.4 Cramér-von Mises Estimation

Cramér-von Mises Estimation (CVM) is a minimum distance estimation technique that involves measuring the discrepancy between the estimated CDF and the empirical distribution function (EDF) Louzada *et al.* (2016). Macdonald (1971) asserts that the CVM provides a smaller bias compared to the other minimum distance estimators.

Suppose $y_1, y_2, ..., y_n$ is a random sample of size n from an EDF with CDF $G(y_b)$ and $y_{(1)} < y_{(2)} < ... < y_{(n)}$ represents the order statistics of the observed sample, the

Cramér-Von Mises estimates are obtained by minimising Equation (3.34).

$$CVM(\varphi) = \frac{1}{12n} + \sum_{b=1}^{n} \left\{ \left(G\left(y_{(b)} \right) | \varphi \right) - \frac{2b-1}{2n} \right\}^2, \tag{3.34}$$

with respect to the parameter, where $b = 1, 2, ..., n$. The CVM, $\hat{\varphi}$ is derived by taking the derivative of the CVM function and setting it to zero thus $CVM'(\varphi) = 0$. In situations where φ is a vector of parameters, the initial partial derivatives of CVM function are taken with respect to the various parameters $(\varphi_1, \varphi_2, ..., \varphi_n)$ and set to zero to obtain the CVM estimates $\hat{\varphi}_1, \hat{\varphi}_2, ..., \hat{\varphi}_n$ thus $\partial CVM/\partial \varphi_b = 0$, where $b = 1, 2, ..., n$.

3.6.5 Anderson-Darling Estimation

The Anderson–Darling estimation (AD) just like the Cramér–von Mises estimation belong to the class of quadratic EDF and also a minimum distance estimation method. The AD was proposed by Anderson and Darling (1952).

Suppose $y_1, y_2, ..., y_n$ is random sample of size n from an EDF with CDF $G(y_b)$ and $y_{(1)} < y_{(2)} < ... < y_{(n)}$ represents the order statistics of the observed sample, the Anderson-Darling estimates are obtained by minimising Equation (3.35).

$$AD(\varphi) = -n - \frac{1}{n} \sum_{b=1}^{n} (2b-1) \left\{ \left(\log G\left(y_{(b)} \right) \right) + \log\left(1 - G\left(y_{(n+1-b)} \right) \right) \right\}, \tag{3.35}$$

with respect to the parameter, where $b = 1, 2, ..., n$. The AD, $\hat{\varphi}$ is derived by taking the derivative of the AD function and setting it to zero thus $AD'(\varphi) = 0$. In situations where φ is a vector of parameters, the initial partial derivatives of AD function are taken with respect to the various parameters $(\varphi_1, \varphi_2, ..., \varphi_n)$ and set to zero to obtain the AD estimates $\hat{\varphi}_1, \hat{\varphi}_2, ..., \hat{\varphi}_n$ thus $\partial AD/\partial \varphi_b = 0$, where $b = 1, 2, ..., n$.

3.7 Total Time on Test Transform

The total time on test (TTT) transform was proposed by Richard E. Barlow and Raphael Campo in 1975 to deduce the shape of a failure rate function and how close a data distribution is to the model (Chaubey and Zhang, 2013).

If $G(\cdot)$ is the CDF of a distribution with $G^{-1}(\cdot)$, $\bar{G}(\cdot)$ as its quantile function and survival function respectively, then the TTT transform function defined on $[0, 1]$ is given by

$$H_G^{-1}(p) = \int_0^{G^{-1}(p)} (1 - G(x))\, \mathrm{d}x. \tag{3.36}$$

The scaled TTT transform is obtained using

$$\Phi_G(p) = \frac{H_G^{-1}(p)}{H_G^{-1}(1)}. \tag{3.37}$$

If G is a life distribution with a finite mean μ, then $H_G^{-1}(1) = \mu$, the scale TTT transform of G can also be expressed as

$$\Phi_G(p) = \frac{1}{\mu} \int_0^{G^{-1}(p)} (1 - G(x))\, \mathrm{d}x. \tag{3.38}$$

Suppose $y_{(1)} \leq y_{(2)} \leq ... \leq y_{(n)}$ represents the order statistics of the observed sample, the TTT plots can be computed in the following way;

i. First compute the TTT values $t_b = ny_{(b)} + (n-1)(y_{(2)} - y_{(1)}) + ... + (n-b+1)(y_{(b)} - y_{(b-1)})$ for $b = 1, 2, ..., n$ and $t_0 = 0$.

ii. Compute $\phi_b = t_b/t_n$ for $b = 0, 1, 2, ..., n$ to normalise the TTT values.

iii. Plot $(b/n, \phi_b)$ for $b = 0, 1, 2, ..., n$.

The TTT plots could be seen to be approximately either linear, concave, convex, convex-concave or concave-convex. A linear shape shows the exhibiting of no trend, a concave shape shows the exhibiting of an increasing failure rate function, a convex shape shows the exhibiting of a decreasing failure rate function, a convex-concave shape shows the exhibiting of a bathtub failure rate function while a concave-convex shape shows the exhibiting of an upside down bathtub failure rate function.

3.8 Data and Source

In the study, eleven (11) complete data sets were employed. The data set descriptions and sources are presented in this section.

3.8.1 Data sets for First Model Developed

The first four data sets were used to ascertain how applicable the harmonic mixture Gompertz distribution and its regression model are. They include the 63 observations of the strength of 1.5cm glass fibres, the failure times (10^3h) of 40 turbochargers in a type of diesel engine, the transformed total production of milk recorded in the first birth of cows (107) used in the SINDI race and the relationship between Survival time (T) and duration of diabetes(DUR) in years of 40 male patients. The strength of 1.5cm glass fibres data set were employed by (Eghwerido *et al.*, 2021b) and (Khaleel *et al.*, 2020), the turbochargers failure times data set were employed by (Guerra *et al.*, 2021), the transformed total milk production data set were employed by Nasiru *et al.* (2021) and the survival time and duration of diabetes data set were retrieved from Lee and Wang (2003).

3.8.2 Data sets for Second Model Developed

The next three data sets were employed to demonstrate the applicability of the harmonic mixture Fréchet distribution. Firstly, the dataset consists of yearly maximum temperature records from a specific location in the Upper East Region of Ghana, which is known for its relatively high yearly temperature values. The temperature data spans from 1970 to 2020 and is measured in degrees Celsius ($°C$). These temperature records were generated based on the given latitude (10.9922) and longitude (-1.1133) of the location from `https://www.globalclimatemonitor.org/`. Secondly, the dataset includes yearly unemployment rate data for Ghana, covering the period from 1991 to 2021. The unemployment rate data provide insights into the employment situation in Ghana over the specified time frame from the World Bank database. Lastly, the study incorporates survival times data from 128 patients diagnosed with bladder cancer. The survival times represent the duration between the diagnosis of bladder cancer and either the occurrence of an event (such as death) or the end of the study period. These survival times are crucial for analysing the progression and outcomes of bladder cancer patients. The bladder cancer data set were employed by Anafo *et al.* (2021) and Nasiru and Abubakari (2022).

3.8.3 Data sets for Third Model Developed

The last four data sets were employed to assess the applicability of the harmonic mixture Burr XII distribution and its regression model. These datasets include the taxes revenues (Bhatti *et al.*, 2018b), the failure times of epoxy strands (Ghosh and Bourguinon, 2017), the precipitation (in inches) in Minneapolis (Nasir *et al.*, 2019) and a regression data set regarding proportion of fat in the arms from `http://www.leg.ufpr.br/doku.php/publications:papercompanions:multquasibeta`.

3.9 Software Packages

The study extensively utilises the R programming language as a key tool for data analysis and computations. Throughout the research, the R package, along with the Mathematica package, is employed to perform various calculations and statistical operations. Specifically, the R package is utilised for generating plots, shapes, and conducting simulations. The package's robust functionality enables the creation of visual representations, such as graphs and charts, to visualise data patterns and relationships. Additionally, the R package provides tools for conducting simulations, allowing researchers to explore different scenarios and assess the behaviour of modified distributions. On the other hand, the Mathematica package is utilised in the study for specific computations and analyses. This software provides a powerful environment for mathematical and statistical computations, offering a range of specialised functions and capabilities.

CHAPTER 4

THEORETICAL RESULTS

4.1 Introduction

This chapter presents the theoretical results of the Harmonic Mixture Gompertz (HMGOM), Harmonic Mixture Fréchet (HMFR) and Harmonic Mixture Burr XII (HMBRXII) distributions. Some statistical properties associated with the developed distributions are presented. By exploring these properties, researchers can gain a deeper understanding of the distribution's moments, quantiles, variability, reliability, and order-based statistics. Estimators for the parameters of the proposed distributions are derived using the estimation techniques discussed in chapter 3. Regression models of the HMGOM and HMBRXII distributions are derived.

We can prove from Theorem 4.1 that the HMG family is heavy-tailed.

Proposition 4.1. A random variable Y from the HMG family is heavy-tailed.

Proof. For a random variable Y from the HMG family with complementary cumulative distribution function (CCDF), $\bar{F}_{Hm}(y)$,

$$\lim_{y\to\infty} \bar{F}_{Hm}(y)e^{\lambda y} = \infty,$$

implies the random variable Y is heavy-tailed.

By substitution,

$$\lim_{y\to\infty} \bar{F}_{Hm}(y)e^{\lambda y} = \lim_{y\to\infty} \frac{\bar{G}^{\alpha}(y)}{1-\rho\left(1-\bar{G}^{\alpha-1}(y)\right)}e^{\lambda y}.$$

Since $0 \leq \rho \leq 1$,

$$\lim_{y\to\infty} \bar{F}_{Hm}(y)e^{\lambda y} = \infty.$$

The proof is complete.

4.2 The Development of the Harmonic Mixture Gompertz Distribution

This sections presents the PDF, CDF, FRF and SF of the HMGOM distribution. The substitution of equations (3.2) and (3.3) into equation (3.21) gives the PDF of the HMGOM distribution as Equation (4.1).

$$f(y) = \frac{g\alpha\left(1-\rho\right)e^{fy}e^{-\frac{g\alpha}{f}\left(e^{fy}-1\right)} + g\rho e^{fy}e^{-\frac{g(2\alpha-1)}{f}\left(e^{fy}-1\right)}}{\left[1-\rho\left(1-e^{-\frac{g(\alpha-1)}{f}\left(e^{fy}-1\right)}\right)\right]^{2}}, \tag{4.1}$$

where $\alpha > 0$, $f > 0$, $g > 0$, $y > 0$ and $0 < \rho < 1$.

Figure 4.1 displays the density plots of the HMGOM distribution. The densities exhibited decreasing, left-skewed and right-skewed shapes.

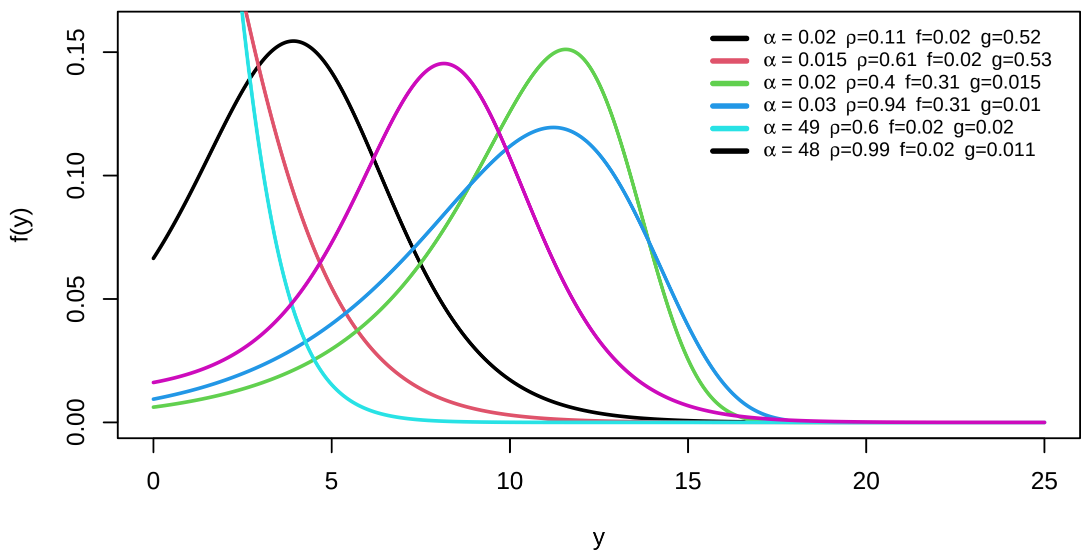

Figure 4.1: The density plots of the HMGOM

To obtain the CDF of the HMGOM distribution, substitute equation (3.3), the SF of the Gompertz distribution into equation (3.20). By performing this substitution, we can derive the expression given as Equation (4.2).

$$F(y) = 1 - \frac{e^{-\frac{g\alpha}{f}\left(e^{ay}-1\right)}}{\left[1-\rho\left(1-e^{-\frac{g(\alpha-1)}{f}\left(e^{fy}-1\right)}\right)\right]}, y > 0. \tag{4.2}$$

The Figure 4.2 displays the CDF of the HMGOM distribution for various parameter values. As x approaches 0 the CDF approaches 0 and approaches 1 as y approaches infinity.

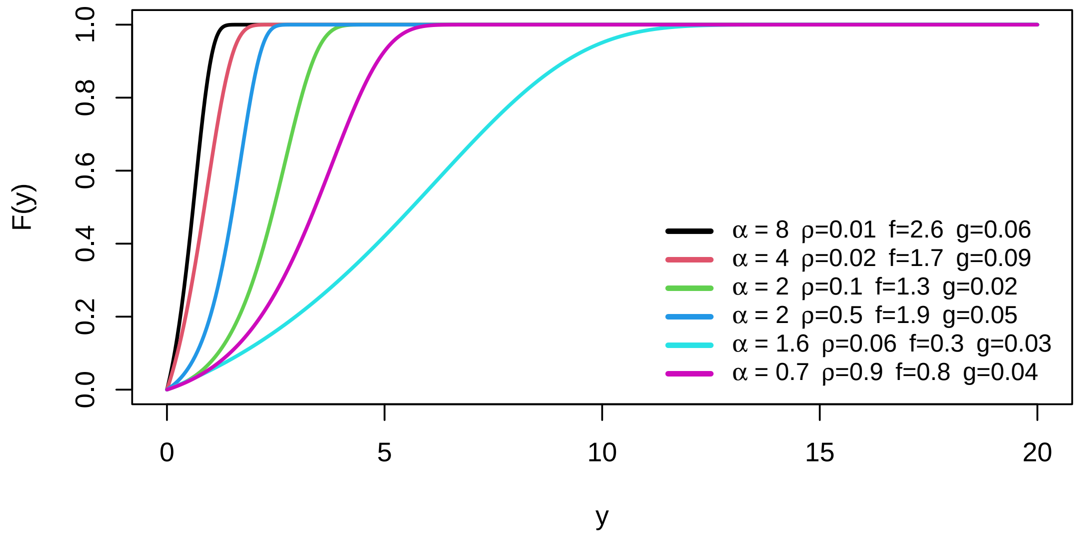

Figure 4.2: The CDF plot of the HMGOM

The SF of the HMGOM distribution can be derived as the complement of the CDF of the HMGOM distribution. The SF is given by Equation (4.3).

$$S(y) = \frac{e^{-\frac{g\alpha}{f}\left(e^{fy}-1\right)}}{\left[1-\rho\left(1-e^{-\frac{g(\alpha-1)}{f}\left(e^{fy}-1\right)}\right)\right]}, y > 0. \tag{4.3}$$

To obtain the FRF, we substitute equations (3.2) and (3.3) into equation (3.22).The FRF of the HMGOM distribution is expressed as Equation (4.4).

$$h(y) = \frac{g\alpha\left(1-\rho\right)e^{fy}e^{-\frac{g\alpha}{f}\left(e^{fy}-1\right)} + g\rho e^{fy}e^{-\frac{g(2\alpha-1)}{f}\left(e^{fy}-1\right)}}{e^{-\frac{g\alpha}{f}\left(e^{fy}-1\right)}\left[1-\rho\left(1-e^{-\frac{g(\alpha-1)}{f}\left(e^{fy}-1\right)}\right)\right]}, y > 0. \tag{4.4}$$

Figure 4.3 illustrates the plots of the FRF for the HMGOM distribution. By manipulating certain parameters, the FRF plots exhibit distinct patterns, thus increasing trends.

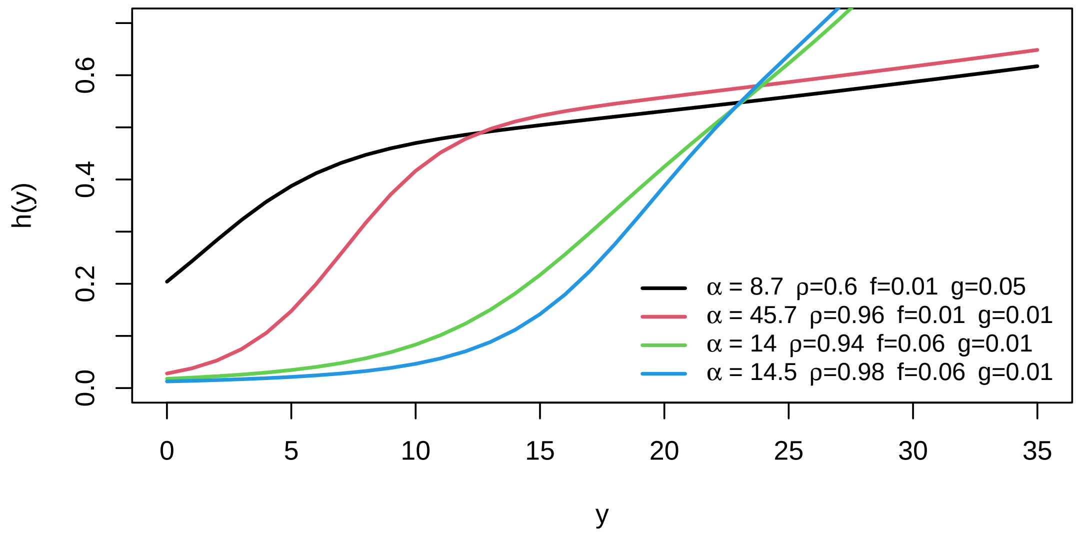

Figure 4.3: The FRF plots of the HMGOM

We assess the improvement of the introduction of the extra parameters from the HMG family brings to the Gompertz distribution (black curve) in Figure 4.4. While varying the values of the parameters ρ and α and keeping the values of the parameters from the Gompertz distribution constant, the plots showed an improvement in the kurtosis (peakness) and skewness of the Gompertz Distribution.

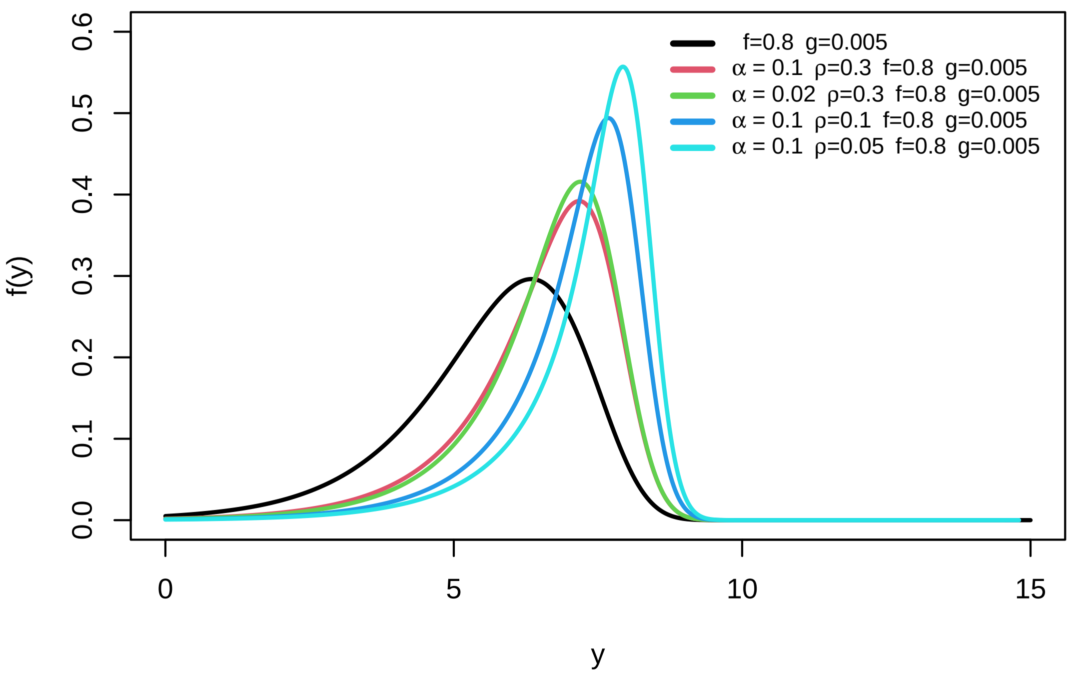

Figure 4.4: Assessing the densities of the HMGOM Distribution and the Gompertz Distribution

Lemma 4.1. The linear representation of the PDF of the HMGOM distribution provided $\alpha > 1$ is given by Equation (4.5).

$$f(y) = \sum_{a=0}^{\infty}\sum_{b=0}^{a}\sum_{k=0}^{\infty}\sum_{l=0}^{k}\sum_{m=0}^{\infty} \varpi_{abklm} y^m e^{-fly}, \tag{4.5}$$

where $\varpi_{abklm} = [g\alpha(1-\rho)\tau_{abklm} + g\rho\tau^*_{abklm}]$,
$\tau_{abklm} = \frac{(-1)^{b+k+l}}{k!m!}(a+1)\binom{a}{b}\binom{l}{k}\rho^a\left(\frac{g}{f}(\alpha(b+1)-b\right)^k(f(k+1))^m$,
$\tau^*_{abklm} = \frac{(-1)^{b+k+l}}{k!m!}(a+1)\binom{a}{b}\binom{l}{k}\rho^a\left(\frac{g}{f}(\alpha(b+2)-(b+1)\right)^k(f(k+1))^m$,
$y > 0, f > 0, g > 0, \alpha > 1$ and $0 < \rho < 1$.

Proof. Given that $\eta > 0$, the Taylor series for $(1-w)^{-\eta}$,$(1-w)^{\lambda}$ for $|w| < 1$ and e^{-t} are $(1-w)^{-\eta} = \sum_{a=0}^{\infty}\binom{\eta+a-1}{a}(w)^a$, $(1-w)^{\lambda} = \sum_{b=0}^{\infty}(-1)^b\binom{\lambda}{b}(w)^b$ and $e^{-h} = \sum_{t=0}^{\infty}\frac{(-1)^t}{t!}(h)^t$. Since $0 < e^{-\frac{g(\alpha-1)}{f}(e^{fy}-1)} < 1$ provided $\alpha > 1$, we use the Taylor series twice to obtain

$$\left[1-\rho\left(1-e^{-\frac{g(\alpha-1)}{f}(e^{fy}-1)}\right)\right]^{-2}=\sum_{a=0}^{\infty}\sum_{b=0}^{a}(-1)^{b}(a+1)\binom{a}{b}\rho^{a}e^{\frac{-g(\alpha-1)b}{f}(e^{fy}-1)}.$$

It follows that

$$\begin{aligned}f(y)=g\alpha(1-\rho)\sum_{a=0}^{\infty}\sum_{b=0}^{a}(-1)^{b}(a+1)\binom{a}{b}\rho^{a}e^{fy}e^{-\frac{g}{f}(\alpha(b+1)-b)(e^{fy}-1)}\\+g\rho\sum_{a=0}^{\infty}\sum_{b=0}^{a}(-1)^{b}(a+1)\binom{a}{b}\rho^{a}e^{fy}e^{-\frac{g}{f}(\alpha(b+2)-(b+1))(e^{fy}-1)}.\end{aligned} \tag{4.6}$$

We then use Taylor series expansion to obtain

$$e^{-\frac{g}{f}(\alpha(b+1)-b)(e^{fy}-1)}=\sum_{k=0}^{\infty}\frac{(-1)^{k}}{k!}\left(\frac{g}{f}(\alpha(b+1)-b)\right)^{k}(e^{fy}-1)^{k}$$

and

$$e^{-\frac{g}{f}(\alpha(b+2)-(b+1))(e^{fy}-1)}=\sum_{k=0}^{\infty}\frac{(-1)^{k}}{k!}\left(\frac{g}{f}(\alpha(b+2)-(b+1))\right)^{k}(e^{fy}-1)^{k}.$$

Similarly,

$$(e^{fy}-1)^{k}=e^{fky}\left(1-e^{-fy}\right)^{k}=e^{fky}\sum_{l=0}^{k}(-1)^{l}\binom{l}{k}e^{-fly}$$

and

$$e^{fy}\cdot e^{fky}=e^{f(k+1)y}=\sum_{m=0}^{\infty}\frac{(f(k+1))^{m}}{m!}x^{m}$$

Substituting these expansions into equation (4.6) and applying the Taylor series expansion once more, we obtain

$$f(y)=g\alpha(1-\rho)\sum_{a=0}^{\infty}\sum_{b=0}^{a}\sum_{k=0}^{\infty}\sum_{l=0}^{k}\sum_{m=0}^{\infty}\omega_{abklm}y^{m}e^{-fly}+g\rho\sum_{a=0}^{\infty}\sum_{b=0}^{a}\sum_{k=0}^{\infty}\sum_{l=0}^{k}\sum_{m=0}^{\infty}\omega^{*}_{abklm}y^{m}e^{-fly}.$$

4.3 Statistical Properties of the HMGOM distribution

The statistical properties of the HMGOM distribution are derived in this section. Properties such as the quantile function, non-central moments, incomplete moments, inequality measures, mean and median deviations, moment generating functions, characteristic function, entropy, stress-strength reliability, order statistics and identifiability are deduced.

4.3.1 Quantile Function

The quantile function, also known as the inverse CDF, operates in the opposite direction of the CDF. It also provides another way for describing the shapes and characteristics of a distribution.

Lemma 4.2. The quantile function of the HMGOM distribution can be expressed as Equation 4.7.

$$(1-p)\left[1-\rho\left(1-e^{-\frac{g(\alpha-1)}{f}(e^{fy_p}-1)}\right)\right]-e^{-\frac{g\alpha}{f}(e^{fy_p}-1)}=0, \tag{4.7}$$

where $p \in (0,1)$ and $Q(p) = y_p$ is the quantile function.

Proof. By definition, the quantile function is defined by

$$Q(p) = \mathbf{P}(Y \leq y_p) = p.$$

To obtain the quantile function of the HMGOM distribution, we substitute equation (3.1) into equation (3.24) and letting $Q(p) = y_p$.
The quantile function of the HMGOM distribution is without an analytical expression or closed form. This means that there is no direct formula available to calculate the exact quantiles of the HMGOM distribution. Instead, numerical methods or approximation techniques may be employed to estimate the quantiles based on the

distribution's parameters and desired probability values.

4.3.2 Moments

In this section, we focus on deriving the r^{th} moments of the HMGOM distribution for the random variable Y. Obtaining the moments are essential as they aid in statistical analysis. Measures including mean(μ), variance (σ^2), coefficient of variation (CV), coefficient of skewness (CS) and coefficient of kurtosis (CK) can be obtained using moments. The μ, σ^2, CV, CS and CK respectively are defined by

$$\mu = \mu_1^{'},$$

$$\sigma^2 = \mu_2^{'} - (\mu)^2,$$

$$CV = \frac{\sqrt{\mu_2^{'} - (\mu)^2}}{\mu},$$

$$CS = \frac{E(Y-\mu)^3}{[E(Y-\mu)^2]^{\frac{3}{2}}} = \frac{\mu_3^{'} - 3\mu\mu_2^{'} + 2\mu^3}{(\mu_2^{'} - \mu^2)^{\frac{3}{2}}}$$

and

$$CK = \frac{E(Y-\mu)^4}{[E(Y-\mu)^2]^2} = \frac{\mu_4^{'} - 4\mu\mu_3^{'} + 6\mu^2\mu_2^{'} - 3\mu^4}{(\mu_2^{'} - \mu^2)^2}.$$

Proposition 4.2. The r^{th} non-central moment of the HMGOM distribution for $\alpha > 1$ is expressed as Equation (4.8).

$$\mu_r^{'} = \sum_{a=0}^{\infty}\sum_{b=0}^{a}\sum_{k=0}^{\infty}\sum_{l=0}^{k}\sum_{m=0}^{\infty} \varpi_{abklm} \left(\frac{1}{fl}\right)^{r+m+1} \Gamma(r+m+1), r = 1, 2, ... \quad (4.8)$$

Proof. Mathematically,

$$\mu_r^{'} = E(Y^r) = \int_0^{\infty} y^r f(y) \mathrm{d}y. \quad (4.9)$$

The substitution of equation (4.5) into equation (4.9) produces

$$E(Y^r) = \int_0^\infty y^r \sum_{a=0}^\infty \sum_{b=0}^a \sum_{k=0}^\infty \sum_{l=0}^k \sum_{m=0}^\infty \varpi_{abklm} y^m e^{-fly} \mathrm{d}y.$$

We then obtain

$$\mu_r^{'} = \sum_{a=0}^\infty \sum_{b=0}^a \sum_{k=0}^\infty \sum_{l=0}^k \sum_{m=0}^\infty \varpi_{abklm} \int_0^\infty y^{r+m} e^{-fly} \mathrm{d}y.$$

Letting $u = fly$, which implies $y = \frac{u}{fl}$ and $dy = \frac{du}{fl}$, we obtain

$$\mu_r^{'} = \sum_{a=0}^\infty \sum_{b=0}^a \sum_{k=0}^\infty \sum_{l=0}^k \sum_{m=0}^\infty \varpi_{abklm} \left(\frac{1}{fl}\right)^{r+m+1} \int_0^\infty u^{r+m} e^{-u} \mathrm{d}u.$$

Using the identity

$$\Gamma(S) = \int_0^\infty y^{S-1} e^{-y} \mathrm{d}y,$$

we obtain

$$\mu_r^{'} = \sum_{a=0}^\infty \sum_{b=0}^a \sum_{k=0}^\infty \sum_{l=0}^k \sum_{m=0}^\infty \varpi_{abklm} \left(\frac{1}{fl}\right)^{r+m+1} \Gamma(r+m+1).$$

The Table 4.1 shows some measures of dispersion and asymmetry for the HMGOM distribution obtained through the use of the non-central moments. The HMGOM distribution could exhibit high skewness, moderate skewness and even could be approximately symmetric. As ρ approaches one, the distribution exhibits negative skewness and as ρ approaches zero, positive skewness. Furthermore, the HMGOM distribution demonstrates different characteristics, such as platykurtic or leptokurtic behaviour.

Table 4.1: Moments of the HMGOM for Different Parameter Values

r	α=12, ρ=0.99, f=0.35, g=0.05	α=10,ρ=0.90, f=0.35,g=0.05	α=10, ρ=0.80, f=0.35,g=0.05	α=55, ρ=0.60, f=0.60, g=0.05	α=55, ρ=0.60, f=0.60, g=0.55
μ_1'	3.2339	2.5583	2.1978	0.4476	4.9056×10^{-2}
μ_2'	11.8953	7.9458	6.1421	0.2947	3.8992×10^{-3}
μ_3'	46.5277	27.2857	19.4507	0.2400	4.1385×10^{-4}
μ_4'	189.6091	100.4260	67.1160	0.2268	5.4523×10^{-5}
μ_5'	797.5481	390.1568	247.4523	0.2405	8.5639×10^{-6}
σ^2	1.4372	1.4007	1.3116	0.0943	0.0015
CV	0.3707	0.4626	0.5211	0.6861	0.7895
CS	-0.7174	-0.1263	0.1238	0.6916	1.3199
CK	2.0360	1.7190	1.8317	3.4754	5.4944

4.3.3 Incomplete Moments

We derive the HMGOM distribution's incomplete moments. Incomplete moments play a crucial role in various fields, including finance, economics, and actuarial science.

Proposition 4.3. The r^{th} incomplete moments of the HMGOM distribution for $\alpha > 1$ can be expressed as Equation (4.10).

$$m_r(z) = \sum_{a=0}^{\infty}\sum_{b=0}^{a}\sum_{k=0}^{\infty}\sum_{l=0}^{k}\sum_{m=0}^{\infty} \varpi_{abklm} \left(\frac{1}{fl}\right)^{r+m+1} \gamma(r+m+1, flz), r = 1, 2, 3, ..., \tag{4.10}$$

$\gamma(\cdot, \cdot)$ is an lower incomplete gamma function.

Proof. Mathematically,

$$m_r(z) = E(Y^r|Y \leq z) = \int_0^z y^r f(y)\mathrm{d}y. \tag{4.11}$$

When equation (4.5) is substituted into equation (4.11), we have

$$m_r(z) = \int_0^z y^r \sum_{a=0}^{\infty}\sum_{b=0}^{a}\sum_{k=0}^{\infty}\sum_{l=0}^{k}\sum_{m=0}^{\infty} \varpi_{abklm} y^m e^{-fly}\mathrm{d}y.$$

We then obtain

$$m_r(z) = \sum_{a=0}^{\infty}\sum_{b=0}^{a}\sum_{k=0}^{\infty}\sum_{l=0}^{k}\sum_{m=0}^{\infty} \varpi_{abklm} \int_0^z y^{r+m} e^{-fly}\mathrm{d}y.$$

Letting $u = fly$, which implies $x = \frac{u}{fl}$ and $dy = \frac{du}{fl}$, we obtain

$$\mu_r^{'} = \sum_{a=0}^{\infty}\sum_{b=0}^{a}\sum_{k=0}^{\infty}\sum_{l=0}^{k}\sum_{m=0}^{\infty}\varpi_{abklm}\left(\frac{1}{fl}\right)^{r+m+1}\int_0^{flz} u^{r+m}e^{-u}\mathrm{d}u.$$

The identity

$$\gamma(a, x) = \int_0^x t^{a-1}e^{-t}\mathrm{d}t,$$

helps obtain

$$\mu_r^{'} = \sum_{a=0}^{\infty}\sum_{b=0}^{a}\sum_{k=0}^{\infty}\sum_{l=0}^{k}\sum_{m=0}^{\infty}\varpi_{abklm}\left(\frac{1}{fl}\right)^{r+m+1}\gamma(r+m+1, flz).$$

4.3.4 The measures of Inequality

By utilising both the Lorenz curve and the Bonferroni curve, researchers can gain insights into income inequality trends, analyse income distributions across nations or over time, and make more accurate and meaningful comparisons by accounting for differences in population sizes.

Proposition 4.4. The Lorenz curve for the HMGOM distribution for $\alpha > 1$ is given by Equation (4.12).

$$L(y) = \frac{1}{\mu}\sum_{a=0}^{\infty}\sum_{b=0}^{a}\sum_{k=0}^{\infty}\sum_{l=0}^{k}\sum_{m=0}^{\infty}\varpi_{abklm}\left(\frac{1}{fl}\right)^{m+2}\gamma(m+2, flz). \tag{4.12}$$

Proof. By definition the Lorenz curve is given by

$$L_F(y) = \frac{1}{\mu}\int_0^z yf(y)\mathrm{d}y.$$

$\int_0^z yf(y)\mathrm{d}y$ can be obtained using the first incomplete moment.

Proposition 4.5. The Bonferroni curve for the HMGOM distribution for $\alpha > 1$ can be expressed as Equation (4.13).

$$B(y) = \frac{1}{\mu F(y)} \sum_{a=0}^{\infty} \sum_{b=0}^{a} \sum_{k=0}^{\infty} \sum_{l=0}^{k} \sum_{m=0}^{\infty} \varpi_{abklm} \left(\frac{1}{fl}\right)^{m+2} \gamma(m+2, flz). \tag{4.13}$$

Proof.

$$B(y) = \frac{L(y)}{F(y)}. \tag{4.14}$$

The substitution of equation (4.12) completes the proof.

4.3.5 Mean Deviation and Median Deviation

By considering both mean and median deviations, researchers can gain a comprehensive understanding of the variation present in distributions. These measures help quantify the extent to which data points deviate from the central tendency, providing valuable insights into the overall spread and dispersion of the data.

Proposition 4.6. The mean deviation of the HMGOM distribution for $\alpha > 1$ can be expressed as Equation (4.15).

$$\Delta_1(y) = 2\mu F(\mu) - 2 \sum_{a=0}^{\infty} \sum_{b=0}^{a} \sum_{k=0}^{\infty} \sum_{l=0}^{k} \sum_{m=0}^{\infty} \varpi_{abklm} \left(\frac{1}{fl}\right)^{m+2} \gamma(m+2, fl\mu). \tag{4.15}$$

Proof. Mathematically,

$$\begin{aligned}
\Delta_1(y) &= \int_0^{\infty} |y-\mu| f(y) \mathrm{d}y \\
&= \int_0^{\mu} (\mu - y) f(y) \mathrm{d}y + \int_{\mu}^{\infty} (y-\mu) f(y) \mathrm{d}y \\
&= \mu \int_0^{\mu} f(y) \mathrm{d}y - \int_0^{\mu} y f(y) \mathrm{d}y + \mu \int_0^{\mu} f(y) \mathrm{d}y - \int_0^{\mu} y f(y) \mathrm{d}y \\
&+ \int_0^{\infty} y f(y) \mathrm{d}x - \mu \int_0^{\infty} f(y) \mathrm{d}y \\
&= 2\mu F(\mu) - 2 \int_0^{\mu} y f(y) \mathrm{d}y.
\end{aligned}$$

$\int_0^\mu yf(y)\mathrm{d}y$ is obtained using the first r^{th} incomplete moment of the HMGOM distribution.

Proposition 4.7. The median deviation for the HMGOM distribution for $\alpha > 1$ can be expressed as Equation (4.16).

$$\Delta_2(y) = \mu - 2\sum_{a=0}^{\infty}\sum_{b=0}^{a}\sum_{k=0}^{\infty}\sum_{l=0}^{k}\sum_{m=0}^{\infty}\varpi_{abklm}\left(\frac{1}{fl}\right)^{m+2}\gamma(m+2, flH). \tag{4.16}$$

Proof. Mathematically,

$$\begin{aligned}
\Delta_2(y) &= \int_0^\infty |y-H|f(y)\mathrm{d}y \\
&= \int_0^H (H-y)f(y)\mathrm{d}y + \int_H^\infty (y-H)f(y)\mathrm{d}y \\
&= H\int_0^H f(y)\mathrm{d}y - \int_0^H yf(y)\mathrm{d}y + H\int_0^H f(y)\mathrm{d}y - \int_0^H yf(y)\mathrm{d}y \\
&+ \int_0^\infty yf(y)\mathrm{d}y - H\int_0^\infty f(y)\mathrm{d}y.
\end{aligned}$$

Using the identity $F(H) = 0.5$, we have

$$\Delta_2(y) = \mu - 2\int_0^H yf(y)\mathrm{d}y.$$

The integral $\int_0^H yf(y)\mathrm{d}y$ is derived using the first incomplete moment.

4.3.6 Mean Residuals

The mean residuals provide an estimate of the remaining lifespan beyond time t for an individual or unit that has already survived up to time t. It quantifies the expected added lifetime, on average, from the current time t onwards.

Proposition 4.8. The mean residuals of the HMGOM distribution for $\alpha > 1$ can be expressed as Equation (4.17).

$$m(t) = \frac{1}{S_G(t)}\left[\mu - \sum_{a=0}^{\infty}\sum_{b=0}^{a}\sum_{k=0}^{\infty}\sum_{l=0}^{k}\sum_{m=0}^{\infty}\varpi_{abklm}\left(\frac{1}{fl}\right)^{m+2}\gamma(m+2, flt)\right] - t. \quad (4.17)$$

Proof. The mean residual life of a non-negative random variable Y is defined as

$$m(t) = E(Y - t|Y > t) = \frac{1}{S(t)}\int_t^{\infty}(y - t)f(y)\mathrm{d}y, t \geq 0.$$

It follows that

$$m(t) = \frac{1}{S_G(t)}\left[\mu - \int_0^t (y)f(y)\mathrm{d}y\right] - t. \quad (4.18)$$

Substituting equation (3.3) and $\int_0^t yf(y)\mathrm{d}y$, which is the first r^{th} incomplete moment into equation (4.18) completes the proof.

4.3.7 Moment Generating Function

The MGF is one of the powerful tools used to derive the moments of a probability distribution, provided the MGF exists for that distribution.

Proposition 4.9. The MGF for the HMGOM distribution for $\alpha > 1$ is given by Equation (4.19).

$$M_G(t) = \sum_{a=0}^{\infty}\sum_{b=0}^{a}\sum_{k=0}^{\infty}\sum_{l=0}^{k}\sum_{m=0}^{\infty}\sum_{r=0}^{\infty}\varpi_{abklm}\frac{t^r}{r!}\left(\frac{1}{fl}\right)^{r+m+1}\Gamma(r + m + 1). \quad (4.19)$$

Proof. Using the identity

$$e^{tY} = \sum_{r=0}^{\infty}\frac{t^r Y^r}{r!},$$

the MGF can be deduced as

$$M_G(t) = E(e^{tY}) = \sum_{r=0}^{\infty}\frac{t^r E(Y^r)}{r!} = \sum_{r=0}^{\infty}\frac{t^r}{r!}\mu_r'. \quad (4.20)$$

The substitution of equation (4.9) completes the proof.

4.3.8 Characteristic Function

In situations where the moment generating function fails to exist, characteristic functions provide a reliable means to characterise the distribution of heavy-tailed random variables.

Proposition 4.10. The characteristic function of the HMGOM distribution for $\alpha > 1$ is given by (4.21).

$$C(t) = \sum_{a=0}^{\infty}\sum_{b=0}^{a}\sum_{k=0}^{\infty}\sum_{l=0}^{k}\sum_{m=0}^{\infty}\sum_{r=0}^{\infty} \varpi_{abklm} \frac{(zt)^r}{r!} \left(\frac{1}{fl}\right)^{r+m+1} \Gamma(r+m+1). \tag{4.21}$$

Proof. Using the identity

$$e^{ztY} = \sum_{r=0}^{\infty} \frac{z^r t^r Y^r}{r!},$$

where $z = \sqrt{-1}$. We can define the characteristic function as

$$C(t) = E(e^{ztY}) = \sum_{r=0}^{\infty} \frac{(zt)^r E(Y^r)}{r!} = \sum_{r=0}^{\infty} \frac{(zt)^r}{r!} \mu_r^{'}. \tag{4.22}$$

The substitution of equation (4.9) completes the proof.

4.3.9 Entropy

By examining the entropy of the HMGOM distribution, researchers can gain insights into the level of uncertainty or variability inherent in the random variable. This information can be valuable for decision-making, risk assessment, and understanding the overall characteristics of the distribution.

Proposition 4.11. The Rényi entropy of the HMGOM distribution for $\alpha > 1$ is given by Equation (4.23).

$$I_R(\lambda) = \frac{1}{1-\lambda} \log \left[\sum_{a=0}^{\infty}\sum_{b=0}^{a}\sum_{k=0}^{\infty}\sum_{l=0}^{\infty}\sum_{m=0}^{l}\sum_{n=0}^{\infty} \psi^{*}_{abklmn} \left(\frac{1}{fm}\right)^{n+1} \Gamma(n+1) \right], \lambda \neq 1, \tag{4.23}$$

where

$\psi^*_{abklmn} = \frac{(-1)^{b+l+m}}{l!n!}\binom{2\lambda+a-1}{a}\binom{a}{b}\binom{k}{\lambda}\binom{m}{l}\rho^{a+k}g^{\lambda}(\alpha(1-\rho))^{\lambda-k}\left(\frac{g}{f}\left(\alpha(\lambda+b+k)-(b+k)\right)\right)^{l}$ $(f(l+1))^n$.

Proof. Mathematically,

$$I_R(\lambda) = \frac{1}{1-\lambda}\log\int_0^{\infty} f^{\lambda}(y)\mathrm{d}y, \lambda \neq 1. \tag{4.24}$$

The PDF of HMGOM to the power λ is given as

$$f^{\lambda}(y) = \frac{g^{\lambda}e^{\lambda fy}e^{-\frac{g\alpha\lambda}{f}(e^{fy}-1)}(\alpha(1-\rho))^{\lambda}\left(1+\frac{\rho e^{-\frac{g(\alpha-1)}{f}(e^{fy}-1)}}{\alpha(1-\rho)}\right)^{\lambda}}{\left[1-\rho\left(1-e^{-\frac{g(\alpha-1)}{f}(e^{fy}-1)}\right)\right]^{2\lambda}}$$

Using Taylor series, we obtain

$$\left[1-\rho\left(1-e^{-\frac{g(\alpha-1)}{f}(e^{fy}-1)}\right)\right]^{-2\lambda} = \sum_{a=0}^{\infty}\sum_{b=0}^{a}(-1)^b\binom{2\lambda+a-1}{a}\binom{a}{b}\rho^a e^{\frac{-g(\alpha-1)j}{f}(e^{fy}-1)}$$

and

$$\left(1+\frac{\rho e^{-\frac{g(\alpha-1)}{f}(e^{fy}-1)}}{\alpha(1-\rho)}\right)^{\lambda} = \sum_{k=0}^{\infty}\binom{k}{\lambda}\rho^k(\alpha(1-\rho))^{-k}e^{-\frac{g(\alpha-1)k}{f}(e^{fy}-1)}$$

Also,

$$e^{-\frac{g}{f}(\alpha(\lambda+b+k)-(b+k))}(e^{fy}-1) = \sum_{l=0}^{\infty}\frac{(-1)^l}{l!}\left(\frac{g}{f}\left(\alpha(\lambda+b+k)-(b+k)\right)\right)^{l}(e^{fy}-1)^l,$$

$$(e^{fy}-1)^l = e^{fly}(1-e^{-fy})^l = e^{fly}\sum_{m=0}^{l}(-1)^m\binom{m}{l}e^{-fmy}$$

and

$$e^{fy}\cdot e^{fly} = e^{f(l+1)y} = \sum_{n=0}^{\infty}\frac{1}{n!}(f(l+1))^n y^n$$

We then obtain

$$f^{\lambda}(y) = \sum_{a=0}^{\infty}\sum_{b=0}^{a}\sum_{k=0}^{\infty}\sum_{l=0}^{\infty}\sum_{m=0}^{l}\sum_{n=0}^{\infty}\psi^*_{abklmn}y^n e^{-fmy}, \tag{4.25}$$

We substitute equation (4.25) into equation (4.24) and obtain

$$I_R(\lambda) = \frac{1}{1-\lambda} \log \int_0^\infty \sum_{a=0}^{\infty} \sum_{b=0}^{a} \sum_{k=0}^{\infty} \sum_{l=0}^{\infty} \sum_{m=0}^{l} \sum_{n=0}^{\infty} \psi^*_{abklmn} y^n e^{-fmy} \mathrm{d}y. \tag{4.26}$$

Letting $u = fmy$, which implies $y = \frac{u}{fm}$ and $dy = \frac{du}{fm}$, we obtain

$$f^\lambda(y) = \sum_{a=0}^{\infty} \sum_{b=0}^{a} \sum_{k=0}^{\infty} \sum_{l=0}^{\infty} \sum_{m=0}^{l} \sum_{n=0}^{\infty} \psi^*_{abklmn} \left(\frac{1}{fm}\right)^{n+1} \int_0^\infty u^n e^{-u} \mathrm{d}u.$$

But $\int_0^\infty u^n e^{-u} \mathrm{d}u = \Gamma(n+1)$.

We obtain the Rényi entropy of the HMGOM distribution after correctly substituting into equation (4.26).

4.3.10 Stress-Strength Reliability

This concept is particularly relevant in various fields such as engineering, structural analysis, and reliability engineering. By quantifying the stress-strength reliability, engineers and analysts can make informed decisions regarding the design, operation, and maintenance of systems to ensure they can withstand the anticipated stresses and perform reliably under normal or extreme conditions.

Proposition 4.12. The stress-strength reliability of the HMGOM distribution for $\alpha > 1$ is given as Equation (4.27).

$$R_{ss} = 1 - \left[\sum_{a=0}^{\infty} \sum_{b=0}^{a} \sum_{k=0}^{\infty} \sum_{l=0}^{k} \sum_{m=0}^{\infty} \delta_{abklm} \left(\frac{1}{fl}\right)^{m+1} \Gamma(m+1) \right], \tag{4.27}$$

where $\delta_{abklm} = [g\alpha(1-\rho)\eta_{abklm} + g\rho\eta^*_{abklm}]$,

$\eta_{abklm} = \frac{(-1)^{b+k+l}}{k!m!} \binom{a+2}{2} \binom{a}{b} \binom{l}{k} \rho^a \left(\frac{g}{f}(\alpha(b+2) - b\right)^k (f(k+1))^m$,

$\eta^*_{abklm} = \frac{(-1)^{b+k+l}}{k!m!} \binom{a+2}{2} \binom{a}{b} \binom{l}{k} \rho^a \left(\frac{g}{f}(\alpha(b+3) - (b+1)\right)^k (f(k+1))^m$.

Proof. By definition

$$R_{ss} = \int_0^\infty f(y) \cdot F(y) \mathrm{d}y = 1 - \int_0^\infty f(y) \cdot S(y) \mathrm{d}y. \tag{4.28}$$

Multiplying equations (3.2) and (3.3), we have

$$f(y) \cdot S(y) = \frac{g\alpha(1-\rho)e^{fy}e^{-\frac{2g\alpha}{f}(e^{fy}-1)} + g\rho e^{fy}e^{-\frac{g(3\alpha-1)}{f}(e^{fy}-1)}}{\left[1-\rho\left(1-e^{-\frac{g(\alpha-1)}{f}(e^{fy}-1)}\right)\right]^3}. \tag{4.29}$$

Simplifying equation(4.29) using the Taylor series, we obtain

$$f(y) \cdot S(y) = \sum_{a=0}^{\infty}\sum_{b=0}^{a}\sum_{k=0}^{\infty}\sum_{l=0}^{k}\sum_{m=0}^{\infty} \delta_{abklm} y^m e^{-fly}. \tag{4.30}$$

We substitute equation (4.30) into equation (4.28) and obtain

$$R_{ss} = 1 - \left[\sum_{a=0}^{\infty}\sum_{b=0}^{a}\sum_{k=0}^{\infty}\sum_{l=0}^{k}\sum_{m=0}^{\infty} \delta_{abklm} \int_0^\infty y^m e^{-fly} \mathrm{d}y\right].$$

Letting $u = fly$, which implies $x = \frac{u}{fl}$ and $dy = \frac{du}{fl}$, we obtain

$$R_{ss} = 1 - \left[\sum_{a=0}^{\infty}\sum_{b=0}^{a}\sum_{k=0}^{\infty}\sum_{l=0}^{k}\sum_{m=0}^{\infty} \delta_{abklm} \left(\frac{1}{fl}\right)^{m+1} \int_0^\infty u^m e^{-u} \mathrm{d}u\right]. \tag{4.31}$$

But $\int_0^\infty u^m e^{-u} \mathrm{d}u = \Gamma(m+1)$.

We obtain the stress-strength reliability of the HMGOM distribution after correctly substituting into equation (4.31).

4.3.11 Order Statistics

Order statistics can help identify maximum and minimum values of a random variable.

Proposition 4.13. If $Y_1, Y_2, Y_3, ..., Y_n$ is a random variable from the HMGOM distribution for $\alpha > 1$ with order statistics $Y_{(1)}, Y_{(2)}, Y_{(3)}, ..., Y_{(n)}$, then the PDF of the p^{th}

order statistics Y_P is given as Equation (4.32).

$$f_{p:n}(y)=\frac{1}{\beta(p,n-p+1)}\left[\sum_{a=0}^{\infty}\sum_{b=0}^{a}\sum_{k=0}^{\infty}\sum_{l=0}^{n-p}\sum_{m=0}^{p+l-1}\sum_{q=0}^{k}\sum_{s=0}^{\infty}\gamma_{abklmqs}y^{s}e^{-fqy}\right], \tag{4.32}$$

where $\gamma_{abklmqs}=\left[g\alpha(1-\rho)\psi_{abklmqs}+g\rho\psi^{*}_{abklmqs}\right]$, $\psi_{abklmqs}=\frac{(-1)^{b+k+l+m+q}}{k!s!}\binom{n-p}{l}\binom{p+l-1}{m}\binom{m+a-1}{a}\binom{a}{b}\binom{q}{k}\rho^{a}\left(\frac{g}{f}(\alpha(m+b+1)-j\right)^{k}(f(k+1))^{s}$ and $\psi^{*}_{abklmqs}=\frac{(-1)^{b+k+l+m+q}}{k!s!}\binom{n-p}{l}\binom{p+l-1}{m}\binom{m+a-1}{a}\binom{a}{b}\binom{q}{k}\rho^{a}\left(\frac{\beta}{a}(\alpha(m+b+2)-(b+1)\right)^{k}(f(k+1))^{s}$.

Proof. By definition

$$f_{p:n}(y)=\frac{1}{\beta(p,n-p+1)}\left(F(y)\right)^{p-1}\left(1-F(y)\right)^{n-p}f(y). \tag{4.33}$$

Applying the Taylor series,

$$\left(1-F(y)\right)^{n-p}=\sum_{l=0}^{n-p}(-1)^{l}\binom{n-p}{l}\left(F(y)\right)^{l}.$$

We then obtain,

$$f_{p:n}(y)=\frac{1}{\beta(p,n-p+1)}\sum_{l=0}^{n-p}\sum_{m=0}^{p+l-1}(-1)^{l+m}\binom{n-p}{l}\binom{p+l-1}{m}\left(S(y)\right)^{m}f(y). \tag{4.34}$$

Raising equation (3.3) to the power m and subsequently multiplying it with equation (3.2), we obtain

$$\left(S(y)\right)^{m}f(y)=\frac{g\alpha(1-\rho)e^{fy}e^{-\frac{g\alpha(m+1)}{f}(e^{fy}-1)}+g\rho e^{fy}e^{-\frac{g(\alpha(m+2)-1)}{f}(e^{fy}-1)}}{\left[1-\rho\left(1-e^{-\frac{g(\alpha-1)}{f}(e^{fy}-1)}\right)\right]^{m+2}}$$

Applying the expansion series equations, we have

$$\left(S(y)\right)^{m}f(y)=\sum_{a=0}^{\infty}\sum_{b=0}^{a}\sum_{k=0}^{\infty}\sum_{q=0}^{k}\sum_{s=0}^{\infty}\tau_{abkqs}y^{s}e^{-fqy}+\sum_{a=0}^{\infty}\sum_{b=0}^{a}\sum_{k=0}^{\infty}\sum_{q=0}^{k}\sum_{s=0}^{\infty}\tau^{*}_{abkqs}y^{s}e^{-fqy}, \tag{4.35}$$

where $\tau_{abkqs} = \beta\alpha(1-\rho)\frac{(-1)^{b+k+q}}{k!s!}\binom{m+a-1}{a}\binom{a}{b}\binom{q}{k}\rho^{a}\left(\frac{g}{f}(\alpha(m+b+1)-b\right)^{k}(f(k+1))^{s}$

and

$\tau^{*}_{abkqs} = g\rho\frac{(-1)^{b+k+q}}{k!s!}\binom{m+a-1}{a}\binom{a}{b}\binom{q}{k}\rho^{a}\left(\frac{g}{f}(\alpha(m+b+2)-(b+1)\right)^{k}(f(k+1))^{s}$.

Substituting equation (4.35) into equation (4.34) completes the proof.

Proposition 4.14. The r^{th} moment of the p^{th} order statistics can be expressed as Equation (4.36).

$$\mu_{r}^{p:n} = \frac{1}{\beta(p,n-p+1)}\left[\sum_{a=0}^{\infty}\sum_{b=0}^{a}\sum_{k=0}^{\infty}\sum_{l=0}^{n-p}\sum_{m=0}^{p+l-1}\sum_{q=0}^{k}\sum_{s=0}^{\infty}\gamma_{abklmqs}\left(\frac{1}{fq}\right)^{r+s+1}\Gamma(r+s+1)\right]. \tag{4.36}$$

Proof. By definition

$$\mu_{r}^{p:n} = \int_{0}^{\infty} y^{r} f_{p:n}(y)\mathrm{d}y. \tag{4.37}$$

We substitute equation (4.32) into equation (4.37), obtaining

$$\mu_{r}^{p:n} = \frac{1}{\beta(p,n-p+1)}\left[\sum_{a=0}^{\infty}\sum_{b=0}^{a}\sum_{k=0}^{\infty}\sum_{l=0}^{n-p}\sum_{m=0}^{p+l-1}\sum_{q=0}^{k}\sum_{s=0}^{\infty}\gamma_{abklmqs}\int_{0}^{\infty} y^{r+s}e^{-fqy}\mathrm{d}y\right].$$

$\int_{0}^{\infty} y^{r+s}e^{-fqy}\mathrm{d}y$ is derived from the method used to derive the non-central moment. We then obtain the desired equation after substituting correctly and that completes the proof.

4.3.12 Identifiability

To ensure that accurate inferences are made, the HMGOM distribution's identifiability property is presented.

Proposition 4.15. If Y_1 and Y_2 are random variables from the HMGOM distribution with CDF $F_Y(y;\alpha_1,\rho_1,f_1,g_1)$ and $F_Y(y;\alpha_2,\rho_2,f_2,g_2)$ respectively, then the HMGOM distribution is identifiable if and only if $\alpha_1=\alpha_2$, $\rho_1=\rho_2$, $f_1=f_2$ and $g_1=g_2$.

Proof. For HMGOM distribution to be idenfiable, $F_Y(y;\alpha_1,\rho_1,f_1,g_1) = F_Y(y;\alpha_2,\rho_2,f_2,g_2)$. Then

$$1 - \frac{e^{-\frac{g_1\alpha_1}{f_1}(e^{f_1 y}-1)}}{\left[1-\rho_1\left(1-e^{-\frac{g_1(\alpha_1-1)}{f_1}(e^{f_1 y}-1)}\right)\right]} = 1 - \frac{e^{-\frac{g_2\alpha_2}{f_2}(e^{f_2 y}-1)}}{\left[1-\rho_2\left(1-e^{-\frac{g_2(\alpha_2-1)}{f_2}(e^{f_2 y}-1)}\right)\right]}.$$

If $\alpha_1 = \alpha_2$, $\rho_1 = \rho_2$, $f_1 = f_2$ and $g_1 = g_2$, then

$$\frac{e^{-\frac{g_1\alpha_1}{f_1}(e^{f_1 y}-1)}}{\left[1-\rho_1\left(1-e^{-\frac{g_1(\alpha_1-1)}{f_1}(e^{f_1 y}-1)}\right)\right]} - \frac{e^{-\frac{g_2\alpha_2}{f_2}(e^{f_2 y}-1)}}{\left[1-\rho_2\left(1-e^{-\frac{g_2(\alpha_2-1)}{f_2}(e^{f_2 y}-1)}\right)\right]} = 0.$$

The identifiability requirement has been met.

4.4 Estimation of Parameters of the HMGOM Distribution

This section focuses on obtaining estimates of the parameters for the HMGOM distribution. By applying these estimation techniques, we aim to determine the most suitable parameter values that best fit the HMGOM distribution to the given data. Each method offers a different approach to parameter estimation, allowing for a comprehensive analysis of the distribution and the selection of the most appropriate estimation method based on the specific characteristics of the data.

4.4.1 Maximum Likelihood Estimation

By applying the MLE to the HMGOM distribution, researchers can obtain parameter estimates that are optimal in terms of maximising the likelihood of the observed data and capturing the underlying characteristics of the distribution. For the HMGOM distribution, the likelihood function can be expressed as Equation (4.38).

$$L\left(y,\alpha,\rho,f,g\right) = \prod_{a=1}^{n} f(y_a,\alpha,\rho,f,g). \tag{4.38}$$

We substitute equation (4.1) into (4.38) and thereafter obtain the log-likelihood function given as Equation (4.39).

$$l(y,\alpha,\rho,f,g) = n\ln g + f\sum_{a=1}^{n} y_a - \frac{g}{f}\alpha\sum_{a=1}^{n}\left(e^{fy_a}-1\right) + \sum_{a=1}^{n}\ln\left[\alpha(1-\rho)+\rho e^{-\frac{g(\alpha-1)}{f}(e^{fy_a}-1)}\right]$$
$$-2\sum_{a=1}^{n}\ln\left[1-\rho\left(1-e^{-\frac{g(\alpha-1)}{f}(e^{fy_a}-1)}\right)\right]. \tag{4.39}$$

To estimate the parameters using the MLE approach, we utilise the method of differentiation. By differentiating equation (4.39) with respect to the parameters (α,ρ,f,g) and setting the equations obtained to zero, we can derive a system of equations. These equations when solved using numerical methods gives the parameter estimates. The derivatives obtained are as follows

$$\frac{\partial l}{\partial\alpha} = -\frac{g}{f}\sum_{a=1}^{n}\left(e^{fy_a}-1\right) + \sum_{a=1}^{n}\frac{(1-\rho)-\frac{g\rho}{f}\left(e^{fy_a}-1\right)e^{-\frac{g(\alpha-1)}{f}(e^{fy_a}-1)}}{\alpha(1-\rho)+\rho e^{-\frac{g(\alpha-1)}{f}(e^{fy_a}-1)}}$$
$$-\sum_{a=1}^{n}\frac{g\rho\left(e^{fy_a}-1\right)e^{-\frac{g(\alpha-1)}{f}(e^{fy_a}-1)}}{f\left[1-\rho+\rho e^{-\frac{g(\alpha-1)}{f}(e^{fy_a}-1)}\right]},$$

$$\frac{\partial l}{\partial\rho} = \sum_{a=1}^{n}\frac{e^{-\frac{g(\alpha-1)}{f}(e^{fy_a}-1)}-1}{1-\rho+\rho e^{-\frac{g(\alpha-1)}{f}(e^{fy_a}-1)}} + \sum_{a=1}^{n}\frac{e^{-\frac{g(\alpha-1)}{f}(e^{fy_a}-1)}-\alpha}{\alpha(1-\rho)+\rho e^{-\frac{g(\alpha-1)}{f}(e^{fy_a}-1)}},$$

$$\frac{\partial l}{\partial f} = \sum_{a=1}^{n} y_a - \sum_{a=1}^{n}\frac{\alpha g(e^{fy_a}-1)}{f^2} - \sum_{a=1}^{n}\frac{g\rho(\alpha-1)\left(1+e^{fy_a}(fy_a-1)\right)e^{-\frac{g(\alpha-1)}{f}(e^{fy_a}-1)}}{f^2\left[\alpha(1-\rho)+\rho e^{-\frac{g(\alpha-1)}{f}(e^{fy_a}-1)}\right]}$$
$$-\sum_{a=1}^{n}\frac{\alpha g y_a e^{fy_a}}{f} - \sum_{a=1}^{n}\frac{g\rho(\alpha-1)\left(1+e^{fy_a}(fy_a-1)\right)e^{-\frac{g(\alpha-1)}{f}(e^{fy_a}-1)}}{f^2\left[1-\rho+\rho e^{-\frac{g(\alpha-1)}{f}(e^{fy_a}-1)}\right]},$$

$$\frac{\partial l}{\partial g} = \frac{n}{g} - \sum_{a=1}^{n}\frac{\rho(\alpha-1)(e^{fy_a}-1)e^{-\frac{g(\alpha-1)}{f}(e^{fy_a}-1)}}{f\left[\alpha(1-\rho)+\rho e^{-\frac{g(\alpha-1)}{a}(e^{fy_a}-1)}\right]} - \sum_{a=1}^{n}\frac{\rho(\alpha-1)(e^{fy_a}-1)e^{-\frac{g(\alpha-1)}{f}(e^{fy_a}-1)}}{f\left[1-\rho+\rho e^{-\frac{g(\alpha-1)}{f}(e^{fy_a}-1)}\right]}$$
$$-\sum_{a=1}^{n}\frac{\alpha(e^{fy_a}-1)}{f}.$$

4.4.2 Ordinary Least Squares

To perform the OLSS estimation, a specific objective function is defined, which represents the discrepancy between the observed data and the model predictions. The goal is to minimise Equation (4.40).

$$LS(\alpha, \rho, f, g) = \sum_{a=1}^{n} \left\{ \left(F(y_{(a)})\right) - \frac{a}{n+1} \right\}^2. \tag{4.40}$$

The method of differentiation is employed to minimise equation (4.40). We differentiate with respect to each parameter and equate the resulting equations to zero, obtaining

$$\frac{\partial LS}{\partial \alpha} = \sum_{a=1}^{n} \left\{ \left(F(y_{(a)})\right) - \frac{a}{n+1} \right\} \cdot \Lambda_1(y_{(a)}; \alpha, \rho, f, g) = 0, \tag{4.41}$$

$$\frac{\partial LS}{\partial \rho} = \sum_{a=1}^{n} \left\{ \left(F(y_{(a)})\right) - \frac{a}{n+1} \right\} \cdot \Lambda_2(y_{(a)}; \alpha, \rho, f, g) = 0, \tag{4.42}$$

$$\frac{\partial LS}{\partial f} = \sum_{a=1}^{n} \left\{ \left(F(y_{(a)})\right) - \frac{a}{n+1} \right\} \cdot \Lambda_3(y_{(a)}; \alpha, \rho, f, g) = 0, \tag{4.43}$$

$$\frac{\partial LS}{\partial g} = \sum_{a=1}^{n} \left\{ \left(F(y_{(a)})\right) - \frac{a}{n+1} \right\} \cdot \Lambda_4(y_{(a)}; \alpha, \rho, f, g) = 0, \tag{4.44}$$

where

$$\Lambda_1(y_{(a)}) = \frac{g(e^{fy_{(a)}} - 1) \left\{ \rho e^{-\frac{g(2\alpha-1)}{f}(e^{fy_{(a)}}-1)} + e^{-\frac{g\alpha}{f}(e^{fy_{(a)}}-1)} \left[1 - \rho(1 - e^{-\frac{g(\alpha-1)}{f}(e^{fy_{(a)}}-1)})\right] \right\}}{f\left[1 - \rho\left(1 - e^{-\frac{g(\alpha-1)}{f}(e^{fy_{(a)}}-1)}\right)\right]^2}, \tag{4.45}$$

$$\Lambda_2(y_{(a)}) = \frac{e^{-\frac{g\alpha}{f}(e^{fy_{(a)}}-1)} \left(e^{-\frac{g(\alpha-1)}{f}(e^{fy_{(a)}}-1)} - 1\right)}{\left[1 - \rho\left(1 - e^{-\frac{g(\alpha-1)}{f}(e^{fy_{(a)}}-1)}\right)\right]^2}, \tag{4.46}$$

$$\Lambda_3(y_{(a)}) = \frac{g\rho(\alpha-1)(1+e^{fy_{(a)}}(fy_{(a)}-1))e^{-\frac{g(2\alpha-1)}{f}(e^{fy_{(a)}}-1)}}{f^2\left[1-\rho\left(1-e^{-\frac{g(\alpha-1)}{f}(e^{fy_{(a)}}-1)}\right)\right]^2} + \frac{\alpha g(1+e^{fy_{(a)}}(fy_{(a)}-1))e^{-\frac{g\alpha}{f}(e^{fy_{(a)}}-1)}\left[1-\rho(1-e^{-\frac{g(\alpha-1)}{f}(e^{fy_{(a)}}-1)})\right]}{f^2\left[1-\rho\left(1-e^{-\frac{g(\alpha-1)}{f}(e^{fy_{(a)}}-1)}\right)\right]^2}, \tag{4.47}$$

$$\Lambda_4(y_{(a)}) = \frac{\rho(\alpha-1)(e^{fy_{(a)}}-1)e^{-\frac{g(2\alpha-1)}{f}(e^{fy_{(a)}}-1)}}{f\left[1-\rho\left(1-e^{-\frac{g(\alpha-1)}{f}(e^{fy_{(a)}}-1)}\right)\right]^2} + \frac{\alpha(e^{fy_{(a)}}-1)e^{-\frac{g\alpha}{f}(e^{fy_{(a)}}-1)}\left[1-\rho(1-e^{-\frac{g(\alpha-1)}{f}(e^{fy_{(a)}}-1)})\right]}{f\left[1-\rho\left(1-e^{-\frac{g(\alpha-1)}{f}(e^{fy_{(a)}}-1)}\right)\right]^2}. \tag{4.48}$$

These equations obtained are solved simultaneously using numerical methods to obtain the parameter estimates.

4.4.3 Weighted Least Squares

The WLSS estimates are obtained by solving the minimisation problem, which involves finding the parameter values that minimise the weighted discrepancy between the observed data and the predictions of the HMGOM distribution.The minimisation function is given as Equation (4.49).

$$WLS(\alpha,\rho,f,g) = \sum_{a=1}^{n}\frac{(n+1)^2(n+2)}{a(n-a+1)}\left\{(F(y_{(a)})) - \frac{a}{n+1}\right\}^2. \tag{4.49}$$

The method of differentiation is employed to minimise equation (4.49). We differentiate with respect to each parameter and equate the resulting equations to zero, obtaining

$$\frac{\partial WLS}{\partial\alpha} = \sum_{a=1}^{n}\frac{(n+1)^2(n+2)}{a(n-a+1)}\left\{(F(y_{(a)})) - \frac{a}{n+1}\right\}\cdot\Lambda_1(y_{(a)};\alpha,\rho,f,g) = 0, \tag{4.50}$$

$$\frac{\partial WLS}{\partial \rho} = \sum_{a=1}^{n} \frac{(n+1)^2(n+2)}{a(n-a+1)} \left\{ (F(y_{(a)})) - \frac{a}{n+1} \right\} \cdot \Lambda_2(y_{(a)}; \alpha, \rho, f, g) = 0, \quad (4.51)$$

$$\frac{\partial WLS}{\partial f} = \sum_{a=1}^{n} \frac{(n+1)^2(n+2)}{a(n-a+1)} \left\{ (F(y_{(a)})) - \frac{a}{n+1} \right\} \cdot \Lambda_3(y_{(a)}; \alpha, \rho, f, g) = 0, \quad (4.52)$$

$$\frac{\partial WLS}{\partial g} = \sum_{a=1}^{n} \frac{(n+1)^2(n+2)}{a(n-a+1)} \left\{ (F(y_{(a)})) - \frac{a}{n+1} \right\} \cdot \Lambda_4(y_{(a)}; \alpha, \rho, f, g) = 0. \quad (4.53)$$

$\Lambda_m(y_{(a)}; \alpha, \rho, f, g)$, $(m = 1, 2, 3, 4)$, can be obtained through equations (4.45), (4.46), (4.47) and (4.48).

These equations obtained are solved simultaneously using numerical methods to obtain the parameter estimates.

4.4.4 Cramér-von Mises Estimation

The CVM estimates are obtained by solving the minimisation problem, which involves finding the parameter values that minimise the discrepancy between the observed data and the HMGOM distribution as measured by the Cramér-von Mises statistic. The minimisation function is given as Equation (4.54).

$$CVM(\alpha, \rho, f, g) = \frac{1}{12n} + \sum_{a=1}^{n} \left\{ (F(y_{(a)})) - \frac{2a-1}{2n} \right\}^2. \quad (4.54)$$

The method of differentiation is employed to minimise equation (4.54). We differentiate with respect to each parameter and equate the resulting equations to zero, obtaining

$$\frac{\partial CVM}{\partial \alpha} = \sum_{a=1}^{n} \left\{ (F(y_{(a)})) - \frac{2a-1}{2n} \right\} \cdot \Lambda_1(y_{(a)}; \alpha, \rho, f, g) = 0, \quad (4.55)$$

$$\frac{\partial CVM}{\partial \rho} = \sum_{a=1}^{n} \left\{ (F(y_{(a)})) - \frac{2a-1}{2n} \right\} \cdot \Lambda_2(y_{(a)}; \alpha, \rho, f, g) = 0, \quad (4.56)$$

$$\frac{\partial CVM}{\partial f} = \sum_{a=1}^{n} \left\{ \left(F(y_{(a)})\right) - \frac{2a-1}{2n} \right\} \cdot \Lambda_3(y_{(a)}; \alpha, \rho, f, g) = 0, \tag{4.57}$$

$$\frac{\partial CVM}{\partial g} = \sum_{a=1}^{n} \left\{ \left(F(y_{(a)})\right) - \frac{2a-1}{2n} \right\} \cdot \Lambda_4(y_{(a)}; \alpha, \rho, f, g) = 0, \tag{4.58}$$

$\Lambda_m(y_{(a)}; \alpha, \rho, f, g)$, $(m = 1, 2, 3, 4)$, can be obtained through equations (4.45), (4.46), (4.47) and (4.48).

These equations obtained are solved simultaneously using numerical methods to obtain the parameter estimates.

4.4.5 Anderson-Darling Estimation

The AD estimates are obtained by solving the minimisation problem, which involves finding the parameter values that minimise the discrepancy between the observed data and the HMGOM distribution as measured by the Anderson-Darling statistic. The minimisation function is given as Equation (4.59).

$$AD(\alpha, \rho, f, g) = -n - \frac{1}{n} \sum_{a=1}^{n} (2a-1) \left\{ \left(\log F(y_{(a)})\right) + \log\left(1 - F(y_{(n+1-a)})\right) \right\}. \tag{4.59}$$

The method of differentiation is employed to minimise equation (4.59). We differentiate with respect to each parameter and equate the resulting equations to zero, obtaining

$$\frac{\partial AD}{\partial \alpha} = \sum_{a=1}^{n} (2a-1) \left\{ \frac{\Lambda_1(y_{(a)}; \alpha, \rho, f, g)}{\left(F(y_{(a)})\right)} - \frac{\Lambda_1(y_{(n+1-a)}; \alpha, \rho, f, g)}{1 - \left(F(y_{(n+1-a)})\right)} \right\} = 0, \tag{4.60}$$

$$\frac{\partial AD}{\partial \rho} = \sum_{a=1}^{n} (2a-1) \left\{ \frac{\Lambda_2(y_{(a)}; \alpha, \rho, f, g)}{\left(F(y_{(a)})\right)} - \frac{\Lambda_2(y_{(n+1-a)}; \alpha, \rho, f, g)}{1 - \left(F(y_{(n+1-a)})\right)} \right\} = 0, \tag{4.61}$$

$$\frac{\partial AD}{\partial f} = \sum_{a=1}^{n} (2a-1) \left\{ \frac{\Lambda_3(y_{(a)}; \alpha, \rho, f, g)}{\left(F(y_{(a)})\right)} - \frac{\Lambda_3(y_{(n+1-a)}; \alpha, \rho, f, g)}{1 - \left(F(y_{(n+1-a)})\right)} \right\} = 0, \tag{4.62}$$

$$\frac{\partial AD}{\partial g} = \sum_{a=1}^{n} (2a-1) \left\{ \frac{\Lambda_4(y_{(a)}; \alpha, \rho, f, g)}{\left(F(y_{(a)})\right)} - \frac{\Lambda_4(y_{(n+1-a)}; \alpha, \rho, f, g)}{1 - \left(F(y_{(n+1-a)})\right)} \right\} = 0, \tag{4.63}$$

where $\Lambda_m(y_{(\cdot)}; \alpha, \rho, f, g)$, $(m = 1, 2, 3, 4)$, can be derived from the equations (4.45), (4.46), (4.47) and (4.48).

These equations obtained are solved simultaneously using numerical methods to obtain the parameter estimates.

4.5 HMGOM Regression Model

The HMGOM distribution is used to study the impact some explanatory variables have on the response variable. To achieve this, we introduce the HMGOM regression model considering the parameters f, g and α are varying across observations using the logarithmic link functions $\log(f_a) = x_a^T f_a$, $\log(g_a) = x_a^T g_a$ and $\log(\alpha_a) = x_a^T \alpha_a$, $a = 1, 2, 3..., n$.

The survival function of the HMGOM regression model is obtained through a substitution of the logarithmic link functions into the survival function of the HMGOM distribution and given as Equation (4.64).

$$S(y|x) = \frac{e^{-\frac{\exp(x_a^T g_a)\exp(x_a^T \alpha_a)}{\exp(x_a^T f_a)}\left(e^{\exp(x_a^T f_a) y} - 1\right)}}{\left[1 - \rho\left(1 - e^{-\frac{\exp(x_a^T g_a)(\exp(x_a^T \alpha_a) - 1)}{\exp(x_a^T f_a)}\left(e^{\exp(x_a^T f_a) y} - 1\right)}\right)\right]}. \tag{4.64}$$

By maximising log-likelihood function, the MLE provides estimates for the parameters that best align with the observed data and the assumed HMGOM regression model. The log-likelihood function is given by Equation (4.65).

$$\ell = n\sum_{a=1}^{n} \ln g_a + \sum_{a=1}^{n} f_a x_a - \sum_{a=1}^{n} \frac{g_a}{f_a}\alpha_a\left(e^{f x_a} - 1\right) + \sum_{a=1}^{n} \ln\left[\alpha_a(1-\rho) + \rho e^{-\frac{g_a(\alpha_a - 1)}{f_a}(e^{f_a x_a} - 1)}\right]$$
$$- 2\sum_{a=1}^{n} \ln\left[1 - \rho\left(1 - e^{-\frac{g_a(\alpha_a - 1)}{f_a}(e^{f_a x_a} - 1)}\right)\right]. \tag{4.65}$$

4.6 Development of the Harmonic Mixture Fréchet Distribution

In this section, we explore the the PDF, CDF, FRF and SF of the HMFR distribution. To obtain the PDF of the HMFR distribution, we substitute equations (3.7) and (3.9) into equation (3.21). This substitution allows us to express the PDF in terms of the parameters and the corresponding equations that define the HMFR distribution. The PDF of the HMFR distribution is expressed as Equation (4.66).

$$f_{HMFR}(x) = \frac{\alpha\,(1-\rho)\,dg^{d}x^{-d-1}e^{-\alpha(\frac{g}{x})^{d}}\left(1-e^{-(\frac{g}{x})^{d}}\right)^{\alpha-1} + \rho dg^{d}x^{-d-1}e^{-(\frac{g}{x})^{d}}\left(1-e^{-(\frac{g}{x})^{d}}\right)^{2\alpha-2}}{\left[1-\rho\left(1-\left(1-e^{-(\frac{g}{x})^{d}}\right)^{\alpha-1}\right)\right]^{2}}, \tag{4.66}$$

where $d > 0$, $\alpha > 0$, $g > 0$, $x > 0$, $0 < \rho < 1$.

The density plot visually represents how the distribution's shape can be influenced by adjusting the parameters. Different combinations of parameter values result in distinct shapes of the probability density function as shown in 4.5. This variability in shape highlights the flexibility and versatility of the HMFR distribution in modelling a wide range of data patterns.

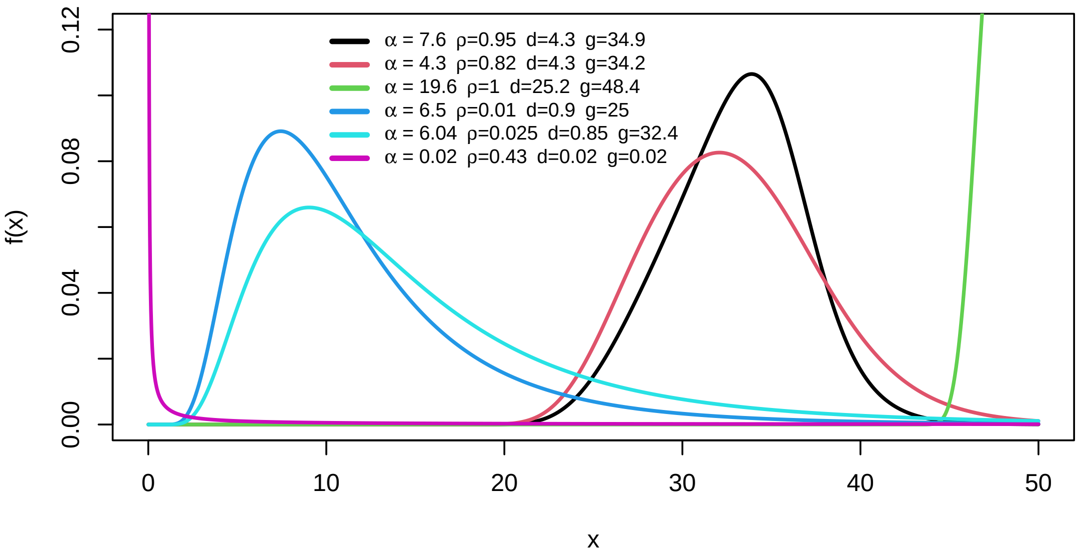

Figure 4.5: The density plot of the HMFR

The CDF of the HMFR distribution is derived by the substitution of equation (3.9) into equation (3.20). The CDF of the HMFR distribution can therefore be expressed as Equation (4.67).

$$F_{HMFR}(x) = 1 - \frac{\left(1 - e^{-\left(\frac{g}{x}\right)^d}\right)^{\alpha}}{\left[1 - \rho\left(1 - \left(1 - e^{-\left(\frac{g}{x}\right)^d}\right)^{\alpha-1}\right)\right]}, x > 0. \qquad (4.67)$$

The Figure 4.6 offers a visual representation of the CDF of the HMFR distribution for a range of parameter values. The CDF approaches 0 as x approaches 0 and approaches 1 as x approaches infinity.

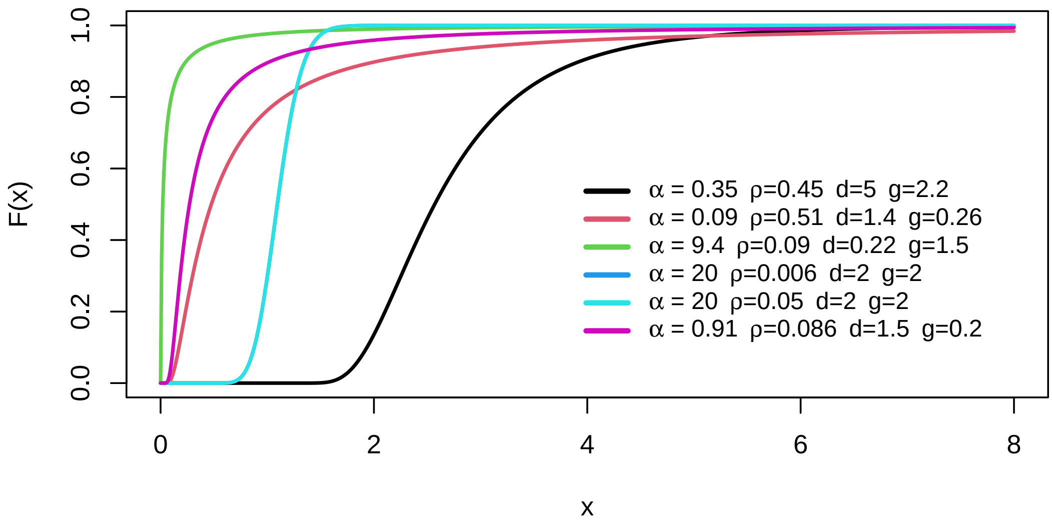

Figure 4.6: The CDF plot of the HMFR

The SF of the HMFR distribution can be derived from the CDF of the HMFR distribution. The survival function is given by Equation (4.68).

$$S_{HMFR}(x) = \frac{\left(1 - e^{-\left(\frac{g}{x}\right)^d}\right)^{\alpha}}{\left[1 - \rho\left(1 - \left(1 - e^{-\left(\frac{g}{x}\right)^d}\right)^{\alpha-1}\right)\right]}, x > 0. \tag{4.68}$$

The substitutions of equations (3.7) and (3.9) into equation (3.22) gives the FRF of the HMFR distribution.The FRF of the HMFR distribution can then be expressed as Equation (4.69).

$$h_{HMFR}(x) = \frac{dg^d x^{-d-1} e^{-\left(\frac{g}{x}\right)^d}\left(1 - e^{-\left(\frac{g}{x}\right)^d}\right)^{\alpha-1}}{\left(1 - e^{-\left(\frac{g}{x}\right)^d}\right)^{\alpha}} \frac{\alpha\left(1-\rho\right) + \rho\left(1 - e^{-\left(\frac{g}{x}\right)^d}\right)^{\alpha-1}}{\left[1 - \rho\left(1 - \left(1 - e^{-\left(\frac{g}{x}\right)^d}\right)^{\alpha-1}\right)\right]}, x > 0. \tag{4.69}$$

Figure 4.7 gives the visual representation of the FRF for the HMFR distribution. By exploring different parameter values, the plots exhibit a range of desirable shapes, including decreasing, increasing, and unimodal patterns. The FRF of the HMFR distribution can take on various forms, such as being monotonically increasing, monotonically decreasing, or resembling an upside-down bathtub shape. The flexibility of the

HMFR distribution allows it to accurately model both monotonic and non-monotonic failure rates. Depending on the specific parameter values chosen, the HMFR distribution can effectively capture different types of failure rate behaviours observed in real-world scenarios.

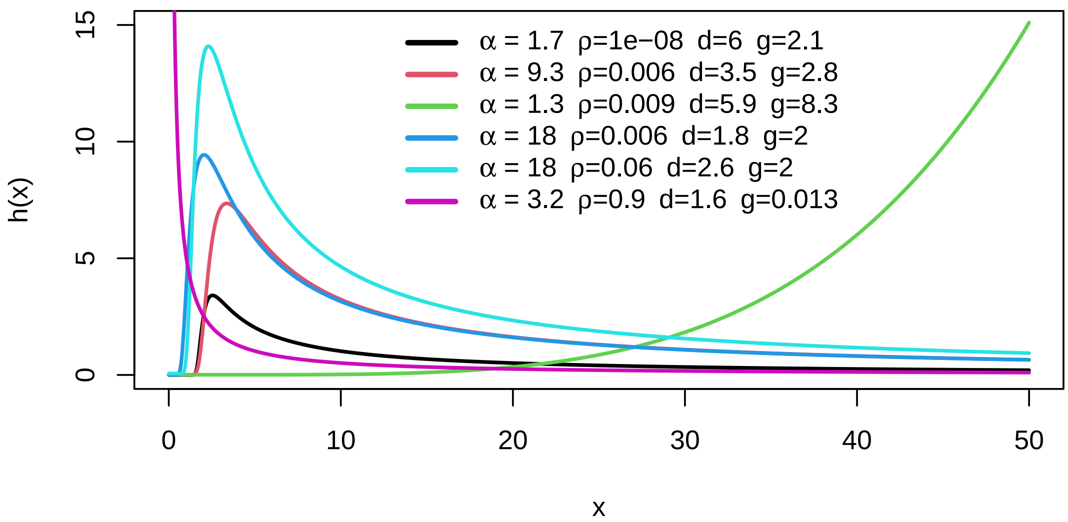

Figure 4.7: The FRF plot of the HMFR

We examined the impact of incorporating additional parameters from the HMG family on the Fréchet distribution (black curve) in Figure 4.8. By varying the values of the parameters ρ and α while keeping the Fréchet distribution parameters constant, we observed notable improvements in terms of kurtosis (peakness) and skewness. These enhancements indicate that the introduction of the extra parameters from the HMG family contributes to a more refined and flexible modelling of the distribution.

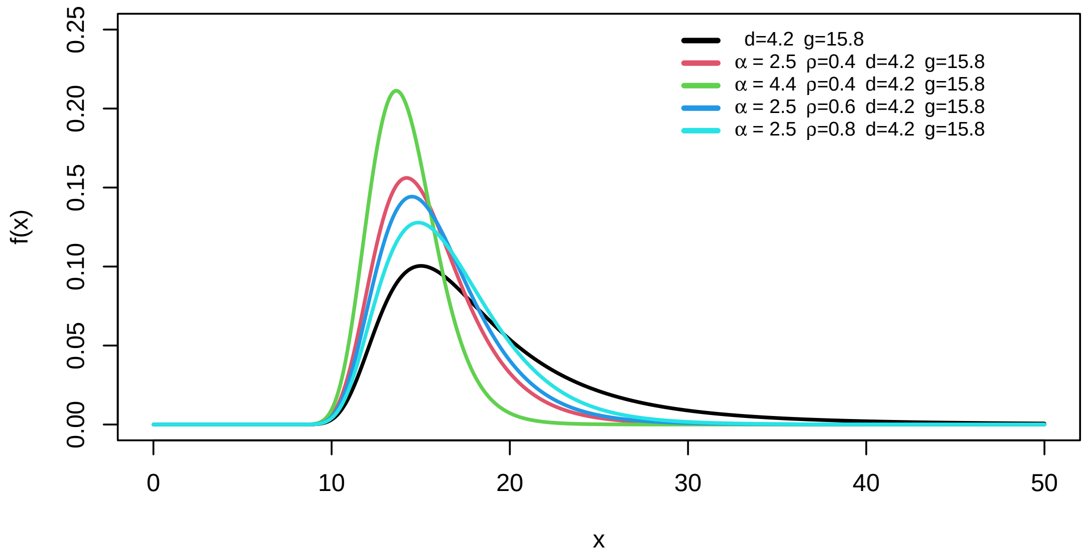

Figure 4.8: Assessing the densities of the HMFR Distribution and the Fréchet Distribution

Lemma 4.3. The linear representation of the PDF for the HMFR distribution is given by Equation (4.70).

$$f_{HMFR}(x) = \sum_{a=0}^{\infty}\sum_{b=0}^{a}\sum_{k=0}^{\infty}\Omega_{abk} d g^{d} x^{-g-1} e^{-\left(\frac{g}{x}\right)^{d}(k+1)}, \tag{4.70}$$

where $\Omega_{abk} = [\alpha(1-\rho)\tau_{abk} + \rho\tau^{*}_{abk}]$, $\tau_{abk} = (-1)^{b+k}(a+1)\binom{a}{b}\binom{(\alpha-1)(b+1)}{k}\rho^{a}$, $\tau^{*}_{abk} = (-1)^{b+k}(a+1)\binom{a}{b}\binom{(\alpha-1)(b+2)}{k}\rho^{a}$, $x > 0, d > 0, g > 0, \alpha > 0$ and $0 < \rho < 1$.

Proof. For $\eta > 0$, the Taylor series for $(1-z)^{-\eta}$, for $|z| < 1$ is

$$(1-z)^{-\eta} = \sum_{a=0}^{\infty}(-1)^{a}\binom{-\eta}{a}(z)^{a}. \tag{4.71}$$

For $0 < \left(1 - e^{-\left(\frac{g}{x}\right)^{d}}\right) < 1$, the Taylor series can be employed to obtain

$$\left[1 - \rho\left(1 - \left(1 - e^{-\left(\frac{g}{x}\right)^{d}}\right)^{\alpha-1}\right)\right]^{-2} = \sum_{a=0}^{\infty}\sum_{b=0}^{a}(-1)^{b}(a+1)\binom{a}{b}\rho^{a}\left(1 - e^{-\left(\frac{g}{x}\right)^{d}}\right)^{b(\alpha-1)}. \tag{4.72}$$

Substituting equation (4.72) into equation (4.66) yields

$$f_{HMFR}(x) = \alpha\,(1-\rho)\,dg^d x^{-d-1} e^{-\left(\frac{g}{x}\right)^d} \sum_{a=0}^{\infty}\sum_{b=0}^{a} (-1)^b (a+1) \binom{a}{b} \rho^a \left(1 - e^{-\left(\frac{g}{x}\right)^d}\right)^{(b+1)(\alpha-1)}$$
$$+ \rho dg^d x^{-d-1} e^{-\left(\frac{g}{x}\right)^d} \sum_{a=0}^{\infty}\sum_{b=0}^{a} (-1)^b (a+1) \binom{a}{b} \rho^a \left(1 - e^{-\left(\frac{g}{x}\right)^d}\right)^{(b+2)(\alpha-1)}. \tag{4.73}$$

Applying equation (4.71) again,

$$\left(1 - e^{-\left(\frac{g}{x}\right)^d}\right)^{(\alpha-1)(b+1)} = \sum_{k=0}^{\infty} (-1)^k \binom{(\alpha-1)(b+1)}{k} e^{-k\left(\frac{g}{x}\right)^d} \tag{4.74}$$

and

$$\left(1 - e^{-\left(\frac{g}{x}\right)^d}\right)^{(\alpha-1)(b+2)} = \sum_{k=0}^{\infty} (-1)^k \binom{(\alpha-1)(b+2)}{k} e^{-k\left(\frac{g}{x}\right)^d}. \tag{4.75}$$

The substitution of equation (4.74) and equation (4.75) into equation (4.73) gives

$$f_{HMFR}(x) = \alpha\,(1-\rho)\,dg^d x^{-d-1} \sum_{a=0}^{\infty}\sum_{b=0}^{a}\sum_{k=0}^{\infty} (-1)^{b+k} (a+1) \binom{a}{b} \binom{(\alpha-1)(b+1)}{k} \rho^a e^{-\left(\frac{g}{x}\right)^d (k+1)}$$
$$+ \rho dg^d x^{-d-1} \sum_{a=0}^{\infty}\sum_{b=0}^{a}\sum_{k=0}^{\infty} (-1)^{b+k} (a+1) \binom{a}{b} \binom{(\alpha-1)(b+2)}{k} \rho^a e^{-\left(\frac{g}{x}\right)^d (k+1)}.$$

Hence,

$$f_{HMFR}(x) = \alpha\,(1-\rho)\,dg^d x^{-d-1} \sum_{a=0}^{\infty}\sum_{b=0}^{a}\sum_{k=0}^{\infty} \tau_{abk} e^{-\left(\frac{g}{x}\right)^d (k+1)}$$
$$+ \rho dg^d x^{-d-1} \sum_{a=0}^{\infty}\sum_{b=0}^{a}\sum_{k=0}^{\infty} \tau^*_{abk} e^{-\left(\frac{g}{x}\right)^d (k+1)}.$$

4.7 Statistical Properties of HMFR Distribution

This section is dedicated to deriving the statistical properties of the HMFR distribution.These properties include the quantile function, non-central moments, incomplete moments, inequality measures, mean and median deviations, moment generating functions, characteristic function, entropy, stress-strength reliability, order statistics, and identifiability. Through our analysis, we explore and derive these properties, which provide valuable insights into the distribution's behaviour and characteristics.

4.7.1 Quantile Function

A distribution's quantile function is its CDF's inverse. It provides another means of explaining the some features and shapes of the HMFR distribution.

Lemma 4.4. The expression for the quantile function of the HMFR distribution can be expressed as Equation (4.76).

$$(1-p)\left\{1-\rho+\rho\left[1-e^{-x_p^{-d}g^d}\right]^{\alpha-1}\right\}-\left[1-e^{-x_p^{-d}g^d}\right]^{\alpha}=0, \tag{4.76}$$

where $p \in (0,1)$ and $p_{HMFR}(p) = x_p$ is the quantile function.

Proof. Mathematically,

$$Q_{HMFR}(p) = \mathbf{p}(X \leq x_p) = p.$$

The quantile function of the HMFR distribution can be obtained through the substitution of equation (3.8) into equation (3.24) and letting $Q_{HMFR}(p) = x_p$.
It is apparent that the quantile function of the HMFR distribution cannot be expressed in a closed form. Numerical techniques involving iterative algorithms that aim to find the value of the quantile corresponding to a given probability level are used to estimate the quantiles.

4.7.2 Moments

Moments play a crucial role in statistical analysis as they are instrumental in deriving some essential measures of the HMFR distribution.

Proposition 4.16. The r^{th} non-central moment of the HMFR distribution is given as Equation (4.77).

$$\mu_r^{'} = g^r \sum_{a=0}^{\infty}\sum_{b=0}^{a}\sum_{k=0}^{\infty} \Omega_{abk}(k+1)^{\frac{r}{d}}\Gamma(1-r/d), r < d. \tag{4.77}$$

Proof. Mathematically,

$$\mu_r^{'} = E(X^r) = \int_0^{\infty} x^r f_{HMFR}(x)\mathrm{d}x. \tag{4.78}$$

After substituting equation (4.70) into equation (4.78) gives

$$\begin{aligned} E(X^r) &= \int_0^{\infty} x^r \sum_{a=0}^{\infty}\sum_{b=0}^{a}\sum_{k=0}^{\infty} \Omega_{abk} d g^d x^{-d-1} e^{-(\frac{g}{x})^d (k+1)}\mathrm{d}x, \\ &= d g^d \sum_{a=0}^{\infty}\sum_{b=0}^{a}\sum_{k=0}^{\infty} \Omega_{abk} \int_0^{\infty} x^{r-d-1} e^{-(\frac{g}{x})^d (k+1)}\mathrm{d}x. \end{aligned}$$

Letting $v = (\frac{g}{x})^d (k+1)$, which implies $x = (\frac{v}{b^d (k+1)})^{-\frac{1}{d}}$ and $dx = \frac{-dv}{dg^d (k+1) x^{-d-1}}$. $x \to 0, v \to \infty$ while $x \to \infty, v \to 0$. Which gives

$$\mu_r^{'} = g^r \sum_{a=0}^{\infty}\sum_{b=0}^{a}\sum_{k=0}^{\infty} \Omega_{abk}(k+1)^{\frac{r}{d}} \int_0^{\infty} u^{-\frac{r}{d}} e^{-u}\mathrm{d}u.$$

Using the identity

$$\Gamma(S) = \int_0^{\infty} x^{S-1} e^{-x}\mathrm{d}x,$$

we obtain

$$\mu_r^{'} = g^r \sum_{a=0}^{\infty}\sum_{b=0}^{a}\sum_{k=0}^{\infty} \Omega_{abk}(k+1)^{\frac{r}{d}}\Gamma(1-r/d).$$

The σ^2, CV, CS and CK for the HMFR distribution are displayed in the Table 4.2. The HMFR distribution can exhibit significant skewness, indicated by a coefficient of skewness (CS) lower than -1 or higher than $+1$. In some cases, the distribution shows moderate skewness, with CS values ranging between -1 and -0.5, or between 0.5 and 1. For certain parameter values, the HMFR distribution appears approximately symmetric, with CS values between -0.5 and $+0.5$. Furthermore, depending on the parameter values, the HMFR distribution can demonstrate positive skewness or negative skewness. This indicates that the distribution's tail may be elongated towards the right or the left, respectively. Regarding kurtosis, the HMFR distribution can exhibit platykurtic behaviour, characterised by a kurtosis coefficient (CK) less than 3, for specific parameter values. Alternatively, the distribution can display leptokurtic behaviour, with CK values greater than 3, for other parameter values. Platykurtic distributions have lighter tails and a flatter peak, while leptokurtic distributions have heavier tails and a sharper peak.

Table 4.2: First Five Moments of the HMFR

r	α=9, ρ=0.45, d=6, g=1.5	α=3.5,ρ=0.4, d=10,g=2.0	α=6.5, ρ=0.03, d=10.0,g=2.5	α=10.0, ρ=0.04, d=11.0, g=0.5	α=5.4, ρ=0.004, d=8.00, g=0.05
μ_1'	1.3124	1.9338	2.3091	0.4577	1.7195×10^{-6}
μ_2'	1.7315	3.7557	5.3444	0.2098	1.004×10^{-7}
μ_3'	2.2963	7.3266	12.3991	0.0963	6.2950×10^{-9}
μ_4'	3.0614	14.3573	28.8352	0.0442	4.1241×10^{-10}
μ_5'	4.1028	28.2661	67.2217	0.0204	2.7705×10^{-11}
σ^2	0.0091	0.0161	0.0125	3.1071×10^{-4}	1.004×10^{-7}
CV	0.0727	0.0657	0.0483	0.0385	1.8427×10^{-4}
CS	-0.0261	0.7287	0.5870	-1.8047	197.8694
CK	9.3037	-1.3403	-3.0848	-602.9542	4.0911×10^{4}

4.7.3 Incomplete Moments

The Lorenz curve, the Bonferroni curve, the mean deviation, and the median deviation can all be obtained using the incomplete moments.

Proposition 4.17. The r^{th} incomplete moment of the HMFR distribution can be expressed as Equation (4.79).

$$m_r(y) = g^r \sum_{a=0}^{\infty} \sum_{b=0}^{a} \sum_{k=0}^{\infty} \Omega_{abk}(k+1)^{\frac{r}{d}} \Gamma\Big((1-r/d)\,, (g/y)^d(k+1)\Big), r < d, r = 1, 2, ... \tag{4.79}$$

$\Gamma(\cdot, \cdot)$ is the upper incomplete gamma function.

Proof. Mathematically,

$$m_r(y) = E(X^r | X \leq y) = \int_0^y x^r f_{HMFR}(x) \mathrm{d}x. \tag{4.80}$$

After substituting equation (4.70) into equation (4.80), gives

$$m_r(y) = dg^d \sum_{a=0}^{\infty}\sum_{b=0}^{a}\sum_{k=0}^{\infty}\Omega_{abk}\int_0^y x^{r-d-1}e^{-(\frac{g}{x})^d(k+1)}\mathrm{d}x.$$

Let $v = (\frac{g}{x})^d(k+1)$, then $x = (\frac{v}{g^d(k+1)})^{-\frac{1}{d}}$ and $dx = \frac{-dv}{dg^d(k+1)x^{-d-1}}$. $x \to 0, v \to \infty$ while $x \to y, v \to (\frac{g}{y})^d(k+1)$. This gives

$$m_r(y) = g^r \sum_{a=0}^{\infty}\sum_{b=0}^{a}\sum_{k=0}^{\infty}\Omega_{abk}(k+1)^{\frac{r}{d}}\int_{(\frac{g}{y})^d(k+1)}^{\infty} v^{-\frac{r}{d}}e^{-v}\mathrm{d}v.$$

Using the identity

$$\Gamma(d,z) = \int_z^{\infty} t^{d-1}e^{-t}\mathrm{d}t,$$

we obtain

$$m_r(y) = g^r \sum_{a=0}^{\infty}\sum_{b=0}^{a}\sum_{k=0}^{\infty}\Omega_{abk}(k+1)^{\frac{r}{d}}\Gamma\Big((1-r/d)\,,(g/y)^d(k+1)\Big).$$

4.7.4 Inequality Measures

By utilising both the Lorenz and Bonferroni curves, researchers gain insights into income inequality trends and make more accurate and meaningful comparisons by accounting for differences in population sizes (Trapeznikova, 2019). They provide a convenient descriptive tool to make these comparisons (Creedy, 2001).

Proposition 4.18. The Lorenz curve for the HMFR distribution can be expressed as Equation (4.81).

$$L_{HMFR}(y) = \frac{g}{\mu}\sum_{a=0}^{\infty}\sum_{b=0}^{a}\sum_{k=0}^{\infty}\Omega_{abk}(k+1)^{\frac{1}{d}}\Gamma\Big((1-1/d)\,,(g/y)^d(k+1)\Big), d>1. \quad (4.81)$$

Proof. By definition the Lorenz curve is given by

$$L_F(y) = \frac{1}{\mu}\int_0^y x f_{HMFR}(x)\mathrm{d}x.$$

$\int_0^y x f_{HMFR}(x)\mathrm{d}x$ is the first incomplete moment of the HMFR distribution.

Proposition 4.19. The Bonferroni curve for the HMFR distribution is Equation (4.82).

$$B_{HMFR}(y) = \frac{g}{\mu F(y)} \sum_{a=0}^{\infty}\sum_{b=0}^{a}\sum_{k=0}^{\infty} \Omega_{abk}(k+1)^{\frac{1}{d}}\Gamma\Big((1-1/d)\,,(g/y)^{d}(k+1)\Big), d > 1. \tag{4.82}$$

Proof.

$$B_{HMFR}(y) = \frac{L_{HMFR}(y)}{F(y)}. \tag{4.83}$$

After substituting equation (4.81) into equation (4.83), we obtain the Bonferroni curve of the distribution.

4.7.5 Mean Deviation and Median Deviation

The mean and median deviations serve as useful measures for quantifying the total variation present in distributions. These statistical measures provide insights into the dispersion or spread of data points around the central tendency of the distribution.

Proposition 4.20. The mean deviation of the HMFR distribution can be expressed as Equation (4.84).

$$\Delta_1(x) = 2\mu F_{HMFR}(\mu) - 2g \sum_{a=0}^{\infty}\sum_{b=0}^{a}\sum_{k=0}^{\infty} \Omega_{abk}(k+1)^{\frac{1}{d}}\Gamma\Big((1-1/d)\,,(g/\mu)^{d}(k+1)\Big), d > 1. \tag{4.84}$$

Proof. Mathematically,

$$\begin{aligned}\Delta_1(x) &= \int_0^{\infty} |x-\mu| f_{HMFR}(x)\mathrm{d}x \\ &= \int_0^{\mu} (\mu - x) f_{HMFR}(x)\mathrm{d}x + \int_{\mu}^{\infty} (x-\mu) f_{HMFR}(x)\mathrm{d}x \\ &= \mu \int_0^{\mu} f_{HMFR}(x)\mathrm{d}x - \int_0^{\mu} x f_{HMFR}(x)\mathrm{d}x + \mu \int_0^{\mu} f_{HMFR}(x)\mathrm{d}x - \int_0^{\mu} x f_{HMFR}(x)\mathrm{d}x \\ &+ \int_0^{\infty} x f_{HMFR}(x)\mathrm{d}x - \mu \int_0^{\infty} f_{HMFR}(x)\mathrm{d}x \\ &= 2\mu F_{HMFR}(\mu) - 2\int_0^{\mu} x f_{HMFR}(x)\mathrm{d}x.\end{aligned}$$

$\int_0^{\mu} x f_{HMFR}(x)\mathrm{d}x$ as the first incomplete moment gives the mean deviation.

Proposition 4.21. The median deviation of the HMFR distribution can be expressed as Equation (4.85).

$$\Delta_2(x) = \mu - 2g \sum_{a=0}^{\infty} \sum_{b=0}^{a} \sum_{k=0}^{\infty} \Omega_{abk} (k+1)^{\frac{1}{d}} \Gamma\Big((1-1/d), (g/H)^d (k+1)\Big), \tag{4.85}$$

where H is the median.

Proof. Mathematically,

$$\begin{aligned}\Delta_2(x) &= \int_0^{\infty} |x-H| f_{HMFR}(x)\mathrm{d}x \\ &= \int_0^{H} (M - x) f_{HMFR}(x)\mathrm{d}x + \int_{H}^{\infty} (x-H) f_{HMFR}(x)\mathrm{d}x \\ &= H \int_0^{H} f_{HMFR}(x)\mathrm{d}x - \int_0^{H} x f_{HMFR}(x)\mathrm{d}x + H \int_0^{H} f_{HMFR}(x)\mathrm{d}x - \int_0^{H} x f_{HMFR}(x)\mathrm{d}x \\ &+ \int_0^{\infty} x f_{HMFR}(x)\mathrm{d}x - H \int_0^{\infty} f_{HMFR}(x)\mathrm{d}x.\end{aligned}$$

Using the identity $F(H) = 0.5$, we have

$$\Delta_2(x) = \mu - 2\int_0^{H} x f_{HMFR}(x)\mathrm{d}x.$$

$\int_0^H xf_{HMFR}(x)\mathrm{d}x$ as the first incomplete moment gives the median deviation.

4.7.6 Mean Residuals

The mean residuals at a specific time, denoted as t, provides an estimate of the expected additional lifespan that a unit has survived up to that time (Gupta and Bradley, 2003). This function is particularly important in the field of survival or reliability analysis, as it offers valuable insights into the remaining lifetime of a unit or system at a given point in time. By considering the mean residuals, analysts can make informed decisions regarding maintenance, replacement, or other reliability-related considerations.

Proposition 4.22. The mean residuals for the HMFR distribution can be expressed as Equation (4.86).

$$m_{HMFR}(t) = \frac{1}{S_{HMFR}}\left[\mu - g\sum_{a=0}^{\infty}\sum_{b=0}^{a}\sum_{k=0}^{\infty}\Omega_{abk}(k+1)^{\frac{1}{d}}\Gamma\Big((1-1/d)\,,(g/t)^d(k+1)\Big)\right] - t, d > 1. \tag{4.86}$$

Proof. Mathematically,

$$m(t) = E(X - t|X > t) = \frac{1}{S(t)}\int_t^{\infty}(x-t)f(x)\mathrm{d}x, t \geq 0.$$

Hence,

$$m(t) = \frac{1}{S(t)}\left[\mu - \int_0^t (x)f(x)\mathrm{d}x\right] - t. \tag{4.87}$$

The substitution of the equation (3.9) and

$$\int_0^t xf(x)\mathrm{d}x = g\sum_{a=0}^{\infty}\sum_{b=0}^{a}\sum_{k=0}^{\infty}\Omega_{abk}(k+1)^{\frac{1}{d}}\Gamma\Big((1-1/d)\,,(g/t)^d(k+1)\Big)$$

into equation (4.87) completes the proof.

4.7.7 Moment Generating Function

The MGF is one of the powerful tools used to derive the moments of a probability distribution, provided the MGF exists for that distribution.

Proposition 4.23. The moment generating function of the HMFR distribution can be expressed as Equation (4.88).

$$M_{HMFR}(t) = \sum_{a=0}^{\infty}\sum_{b=0}^{a}\sum_{k=0}^{\infty}\sum_{r=0}^{\infty}\Omega_{abk}\frac{(k+1)^{\frac{r}{d}}(gt)^{r}}{r!}\Gamma(1-r/d), r < d. \tag{4.88}$$

Proof. Using the identity

$$e^{tX} = \sum_{r=0}^{\infty}\frac{t^{r}X^{r}}{r!}.$$

We deduce the MGF as

$$M_{HMFR}(t) = E(e^{tX}) = \sum_{r=0}^{\infty}\frac{t^{r}E(X^{r})}{r!} = \sum_{r=0}^{\infty}\frac{t^{r}}{r!}\mu_{r}^{'}. \tag{4.89}$$

After substituting equation (4.78) into equation (4.89), we obtain the MGF.

4.7.8 Characteristic Function

Characteristic functions are valuable in dealing with heavy-tailed random variables that lack a moment generating function (Nadarajah and Pogány, 2013).

Proposition 4.24. The characteristic function of the HMFR distribution is given as Equation (4.90).

$$C_{HMFR}(t) = \sum_{a=0}^{\infty}\sum_{b=0}^{a}\sum_{k=0}^{\infty}\sum_{r=0}^{\infty}\varpi_{abk}\frac{(k+1)^{\frac{r}{d}}(zgt)^{r}}{r!}\Gamma(1-r/d), r < d. \tag{4.90}$$

Proof. Using the identity

$$e^{ztX} = \sum_{r=0}^{\infty}\frac{z^{r}t^{r}X^{r}}{r!},$$

where $z = \sqrt{-1}$. We can define the characteristic function as

$$C_{HMF}(t) = E(e^{ztX}) = \sum_{r=0}^{\infty} \frac{(zt)^r E(X^r)}{r!} = \sum_{r=0}^{\infty} \frac{(zt)^r}{r!} \mu_r^{'}. \tag{4.91}$$

After substituting equation (4.78) into equation (4.91), we obtain the characteristic function.

4.7.9 Entropy

By examining the entropy of the HMFR distribution, researchers can gain insights into the level of uncertainty or variability inherent in the random variable. A lower entropy value indicates less uncertainty and a higher level of predictability, while a higher entropy value indicates greater uncertainty and a lower level of predictability.

Proposition 4.25. The Rényi entropy of the HMFR distribution can be expressed as Equation (4.92).

$$I_R(\lambda) = \frac{1}{1-\lambda} \log \left\{ K^* \sum_{a=0}^{\infty} \sum_{b=0}^{a} \sum_{k=0}^{\infty} \sum_{m=0}^{\infty} \psi_{abkm}^{*} \Gamma\big(\lambda + \frac{1}{d}(\lambda - 1)\big) \right\}, \tag{4.92}$$

where $K^* = (dg^d)^{\lambda-1} g^{(d+1)(1-\lambda)} (\alpha(1-\rho))^{\lambda}$ and
$\psi_{abkm}^{*} = (-1)^{b+k} \binom{2\lambda+a-1}{a} \binom{a}{b} \binom{(\alpha-1)(\lambda+m+b)}{k} \binom{\lambda}{m} (\lambda+k)^{(1-\lambda)(1+\frac{1}{d})} \rho^{a+m} (\alpha(1-\rho))^{-m}$.

Proof. Mathematically,

$$I_R(\lambda) = \frac{1}{1-\lambda} \log \int_0^{\infty} f_{HMFR}^{\lambda}(x) \mathrm{d}x. \tag{4.93}$$

The PDF of HMFR to the power λ is given as

$$f_{HMFR}^{\lambda}(x) = \frac{(dg^d)^{\lambda} x^{-\lambda(d+1)} e^{-\lambda x^{-d} g^d} (1 - e^{x^{-d} g^d})^{\lambda(\alpha-1)} (\alpha(1-\rho))^{\lambda} \left(1 + \frac{\rho(1-e^{-x^{-d}g^d})^{\alpha-1}}{\alpha(1-\rho)}\right)^{\lambda}}{\left[1 - \rho\left(1 - \left(1 - e^{-x^{-d} g^d}\right)^{\alpha-1}\right)\right]^{2\lambda}}.$$

The Taylor series in equation (4.71) helps to obtain

$$\left[1-\rho\left(1-\left(1-e^{-(\frac{g}{x})^d}\right)^{\alpha-1}\right)\right]^{-2\lambda}=\sum_{a=0}^{\infty}\sum_{b=0}^{a}(-1)^b\binom{2\lambda+a-1}{a}\binom{a}{b}\rho^a\left(1-e^{-(\frac{g}{x})^d}\right)^{b(\alpha-1)}$$

and

$$\left(1+\frac{\rho(1-e^{-(\frac{g}{x})^d})^{\alpha-1}}{\alpha(1-\rho)}\right)^{\lambda}=\sum_{m=0}^{\infty}\binom{\lambda}{m}\rho^m(\alpha(1-\rho))^{-m}(1-e^{-(\frac{g}{x})^d})^{m(\alpha-1)}.$$

We then obtain

$$f^{\lambda}_{HMFR}(x)=(dg^d)^{\lambda}(\alpha(1-\rho))^{\lambda}x^{-\lambda(d+1)}\sum_{a=0}^{\infty}\sum_{b=0}^{a}\sum_{k=0}^{\infty}\sum_{m=0}^{\infty}\psi_{abkm}e^{-(\frac{g}{x})^d(k+\lambda)}, \tag{4.94}$$

where $\psi_{abkm}=(-1)^{b+k}\binom{2\lambda+a-1}{a}\binom{a}{b}\binom{(\alpha-1)(\lambda+m+b)}{k}\binom{\lambda}{m}\rho^{a+m}(\alpha(1-\rho))^{-m}$.

Substituting equation (4.94) into equation (4.93), we have

$$I_R(\lambda)=\frac{1}{1-\lambda}\log\int_0^{\infty}(dg^d)^{\lambda}(\alpha(1-\rho))^{\lambda}x^{-\lambda(d+1)}\sum_{a=0}^{\infty}\sum_{b=0}^{a}\sum_{k=0}^{\infty}\sum_{m=0}^{\infty}\psi_{abkm}e^{-(\frac{g}{x})^d(k+\lambda)}\mathrm{d}x. \tag{4.95}$$

Let

$$\phi(x)=\int_0^{\infty}(dg^d)^{\lambda}(\alpha(1-\rho))^{\lambda}x^{-\lambda(d+1)}\sum_{a=0}^{\infty}\sum_{b=0}^{a}\sum_{k=0}^{\infty}\sum_{m=0}^{\infty}\psi_{abkm}e^{-(\frac{g}{x})^d(k+\lambda)}\mathrm{d}x.$$

Let $v=(\frac{g}{x})^d(k+\lambda)$ then $x=\left(\frac{v}{g^d(k+\lambda)}\right)^{-\frac{1}{d}}$ and $dx=\frac{-dv}{dg^d(k+\lambda)x^{-d-1}}$. $x\to 0, v\to\infty$ while $x\to\infty, v\to 0$, This gives

$$\phi(x)=K^*\sum_{a=0}^{\infty}\sum_{b=0}^{a}\sum_{k=0}^{\infty}\sum_{m=0}^{\infty}\psi_{abkm}\,(\lambda+k)^{(1-\lambda)(1+\frac{1}{d})}\int_0^{\infty}v^{-(1-\lambda)(1+\frac{1}{d})}e^{-v}\mathrm{d}u,$$

where $K^*=(dg^d)^{\lambda-1}g^{(d+1)(1-\lambda)}(\alpha(1-\rho))^{\lambda}$.

Using the identity $\Gamma(S)=\int_0^{\infty}x^{S-1}e^{-x}\mathrm{d}x$ gives

$$\phi(x)=K^*\sum_{a=0}^{\infty}\sum_{b=0}^{a}\sum_{k=0}^{\infty}\sum_{m=0}^{\infty}\psi_{abkm}\,(\lambda+k)^{(1-\lambda)(1+\frac{1}{d})}\,\Gamma\big(\lambda+\frac{1}{d}(\lambda-1)\big). \tag{4.96}$$

Substituting equation(4.96) into equation (4.95) completes the proof.

4.7.10 Stress-Strength Reliability

Stress-strength reliability is a measure that evaluates the capacity of a system to endure the stress or load it encounters (Alamri *et al.*, 2021). By comparing the strength of the system to the stress it can handle, stress-strength reliability provides an indication of the system's ability to function without failure or breakdown.

Proposition 4.26. For HMFR distribution, the stress-strength reliability can be expressed as Equation (4.97).

$$R_{ss} = 1 - \sum_{a=0}^{\infty}\sum_{b=0}^{a}\sum_{k=0}^{\infty} \frac{\delta_{abk}}{(k+1)}, \tag{4.97}$$

where $\delta_{abk} = [\alpha(1-\rho)\eta_{abk} + \rho\eta^*_{abk}]$, $\eta_{abk} = (-1)^{b+k}\binom{a+2}{2}\binom{a}{b}\binom{b(\alpha-1)+(2\alpha-1)}{k}\rho^a$, and $\eta^*_{abk} = (-1)^{b+k}\binom{a+2}{2}\binom{a}{b}\binom{b(\alpha-1)+(3\alpha-2)}{k}\rho^a$.

Proof. By definition

$$R_{ss} = \int_0^{\infty} f_{HMFR}(x)F_{HMFR}(x)\mathrm{d}x = 1 - \int_0^{\infty} f_{HMFR}(x)S_{HMFR}(x)\mathrm{d}x. \tag{4.98}$$

Multiplying equations (3.7) and (3.9) and using the series expansion equation (4.71), we have

$$\begin{aligned} f_{HMFR}(x)\cdot S_{HMFR}(x) = {} & \alpha\,(1-\rho)\,dg^d x^{-d-1}\sum_{a=0}^{\infty}\sum_{b=0}^{a}\sum_{k=0}^{\infty}\eta_{abk}\binom{b(\alpha-1)+(2\alpha-1)}{k}e^{-\left(\frac{g}{x}\right)^d(k+1)} \\ & + \rho dg^d x^{-d-1}\sum_{a=0}^{\infty}\sum_{b=0}^{a}\sum_{k=0}^{\infty}\eta_{abk}\binom{b(\alpha-1)+(3\alpha-2)}{k}e^{-\left(\frac{g}{x}\right)^d(k+1)}, \end{aligned} \tag{4.99}$$

where $\eta_{abk} = (-1)^{b+k}\binom{a+2}{2}\binom{a}{b}\rho^a$.

The substitution of equation (4.99) into equation (4.98) gives

$$R_{ss} = 1 - \Bigg[\alpha\,(1-\rho)\,dg^{d}\sum_{a=0}^{\infty}\sum_{b=0}^{a}\sum_{k=0}^{\infty}\eta_{abk}\binom{b(\alpha-1)+(2\alpha-1)}{k}\int_{0}^{\infty}x^{-d-1}e^{-(\frac{g}{x})^{d}(k+1)}\mathrm{d}x$$
$$-\rho dg^{d}\sum_{a=0}^{\infty}\sum_{b=0}^{a}\sum_{k=0}^{\infty}\eta_{abk}\binom{b(\alpha-1)+(3\alpha-2)}{k}\int_{0}^{\infty}x^{-d-1}e^{-(\frac{g}{x})^{d}(k+1)}\mathrm{d}x\Bigg].$$

Let $v = (\frac{g}{x})^{d}(k+1)$, then $x = \left(\frac{v}{g^{d}(k+1)}\right)^{-\frac{1}{d}}$ and $dx = \frac{-dv}{dg^{d}(k+1)x^{-d-1}}$. As $x \to 0, v \to \infty$ and as $x \to \infty, v \to 0$, we obtain

$$R_{ss} = 1 - \Bigg[\alpha\,(1-\rho)\sum_{a=0}^{\infty}\sum_{b=0}^{a}\sum_{k=0}^{\infty}\eta_{abk}\binom{b(\alpha-1)+(2\alpha-1)}{k}\int_{0}^{\infty}\frac{e^{-u}}{(k+1)}\mathrm{d}u$$
$$-\rho\sum_{a=0}^{\infty}\sum_{b=0}^{a}\sum_{k=0}^{\infty}\eta_{abk}\binom{b(\alpha-1)+(3\alpha-2)}{k}\int_{0}^{\infty}\frac{e^{-u}}{(k+1)}\mathrm{d}u\Bigg].$$

Using the identity $\int_{0}^{\infty}e^{-u}\mathrm{d}u = 1$, we obtain

$$R_{ss} = 1 - \Bigg[\alpha\,(1-\rho)\sum_{a=0}^{\infty}\sum_{b=0}^{a}\sum_{k=0}^{\infty}\eta_{abk}\binom{b(\alpha-1)+(2\alpha-1)}{k}\frac{1}{(k+1)}$$
$$-\rho\sum_{a=0}^{\infty}\sum_{b=0}^{a}\sum_{k=0}^{\infty}\eta_{abk}\binom{b(\alpha-1)+(3\alpha-2)}{k}\frac{1}{(k+1)}\Bigg].$$

4.7.11 Order Statistics

Order statistics play a significant role in identifying the maximum and minimum values of a random variable within a set of observations. They involve arranging the data points in ascending or descending order to determine the extreme values. By utilising order statistics, analysts can gain insights into the distribution of extreme events and evaluate their likelihood. This approach is particularly relevant in extreme value theory, which focuses on the statistical analysis of rare and extreme events (Abonongo, 2021).

Proposition 4.27. If $X_{11}, X_{12}, X_{13}, ..., X_{1n}$ is a random variable from the HMFR distribution with order statistics $X_{(11)}, X_{(12)}, X_{(13)}, ..., X_{(1n)}$, then the PDF of the r^{th}

order statistics X_{1r} is given as Equation (4.100).

$$f_{r:n}(x) = \frac{1}{\beta(r, n-r+1)} \sum_{a=0}^{\infty} \sum_{b=0}^{a} \sum_{k=0}^{\infty} \sum_{l=0}^{n-r} \sum_{m=0}^{r+l-1} \sum_{n=0}^{\infty} \sum_{q=0}^{n} \varpi_{abklmnq} d g^{d} x^{-d-1} e^{-(\frac{g}{x})^{d}(k+1)}, \tag{4.100}$$

where $\varpi_{abklmnq} = \left[\alpha(1-\rho)\omega_{abklmnq} + \rho\omega^{*}_{abklmnq}\right]$,

$\omega_{abklmnq} = (-1)^{b+k+l+m+q}(a+1)\binom{a}{b}\binom{m\alpha+q+(\alpha-1)(b+1)}{k}\binom{n-r}{l}\binom{r+l-1}{m}\binom{m+n-1}{n}\binom{n}{q}(\rho)^{a+n}$

and

$\omega^{*}_{abklmnq} = (-1)^{b+k+l+m+q}(a+1)\binom{a}{b}\binom{m\alpha+q+(\alpha-1)(b+2)}{k}\binom{n-p}{l}\binom{p+l-1}{m}\binom{m+n-1}{n}\binom{n}{q}(\rho)^{a+n}$.

Proof. By definition,

$$f_{r:n}(x) = \frac{1}{\beta(r, n-r+1)} \left(F_{HMFR}(x)\right)^{r-1} \left(1 - F_{HMFR}(x)\right)^{n-r} f_{HMFR}(x). \tag{4.101}$$

Applying the series expansion equation in (4.71),

$$\left(1 - F_{HMFR}(x)\right)^{n-r} = \sum_{l=0}^{n-r} (-1)^{l} \binom{n-r}{l} \left(F_{HMFR}(x)\right)^{l}.$$

We then obtain,

$$f_{r:n}(x) = \frac{1}{\beta(r, n-r+1)} \sum_{l=0}^{n-r} \sum_{m=0}^{r+l-1} (-1)^{l+m} \binom{n-r}{l} \binom{r+l-1}{m} \left(S_{HMFR}(x)\right)^{m} f_{HMFR}(x). \tag{4.102}$$

Applying the series expansion equation in (4.71) again and simplifying, we have

$$\left(S_{HMFR}(x)\right)^{m} \cdot f_{HMFR}(x) = \sum_{a=0}^{\infty} \sum_{b=0}^{a} \sum_{k=0}^{\infty} \sum_{n=0}^{\infty} \sum_{q=0}^{n} \varphi_{abknq} d g^{d} x^{-d-1} e^{-(\frac{g}{x})^{d}(k+1)}, \tag{4.103}$$

where $\varphi_{abknq} = \left[\alpha(1-\rho)\Omega_{ijknq} + \rho\Omega^{*}_{abknq}\right]$,

$\Omega_{abknq} = (-1)^{b+k+q}(a+1)\binom{a}{b}\binom{m\alpha+q+(\alpha-1)(b+1)}{k}\binom{m+n-1}{n}\binom{n}{q}(\rho)^{a+n}$ and

$\Omega^{*}_{abknq} = (-1)^{b+k+q}(a+1)\binom{a}{b}\binom{m\alpha+q+(\alpha-1)(b+2)}{k}\binom{m+n-1}{n}\binom{n}{q}(\rho)^{a+n}$.

Substituting equation (4.103) into equation (4.102) completes the proof.

Proposition 4.28. The t^{th} non-central moment of the r^{th} order statistics is given by

Equation (4.104).

$$\mu_t^{r:n} = \frac{g^t}{\beta(r, n-r+1)} \sum_{a=0}^{\infty} \sum_{b=0}^{a} \sum_{k=0}^{\infty} \sum_{l=0}^{n-r} \sum_{m=0}^{r+l-1} \sum_{n=0}^{\infty} \sum_{q=0}^{n} \varpi_{abklmnq}(k+1)^{\frac{t}{d}} \Gamma\big(1 - \frac{t}{d}\big), t < d. \tag{4.104}$$

Proof. By definition

$$\mu_t^{r:n} = \int_0^{\infty} x^t f_{r:n}(x) \mathrm{d}x. \tag{4.105}$$

The substitution of equation (4.100) into equation (4.105) gives

$$\mu_t^{r:n} = \frac{dg^d}{\beta(r, n-r+1)} \sum_{a=0}^{\infty} \sum_{b=0}^{a} \sum_{k=0}^{\infty} \sum_{l=0}^{n-r} \sum_{m=0}^{r+l-1} \sum_{n=0}^{\infty} \sum_{q=0}^{n} \varpi_{abklmnq} \int_0^{\infty} x^{t-d-1} e^{-(\frac{g}{x})^d (k+1)} \mathrm{d}x.$$

$\int_0^{\infty} x^{t-d-1} e^{-(\frac{g}{x})^d (k+1)} \mathrm{d}x = \frac{g^t (k+1)^{\frac{t}{d}}}{dg^d} \Gamma\big(1 - \frac{t}{d}\big)$ can be derived from the same method used for deriving the non-central moment. We then obtain the desired equation after substituting this equation.

The proof is complete.

4.7.12 Identifiability

To ensure that accurate inferences are made, the HMFR distribution's identifiability property is presented.

Proposition 4.29. If X_1 and X_2 are random variables from the HMF distribution with CDF $F_X(x; \alpha_1, \rho_1, d_1, g_1)$ and $F_X(x; \alpha_2, \rho_2, d_2, g_2)$ respectively, then the HMFR distribution is identifiable if and only if $\alpha_1 = \alpha_2$, $\rho_1 = \rho_2$, $d_1 = d_2$ and $g_1 = g_2$.

Proof. For HMFR distribution to be idenfiable, $F_X(x; \alpha_1, \rho_1, d_1, g_1) = F_X(x; \alpha_2, \rho_2, d_2, g_2)$. Then

$$1 - \frac{\left(1 - e^{-(\frac{g_1}{x})^{d_1}}\right)^{\alpha_1}}{\left[1 - \rho_1 \left(1 - \left(1 - e^{-(\frac{g_1}{x})^{d_1}}\right)^{\alpha_1 - 1}\right)\right]} = 1 - \frac{\left(1 - e^{-(\frac{g_2}{x})^{d}_{2}}\right)^{\alpha_2}}{\left[1 - \rho_2 \left(1 - \left(1 - e^{-(\frac{g_2}{x})^{d_2}}\right)^{\alpha_2 - 1}\right)\right]}$$

If $\alpha_1 = \alpha_2$, $\rho_1 = \rho_2$, $d_1 = d_2$ and $g_1 = g_2$, then

$$\frac{\left(1 - e^{-(\frac{g_1}{x})^{d_1}}\right)^{\alpha_1}}{\left[1 - \rho_1 \left(1 - \left(1 - e^{-(\frac{g_1}{x})^{d_1}}\right)^{\alpha_1 - 1}\right)\right]} - \frac{\left(1 - e^{-(\frac{g_2}{x})^{d}_{2}}\right)^{\alpha_2}}{\left[1 - \rho_2 \left(1 - \left(1 - e^{-(\frac{g_2}{x})^{d_2}}\right)^{\alpha_2 - 1}\right)\right]} = 0$$

The identifiability requirement has been met and that completes the proof.

4.8 Estimation of Parameters of the Harmonic Mixture Fréchet Distribution

This section is dedicated to estimating the parameters of the HMFR distribution. The objective is to determine the optimal parameter values that provide the best fit between the HMFR distribution and the given dataset. Various estimation techniques are employed, each offering a different approach to parameter estimation. By considering multiple methods, a thorough analysis of the distribution and the selection of the most suitable estimation technique based on the data's unique characteristics can be achieved.

4.8.1 Maximum Likelihood Estimation

By applying the MLE to the HMFR distribution, researchers can obtain parameter estimates that are optimal in terms of maximising the likelihood of the observed data and capturing the underlying characteristics of the distribution. For the HMFR distribution, the likelihood function can be expressed as Equation (4.106).

$$L\left(x, \alpha, \rho, d, g\right) = \prod_{a=1}^{n} f_{HMFR}(x_a, \alpha, \rho, d, g). \tag{4.106}$$

We substitute equation (4.66) into (4.106) and thereafter obtain the log-likelihood function given as Equation (4.107).

$$l(x,\alpha,\rho,d,g)=n\ln d+dn\ln g+(-d-1)\sum_{a=1}^{n}\ln x_a+(\alpha-1)\sum_{a=1}^{n}\ln\left(1-e^{-\left(\frac{g}{x_a}\right)^d}\right)$$
$$+\sum_{a=1}^{n}\ln\left[\alpha(1-\rho)+\rho\left(1-e^{-\left(\frac{g}{x_a}\right)^d}\right)^{\alpha-1}\right]-2\sum_{a=1}^{n}\ln\left[1-\rho\left(1-\left(1-e^{-\left(\frac{g}{x_a}\right)^d}\right)^{\alpha-1}\right)\right]. \tag{4.107}$$

To estimate the parameters using the MLE approach, we utilise the method of differentiation. By differentiating equation (4.107) with respect to the parameters (α,ρ,d,g) and setting the equations obtained to zero, we can derive a system of equations. These equations when solved using numerical methods gives the parameter estimates. The derivatives obtained are as follows

$$\frac{\partial l}{\partial\alpha}=\sum_{a=1}^{n}\ln\left(1-e^{-\left(\frac{g}{x_a}\right)^d}\right)+\sum_{a=1}^{n}\frac{(1-\rho)+\rho\ln\left(1-e^{-\left(\frac{g}{x_a}\right)^d}\right)}{\alpha(1-\rho)+\rho\left(1-e^{-\left(\frac{g}{x_a}\right)^d}\right)^{\alpha-1}}$$
$$-\sum_{a=1}^{n}\frac{2\rho\ln\left(1-e^{-\left(\frac{g}{x_a}\right)^d}\right)\left(1-e^{-\left(\frac{g}{x_a}\right)^d}\right)^{\alpha-1}}{1-\rho+\rho\left(1-e^{-\left(\frac{g}{x_a}\right)^d}\right)^{\alpha-1}},$$

$$\frac{\partial l}{\partial\rho}=-2\sum_{a=1}^{n}\frac{\left(1-e^{-\left(\frac{g}{x_a}\right)^d}\right)^{\alpha-1}-1}{1-\rho+\rho\left(1-e^{-\left(\frac{g}{x_a}\right)^d}\right)^{\alpha-1}}-\sum_{a=1}^{n}\frac{\left(1-e^{-\left(\frac{g}{x_a}\right)^d}\right)^{\alpha-1}-\alpha}{\alpha(1-\rho)+\rho\left(1-e^{-\left(\frac{g}{x_a}\right)^d}\right)^{\alpha-1}},$$

$$\frac{\partial l}{\partial d}=\frac{n}{d}+n\ln g-\sum_{a=0}^{n}\ln x_a+\sum_{a=1}^{n}\frac{\rho(\alpha-1)\left(\frac{g}{x_a}\right)^d\ln\left(\frac{g}{x_a}\right)e^{-\left(\frac{g}{x_a}\right)^d}\left(1-e^{-\left(\frac{g}{x_a}\right)^d}\right)^{\alpha-2}}{\alpha(1-\rho)+\rho\left(1-e^{-\left(\frac{g}{x_a}\right)^d}\right)^{\alpha-1}}$$
$$-\alpha\sum_{a=1}^{n}\frac{(\alpha-1)\left(\frac{g}{x_a}\right)^d\ln\left(\frac{g}{x_a}\right)}{1-e^{-\left(\frac{g}{x_a}\right)^d}}-\sum_{a=1}^{n}\frac{2\rho(\alpha-1)\left(\frac{g}{x_a}\right)^d\ln\left(\frac{g}{x_a}\right)e^{-\left(\frac{g}{x_a}\right)^d}\left(1-e^{-\left(\frac{g}{x_a}\right)^d}\right)^{\alpha-2}}{1-\rho+\rho\left(1-e^{-\left(\frac{g}{x_a}\right)^d}\right)^{\alpha-1}},$$

$$\frac{\partial l}{\partial g} = \frac{nd}{g} + \sum_{a=1}^{n} \frac{\rho(\alpha-1)\left(\frac{g}{x_a}\right)^d \left(\frac{d}{g}\right) e^{-\left(\frac{g}{x_a}\right)^d} \left(1 - e^{-\left(\frac{g}{x_a}\right)^d}\right)^{\alpha-2}}{\alpha(1-\rho) + \rho\left(1 - e^{-\left(\frac{g}{x_a}\right)^d}\right)^{\alpha-1}}$$

$$+ \sum_{a=1}^{n} \frac{(\alpha-1)\left(\frac{g}{x_a}\right)^d \left(\frac{d}{g}\right) e^{-\left(\frac{g}{x_a}\right)^d}}{1 - e^{-\left(\frac{g}{x_a}\right)^d}} - \sum_{a=1}^{n} \frac{2\rho(\alpha-1)\left(\frac{g}{x_a}\right)^d \left(\frac{d}{g}\right) e^{-\left(\frac{g}{x_a}\right)^d} \left(1 - e^{-\left(\frac{g}{x_a}\right)^d}\right)^{\alpha-2}}{1 - \rho + \rho\left(1 - e^{-\left(\frac{g}{x_a}\right)^d}\right)^{\alpha-1}}.$$

4.8.2 Ordinary Least Squares

To perform the OLSS estimation, a specific objective function is defined, which represents the discrepancy between the observed data and the model predictions. The goal is to minimise Equation (4.108).

$$LS(\alpha, \rho, d, g) = \sum_{b=1}^{n} \left\{ \left(F_{HMFR}(x_{(b)})\right) - \frac{b}{n+1} \right\}^2. \tag{4.108}$$

The method of differentiation is employed to minimise equation (4.108). We differentiate with respect to each parameter and equate the resulting equations to zero, obtaining

$$\frac{\partial LS}{\partial \alpha} = \sum_{b=1}^{n} \left\{ \left(F_{HMFR}(x_{(b)})\right) - \frac{b}{n+1} \right\} \cdot \Lambda_1(x_{(b)}; \alpha, \rho, d, g) = 0, \tag{4.109}$$

$$\frac{\partial LS}{\partial \rho} = \sum_{b=1}^{n} \left\{ \left(F_{HMFR}(x_{(b)})\right) - \frac{b}{n+1} \right\} \cdot \Lambda_2(x_{(b)}; \alpha, \rho, d, g) = 0, \tag{4.110}$$

$$\frac{\partial LS}{\partial d} = \sum_{b=1}^{n} \left\{ \left(F_{HMFR}(x_{(b)})\right) - \frac{b}{n+1} \right\} \cdot \Lambda_3(x_{(b)}; \alpha, \rho, d, g) = 0, \tag{4.111}$$

$$\frac{\partial LS}{\partial g} = \sum_{b=1}^{n} \left\{ \left(F_{HMFR}(x_{(b)})\right) - \frac{b}{n+1} \right\} \cdot \Lambda_4(x_{(b)}; \alpha, \rho, d, g) = 0, \tag{4.112}$$

where

$$\Lambda_1(x_{(b)};\alpha,\rho,d,g)=\frac{(\rho-1)\log\left(1-e^{-\left(\frac{g}{x_{(b)}}\right)^d}\right)\left(1-e^{-\left(\frac{g}{x_{(b)}}\right)^d}\right)^{\alpha}\left(e^{\left(\frac{g}{x_{(b)}}\right)^d}-1\right)^2}{\left[(\rho-1)+e^{\left(\frac{g}{x_{(b)}}\right)^d}\left(1+\rho\left(\left(1-e^{-\left(\frac{g}{x_{(b)}}\right)^d}\right)^{\alpha}-1\right)\right)\right]^2},\tag{4.113}$$

$$\Lambda_2(x_{(b)};\alpha,\rho,d,g)=\frac{\left(1-e^{-\left(\frac{g}{x_{(b)}}\right)^d}\right)^{\alpha}\left(\left(1-e^{\left(\frac{g}{x_{(b)}}\right)^d}\right)^{\alpha-1}-1\right)}{\left[1+\rho\left(\left(1-e^{-\left(\frac{g}{x_{(b)}}\right)^d}\right)^{\alpha-1}-1\right)\right]^2},\tag{4.114}$$

$$\begin{aligned}\Lambda_3(x_{(b)};\alpha,\rho,d,g)=&\left(\frac{g}{x_{(b)}}\right)^d\log\left(\frac{g}{x_{(b)}}\right)\left(1-e^{-\left(\frac{g}{x_{(b)}}\right)^d}\right)^{\alpha}\\&\times\frac{\left[\alpha(\rho-1)+e^{\left(\frac{g}{x_{(b)}}\right)^d}\left(\alpha+\rho(1-\alpha)\left(1-e^{-\left(\frac{g}{x_{(b)}}\right)^d}\right)^{\alpha}\right)\right]}{\left[(\rho-1)+e^{\left(\frac{g}{x_{(b)}}\right)^d}\left(1+\rho\left(\left(1-e^{-\left(\frac{g}{x_{(b)}}\right)^d}\right)^{\alpha}-1\right)\right)\right]^2},\end{aligned}\tag{4.115}$$

$$\begin{aligned}\Lambda_4(x_{(b)};\alpha,\rho,d,g)=&\frac{d}{g}\left(\frac{g}{x_{(b)}}\right)^d\left(1-e^{-\left(\frac{g}{x_{(b)}}\right)^d}\right)^{\alpha}\\&\times\frac{\left[\alpha(\rho-1)+e^{\left(\frac{g}{x_{(b)}}\right)^d}\left(\alpha+\rho(1-\alpha)\left(1-e^{-\left(\frac{g}{x_{(b)}}\right)^d}\right)^{\alpha}\right)\right]}{\left[(\rho-1)+e^{\left(\frac{g}{x_{(b)}}\right)^d}\left(1+\rho\left(\left(1-e^{-\left(\frac{g}{x_{(b)}}\right)^d}\right)^{\alpha}-1\right)\right)\right]^2}.\end{aligned}\tag{4.116}$$

These equations obtained are solved simultaneously using numerical methods to obtain the parameter estimates.

4.8.3 Weighted Least Squares

The WLSS estimates are obtained by solving the minimisation problem, which involves finding the parameter values that minimise the weighted discrepancy between the observed data and the predictions of the HMF distribution.The minimisation function is given as Equation (4.117).

$$WLS(\alpha,\rho,d,g)=\sum_{b=1}^{n}\frac{(n+1)^2(n+2)}{b(n-b+1)}\left\{\left(F_{HMFR}(x_{(b)})\right)-\frac{b}{n+1}\right\}^2. \qquad (4.117)$$

The method of differentiation is employed to minimise equation (4.117). We differentiate with respect to each parameter and equate the resulting equations to zero, obtaining

$$\frac{\partial WLS}{\partial \alpha}=\sum_{b=1}^{n}\frac{(n+1)^2(n+2)}{b(n-b+1)}\left\{\left(F_{HMFR}(x_{(b)})\right)-\frac{b}{n+1}\right\}\cdot\Lambda_1(x_{(b)};\alpha,\rho,d,g)=0, \qquad (4.118)$$

$$\frac{\partial WLS}{\partial \rho}=\sum_{b=1}^{n}\frac{(n+1)^2(n+2)}{b(n-b+1)}\left\{\left(F_{HMFR}(x_{(b)})\right)-\frac{b}{n+1}\right\}\cdot\Lambda_2(x_{(b)};\alpha,\rho,d,g)=0, \qquad (4.119)$$

$$\frac{\partial WLS}{\partial d}=\sum_{b=1}^{n}\frac{(n+1)^2(n+2)}{b(n-b+1)}\left\{\left(F_{HMFR}(x_{(b)})\right)-\frac{b}{n+1}\right\}\cdot\Lambda_3(x_{(b)};\alpha,\rho,d,g)=0, \qquad (4.120)$$

$$\frac{\partial WLS}{\partial g}=\sum_{b=1}^{n}\frac{(n+1)^2(n+2)}{b(n-b+1)}\left\{\left(F_{HMFR}(x_{(b)})\right)-\frac{b}{n+1}\right\}\cdot\Lambda_4(x_{(b)};\alpha,\rho,d,g)=0. \qquad (4.121)$$

$\Lambda_m(x_{(b)};\alpha,\rho,d,g)$, $(m=1,2,3,4)$, are obtained using equations (4.113), (4.114), (4.115) and (4.116).

These equations obtained are solved simultaneously using numerical methods to obtain the parameter estimates.

4.8.4 Cramér-von Mises Estimation

The CVM estimates are obtained by solving the minimisation problem, which involves finding the parameter values that minimise the discrepancy between the observed data and the HMF distribution as measured by the Cramér-von Mises statistic. The minimisation function is given as Equation (4.122).

$$CVM(\alpha, \rho, d, g) = \frac{1}{12n} + \sum_{b=1}^{n} \left\{ \left(F_{HMFR}(x_{(b)})\right) - \frac{2b-1}{2n} \right\}^2. \tag{4.122}$$

The method of differentiation is employed to minimise equation (4.122). We differentiate with respect to each parameter and equate the resulting equations to zero, obtaining

$$\frac{\partial CVM}{\partial \alpha} = \sum_{b=1}^{n} \left\{ \left(F_{HMFR}(x_{(b)})\right) - \frac{2b-1}{2n} \right\} \cdot \Lambda_1(x_{(b)}; \alpha, \rho, d, g) = 0, \tag{4.123}$$

$$\frac{\partial CVM}{\partial \rho} = \sum_{b=1}^{n} \left\{ \left(F_{HMFR}(x_{(b)})\right) - \frac{2b-1}{2n} \right\} \cdot \Lambda_2(x_{(b)}; \alpha, \rho, d, g) = 0, \tag{4.124}$$

$$\frac{\partial CVM}{\partial d} = \sum_{b=1}^{n} \left\{ \left(F_{HMFR}(x_{(b)})\right) - \frac{2b-1}{2n} \right\} \cdot \Lambda_3(x_{(b)}; \alpha, \rho, d, g) = 0, \tag{4.125}$$

$$\frac{\partial CVM}{\partial g} = \sum_{b=1}^{n} \left\{ \left(F_{HMFR}(x_{(b)})\right) - \frac{2b-1}{2n} \right\} \cdot \Lambda_4(x_{(b)}; \alpha, \rho, d, g) = 0, \tag{4.126}$$

$\Lambda_m(x_{(b)}; \alpha, \rho, d, g)$, $(m = 1, 2, 3, 4)$, are obtained using equations (4.113), (4.114), (4.115) and (4.116).

These equations obtained are solved simultaneously using numerical methods to obtain the parameter estimates.

4.8.5 Anderson-Darling Estimation

The AD estimates are obtained by solving the minimisation problem, which involves finding the parameter values that minimise the discrepancy between the observed data and the HMFR distribution as measured by the Anderson-Darling statistic. The minimisation function is given as Equation (4.127).

$$AD(\alpha,\rho,d,g) = -n - \frac{1}{n}\sum_{b=1}^{n}(2b-1)\left\{\left(\log F_{HMFR}(x_{(b)})\right) + \log\left(1 - F_{HMFR}(x_{(n+1-b)})\right)\right\}. \tag{4.127}$$

The method of differentiation is employed to minimise equation (4.127). We differentiate with respect to each parameter and equate the resulting equations to zero, obtaining

$$\frac{\partial AD}{\partial \alpha} = \sum_{b=1}^{n}(2b-1)\left\{\frac{\Lambda_1(x_{(b)};\alpha,\rho,d,g)}{\left(F_{HMFR}(x_{(b)})\right)} - \frac{\Lambda_1(x_{(n+1-b)};\alpha,\rho,d,g)}{1-\left(F_{HMFR}(x_{(n+1-b)})\right)}\right\} = 0, \tag{4.128}$$

$$\frac{\partial AD}{\partial \rho} = \sum_{b=1}^{n}(2b-1)\left\{\frac{\Lambda_2(x_{(b)};\alpha,\rho,d,g)}{\left(F_{HMFR}(x_{(b)})\right)} - \frac{\Lambda_2(x_{(n+1-b)};\alpha,\rho,d,g)}{1-\left(F_{HMFR}(x_{(n+1-b)})\right)}\right\} = 0, \tag{4.129}$$

$$\frac{\partial AD}{\partial d} = \sum_{b=1}^{n}(2b-1)\left\{\frac{\Lambda_3(x_{(b)};\alpha,\rho,d,g)}{\left(F_{HMFR}(x_{(b)})\right)} - \frac{\Lambda_3(x_{(n+1-b)};\alpha,\rho,d,g)}{1-\left(F_{HMFR}(x_{(n+1-b)})\right)}\right\} = 0, \tag{4.130}$$

$$\frac{\partial AD}{\partial g} = \sum_{b=1}^{n}(2b-1)\left\{\frac{\Lambda_4(x_{(b)};\alpha,\rho,d,g)}{\left(F_{HMFR}(x_{(b)})\right)} - \frac{\Lambda_4(x_{(n+1-b)};\alpha,\rho,d,g)}{1-\left(F_{HMFR}(x_{(n+1-b)})\right)}\right\} = 0, \tag{4.131}$$

where $\Lambda_m(x_{(\cdot)};\alpha,\rho,d,g)$, $(m = 1,2,3,4)$, are obtain using equations (4.113), (4.114), (4.115) and (4.116).

The ADE estimates are derived by solving these functions simultaneously employing numerical methods.

4.9 Development of the Harmonic Mixture Burr XII Distribution

This sections presents the PDF, CDF, FRF and SF of the HMBRXII distribution. We can determine the PDF of the HMBRXII distribution by the substituting the equations (3.14) and (3.15) into equation (3.21). The expression obtained is Equation

(4.132).

$$f(x) = \frac{\alpha (1-\rho) dwx^{d-1} \left(1+x^d\right)^{-\alpha w-1} + \rho dwx^{d-1} \left(1+x^d\right)^{-w(2\alpha-1)-1}}{\left[1-\rho\left(1-\left(1+x^d\right)^{-w(\alpha-1)}\right)\right]^2}, \tag{4.132}$$

where $d > 0$, $w > 0$, $\alpha > 0$, $0 < \rho < 1$, and $x > 0$.

The density plots of the HMBRXII distribution are shown in Figure 4.9. By manipulating the parameter values, the density exhibits distinct characteristics, primarily either a decreasing trend or a right-skewed shape. This variation in density highlights the flexibility of the HMBRXII distribution in capturing different data patterns and distributions. It provides a visual representation of how different parameter settings can influence the shape and behaviour of the distribution. Analysing the density plots allows researchers to gain insights into the distribution's characteristics and make informed decisions regarding data analysis and modelling.

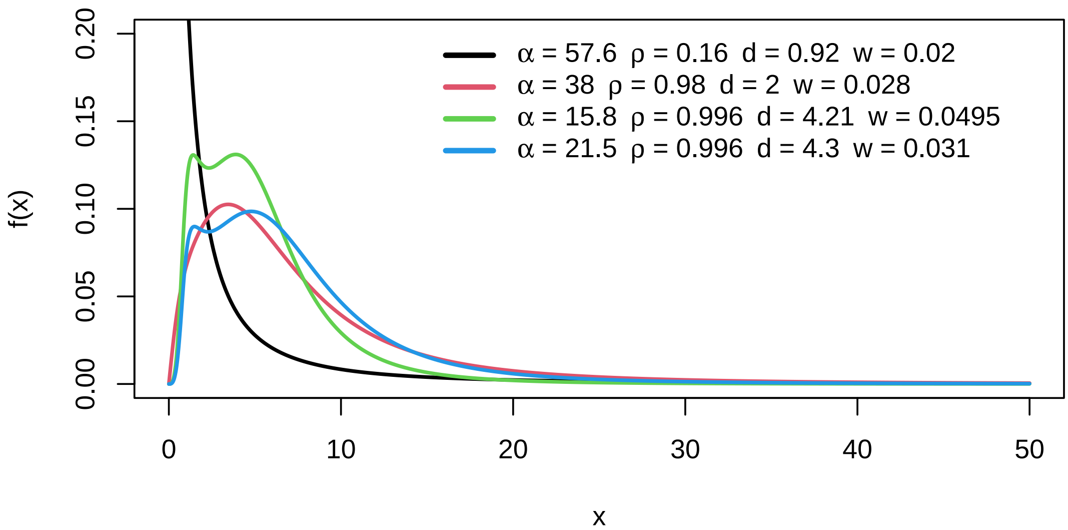

Figure 4.9: The density plots of the HMBRXII

To obtain the corresponding CDF of the HMBRXII distribution, substitute equation (3.15), the SF of the Burr XII distribution into equation (3.20). By performing this substitution, we can derive the expression in Equation (4.133).

$$F(x) = 1 - \frac{\left(1 + x^d\right)^{-\alpha w}}{\left[1 - \rho\left(1 - \left(1 + x^d\right)^{-w(\alpha - 1)}\right)\right]}, x > 0. \tag{4.133}$$

The Figure 4.10 displays the CDF of the HMBRXII distribution as parameter values are varied. The CDF approaches 0 as x approaches 0 and approaches 1 as x approaches infinity.

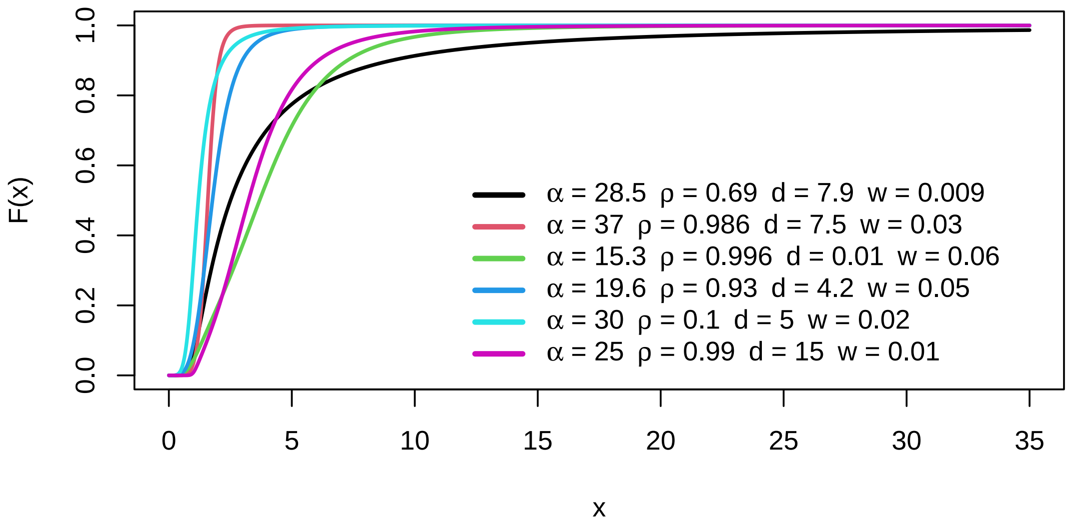

Figure 4.10: The CDF plots of the HMBRXII

The SF is then given by Equation (4.134).

$$S(x) = \frac{\left(1 + x^d\right)^{-\alpha w}}{\left[1 - \rho\left(1 - \left(1 + x^d\right)^{-w(\alpha - 1)}\right)\right]}, x > 0. \tag{4.134}$$

To obtain the FRF, we substitute equations (3.14) and (3.15) into equation (3.22).The FRF of the HMBRXII distribution is expressed as Equation (4.135).

$$h(x) = \frac{\alpha\left(1 - \rho\right) dwx^{d-1}\left(1 + x^d\right)^{-\alpha w - 1} + \rho dwx^{d-1}\left(1 + x^d\right)^{-w(2\alpha - 1) - 1}}{\left(1 + x^d\right)^{-\alpha w}\left[1 - \rho\left(1 - \left(1 + x^d\right)^{-w(\alpha - 1)}\right)\right]}, x > 0. \tag{4.135}$$

The plots of the FRF for the HMBRXII distribution are presented in Figure 4.11. By manipulating certain parameter values, the failure rate plots exhibit distinct patterns, primarily either a decreasing trend or an upside-down bathtub shape. These variations in the failure rate provide insights into the behaviour and characteristics of the distribution under different parameter settings.

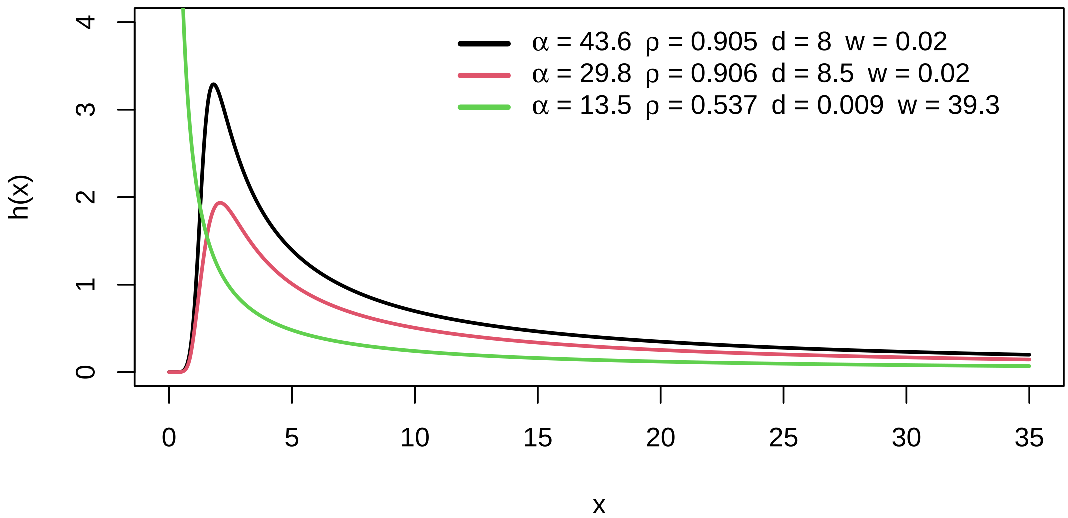

Figure 4.11: The FRF plots of the HMBRXII

In Figure 4.12, we investigated the effect of introducing additional parameters from the HMG family to the Burr XII distribution (black curve). By modifying the values of the parameters α and ρ, while keeping the remaining parameters of the Burr XII distribution constant, we observed significant enhancements in terms of kurtosis (peakness) and skewness. These improvements indicate that the inclusion of the additional parameters from the HMG family provides a valuable augmentation to the Burr XII distribution, enabling a more accurate representation of data with varying characteristics and tail behaviours.

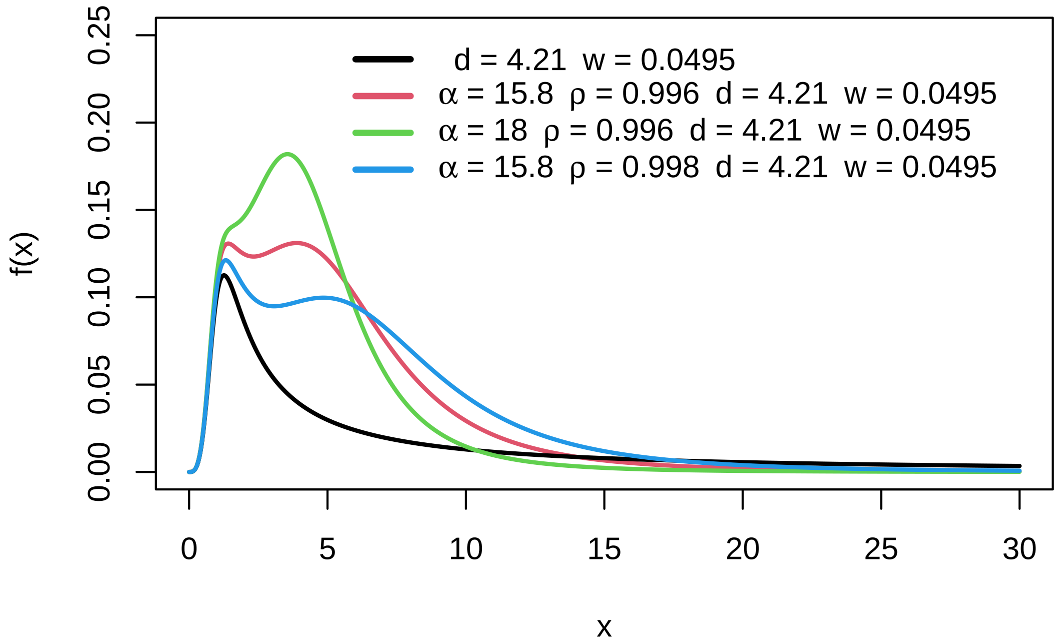

Figure 4.12: Assessing the densities of the HMBRXII Distribution and the BRXII Distribution

Lemma 4.5. The linear representation for the PDF of the HMBRXII distribution provided $\alpha > 1$ is given as Equation (4.136).

$$f(x) = \sum_{a=0}^{\infty}\sum_{b=0}^{a} \varpi_{ab} \left[\alpha(1-\rho)dwx^{d-1}\left(1+x^{c}\right)^{-k(\alpha(b+1)-b)-1} + \rho dwx^{d-1}\left(1+x^{d}\right)^{-w(\alpha(b+2)-(b+1))-1}\right], \tag{4.136}$$

where $\varpi_{ab} = (-1)^b(a+1)\binom{a}{b}\rho$, $x > 0, d > 0, w > 0, \alpha > 1$ and $0 < \rho < 1$.

Proof. For $\eta > 0$, the series expansions for $(1-u)^{-\eta}$ for $|u| < 1$ is $(1-u)^{-\eta} = \sum_{a=0}^{\infty}\binom{\eta+a-1}{a}(u)^a$. Since $0 < \left(1+x^d\right)^{-w} < 1$ for $\alpha > 1$,we use the Taylor series twice to obtain

$$\left[1-\rho\left(1-\left(1+x^{d}\right)^{-w(\alpha-1)}\right)\right]^{-2} = \sum_{a=0}^{\infty}\sum_{b=0}^{a}(-1)^b(a+1)\binom{a}{b}\rho^a\left(1+x^{d}\right)^{-w(\alpha-1)b}.$$

We then obtain

$$
\begin{aligned}
f(x) = \alpha(1-\rho)\sum_{a=0}^{\infty}\sum_{b=0}^{a}(-1)^b(a+1)\binom{a}{b}\rho^a dwx^{d-1}\left(1+x^d\right)^{-w(\alpha(b+1)-b)-1} \\
+\rho\sum_{a=0}^{\infty}\sum_{b=0}^{a}(-1)^b(a+1)\binom{a}{b}\rho^a dwx^{d-1}\left(1+x^d\right)^{-w(\alpha(b+2)-(b+1))-1}.
\end{aligned}
\tag{4.137}
$$

4.10 Statistical Properties of the HMBRXII distribution

The statistical properties of the HMBRXII distribution are derived in this section. Properties such as the quantile function, non-central moments, incomplete moments, inequality measures, mean and median deviations, moment generating functions, characteristic function, entropy, stress-strength reliability, order statistics and identifiability are deduced.

4.10.1 Quantile Function

The quantile function, also known as the inverse CDF, operates in the opposite direction of the CDF. By evaluating the quantile function, researchers can gain insights into the various shapes and nature of a distribution.

Lemma 4.6. The quantile function of the HMBRXII distribution is given by Equation (4.138).

$$
(1-p)\left[1-\rho\left(1-\left(1+x_p^d\right)^{-w(\alpha-1)}\right)\right]-\left(1+x_p^d\right)^{-\alpha w}=0, \tag{4.138}
$$

where $p \in (0,1)$ and $Q(p) = x_p$ is the quantile function.

Proof. Mathematically,

$$
Q(p) = \mathbf{P}(X \leq x_p) = p.
$$

The quantile function of the HMBRXII distribution can be obtained by the substitution of equation (3.13) into equation (3.24) and letting $Q(p) = x_p$.

There is no direct formula available to calculate the exact quantiles of the HMBRXII distribution. Instead, numerical methods or approximation techniques may be employed to estimate the quantiles based on the distribution's parameters and desired probability values.

4.10.2 Moments

The determination of moments holds significant importance in statistical analysis. We gain valuable insights into the behaviour and properties of the distribution, enabling us to compute important statistical measures and make informed interpretations of the data. The moments serve as fundamental building blocks for a wide range of statistical analyses and provide a comprehensive understanding of the distribution's characteristics.

Proposition 4.30. The r^{th} non-central moment of the HMBRXII distribution for $\alpha > 1$ can be expressed as Equation (4.139).

$$\begin{aligned} \mu_r^{'} = \sum_{a=0}^{\infty}\sum_{b=0}^{a} \varpi_{ab} \Bigg[&\alpha(1-\rho)w\mathcal{B}\left(\frac{r}{d}+1, w\left(\alpha(b+1)-b\right)-\frac{r}{d}\right) \\ &+ \rho w\mathcal{B}\left(\frac{r}{d}+1, w\left(\alpha(b+2)-(b+1)\right)-\frac{r}{d}\right)\Bigg], r = 1,2,3,4.... \end{aligned} \tag{4.139}$$

where $\mathcal{B}(\cdot,\cdot)$ is a beta function.

Proof. Mathematically,

$$\mu_r^{'} = E(X^r) = \int_0^{\infty} x^r f(x)\mathrm{d}x. \tag{4.140}$$

The substitution of equation (4.136) into equation (4.140) produces

$$E(X^r) = \int_0^\infty x^r \sum_{a=0}^{\infty}\sum_{b=0}^{a} \varpi_{ab} \Big[\alpha(1-\rho)dwx^{d-1}\left(1+x^d\right)^{-w(\alpha(b+1)-b)-1} + \rho dwx^{d-1}\left(1+x^d\right)^{-w(\alpha(b+2)-(b+1))-1}\Big] dx.$$

We then obtain

$$\mu_r^{'} = dw \sum_{a=0}^{\infty}\sum_{b=0}^{a} \varpi_{ab} \Big[\alpha(1-\rho)\int_0^\infty x^{r+c-1}\left(1+x^d\right)^{-w(\alpha(b+1)-b)-1} dx + \rho \int_0^\infty x^{r+d-1}\left(1+x^d\right)^{-w(\alpha(b+2)-(b+1))-1} dx\Big].$$

Let $v = x^d$, then $x = v^{1/d}$ and $dx = \frac{1}{d}v^{1/d-1}du$. We then have

$$\mu_r^{'} = k \sum_{a=0}^{\infty}\sum_{b=0}^{a} \varpi_{ab} \Big[\alpha(1-\rho)\int_0^\infty v^{r/d}(1+v)^{-w(\alpha(b+1)-b)-1} dv + \rho \int_0^\infty v^{r/d}(1+v)^{-w(\alpha(b+2)-(b+1))-1} dv\Big].$$

Using the identity (see Afify *et al.* (2018))

$$\mathcal{B}(g,h) = \int_0^\infty v^{g-1}(1+v)^{-(g+h)} dv, g>0, h>0$$

we obtain

$$\mu_r^{'} = \sum_{a=0}^{\infty}\sum_{b=0}^{a} \varpi_{ab} \Big[\alpha(1-\rho)k\mathcal{B}\left(\frac{r}{d}+1, w\left(\alpha(b+1)-b\right)-\frac{r}{d}\right) + \rho w\mathcal{B}\left(\frac{r}{d}+1, w\left(\alpha(b+2)-(b+1)\right)-\frac{r}{d}\right)\Big].$$

Table 4.3 presents the values of σ^2, CV, CS, and CK for the HMBRXII distribution. We observe that the HMBRXII distribution is skewed to the right. Furthermore, by varying certain parameter values, we observe different kurtosis characteristics. Specifically, the distribution can exhibit either a platykurtic nature (when CK is less than 3), indicating lighter tails and less extreme values, or a leptokurtic nature (when

CK is greater than 3), indicating heavier tails and more extreme values. These insights into the skewness and kurtosis properties of the HMBRXII distribution allow for a better understanding of its behaviour and provide valuable information for statistical analysis and modelling purposes.

Table 4.3: Moments for HMBRXII

r	α=8.50, ρ=0.20, d=2.90, w=10.50	α=28.50,ρ=0.30, d=1.90,w=15.00	α=8.50, ρ=0.80, d=0.90,w=15.50	α=10.50, ρ=0.50, d=1.20, w=20.50	α=10.50, ρ=0.55, d=1.90, w=8.50
$\mu_1^{'}$	1.980×10^{-1}	4.061×10^{-2}	9.402×10^{-3}	1.406×10^{-2}	1.037×10^{-1}
$\mu_2^{'}$	4.500×10^{-2}	2.081×10^{-3}	1.475×10^{-4}	3.031×10^{-4}	1.323×10^{-2}
$\mu_3^{'}$	1.100×10^{-2}	1.246×10^{-4}	3.052×10^{-6}	8.552×10^{-6}	1.938×10^{-3}
$\mu_4^{'}$	3.000×10^{-3}	8.440×10^{-6}	8.315×10^{-8}	2.957×10^{-7}	3.156×10^{-4}
$\mu_5^{'}$	1.000×10^{-3}	6.201×10^{-7}	2.820×10^{-9}	1.177×10^{-8}	5.610×10^{-5}
σ^2	5.000×10^{-3}	4.000×10^{-4}	5.915×10^{-5}	1.000×10^{-4}	2.500×10^{-3}
CV	0.364	0.512	0.818	0.731	0.480
CS	0.147	0.558	1.214	1.221	0.428
CK	2.738	3.417	6.633	5.126	2.992

4.10.3 Incomplete Moments

By obtaining the incomplete moments, we gain insights into the distribution's shape, spread, and variability. The Lorenz curve, the Bonferroni curve, the mean deviation, and the median deviation can all be obtained using the incomplete moments.

Proposition 4.31. The r^{th} incomplete moment of the HMBRXII distribution for $\alpha > 1$ is given as Equation (4.141).

$$\begin{aligned} m_r(y) =& \sum_{a=0}^{\infty}\sum_{b=0}^{a} \varpi_{ab}\Bigg[\alpha(1-\rho)w\mathcal{B}\left(y^d : \frac{r}{d}+1, (\alpha(b+1)-b)-\frac{r}{d}\right) \\ &+ \rho w\mathcal{B}\left(y^d : \frac{r}{d}+1, (\alpha(b+2)-(b+1))-\frac{r}{d}\right)\Bigg], r = 1, 2, ... \end{aligned} \tag{4.141}$$

where $\mathcal{B}(\cdot : \cdot, \cdot)$ is an incomplete beta function.

Proof. Mathematically,

$$m_r(y) = E(X^r|X \leq y) = \int_0^y x^r f(x)\mathrm{d}x. \tag{4.142}$$

The substitution of equation (4.136) into equation (4.142) gives

$$m_r(y) = \int_0^y x^r \sum_{a=0}^{\infty}\sum_{b=0}^{a} \varpi_{ab} \Big[\alpha(1-\rho)dwx^{d-1}\left(1+x^d\right)^{-w(\alpha(b+1)-b)-1} + \rho dwx^{d-1}\left(1+x^d\right)^{-w(\alpha(b+2)-(b+1))-1}\Big]\mathrm{d}x.$$

We subsequently obtain

$$m_r(y) = dw\sum_{a=0}^{\infty}\sum_{b=0}^{a} \varpi_{ab} \Big[\alpha(1-\rho)\int_0^y x^{r+d-1}\left(1+x^d\right)^{-w(\alpha(b+1)-b)-1}\mathrm{d}x + \rho\int_0^y x^{r+d-1}\left(1+x^d\right)^{-w(\alpha(b+2)-(b+1))-1}\mathrm{d}x\Big].$$

Let $v = x^d$, then $x = v^{1/d}$ and $dx = \frac{1}{d}v^{1/d-1}dv$. It follows that

$$m_r(y) = w\sum_{a=0}^{\infty}\sum_{b=0}^{a} \varpi_{ab} \Big[\alpha(1-\rho)\int_0^{y^d} v^{r/d}(1+v)^{-w(\alpha(b+1)-b)-1}\mathrm{d}v + \rho\int_0^{y^d} v^{r/d}(1+v)^{-w(\alpha(b+2)-(b+1))-1}\mathrm{d}v\Big].$$

Using the identity

$$\mathcal{B}(y:g,h) = \int_0^y v^{g-1}(1+v)^{-(g+h)}\mathrm{d}v,$$

we have

$$m_r(y) = \sum_{a=0}^{\infty}\sum_{b=0}^{a} \varpi_{ab}\Big[\alpha(1-\rho)w\mathcal{B}\left(y^d : \frac{r}{c}+1, w\left(\alpha(b+1)-b\right)-\frac{r}{d}\right) + \rho w\mathcal{B}\left(y^d : \frac{r}{d}+1, w\left(\alpha(b+2)-(b+1)\right)-\frac{r}{d}\right)\Big].$$

4.10.4 Inequality Measures

Comparisons of income distributions across nations can be facilitated using the Lorenz curve and the Bonfenorri curve. These graphical tools enable researchers to visually assess the disparities and changes in income distribution patterns. By examining the shape and positioning of the Lorenz curve, which depicts the cumulative distribution of income, researchers can gain insights into the level of income inequality and the concentration of wealth within a country or across different countries.

Proposition 4.32. The Lorenz curve of the HMBRXII distribution for $\alpha > 1$ is Equation (4.143).

$$\begin{aligned} L(y) = &\frac{1}{\mu}\sum_{a=0}^{\infty}\sum_{b=0}^{a}\varpi_{ab}\Bigg[\alpha(1-\rho)w\mathcal{B}\left(y^d : \frac{1}{d}+1, w\left(\alpha(b+1)-b\right)-\frac{1}{d}\right) \\ &+ \rho w\mathcal{B}\left(y^d : \frac{1}{d}+1, w\left(\alpha(b+2)-(b+1)\right)-\frac{1}{d}\right)\Bigg]. \end{aligned} \tag{4.143}$$

Proof. By definition the Lorenz curve is given by

$$L_F(y) = \frac{1}{\mu}\int_0^y xf(x)\mathrm{d}x.$$

$\int_0^y xf(x)\mathrm{d}x$ as the first incomplete moment completes the proof

Proposition 4.33. The Bonferroni curve of the HMBRXII distribution for $\alpha > 1$ can be expressed as Equation (4.144).

$$\begin{aligned} B(y) = &\frac{1}{\mu F(y)}\sum_{a=0}^{\infty}\sum_{b=0}^{a}\varpi_{ab}\Bigg[\alpha(1-\rho)w\mathcal{B}\left(y^d : \frac{1}{d}+1, w\left(\alpha(b+1)-b\right)-\frac{1}{d}\right) \\ &+ \rho w\mathcal{B}\left(y^d : \frac{1}{d}+1, w\left(\alpha(b+2)-(b+1)\right)-\frac{1}{d}\right)\Bigg]. \end{aligned} \tag{4.144}$$

Proof.

$$B(y) = \frac{L(y)}{F(y)}. \tag{4.145}$$

After substituting equation (4.143) into equation (4.145), we complete the proof.

4.10.5 Mean and Median Deviations

The mean and median deviations serve as useful measures for quantifying the total variation present in distributions. These measures enable researchers to assess the extent of variability or dispersion within a distribution, thereby providing valuable information about the overall pattern and characteristics of the data.

Proposition 4.34. The mean deviation of the HMBRXII distribution for *alpha* > 1 can be expressed as Equation (4.146).

$$\begin{aligned}\Delta_1(x) = 2\mu F(\mu) - 2\sum_{a=0}^{\infty}\sum_{b=0}^{a}\varpi_{ab}\Bigg[&\alpha(1-\rho)w\mathcal{B}\left(\mu^d : \frac{1}{d}+1, w\left(\alpha(b+1)-b\right)-\frac{1}{d}\right)\\ &+\rho w\mathcal{B}\left(\mu^d : \frac{1}{d}+1, w\left(\alpha(b+2)-(b+1)\right)-\frac{1}{d}\right)\Bigg].\end{aligned} \tag{4.146}$$

Proof. Mathematically,

$$\begin{aligned}\Delta_1(x) &= \int_0^{\infty}|x-\mu|f(x)\mathrm{d}x\\ &= \int_0^{\mu}(\mu-x)f(x)\mathrm{d}x + \int_{\mu}^{\infty}(x-\mu)f(x)\mathrm{d}x\\ &= \mu\int_0^{\mu}f(x)\mathrm{d}x - \int_0^{\mu}xf(x)\mathrm{d}x + \mu\int_0^{\mu}f(x)\mathrm{d}x - \int_0^{\mu}xf(x)\mathrm{d}x\\ &+ \int_0^{\infty}xf(x)\mathrm{d}x - \mu\int_0^{\infty}f(x)\mathrm{d}x\\ &= 2\mu F(\mu) - 2\int_0^{\mu}xf(x)\mathrm{d}x.\end{aligned}$$

$\int_0^{\mu}xf(x)\mathrm{d}x$ is the first incomplete moment and if substituted correctly completes the proof.

Proposition 4.35. The median deviation for the HMBRXII distribution for $\alpha > 1$ can be expressed as Equation (4.147).

$$\begin{aligned}\Delta_2(x) = \mu - 2\sum_{a=0}^{\infty}\sum_{b=0}^{a}\varpi_{ab}\Bigg[&\alpha(1-\rho)k\mathcal{B}\left(H^d : \frac{1}{d}+1, w\left(\alpha(b+1)-b\right)-\frac{1}{d}\right)\\ &+\rho w\mathcal{B}\left(H^d : \frac{1}{d}+1, w\left(\alpha(b+2)-(b+1)\right)-\frac{1}{d}\right),\Bigg].\end{aligned} \tag{4.147}$$

where H is the median.

Proof. Mathematically,

$$
\begin{aligned}
\Delta_2(x) &= \int_0^\infty |x - H| f(x)\mathrm{d}x \\
&= \int_0^H (H - x) f(x)\mathrm{d}x + \int_H^\infty (x - H) f(x)\mathrm{d}x \\
&= H\int_0^H f(x)\mathrm{d}x - \int_0^H x f(x)\mathrm{d}x + H\int_0^H f(x)\mathrm{d}x - \int_0^H x f(x)\mathrm{d}x \\
&+ \int_0^\infty x f(x)\mathrm{d}x - H\int_0^\infty f(x)\mathrm{d}x.
\end{aligned}
$$

Using the identity $F(H) = 0.5$, we have

$$
\Delta_2(x) = \mu - 2\int_0^H x f(x)\mathrm{d}x.
$$

$\int_0^H x f(x)\mathrm{d}x$ as the first incomplete moment completes the proof.

4.10.6 Mean Residuals

The mean residual life function is a valuable tool in survival analysis and reliability studies. At any given time point, the mean residual life represents the average remaining lifespan of an individual or system that has already survived up to that time. It provides insights into the additional life expectancy or durability that can be expected for entities that have already reached a certain age.

Proposition 4.36. The mean residual life function of the HMBRXII distribution for $\alpha > 1$ can be expressed as Equation (4.148).

$$
\begin{aligned}
m(t) = \frac{1}{S(t)}\Bigg[\mu - \sum_{a=0}^{\infty}\sum_{b=0}^{a}\varpi_{ab}\Bigg[\alpha(1-\rho)k\mathcal{B}\left(t^d : \frac{1}{d} + 1, w\left(\alpha(b+1) - b\right) - \frac{1}{d}\right) \\
+ \rho w\mathcal{B}\left(t^d : \frac{1}{d} + 1, w\left(\alpha(b+2) - (b+1)\right) - \frac{1}{d}\right)\Bigg]\Bigg] - t.
\end{aligned} \tag{4.148}
$$

Proof. Mathematically,

$$m(t) = E(X - t|X > t) = \frac{1}{S(t)} \int_t^{\infty} (x - t) f(x) \mathrm{d}x, t \geq 0.$$

Hence,

$$m(t) = \frac{1}{S(t)} \left[\mu - \int_0^t (x) f(x) \mathrm{d}x \right] - t. \tag{4.149}$$

The substitution of equation (3.15) and $\int_0^t x f(x) \mathrm{d}x$, the first incomplete moment into equation (4.149) completes the proof.

4.10.7 Moment Generating Function

If the MGF exists for a given distribution, it serves as a useful tool for calculating various moments of that distribution. By manipulating the MGF, we can obtain important statistical measures and characteristics, such as the mean, variance, and higher-order moments.

Proposition 4.37. The MGF of the HMBRXII distribution can be expressed as Equation (4.150).

$$\begin{aligned} M(t) = & \sum_{a=0}^{\infty} \sum_{b=0}^{a} \sum_{r=0}^{\infty} \varpi_{ab} \frac{t^r}{r!} \left[\alpha(1-\rho) w \mathcal{B} \left(\frac{r}{d} + 1, w\left(\alpha(b+1) - b\right) - \frac{r}{d} \right) \right. \\ & \left. + \rho w \mathcal{B} \left(\frac{r}{d} + 1, w\left(\alpha(b+2) - (b+1)\right) - \frac{r}{d} \right) \right], \end{aligned} \tag{4.150}$$

Proof. Using the identity

$$e^{tX} = \sum_{r=0}^{\infty} \frac{t^r X^r}{r!},$$

we deduce the MGF as

$$M(t) = E(e^{tX}) = \sum_{r=0}^{\infty} \frac{t^r E(X^r)}{r!} = \sum_{r=0}^{\infty} \frac{t^r}{r!} \mu_r^{'}. \tag{4.151}$$

After substituting equation (4.140) into equation (4.151), we complete the proof.

4.10.8 Characteristic Function

Characteristic functions are particularly useful in situations where traditional moment generating functions are insufficient for describing heavy-tailed random variables. They provide a powerful tool for analysing and understanding the properties of such distributions.

Proposition 4.38. The characteristic function of the HMBRXII distribution for $\alpha > 1$ is given as Equation (4.152).

$$\begin{aligned} C(t) = & \sum_{a=0}^{\infty}\sum_{b=0}^{a}\sum_{r=0}^{\infty} \varpi_{ab} \frac{(zt)^r}{r!} \left[\alpha(1-\rho) w \mathcal{B}\left(w\left(\alpha(b+1)-b\right) - \frac{r}{d}, \frac{r}{d}+1 \right) \right. \\ & \left. + \rho w \mathcal{B}\left(w\left(\alpha(b+2)-(b+1)\right) - \frac{r}{d}, \frac{r}{d}+1 \right) \right], \end{aligned} \tag{4.152}$$

Proof. Using the identity

$$e^{ztX} = \sum_{r=0}^{\infty} \frac{z^r t^r X^r}{r!},$$

where $z = \sqrt{-1}$. We can define the characteristic function as

$$C(t) = E(e^{ztX}) = \sum_{r=0}^{\infty} \frac{(zt)^r E(X^r)}{r!} = \sum_{r=0}^{\infty} \frac{(zt)^r}{r!} \mu_r^{'}. \tag{4.153}$$

After substituting equation (4.140) into equation (4.153), we complete the proof.

4.10.9 Entropy

The entropy of the HMBRXII distribution allows us to quantify the level of variability or uncertainty present in a distribution. A lower entropy value indicates a reduced level of uncertainty, implying a more predictable distribution. On the other hand, a higher entropy value suggests a greater degree of variation and uncertainty in the distribution, indicating a wider spread of possible outcomes. Thus, the entropy serves as a measure of the randomness within the HMBRXII distribution.

Proposition 4.39. The Rényi entropy of the HMBRXII distribution for $\alpha > 1$ can be expressed as Equation (4.154).

$$I_R(\delta)=\frac{(dw)^{\delta}}{d(1-\delta)}\log\sum_{a=0}^{\infty}\sum_{b=0}^{a}\sum_{l=0}^{\infty}\psi^{*}_{abl}\mathcal{B}\left(w\left(\alpha\delta+(\alpha-1)(b-l)\right)-\frac{(\delta-1)}{d},\delta-\frac{(\delta-1)}{d}\right),\delta\neq 1, \tag{4.154}$$

where

$\psi^{*}_{abl}=(-1)^{b}\binom{2\delta+a-1}{a}\binom{a}{b}\binom{l}{\delta}\rho^{a+l}(\alpha(1-\rho))^{\delta-l}$.

Proof. Mathematically,

$$I_R(\delta)=\frac{1}{1-\delta}\log\int_0^{\infty}f^{\delta}(x)\mathrm{d}x,\delta\neq 1. \tag{4.155}$$

The PDF of HMBRXII to the power δ is given as

$$f^{\delta}(x)=\frac{(dw)^{\delta}x^{\delta(d-1)}\left(1+x^{d}\right)^{-\delta(\alpha w+1)}(\alpha(1-\rho))^{\delta}\left(1+\frac{\rho\left(1+x^{d}\right)^{-w(\alpha-1)}}{\alpha(1-\rho)}\right)^{\delta}}{\left[1-\rho\left(1-\left(1+x^{d}\right)^{-w(\alpha-1)}\right)\right]^{2\delta}}$$

We then use Taylor series to obtain

$$\left[1-\rho\left(1-\left(1+x^{d}\right)^{-w(\alpha-1)}\right)\right]^{2\delta}=\sum_{a=0}^{\infty}\sum_{b=0}^{a}(-1)^{b}\binom{2\delta+a-1}{a}\binom{a}{b}\rho^{a}\left(1+x^{d}\right)^{-w(\alpha-1)b}$$

and

$$\left(1+\frac{\rho\left(1+x^{d}\right)^{-w(\alpha-1)}}{\alpha(1-\rho)}\right)^{\delta}=\sum_{l=0}^{\infty}\binom{l}{\delta}\rho^{l}(\alpha(1-\rho))^{-l}\left(1+x^{d}\right)^{-w(\alpha-1)l}.$$

We then obtain

$$f^{\delta}(x)=(dw)^{\delta}\sum_{a=0}^{\infty}\sum_{b=0}^{a}\sum_{l=0}^{\infty}\psi^{*}_{abl}x^{\delta(c-1)}\left(1+x^{d}\right)^{-w(\alpha\delta+(\alpha-1)(b-l))}, \tag{4.156}$$

Substituting equation (4.156) into equation (4.155) gives

$$I_R(\delta)=\frac{(dw)^{\delta}}{1-\delta}\log\int_0^{\infty}\sum_{a=0}^{\infty}\sum_{b=0}^{a}\sum_{l=0}^{\infty}\psi^{*}_{abl}x^{\delta(d-1)}\left(1+x^{d}\right)^{-w(\alpha\delta+(\alpha-1)(b-l))}\mathrm{d}x. \tag{4.157}$$

Let $v = x^d$ then $x = v^{1/d}$ and $dx = \frac{1}{d}v^{1/d-1}dv$. We then obtain

$$\int_0^\infty f^\delta(x)\mathrm{d}x = \frac{(dw)^\delta}{d}\sum_{a=0}^{\infty}\sum_{b=0}^{a}\sum_{l=0}^{\infty}\psi^*_{abl}v^{\delta-(\frac{\delta-1}{d})-1}(1+v)^{-w(\alpha\delta+(\alpha-1)(b-l))}\,\mathrm{d}v.$$

But $\mathcal{B}(g,h) = \int_0^\infty v^{g-1}(1+v)^{-(g+h)}\mathrm{d}v$.

The Rényi entropy of the HMBRXII distribution is obtained after correctly substituting into equation (4.157).

4.10.10 Stress-Strength Reliability

The concept of stress-strength reliability is particularly relevant in fields such as engineering, materials science, and structural analysis, where it is essential to ensure the reliability and safety of systems and structures. It allows engineers and designers to assess whether the strength of a system or component is sufficient to withstand the expected stress or load it will encounter during its operational lifespan.

Proposition 4.40. For the HMBRXII distribution with $\alpha > 1$, the stress-strength reliability can be expressed as Equation (4.158).

$$R_{ss} = 1 - \left[\sum_{a=0}^{\infty}\sum_{b=0}^{a}\delta_{ab}\left(\frac{\alpha(1-\rho)}{(\alpha(b+2)-b)} + \frac{\rho}{(\alpha(b+3)-(b+1))}\right)\right]., \tag{4.158}$$

where $\delta_{ab} = (-1)^b\binom{a+2}{2}\binom{a}{b}\rho^a$.

Proof. Mathematically,

$$R_{ss} = \int_0^\infty f(x)\cdot F(x)\mathrm{d}x = 1 - \int_0^\infty f(x)\cdot S(x)\mathrm{d}x. \tag{4.159}$$

Multiplying equations (3.14) and (3.15), we have

$$f(x)\cdot S(x) = \frac{\alpha\left(1-\rho\right)dwx^{d-1}\left(1+x^d\right)^{-2\alpha w-1} + \rho dwx^{d-1}\left(1+x^d\right)^{-w(3\alpha-1)-1}}{\left[1-\rho\left(1-\left(1+x^d\right)^{-w(\alpha-1)}\right)\right]^3}, \tag{4.160}$$

Using the Taylor series we simplify equation(4.160) as

$$f(x)\cdot S(x)=\sum_{a=0}^{\infty}\sum_{b=0}^{a}\delta_{ab}\Big[\alpha(1-\rho)dwx^{d-1}\left(1+x^{d}\right)^{-w(\alpha(b+2)-b)-1}$$
$$+\rho dwx^{d-1}\left(1+x^{d}\right)^{-w(\alpha(b+3)-(b+1))-1}\Big]. \tag{4.161}$$

The substitution of equation (4.161) into equation (4.159) yields

$$R_{ss}=1-\Bigg[\sum_{a=0}^{\infty}\sum_{b=0}^{a}\delta_{ab}\int_{0}^{\infty}\Big[\alpha(1-\rho)dwx^{d-1}\left(1+x^{d}\right)^{-w(\alpha(b+2)-b)-1}$$
$$+\rho dwx^{d-1}\left(1+x^{d}\right)^{-w(\alpha(b+3)-(b+1))-1}\Big]\mathrm{d}x\Bigg].$$

Let $v=x^{d}$, then $x=v^{1/d}$ and $dx=\frac{1}{d}v^{1/d-1}dv$. We then have

$$R_{ss}=1-\Bigg[\sum_{a=0}^{\infty}\sum_{b=0}^{a}\delta_{ab}k\int_{0}^{\infty}\Big[\alpha(1-\rho)\left(1+v\right)^{-w(\alpha(b+2)-b)-1}$$
$$+\rho\left(1+v\right)^{-w(\alpha(b+3)-(b+1))-1}\Big]\mathrm{d}v\Bigg].$$

Simplifying further we obtain,

$$R_{ss}=1-\Bigg[\sum_{a=0}^{\infty}\sum_{b=0}^{a}\delta_{ab}\left(\frac{\alpha(1-\rho)}{(\alpha(b+2)-b)}+\frac{\rho}{(\alpha(b+3)-(b+1))}\right)\Bigg].$$

The proof is complete

4.10.11 Order Statistics

Order statistics play a valuable role in identifying both the maximum and minimum values within a set of observations from a random variable. They provide a systematic way to arrange the data in ascending or descending order, allowing us to determine the extreme values within the dataset. This information is particularly useful in analysing the distribution's tail behaviour and understanding the range of values that the random variable can take.

Proposition 4.41. If $X_{11},X_{12},X_{13},...,X_{1n}$ is a random variable from the HMBRXII distribution with order statistics $X_{(11)}, X_{(12)}, X_{(13)}, ..., X_{(1n)}$, then the PDF of the p^{th} order statistics X_{1P} for $\alpha > 1$ is given as Equation (4.162).

$$f_{p:n}(x) = \frac{1}{\beta(p, n-p+1)}\left[\sum_{a=0}^{\infty}\sum_{b=0}^{a}\sum_{l=0}^{n-p}\sum_{m=0}^{p+l-1}\psi^{*}_{ablm}\left(\alpha\left(1-\rho\right)dwx^{d-1}\left(1+x^{d}\right)^{-w(\alpha(b+1)+m)-1}\right.\right.$$
$$\left.\left.+\rho dwx^{d-1}\left(1+x^{d}\right)^{-w(\alpha(b+2)+m-(b+1))-1}\right)\right], \tag{4.162}$$

where $\psi^{*}_{ablm} = (-1)^{b+l+m}\binom{m+a-1}{a}\binom{a}{b}\binom{n-p}{l}\binom{p+l-1}{m}\rho^{a}$

Proof. By definition

$$f_{p:n}(x) = \frac{1}{\beta(p, n-p+1)}\left(F(x)\right)^{p-1}\left(1-F(x)\right)^{n-p}f(x). \tag{4.163}$$

Applying Taylor series,

$$\left(1-F(x)\right)^{n-p} = \sum_{l=0}^{n-p}(-1)^{l}\binom{n-p}{l}\left(F(x)\right)^{l}.$$

We then obtain,

$$f_{p:n}(x) = \frac{1}{\beta(p, n-p+1)}\sum_{l=0}^{n-p}\sum_{m=0}^{p+l-1}(-1)^{l+m}\binom{n-p}{l}\binom{p+l-1}{m}\left(S(x)\right)^{m}f(x). \tag{4.164}$$

Raising equation (3.15) to the power m and subsequently multiplying it with equation (3.14), we obtain

$$\left(S(x)\right)^{m}f(x) = \frac{\alpha\left(1-\rho\right)dwx^{d-1}\left(1+x^{d}\right)^{-w(\alpha+m)-1} + \rho dwx^{d-1}\left(1+x^{d}\right)^{-w(2\alpha+m-1)-1}}{\left[1-\rho\left(1-\left(1+x^{d}\right)^{-w(\alpha-1)}\right)\right]^{m+2}}$$

Applying Taylor series , we have

$$\left(S(x)\right)^{m}f(x) = \sum_{a=0}^{\infty}\sum_{b=0}^{a}\psi_{ab}\left[\alpha\left(1-\rho\right)dwx^{d-1}\left(1+x^{d}\right)^{-w(\alpha(b+1)+m)-1}\right.$$
$$\left.+\rho dwx^{d-1}\left(1+x^{d}\right)^{-w(\alpha(b+2)+m-(b+1))-1}\right], \tag{4.165}$$

where $\psi_{ab} = (-1)^b \binom{m+a-1}{a}\binom{a}{b}\rho^a$

After substituting equation (4.165) into equation (4.164), we complete the proof.

Proposition 4.42. The r^{th} non-central moment of the p^{th} order statistics for $\alpha > 1$ is given by Equation (4.166).

$$\mu_r^{p:n} = \frac{1}{\beta(p, n-p+1)}\Bigg[\sum_{a=0}^{\infty}\sum_{b=0}^{a}\sum_{l=0}^{n-p}\sum_{m=0}^{p+l-1}\psi^*_{ablm}\Bigg(\alpha\,(1-\rho)\,w\mathcal{B}(w(\alpha(b+1)+m)-\frac{r}{d},\frac{r}{d}+1) + \rho w\mathcal{B}(w(\alpha(b+2)+m-(b+1))-\frac{r}{d},\frac{r}{d}+1)\Bigg)\Bigg]. \tag{4.166}$$

Proof. By definition

$$\mu_r^{p:n} = \int_0^{\infty} x^r f_{p:n}(x)\mathrm{d}x. \tag{4.167}$$

The substitution of equation (4.162) into equation (4.167) yields

$$\mu_r^{p:n} = \frac{1}{\beta(p, n-p+1)}\Bigg[\sum_{a=0}^{\infty}\sum_{b=0}^{a}\sum_{l=0}^{n-p}\sum_{m=0}^{p+l-1}\psi^*_{ablm}\int_0^{\infty}\Bigg(\alpha\,(1-\rho)\,dwx^{r+d-1}\left(1+x^d\right)^{-w(\alpha(b+1)+m)-1} + \rho dwx^{r+d-1}\left(1+x^d\right)^{-w(\alpha(b+2)+m-(b+1))-1}\Bigg)\mathrm{d}x\Bigg].$$

The integral required can be derived from the method used in obtaining the non-central moment. We then get the desired equation after substituting correctly.

4.10.12 Identifiability

To ensure that accurate inferences are made, the HMBRXII distribution's identifiability property is presented.

Proposition 4.43. If X_1 and X_2 are random variables from the HMBRXII distribution with CDF $F_X(x;\alpha_1,\rho_1,d_1,w_1)$ and $F_X(x;\alpha_2,\rho_2,d_2,w_2)$ respectively, then the HMBRXII distribution is identifiable if and only if $\alpha_1 = \alpha_2$, $\rho_1 = \rho_2$, $d_1 = d_2$ and $w_1 = w_2$.

Proof. For HMBRXII distribution to be idenfiable, $F_X(x;\alpha_1,\rho_1,d_1,w_1) = F_X(x;\alpha_2,\rho_2,d_2,w_2)$. Then

$$1 - \frac{\left(1+x^{d_1}\right)^{-\alpha_1 w_1}}{\left[1-\rho_1\left(1-(1+x^{d_1})^{-w_1(\alpha_1-1)}\right)\right]} = 1 - \frac{\left(1+x^{d_2}\right)^{-\alpha_2 w_2}}{\left[1-\rho_2\left(1-(1+x^{d_2})^{-w_2(\alpha_2-1)}\right)\right]}$$

If $\alpha_1 = \alpha_2$, $\rho_1 = \rho_2$, $d_1 = d_2$ and $w_1 = w_2$, then

$$\frac{\left(1+x^{c_1}\right)^{-\alpha_1 k_1}}{\left[1-\rho_1\left(1-(1+x^{d_1})^{-w_1(\alpha_1-1)}\right)\right]} - \frac{\left(1+x^{d_2}\right)^{-\alpha_2 k_2}}{\left[1-\rho_2\left(1-(1+x^{d_2})^{-w_2(\alpha_2-1)}\right)\right]} = 0$$

The identifiability requirement has been met.

4.11 Estimation of Parameters of the Harmonic Mixture Burr XII Distribution

In this section, we employ five different estimation methods to obtain the parameter estimates for the HMBRXII distribution. These methods include MLE, OLS, WLS, CVM, and ADE. By employing these estimation techniques, we can determine the most appropriate parameter values that best fit the observed data and characterise the HMBRXII distribution.

4.11.1 Maximum Likelihood Estimation

By applying the MLE to the HMBRXII distribution, researchers can obtain parameter estimates that are optimal in terms of maximising the likelihood of the observed data and capturing the underlying characteristics of the distribution. For the HMBRXII distribution, the likelihood function can be expressed as Equation (4.168).

$$L\left(x,\alpha,\rho,d,w\right) = \prod_{a=1}^{n} f(x_a,\alpha,\rho,d,w). \tag{4.168}$$

We substitute equation (4.132) into (4.168) and thereafter obtain the log-likelihood function given as Equation (4.169).

$$
\begin{aligned}
l(x, \alpha, \rho, d, w) &= n \ln(dw) + (d-1) \sum_{a=1}^{n} \ln x_a + \sum_{a=1}^{n} \ln \left[\alpha(1-\rho) + \rho \left(1 + x_a^d\right)^{-w(\alpha-1)} \right] \\
&- 2 \sum_{a=1}^{n} \ln \left[1 - \rho \left(1 - \left(1 + x_a^d\right)^{-w(\alpha-1)} \right) \right].
\end{aligned}
\tag{4.169}
$$

To estimate the parameters using the MLE approach, we utilise the method of differentiation. By differentiating equation (4.169) with respect to the parameters (α, ρ, d, w) and setting the equations obtained to zero, we can derive a system of equations. These equations when solved using numerical methods gives the parameter estimates. The derivatives obtained are as follows

$$
\begin{aligned}
\frac{\partial l}{\partial \rho} &= \sum_{a=1}^{n} \frac{\left(1 + x_a^d\right)^{-w(\alpha-1)-\alpha}}{\alpha(1-\rho) + \rho\left(1 + x_a^d\right)^{-w(\alpha-1)}} - \sum_{a=1}^{n} \frac{2\left(-1 + \left(1 + x_a^d\right)^{-w(\alpha-1)}\right)}{\left[1 - \rho + \rho\left(1 + x_a^d\right)^{-w(\alpha-1)}\right]}, \\
\frac{\partial l}{\partial \alpha} &= \sum_{a=1}^{n} \left(1 + x_a^d\right)^{-w(\alpha-1)} \left[\frac{2\rho w \ln(1 + x_a^d)}{1 - \rho + \rho\left(1 + x_i^d\right)^{-w(\alpha-1)}} \right. \\
&- \left. \frac{(\rho - 1)\left(1 + x_a^d\right)^{-w(\alpha-1)} + \rho w \ln(1 + x_a^d)}{\alpha(1-\rho) + \rho\left(1 + x_a^d\right)^{-w(\alpha-1)}} \right], \\
\frac{\partial l}{\partial d} &= \frac{n}{d} + \sum_{a=1}^{n} \ln x_a + \sum_{a=1}^{n} w\rho(\alpha-1) x_a^d \ln x_a \left(1 + x_a^d\right)^{-w(\alpha-1)-1} \left[\frac{2}{1 - \rho + \rho\left(1 + x_a^d\right)^{-w(\alpha-1)}} \right. \\
&- \left. \frac{1}{\alpha(1-\rho) + \rho\left(1 + x_a^d\right)^{-w(\alpha-1)}} \right], \\
\frac{\partial l}{\partial w} &= \frac{n}{w} + \sum_{a=1}^{n} \rho(\alpha-1) \ln(1 + x_a^d) \left(1 + x_a^d\right)^{-w(\alpha-1)} \left[\frac{2}{1 - \rho + \rho\left(1 + x_a^d\right)^{-w(\alpha-1)}} \right. \\
&- \left. \frac{1}{\alpha(1-\rho) + \rho\left(1 + x_a^d\right)^{-w(\alpha-1)}} \right].
\end{aligned}
$$

4.11.2 Ordinary Least Squares

The OLSS method is used to estimate the unknown parameters of the HMBRXII distribution by minimising a specific function. The objective of this minimisation is to find the parameter values that minimise the discrepancies between the observed data and the predicted values based on the HMBRXII distribution. These estimates are derived by minimising Equation (4.170).

$$LS(\alpha, \rho, d, w) = \sum_{b=1}^{n} \left\{ \left(F(x_{(b)})\right) - \frac{b}{n+1} \right\}^2. \tag{4.170}$$

The method of differentiation is employed to minimise equation (4.170). We differentiate with respect to each parameter and equate the resulting equations to zero, obtaining

$$\frac{\partial LS}{\partial \alpha} = \sum_{b=1}^{n} \left\{ \left(F(x_{(b)})\right) - \frac{b}{n+1} \right\} \cdot \Lambda_1(x_{(b)}; \alpha, \rho, d, w) = 0, \tag{4.171}$$

$$\frac{\partial LS}{\partial \rho} = \sum_{b=1}^{n} \left\{ \left(F(x_{(b)})\right) - \frac{b}{n+1} \right\} \cdot \Lambda_2(x_{(b)}; \alpha, \rho, d, w) = 0, \tag{4.172}$$

$$\frac{\partial LS}{\partial d} = \sum_{b=1}^{n} \left\{ \left(F(x_{(b)})\right) - \frac{b}{n+1} \right\} \cdot \Lambda_3(x_{(b)}; \alpha, \rho, d, w) = 0, \tag{4.173}$$

$$\frac{\partial LS}{\partial w} = \sum_{b=1}^{n} \left\{ \left(F(x_{(b)})\right) - \frac{b}{n+1} \right\} \cdot \Lambda_4(x_{(b)}; \alpha, \rho, d, w) = 0, \tag{4.174}$$

where

$$\Lambda_1(x_{(b)}) = \frac{w \ln(1 + x_b^d) \left[\left(1 + x_b^d\right)^{-w\alpha} \left(1 - \rho \left(1 - \left(1 + x_b^d\right)^{-w(\alpha-1)}\right)\right) - \rho \left(1 + x_b^d\right)^{-w(2\alpha-1)} \right]}{\left[1 - \rho \left(1 - \left(1 + x_b^d\right)^{-w(\alpha-1)}\right)\right]^2}, \tag{4.175}$$

$$\Lambda_2(x_{(b)}) = \frac{\left(1 + x_b^d\right)^{-w\alpha} \left(\left(1 + x_b^d\right)^{-w(\alpha-1)} - 1\right)}{\left[1 - \rho \left(1 - \left(1 + x_b^d\right)^{-w(\alpha-1)}\right)\right]^2}, \tag{4.176}$$

$$\Lambda_3(x_{(b)}) = \frac{k x_b^d \ln x_b \left[\alpha \left(1 + x_b^d\right)^{-w(\alpha+1)} \left(1 - \rho \left(1 - \left(1 + x_b^d\right)^{-w(\alpha-1)}\right)\right) - \rho(\alpha - 1) \left(1 + x_b^d\right)^{-w(2\alpha-1)}\right]}{\left[1 - \rho \left(1 - \left(1 + x_b^d\right)^{-w(\alpha-1)}\right)\right]^2}, \tag{4.177}$$

$$\Lambda_4(x_{(b)}) = \frac{\ln(1+x_b^d)\left[\alpha\left(1+x_b^d\right)^{-w\alpha}\left(1-\rho\left(1-\left(1+x_b^d\right)^{-w(\alpha-1)}\right)\right)-\rho(\alpha-1)\left(1+x_b^d\right)^{-w(2\alpha-1)}\right]}{\left[1-\rho\left(1-\left(1+x_b^d\right)^{-w(\alpha-1)}\right)\right]^2}. \tag{4.178}$$

These equations obtained are solved simultaneously using numerical methods to obtain the parameter estimates.

4.11.3 Weighted Least Squares

The WLSS method is utilised to estimate the unknown parameters of the HMBRXII distribution by minimising a specific function. This minimisation process aims to find the parameter values that minimise the discrepancies between the observed data and the predicted values based on the HMBRXII distribution, taking into account the weights assigned to each data point. The minimisation function is given as Equation (4.179).

$$WLS(\alpha,\rho,d,w) = \sum_{b=1}^{n}\frac{(n+1)^2(n+2)}{b(n-b+1)}\left\{\left(F(x_{(b)})\right)-\frac{b}{n+1}\right\}^2. \tag{4.179}$$

The method of differentiation is employed to minimise equation (4.179). We differentiate with respect to each parameter and equate the resulting equations to zero, obtaining

$$\frac{\partial WLS}{\partial \alpha} = \sum_{b=1}^{n}\frac{(n+1)^2(n+2)}{b(n-b+1)}\left\{\left(F(x_{(b)})\right)-\frac{b}{n+1}\right\}\cdot\Lambda_1(x_{(b)};\alpha,\rho,d,w)=0, \tag{4.180}$$

$$\frac{\partial WLS}{\partial \rho} = \sum_{b=1}^{n}\frac{(n+1)^2(n+2)}{b(n-b+1)}\left\{\left(F(x_{(b)})\right)-\frac{b}{n+1}\right\}\cdot\Lambda_2(x_{(b)};\alpha,\rho,d,w)=0, \tag{4.181}$$

$$\frac{\partial WLS}{\partial d} = \sum_{b=1}^{n}\frac{(n+1)^2(n+2)}{b(n-b+1)}\left\{\left(F(x_{(b)})\right)-\frac{b}{n+1}\right\}\cdot\Lambda_3(x_{(b)};\alpha,\rho,d,w)=0, \tag{4.182}$$

$$\frac{\partial WLS}{\partial w} = \sum_{b=1}^{n} \frac{(n+1)^2(n+2)}{b(n-b+1)} \left\{ \left(F(x_{(b)})\right) - \frac{b}{n+1} \right\} \cdot \Lambda_4(x_{(b)}; \alpha, \rho, d, w) = 0. \quad (4.183)$$

$\Lambda_p(x_{(b)}; \alpha, \rho, d, w)$, $(p = 1, 2, 3, 4)$, can be obtained through equations (4.175), (4.176), (4.177) and (4.178).

These equations obtained are solved simultaneously using numerical methods to obtain the parameter estimates.

4.11.4 Cramér-Von Mises Estimation

The CVM method is employed to estimate the unknown parameters of the HMBRXII distribution by minimising a specific function. This minimisation process aims to find the parameter values that minimise the discrepancy between the observed data and the theoretical distribution based on the HMBRXII distribution. The minimisation function is given as Equation (4.184).

$$CVM(\alpha, \rho, d, w) = \frac{1}{12n} + \sum_{b=1}^{n} \left\{ \left(F(x_{(b)})\right) - \frac{2b-1}{2n} \right\}^2. \quad (4.184)$$

The method of differentiation is employed to minimise equation (4.184). We differentiate with respect to each parameter and equate the resulting equations to zero, obtaining

$$\frac{\partial CVM}{\partial \alpha} = \sum_{b=1}^{n} \left\{ \left(F(x_{(b)})\right) - \frac{2b-1}{2n} \right\} \cdot \Lambda_1(x_{(b)}; \alpha, \rho, d, w) = 0, \quad (4.185)$$

$$\frac{\partial CVM}{\partial \rho} = \sum_{b=1}^{n} \left\{ \left(F(x_{(b)})\right) - \frac{2b-1}{2n} \right\} \cdot \Lambda_2(x_{(b)}; \alpha, \rho, d, w) = 0, \quad (4.186)$$

$$\frac{\partial CVM}{\partial d} = \sum_{b=1}^{n} \left\{ \left(F(x_{(b)})\right) - \frac{2b-1}{2n} \right\} \cdot \Lambda_3(x_{(b)}; \alpha, \rho, d, w) = 0, \quad (4.187)$$

$$\frac{\partial CVM}{\partial w} = \sum_{b=1}^{n} \left\{ \left(F(x_{(b)})\right) - \frac{2b-1}{2n} \right\} \cdot \Lambda_4(x_{(b)}; \alpha, \rho, d, w) = 0, \quad (4.188)$$

$\Lambda_p(x_{(b)}; \alpha, \rho, d, w)$, $(p = 1, 2, 3, 4)$, can be obtained through equations (4.175), (4.176), (4.177) and (4.178).

These equations obtained are solved simultaneously using numerical methods to obtain the parameter estimates.

4.11.5 Anderson-Darling Estimation

The AD method is utilised to estimate the unknown parameters of the HMBRXII distribution by minimising a specific function. This minimisation process aims to find the parameter values that minimise the difference between the observed data and the theoretical distribution based on the HMBRXII distribution. The minimisation function is given as Equation (4.189).

$$AD(\alpha,\rho,d,w) = -n - \frac{1}{n}\sum_{b=1}^{n}(2b-1)\cdot\left\{\left(\log F(x_{(b)})\right) + \log\left(1 - F(x_{(n+1-b)})\right)\right\}. \quad (4.189)$$

The method of differentiation is employed to minimise equation (4.189). We differentiate with respect to each parameter and equate the resulting equations to zero, obtaining

$$\frac{\partial AD}{\partial \alpha} = \sum_{b=1}^{n}(2b-1)\left\{\frac{\Lambda_1(x_{(b)};\alpha,\rho,d,w)}{\left(F(x_{(b)})\right)} - \frac{\Lambda_1(x_{(n+1-b)};\alpha,\rho,d,w)}{1-\left(F(x_{(n+1-b)})\right)}\right\} = 0, \quad (4.190)$$

$$\frac{\partial AD}{\partial \rho} = \sum_{b=1}^{n}(2b-1)\left\{\frac{\Lambda_2(x_{(b)};\alpha,\rho,d,w)}{\left(F(x_{(b)})\right)} - \frac{\Lambda_2(x_{(n+1-b)};\alpha,\rho,d,w)}{1-\left(F(x_{(n+1-b)})\right)}\right\} = 0, \quad (4.191)$$

$$\frac{\partial AD}{\partial d} = \sum_{b=1}^{n}(2b-1)\left\{\frac{\Lambda_3(x_{(b)};\alpha,\rho,d,w)}{\left(F(x_{(b)})\right)} - \frac{\Lambda_3(x_{(n+1-b)};\alpha,\rho,d,w)}{1-\left(F(x_{(n+1-b)})\right)}\right\} = 0, \quad (4.192)$$

$$\frac{\partial AD}{\partial w} = \sum_{b=1}^{n}(2b-1)\left\{\frac{\Lambda_4(x_{(b)};\alpha,\rho,d,w)}{\left(F(x_{(b)})\right)} - \frac{\Lambda_4(x_{(n+1-b)};\alpha,\rho,d,w)}{1-\left(F(x_{(n+1-b)})\right)}\right\} = 0, \quad (4.193)$$

where $\Lambda_p(x_{(\cdot)};\alpha,\rho,d,w)$, $(p = 1,2,3,4)$, can be derived from the equations (4.175), (4.176), (4.177) and (4.178).

These equations obtained are solved simultaneously using numerical methods to obtain the parameter estimates.

4.12 The Log-Harmonic Mixture Burr XII Regression Model

By applying a log transform to the random variable X that follows the HMBRXII distribution, we define a new variable Y as the natural logarithm of τX, where τ is a positive parameter. This transformation results in a log-linear regression model. To characterise the distribution of Y, we redefine the parameters as $d = 1/\sigma$ and $\tau = e^{\mu}$. This redefinition allows us to express the density function of Y in terms of the new parameters σ and μ in Equation (4.194).

$$f(y) = \frac{\frac{\alpha w(1-\rho)}{\sigma}\exp(\frac{y-\mu}{\sigma})\left(1+\exp(\frac{y-\mu}{\sigma})\right)^{-\alpha w-1} + \frac{\rho w}{\sigma}\exp(\frac{y-\mu}{\sigma})\left(1+\exp(\frac{y-\mu}{\sigma})\right)^{-w(2\alpha-1)-1}}{\left[1-\rho\left(1-\left(1+\exp(\frac{y-\mu}{\sigma})\right)^{-w(\alpha-1)}\right)\right]^2}, \tag{4.194}$$

where $y > 0$, $\sigma > 0$, $w > 0$, $\alpha > 0$, $0 < \rho < 1$ and $\mu \in \mathbb{R}$.

The equation (4.194) represents the PDF of the Log-Harmonic Mixture Burr XII (LHMBXII) distribution. In this distribution, the parameter μ represents the location parameter, while σ represents the scale parameter.

If a random variable X follows the HMBRXII distribution with parameters (α, ρ, d, w), then the logarithmically transformed variable Y, defined as $Y = \log(\tau X)$, follows the LHMBRXII distribution with parameters $(\alpha, \rho, w, \sigma, \mu)$.

The SF of the LHMBRXII can be expressed as Equation (4.195).

$$S(y) = \frac{\left(1+\exp(\frac{y-\mu}{\sigma})\right)^{-\alpha w}}{\left[1-\rho\left(1-\left(1+\exp(\frac{y-\mu}{\sigma})\right)^{-w(\alpha-1)}\right)\right]}. \tag{4.195}$$

We present a log-linear regression model that incorporates the response variable y_i and covariates $Z_a^T = (1, z_{a1}, ..., z_{ap})$. The model is defined as

$$y_a = Z_a^T \boldsymbol{\beta} + \sigma\chi_i.$$

Here, for each observation a ranging from 1 to n, we have the coefficients of the regression of the covariates denoted as $\boldsymbol{\beta} = (\beta_1, \beta_2, ...\beta_p)^T$. The scale parameter is represented as σ, and χ_a corresponds to the random error. The location parameter of y_a is defined as $\mu_a = Z_a^T \boldsymbol{\beta}$. By maximising log-likelihood function, the MLE provides estimates for the parameters that best align with the observed data and the assumed HMGOM regression model. The log-likelihood function, which is used to estimate the parameters $\Omega = (\alpha, \rho, w, \sigma, \beta^T)^T$ of the model, can be written as Equation (4.196).

$$
\begin{aligned}
l(\Omega) &= n\left(\ln(w) - \ln(\sigma)\right) + \sum_{a=1}^{n} \frac{y_a - \mu_a}{\sigma} \\
&+ \sum_{a=1}^{n} \ln\left[\alpha(1-\rho) + \rho\left(1 + e^{\frac{y_a-\mu_a}{\sigma}}\right)^{-w(\alpha-1)}\right] - 2\sum_{a=1}^{n} \ln\left[1 - \rho\left(1 - \left(1 + e^{\frac{y_a-\mu_a}{\sigma}}\right)^{-w(\alpha-1)}\right)\right].
\end{aligned}
\tag{4.196}
$$

CHAPTER 5

SIMULATIONS AND APPLICATIONS

5.1 Introduction

In this chapter, we present the findings of the Monte Carlo simulations and the practical applications of the proposed distributions and regression models on datasets related to lifetimes. We calculate the Average Bias (AB) and their respective Mean Square Error (MSE) for the estimation methods such as MLE, OLSS, WLSS, CVM, and AD with:

$$AB = \frac{1}{1000}\sum_{i=1}^{1000}|\hat{V}_i - V|,$$

and

$$MSE = \frac{1}{1000}\sum_{i=1}^{1000}\left(\hat{V}_i - V\right)^2.$$

The goodness-of-fit of the chosen distributions was evaluated using the Kolmogorov-Smirnov Test (KS), Anderson-Darling Test (A) and Cramér-von Mises Test (W) statistics. The selection of the most suitable model for the dataset was based on the least Akaike Information Criterion (AIC), Consistent Akaike Information Criterion (AICC) and Bayesian Information Criterion (BIC). Furthermore, the model with the lowest values for the KS, A, and W test statistics was considered the best fit for the data.

$$AIC = -2\log(\hat{\theta}) + 2k,$$

$$AICC = AIC + \frac{2k(k+1)}{n-k-1}$$

and

$$BIC = -2\log(\hat{\theta}) + k\log(n).$$

5.2 Monte Carlo Simulations of the Harmonic Mixture Gompertz Distribution

In this section, we conduct simulation experiments to evaluate the accuracy of the estimated parameters in the HMGOM distribution. The experiments are performed using three different parameter combinations: $(\alpha, \rho, f, g) = (0.2, 0.6, 0.5, 0.9)$, $(\alpha, \rho, f, g) = (0.3, 0.7, 0.6, 1.0)$ and $(\alpha, \rho, f, g) = (0.09, 0.6, 0.6, 1.2)$. We replicate the experiments 1000 times using various sample sizes: 30, 80, 200, 500, and 1000. The goal is to ascertain the precision of the estimated parameters in the HMGOM distribution across these different sample sizes.

The results are shown in Table 5.1, 5.2 and 5.3. As the sample sizes increase, we observe a general trend of decreasing ABs and MSEs for the estimators of parameters. Although there may be deviations, the MLE consistently exhibit the least ABs and MSEs, indicating their superior performance as the best estimators. The OLSS and WLSS estimators can be considered as viable alternatives, although they exhibit slightly higher ABs and MSEs at some points compared to the MLE estimators.

Table 5.1: ABs and MSEs for $(\alpha, \rho, f, g) = (0.2, 0.6, 0.5, 0.9)$

Parameter	N	AB					MSE				
		MLE	OLSS	WLSS	CVM	AD	MLE	OLSS	WLSS	CVM	AD
α	30	0.1728	0.1205	0.1627	6.4661	8.0753	0.0334	0.0212	0.0299	111.9517	110.6284
	80	0.1318	0.1361	0.1391	4.1971	10.7874	0.0226	0.0255	0.0251	78.0884	176.0832
	200	0.1446	0.1610	0.1564	7.8795	9.9169	0.0260	0.0300	0.0291	104.5699	124.4208
	500	0.1815	0.1210	0.1449	8.1356	10.8938	0.0353	0.0208	0.0262	88.6376	156.9742
	1000	0.1158	0.1229	0.1362	9.2244	13.7704	0.0181	0.0212	0.0263	133.2229	248.2210
ρ	30	1.1881	1.5707	0.2873	5.5736	3.0961	7.3793	12.6514	0.1332	56.9280	20.4026
	80	0.3462	0.4027	0.3402	4.9603	4.2490	0.1539	0.1958	0.1498	78.0884	40.1785
	200	0.2893	0.2389	0.8352	2.8981	2.7631	0.1152	0.1101	3.1619	18.4375	12.4311
	500	0.2234	0.3470	0.3437	2.6610	4.0440	0.0784	0.1693	0.1587	9.8217	35.6852
	1000	0.4123	1.0902	0.3187	2.2845	2.4518	0.1977	6.3851	0.1316	16.7158	13.1933
f	30	0.4276	0.3338	0.2213	13.5653	14.4995	0.2762	0.1290	0.0896	354.1072	332.2690
	80	0.2649	0.2384	0.2379	13.0908	19.3098	0.0808	0.0814	0.0817	240.0828	393.2078
	200	0.1946	0.2266	0.3252	15.6499	22.3086	0.0498	0.0666	0.1827	259.1609	513.1973
	500	0.1286	0.1755	0.2052	19.5030	28.1683	0.0271	0.0466	0.0597	423.2970	832.7475
	1000	0.1532	0.3147	0.1559	20.2267	24.1433	0.0315	0.1743	0.0410	431.5102	642.7975
g	30	1.3945	2.0766	0.6055	2.1069	2.7606	3.7484	6.4942	0.6311	9.2455	31.06869
	80	1.0232	1.3251	0.8992	2.6983	2.9982	2.2029	3.0258	1.2445	18.4101	17.4671
	200	0.5734	0.8506	0.8384	1.9363	3.2026	0.5469	1.6251	1.0584	6.0719	21.4858
	500	0.3220	0.7811	0.7332	1.8616	2.9325	0.2337	1.1423	0.9002	7.1347	14.5020
	1000	0.7011	0.7927	0.4509	4.9613	5.2361	0.6855	1.0064	0.3930	46.0868	43.8423

Table 5.2: ABs and MSEs for $(\alpha, \rho, f, g) = (0.3, 0.7, 0.6, 1.0)$

Parameter	N	AB					MSE				
		MLE	OLSS	WLSS	CVM	AD	MLE	OLSS	WLSS	CVM	AD
α	30	0.2698	0.2086	0.2371	13.5748	11.3711	0.0765	0.0535	0.0626	268.6568	316.3286
	80	0.2434	0.2228	0.1806	9.1300	22.3308	0.0721	0.0592	0.0522	118.6071	852.4057
	200	0.1193	0.2180	0.1889	10.4509	24.6038	0.0296	0.0621	0.0534	169.6483	827.6018
	500	0.1397	0.1681	0.1404	10.3455	50.9891	0.0303	0.0464	0.0269	142.2032	2916.036
	1000	0.2252	0.1344	0.1347	14.3517	47.1094	0.0639	0.0366	0.0305	228.4411	2465.843
ρ	30	0.6286	0.9968	0.7317	2.0432	1.7773	0.9680	1.8621	0.8903	14.6218	3.927465
	80	1.7077	0.3892	0.7359	3.8029	3.1668	10.4070	0.2265	0.9102	30.5244	33.1390
	200	0.6937	0.7383	1.4451	1.6958	2.3850	0.9408	1.6021	9.0287	6.0972	21.4689
	500	0.4377	0.4484	0.5215	1.7016	1.0061	0.2873	0.2574	0.3233	5.1822	1.0276
	1000	0.3213	0.3698	0.4537	3.0081	0.9283	0.1630	0.2007	0.2708	21.2171	0.8722
f	30	0.2747	0.2936	0.3492	15.8928	33.1261	0.1085	0.1238	0.1403	282.8019	1818.799
	80	0.4215	0.3381	0.3341	18.4690	30.9019	0.3003	0.1424	0.1359,	362.4512	1226.404
	200	0.2751	0.3129	0.3832	20.5009	45.3442	0.0896	0.1304	0.2566	438.7893	2332.963
	500	0.2473	0.2401	0.1923	25.0683	63.0271	0.0955	0.0830,	0.0608	681.9098	4284.441
	1000	0.2464	0.1539	0.2285	27.7694	60.2618	0.0912	0.0392	0.0749	831.2347	3756.44
g	30	1.1085	1.7054	1.9748	2.8332	5.2564	2.3895	3.8585	6.2019	11.2405	35.7389
	80	1.0250	1.6933	1.7599	2.3893	12.2858	2.3002	5.6833	4.8018	9.5992	218.7645
	200	1.2550	0.9142	0.9964	3.5006	9.4239	2.2481	1.0905	1.3969	16.8369	147.4287
	500	1.3039	0.9597	0.9226	4.6598	8.7626	2.8990	1.4930	1.1654	23.3329	96.9149
	1000	0.7671	0.7618	0.9021	4.4774	11.0793	1.1059	1.0287	1.2151	28.0616	127.5515

Table 5.3: ABs and MSEs for $(\alpha, \rho, f, g) = (0.09, 0.6, 0.6, 1.2)$

Parameter	N	AB					MSE				
		MLE	OLSS	WLSS	CVM	AD	MLE	OLSS	WLSS	CVM	AD
α	30	0.1770	0.0866	0.1261	6.8844	8.2518	0.0920	0.0082	0.0403	154.6483	328.7511
	80	0.1177	0.1156	0.1328	6.2260	7.8029	0.0174	0.0163	0.0276	76.2661	624.4194
	200	0.1091	0.1307	0.1958	34.8841	12.0235	0.0141	0.0227	0.0695	2127.1410	871.7330
	500	0.1931	0.1717	0.1205	38.9986	8.6312	0.0426	0.0411	0.0171	1703.0270	1613.0910
	1000	0.1461	0.1360	0.1042	38.1071	15.9033	0.0258	0.0310	0.0140	1983.5160	2087.4670
ρ	30	0.4422	0.4012	0.6517	2.4265	3.7611	0.2241	0.1877	0.8865	6.5368	7.8770
	80	0.3175	1.5238	0.9379	3.4599	3.0609	0.1481	7.4845	2.8595	19.3756	1.7426
	200	0.3290	0.3253	0.8595	2.9609	2.6205	0.1565	0.1496	2.6383	18.5418	8.2478
	500	0.4113	0.2667	0.2709	1.2788	3.4027	0.1997	0.1280	0.1171	1.9222	1.4919,
	1000	0.3412	0.2653	0.1630	1.4268	1.0641	0.1470	0.1157	0.0525	2.8537	3.1897
f	30	0.3906	0.3747	0.3571	24.5892	15.7007	0.2112	0.1805	0.1794	996.1070	1381.2740
	80	0.2590	0.5830	0.2799	36.7441	17.1816	0.0858	0.5543	0.1098	1676.7490	1976.1740
	200	0.2571	0.2001	0.3173	46.5741	25.3394	0.1028	0.0699	0.2288	3191.3390	1735.7010
	500	0.2485	0.1196	0.2000	64.976	27.5783	0.0728	0.0230,	0.0730	4509.726	4166.6540
	1000	0.2220	0.1921	0.1527	58.3461	26.8826	0.0730	0.0692	0.0328	3723.1460	4159.4110
g	30	1.9877	1.3929	0.8649	4.8021	2.0102	7.7005	2.8022	1.5389	26.0589	28.7388
	80	1.1326	2.2593	1.4422	3.7218	4.2053	2.3862	7.6344	2.8845	17.6698	39.0680
	200	1.1010	0.8142	0.6987	12.9255	2.4309	2.0429	1.1326	0.6208	266.0319	40.1133
	500	0.9911	0.3840	0.7037	14.2448	5.1270	1.3039	0.2913	0.9114	242.6935	50.1873
	1000	0.6830	0.6279	0.3421	12.2556	4.5462	0.7551	0.8821	0.2334	178.4128	598.3489

5.3 Applications of the Harmonic Mixture Gompertz Distribution

In this section, we apply the HMGOM distribution to three datasets to assess its empirical importance and evaluate its performance in modelling lifetime data. The

HMGOM distribution is compared with nine(9) other models. These nine(9) distributions can be seen in Table 5.4.

Table 5.4: Compared Models

Models	References
Odd Lindley-Gompertz distribution (OLINGOMD)	Atanda *et al.* (2020)
Kumaraswamy Gompertz distribution (KWGO)	Silva *et al.* (2021)
Rayleigh Gompertz (RGO)	Al-Noor *et al.* (2022)
Exponentiated generalised Weibull-Gompertz distribution (EGWGD)	El-Bassiouny *et al.* (2017)
Rayleigh Gamma Gompertz distribution (RGGOM)	Al-Noor and Assi (2021)
Inverse power Gompertz (IPG)	Abdelhady and Amer (2021)
Odd generalised exponential Gompertz distribution (OGEG)	El-Damcese *et al.* (2015)
Inverted shifted Gompertz distribution(ISGZ)	Chaudhary *et al.* (2020)
Nadarajah Haghighi Gompertz distribution (NHGD)	Ogunde *et al.* (2020b)

5.3.1 The strengths of 1.5 cm glass fibres

The strength 1.5cm glass fibres dataset ranges from a minimum value of 0.5500 to a maximum value of 2.4000. The CS for the dataset is calculated as -0.9220, indicating a negative skew. This suggests that the dataset is skewed towards the left, with a longer tail on the left side of the distribution. Additionally, the CK is determined to be 1.1031. This value implies that the dataset exhibits less peak or concentration in comparison to the normal distribution curve. The flatter peak signifies a platykurtic distribution, indicating that the dataset has lighter tails and lacks extreme outliers. The failure rate behaviour of the strengths of the 1.5cm glass fibres was examined through a TTT plot. The TTT plot displayed an upward trend, indicating an increasing pattern. This observation is evident from the concave shape observed above the 45° line in Figure 5.1.

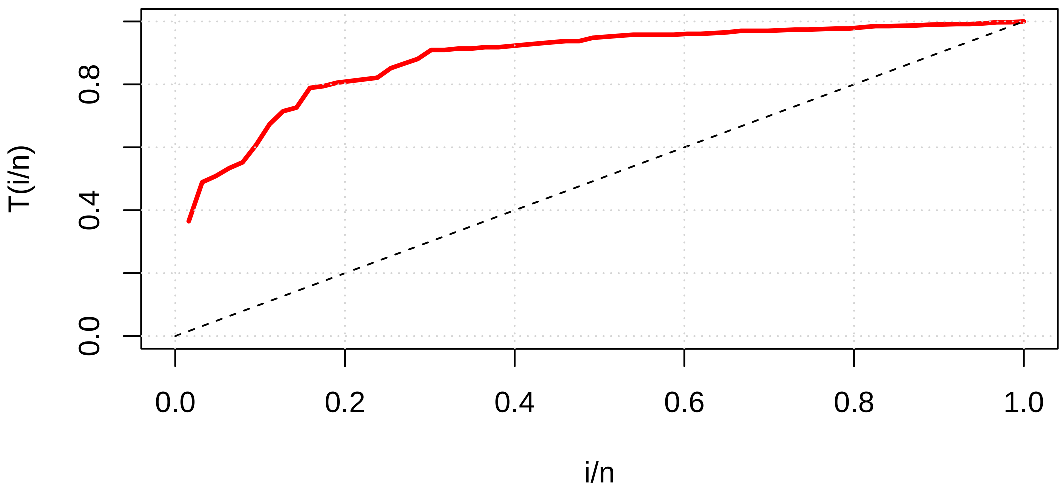

Figure 5.1: The TTT plot of the strengths of 1.5cm glass fibres

Table 5.5 presents the MLEs for the fitted models along with their respective standard errors (SE). The statistical significance of the estimated parameters was assessed at a significance level of 5%. In the case of the HMGOM model, the parameters α and ρ, for KWGO the parameter θ and b, for RGO the parameter α, for EGWGD the parameters a, b, c, and d, and for OGEG the parameters α and β, were found to be statistically insignificant. This means that these estimated parameters do not have a significant impact on the model at the 5% level.

Table 5.5: MLEs for strengths of 1.5cm glass fibres

Models		Estimates	SE	Z-Value	P-Value
HMGOM	α	0.0151	0.0282	0.5341	0.5933
	ρ	0.0089	0.0078	1.1426	0.2532
	f	1.2271	0.0892	13.7637	2.0000×10^{-16}*
	g	0.9833	0.0468	21.0250	2.0000×10^{-16}*
OLINGOMD	α	3.0487	0.9701	3.1426	0.0017 *
	θ	0.0106	0.0066	1.6112	0.1071
	λ	2.6598	0.2773	9.5926	2.2000×10^{-16}*
KWGO	γ	2.9869	0.3959	7.5455	4.5060×10^{-14}*
	θ	0.0265	0.0142	1.8675	0.0618
	a	1.5130	0.3648	4.1476	3.3600×10^{-5}*
	b	1.0979	0.5843	1.8790	0.0603
RGO	α	0.0265	0.0131	2.0189	0.4350
	λ	2.3014	0.2785	8.2634	2.2000×10^{-16}*
	θ	1.0171	0.3288	3.0937	0.0020 *
EGWGD	θ	0.6915	0.3349	2.0651	0.0389*
	a	0.1820	0.4658	0.3908	0.6960
	b	5.4824	7.8627	0.6973	0.4856
	c	0.1133	0.3182	0.3561	0.7217
	d	1.4886	5.1564	0.2887	0.7728
RGGOM	α	2.2785	0.7811	2.9170	0.0035*
	λ	0.4422	0.1516	2.9170	0.0035*
	θ	21.0836	7.0275	3.0002	0.0027*
IPG	α	2.4742	0.2257	10.9619	2.2000×10^{-16}*
	β	0.2177	0.0713	3.0542	0.0023*
	θ	6.9429	2.6243	2.6456	0.0082*
OGEG	α	11.5380	6.1085	1.8889	0.0589
	β	4.7064	3.1616	1.4886	0.1366
	λ	0.0287	0.0133	2.1578	0.0309 *
	c	1.4186	0.4852	2.9234	0.0035 *
ISGZ	α	33.7053	9.4491	3.5670	0.0004 *
	θ	5.7713	0.4573	12.6200	2.2000×10^{-16}*
NHGD	α	0.0937	0.0326	2.8738	0.0041*
	λ	0.0919	0.0320	2.8738	0.0041 *
	β	2.9280	0.4258	6.8757	6.1670×10^{-12}*
	δ	2.0318	0.9085	2.2366	0.0253*

* means significant at 5%.

Based on multiple evaluation criteria as shown in Table 5.6, the HMGOM model demonstrates a better fit than the other models considered. It achieves the highest log-likelihood value, the lowest values for AIC, AICC, and BIC, and the lowest values for A, KS, and W. These results indicate that the HMGOM model provides an improved fit to the dataset, making it a preferred choice for analysing the data.

Table 5.6: Comparison criteria for strengths of 1.5cm glass fibres

Models	ℓ	AIC	AICC	BIC	KS	A	W
HMGOM	-12.0840	32.1681	32.5749	40.7406	0.0918	0.3785	0.0611
OLINGOMD	-18.7784	43.5567	43.9635	49.9861	0.1447	1.7788	0.3092
KWGO	-14.2142	36.4284	45.0009	37.1180	0.1119	0.8936	0.1441
RGO	-16.8399	41.3723	41.7791	47.8017	0.1637	1.7808	0.3074
EGWGD	-14.6649	39.3298	40.3824	50.0455	0.1457	1.0828	0.1966
RGGOM	-34.4107	74.8214	75.2281	81.2508	0.2181	4.9108	0.9045
IPG	-51.5801	109.1601	110.2127	115.5895	0.2646	7.7531	1.5242
OGEG	-16.4297	40.8594	41.5490	49.4319	0.1402	1.4076	0.2103
ISGZ	-27.2560	58.5120	58.8363	62.7983	0.2192	3.8317	0.7204
NHGD	-16.9935	41.9869	42.6766	50.5595	0.1434	1.5199	0.2678

Figure 5.2 and Figure 5.3 present the fitted PDFs and CDFs of the compared models. These figures offer a visual representation of the goodness of fit for each model. Upon examination, it is evident that the HMGOM model demonstrates a better fit to the strengths of the 1.5cm glass fibres. The PDF and CDF curves of the HMGOM model align more closely with the observed data, indicating a higher level of agreement. This suggests that the HMGOM model effectively captures the underlying patterns and distribution characteristics of the dataset.

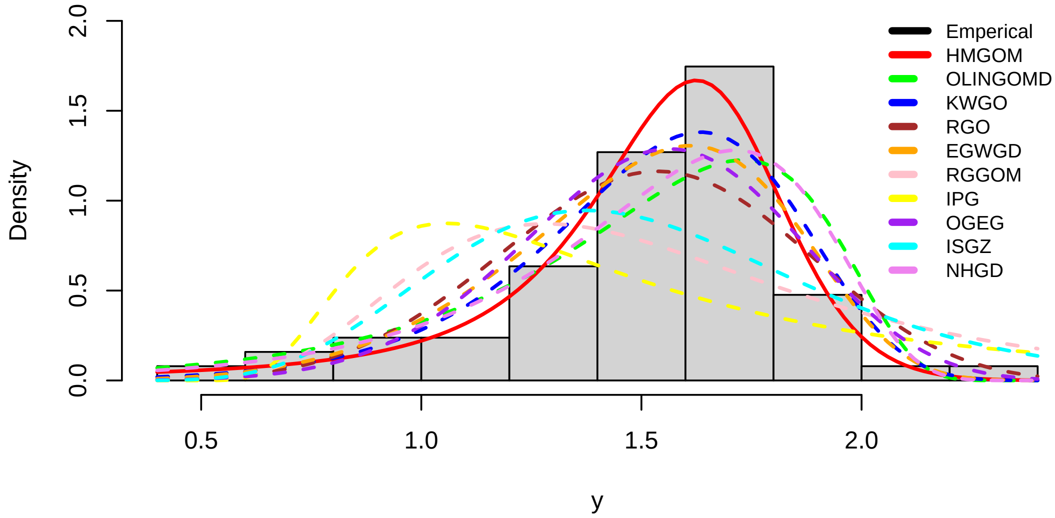

Figure 5.2: The fitted PDFs for strengths of 1.5cm glass fibres

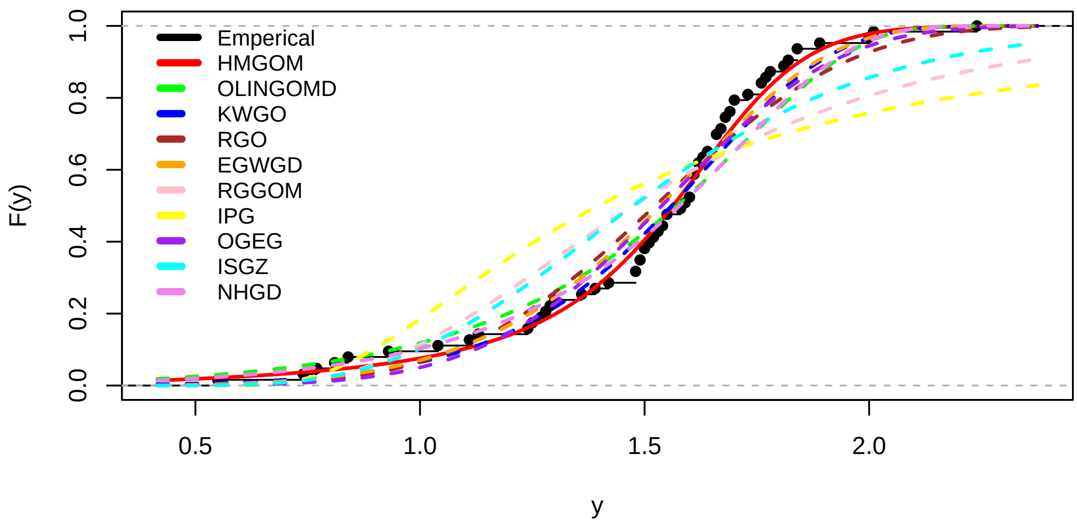

Figure 5.3: The fitted CDFs for strengths of 1.5cm glass fibres

The profile log-likelihood plots in Figure 5.4 provide visual evidence that the estimated parameter values of the HMGOM distribution correspond to the real maxima, validating the accuracy of the estimation process for analysing the strengths of the 1.5cm glass fibres.

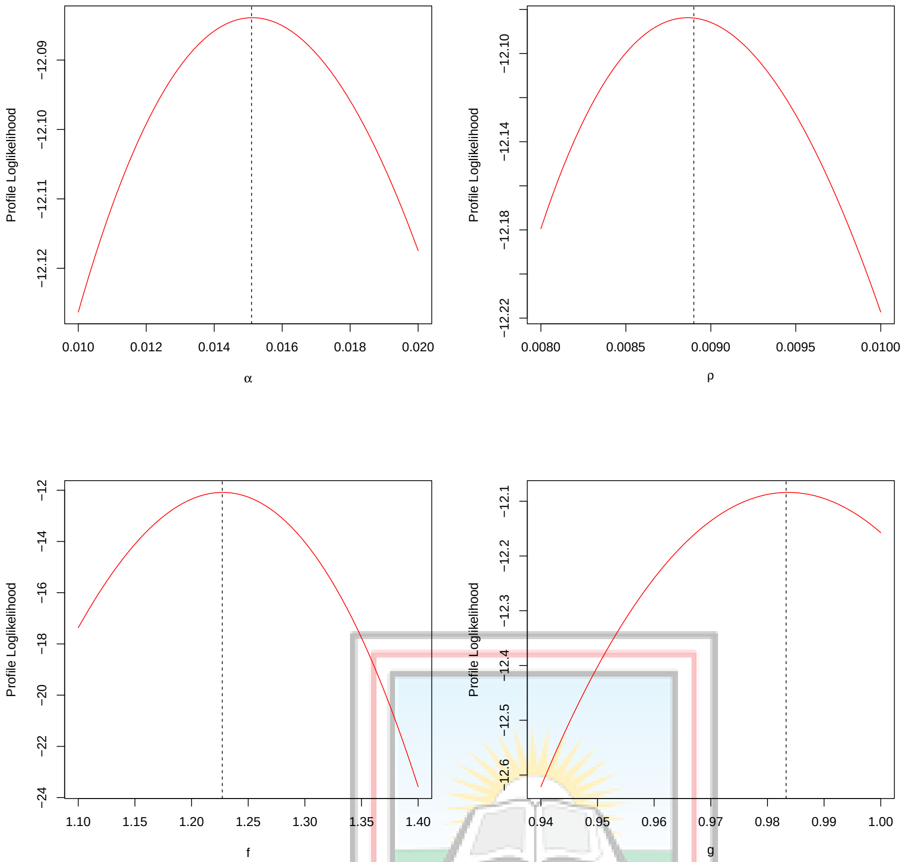

Figure 5.4: Profile log-likelihood plots of HMGOM for strengths of 1.5cm glass fibres

5.3.2 Turbochargers failure time

The dataset pertaining to turbochargers failure time exhibits a range from a minimum value of 1.6000 to a maximum value of 9.0000. The CS for this dataset is calculated as -0.6887, indicating a negative skew. This implies that the data distribution is skewed towards the left, with a longer tail on the left side. Moreover, the CK for the dataset is determined to be -0.2418. This suggests that the dataset has a flatter peak compared to the normal distribution curve, indicating a platykurtic distribution. In other words, the dataset displays lighter tails and a reduced concentration of values compared to a normal distribution.

The failure rate behaviour of the turbochargers failure time was examined through a TTT plot. The TTT plot displayed an upward trend, indicating an increasing pattern. This observation is evident from the concave shape observed above the 45°

line in Figure 5.5.

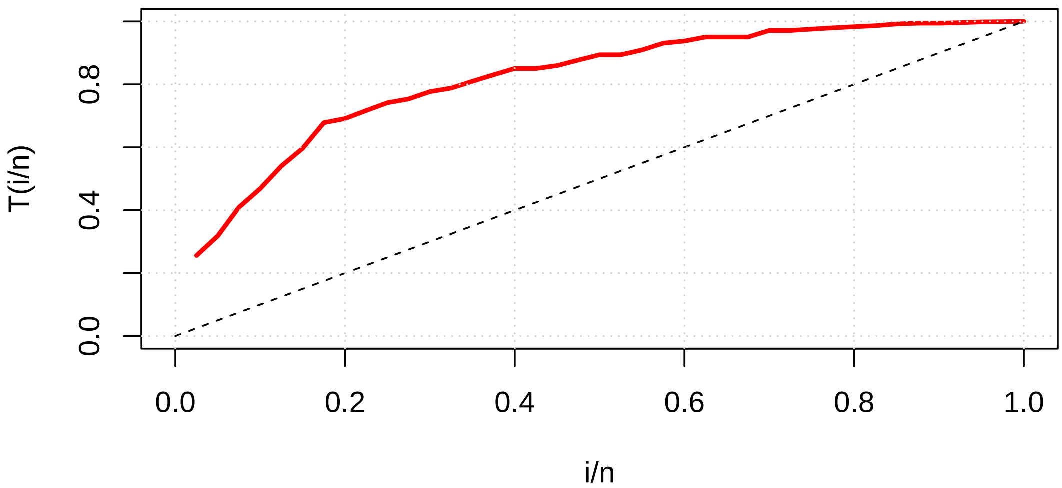

Figure 5.5: The TTT plot of the turbochargers failure time

Table 5.7 presents the MLEs for the fitted models along with their corresponding SEs. The statistical significance of the estimated parameters was assessed at a significance level of 5%. In the case of the HMGOM model, the parameters α, ρ, and g were found to be statistically insignificant. Similarly, for the RGGOM model, the parameters α and λ were not significant. Additionally, the parameters α and θ for the RGO model, θ for the IPG model, β and λ for the OGEG model, and α for the NHGD model were also not significant at the 5%.

Table 5.7: MLEs for turbochargers failure time

Models		Estimates	SE	Z-Value	P-Value
HMGOM	α	0.2402	0.2521	0.9528	0.3407
	ρ	0.0014	0.0162	0.0889	0.9292
	f	0.5403	0.1061	5.0915	3.5520×10^{-7}*
	g	0.0441	0.0580	0.7607	0.4469
OLINGOMD	α	19.9310	3.7279×10^{-3}	5346.4782	2.0000×10^{-16}*
	θ	8.1407×10^{-4}	7.7504×10^{-4}	1.0504	0.2936
	λ	0.5089	0.1485	3.4271	0.0006 *
KWGO	γ	0.1979	0.0694	2.8521	0.0043 *
	θ	0.0538	0.0245	2.1940	0.0282*
	a	2.8612	0.7997	3.5776	0.0003*
	b	4.5520	2.1160	2.1512	0.0315*
RGO	α	0.0208	0.0218	0.9547	0.3397
	λ	0.3267	0.1300	2.5130	0.0120*
	θ	1.2114	0.9450	1.2819	0.1999
EGWGD	θ	1.6283	0.3982	4.0888	4.3370×10^{-5}*
	a	6.4060	0.0435	147.2327	2.2000×10^{-16}*
	b	1.9263	0.0737	26.1349	2.2000×10^{-16}*
	c	0.0014	0.0004	3.3205	0.0009*
	d	0.6035	0.0739	8.1687	3.1170×10^{-16}*
RGGOM	α	6.2600	8.1329	0.7697	0.4415
	λ	0.0245	0.0319	0.7697	0.4415
	θ	5.0530	1.7069	2.9603	0.0031*
IPG	α	1.8488	0.1983	9.3250	2.0000×10^{-16}*
	β	0.6525	0.3035	2.1500	0.0316*
	θ	24.3526	12.6022	1.9324	0.0533
OGEG	α	12.2469	0.7449	16.4421	2.0000×10^{-16}*
	β	3.4789	1.8425	1.8881	0.0590
	λ	0.0089	0.0064	1.3793	0.1678
	c	0.2348	0.1027	2.2862	0.0222*
ISGZ	α	17.4313	7.3819	2.3613	0.01821 *
	θ	19.3358	2.6878	7.1939	6.2980×10^{-13}*
NHGD	α	0.8923	0.5065	1.7617	0.0781
	λ	0.0037	0.0021	1.7617	0.0781 *
	β	0.5336	0.0871	6.1245	9.0960×10^{-10}*
	δ	2.6972	1.3429	2.0085	0.0446*

* means significant at 5%.

Once again, the proposed HMGOM model demonstrated superior goodness of fit, as illustrated in Table 5.8. Among the compared models, the HMGOM model exhibited several favourable characteristics. It achieved the highest log-likelihood value, indicating a better fit to the data and suggesting that it captured the underlying patterns more effectively. Furthermore, the HMGOM model showcased the lowest values across various evaluation criteria, including AIC, AICC, and BIC. These criteria are commonly used for model selection, with lower values indicating a better balance between model complexity and fit to the data. Additionally, the HMGOM model displayed superior performance in terms of other assessment metrics such as A , KS , and W . These statistics are employed to evaluate the agreement between the model and the observed data, and lower values suggest a closer fit.

Table 5.8: Comparison criteria for turbochargers failure times

Models	ℓ	AIC	AICC	BIC	KS	A	W
HMGOM	-78.2964	164.5928	165.7359	171.3483	0.0537	0.0971	0.0139
OLINGOMD	-80.7292	167.4584	172.5250	168.1251	0.1157	0.7601	0.1354
KWGO	-82.1978	172.3956	173.5385	179.1511	0.0837	0.4691	0.0399
RGO	-83.8853	173.7705	174.4372	178.8372	0.1027	0.7847	0.0986
EGWGD	-85.7540	181.5080	183.2727	189.9524	0.1595	1.2566	0.1393
RGGOM	-92.6762	191.3525	192.0192	196.4191	0.1900	2.2561	0.3829
IPG	-102.4359	210.8718	211.5385	215.9384	0.2405	3.8758	0.7149
OGEG	-82.5932	173.1865	174.3293	179.9420	0.0919	0.5940	0.0582
ISGZ	-91.5428	187.0855	187.4098	190.4633	0.1456	1.9066	0.2681
NHGD	-79.3480	166.6960	167.8389	173.4515	0.0744	0.2379	0.0388

The visual comparison of the fitted PDFs in Figure 5.6 and CDFs in Figure 5.7 is made. The close alignment between the model curves and the observed data supports the conclusion that the HMGOM model provides a better fit and is more suitable for analysing the dataset.

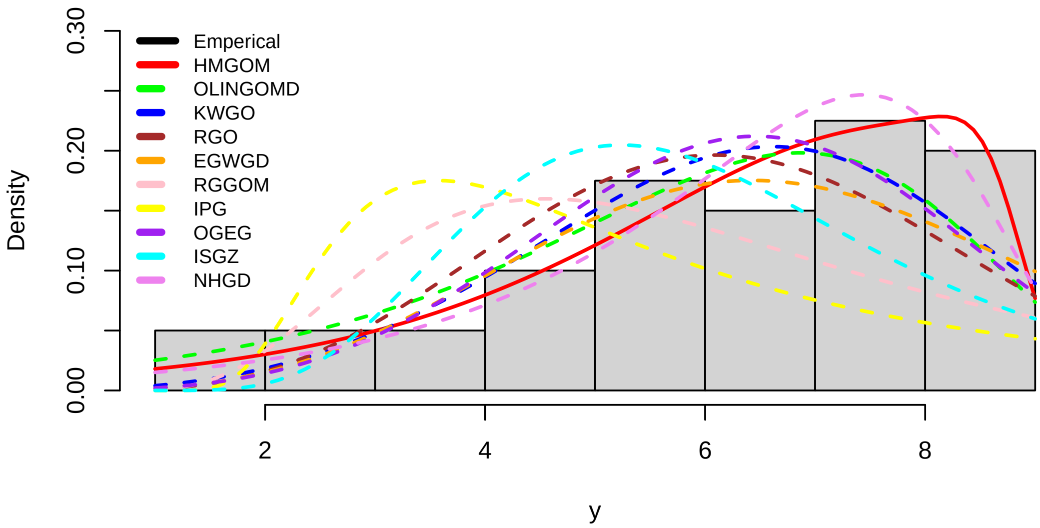

Figure 5.6: The fitted PDFs for turbochargers failure time

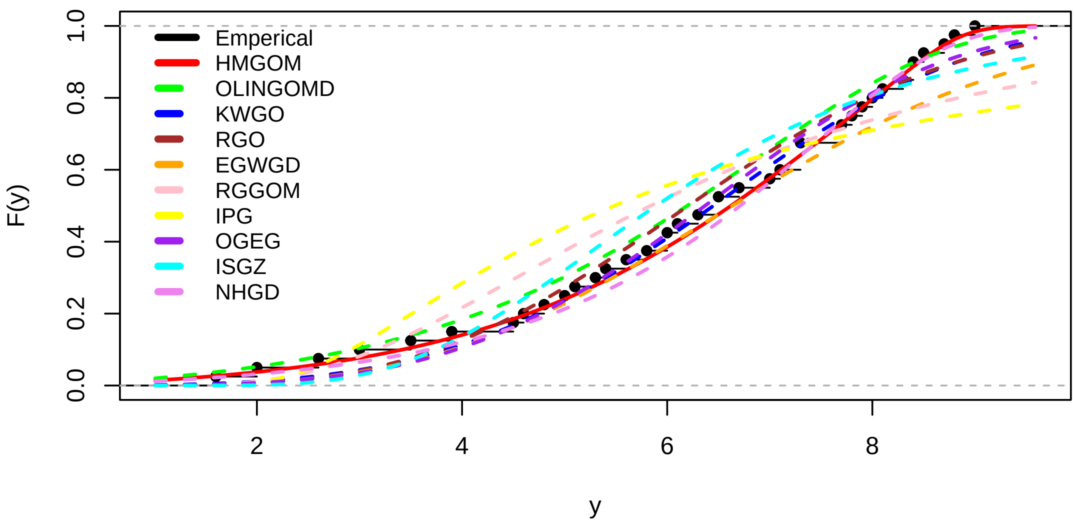

Figure 5.7: The fitted CDFs for turbochargers failure time

The profile log-likelihood plots in Figure 5.8 provide visual evidence that the estimated parameter values of the HMGOM distribution correspond to the real maxima, validating the accuracy of the estimation process for analysing the the turbochargers failure time.

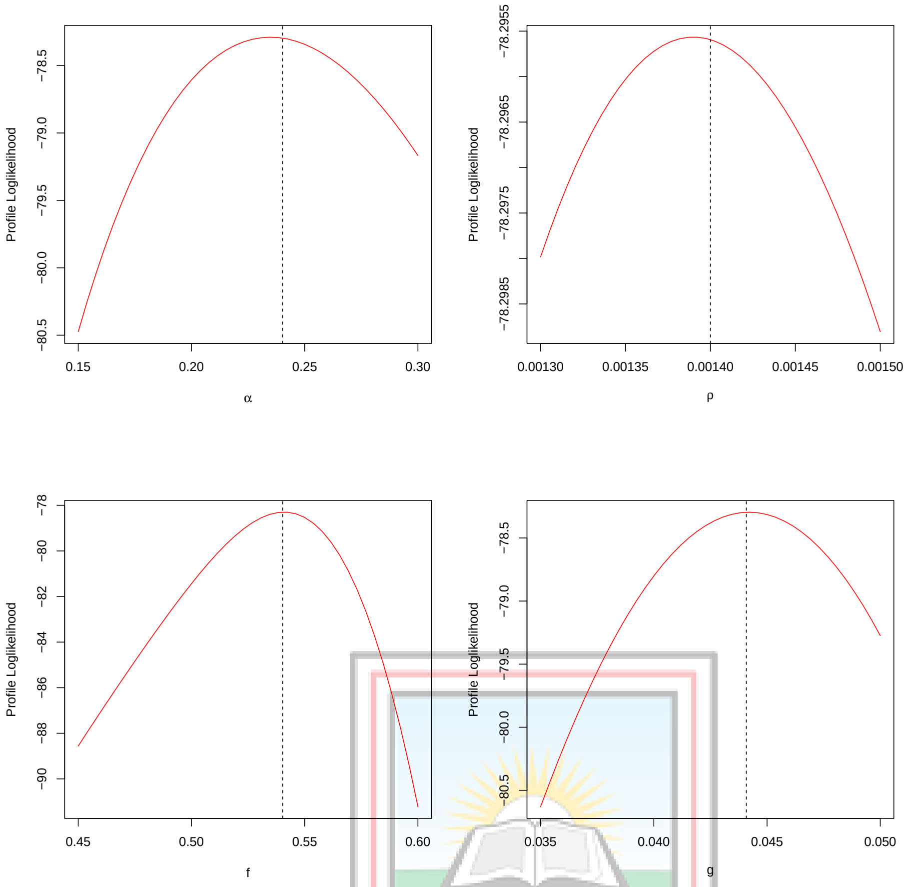

Figure 5.8: Profile log-likelihood plots of HMGOM for turbochargers failure time

5.3.3 Transformed total milk production

The transformed total milk production dataset ranges from a minimum value of 0.0168 to a maximum value of 0.8781. The CS is calculated as -0.3401, suggesting a slight negative skew. This indicates that the dataset is approximately symmetric, with a slightly longer tail on the left side. The CK is determined to be -0.2708, indicating a platykurtic distribution. This means that the dataset has a flatter peak compared to the normal distribution curve, implying a lower concentration of values near the mean and lighter tails compared to a normal distribution.

The failure rate behaviour of the turbochargers failure time dataset was examined through a TTT plot. The TTT plot displayed an upward trend, indicating an increasing pattern. This observation is evident from the concave shape observed above the 45° line in Figure 5.9.

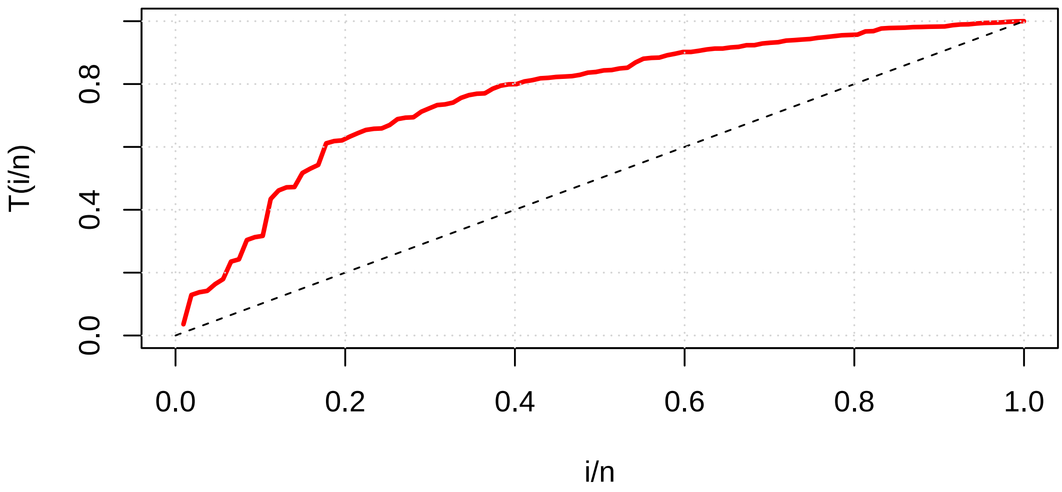

Figure 5.9: The TTT plot of the transformed total milk production

Table 5.7 presents the MLEs for the fitted models, along with their respective SEs. The statistical significance of the estimated parameters was assessed at a 5% significance level. Upon examination, it was found that some parameters across different models were not statistically significant at the 5% level. In the HMGOM model, the parameters α and ρ did not demonstrate significant effects. Similarly, in the RGGOM model, the parameters α and λ were not significant. The RGO model had a non-significant parameter, namely α. Furthermore, the KWGO model showed non-significant parameters θ and b. The EGWGD model had non-significant parameters a, b, c, and d. Similarly, the NHGD model had non-significant parameters α, λ, and δ. Lastly, the OGEG model had non-significant parameters α and λ.

Table 5.9: MLEs for transformed total milk production

Models		Estimates	SE	Z-Value	P-Value
HMGOM	α	0.0525	0.0422	1.2440	0.2135
	ρ	0.0350	0.0302	1.1581	0.2468
	f	1.5058	0.6701	2.2472	0.0246 *
	g	4.4138	1.7451	2.5293	0.0114 *
OLINGOMD	α	19.4207	0.0568	342.1120	2.0000×10^{-16}*
	θ	0.0042	0.0016	2.5350	0.0112 *
	λ	7.7273	0.6355	12.1590	2.0000×10^{-16}*
KWGO	γ	5.2184	1.0590	4.9276	8.3240×10^{-7}*
	θ	0.1913	0.1976	0.9682	0.3330
	a	0.9924	0.2390	4.1515	3.3030×10^{-5}*
	b	1.5953	1.5336	1.0402	0.2983
RGO	α	0.0586	0.0436	1.3462	0.1782
	λ	5.5583	1.0720	5.1852	2.1500×10^{-7}*
	θ	0.3049	0.1015	3.0048	0.0027 *
EGWGD	θ	0.2927	0.1136	2.5777	0.0099 *
	a	17.0403	13.7372	1.2405	0.2148
	b	5.3236	4.5239	1.1768	0.2393
	c	0.4434	0.2942	1.5073	0.1317
	d	0.6923	3.2949	0.2101	0.8336
RGGOM	α	1.2819	1.5692	0.8169	0.4140
	λ	1.0251	1.2549	0.8169	0.4140
	θ	1.7727	0.3305	5.3631	8.1790×10^{-8}*
IPG	α	0.8106	0.0792	10.2297	2.0000×10^{-16}*
	β	0.0528	0.0264	2.0044	0.0450 *
	θ	5.6909	2.3721	2.3991	0.0164 *
OGEG	α	11.3691	7.8930	1.4404	0.1498
	β	1.1768	0.2787	4.2222	2.4190×10^{-5}*
	λ	0.0423	0.0338	1.2506	0.2111
	C	4.2717	0.8151	5.2408	1.5990×10^{-7}*
ISGZ	α	1.4859	0.6540	2.2719	0.0231 *
	θ	0.4904	0.0789	6.2162	5.0930×10^{-10}*
NHGD	α	0.9620	0.7516	1.2800	0.2005
	λ	0.3211	0.2508	1.2800	0.2005
	β	5.0467	1.2835	3.9319	8.4270×10^{-5}*
	δ	1.0470	0.5951	1.7595	0.0785

* means significant at 5%.

As demonstrated in Figure 5.10, the proposed HMGOM model once again exhibited a superior fit. The HMGOM model achieved the highest log-likelihood value and the lowest values for the AIC, AICC, and BIC criteria, indicating its superior performance in terms of model selection and goodness-of-fit measures. Moreover, the HMGOM model yielded the lowest values for the A-statistic, KS-statistic, and W-statistic. This further supports the conclusion that the HMGOM model outperforms the other models in accurately capturing the distribution of the transformed total milk production.

Table 5.10: Comparison criteria for transformed total milk production

Models	ℓ	AIC	AICC	BIC	KS	A	W
HMGOM	29.3006	-50.6013	-50.2091	-39.9100	0.0492	0.1745	0.0264
OLINGOMD	12.4678	-18.9356	-18.7025	-10.9171	0.1976	8.0068	1.3375
KWGO	29.1187	-50.2373	-49.8451	-39.5460	0.0496	0.2426	0.0370
RGO	26.2360	-46.4719	-46.2389	-38.4535	0.0792	0.9227	0.1544
EGWGD	27.7457	-45.4913	-44.8972	-32.1272	0.0728	0.5437	0.0854
RGGOM	-6.6205	19.2410	19.4740	27.2594	0.1833	6.7351	1.2164
IPG	-62.5657	131.1314	131.3644	139.1499	0.2911	15.5810	3.0403
OGEG	28.9825	-49.9651	-49.5729	-39.2738	0.0504	0.2767	0.0385
ISGZ	-47.3555	98.7109	98.8263	104.0565	0.2521	11.8160	2.2307
NHGD	29.0995	-50.1989	-49.8067	-39.5076	0.0521	0.2537	0.0397

Figure 5.10 displays the fitted PDFs of the compared models, while Figure 5.11 presents the corresponding CDFs. Upon examination, it is evident that the HMGOM model provides a better fit for the transformed total milk production. The fitted PDF plot in Figure 5.10 demonstrates that the HMGOM model closely aligns with the observed data distribution, capturing its shape and characteristics more accurately compared to the other models. Similarly, the fitted CDF plot in Figure 5.11 shows that the HMGOM model exhibits a closer match to the empirical cumulative distribution of the transformed total milk production. This indicates that the HMGOM model better captures the overall distributional behaviour and provides a more accurate representation of the data compared to the alternative models.

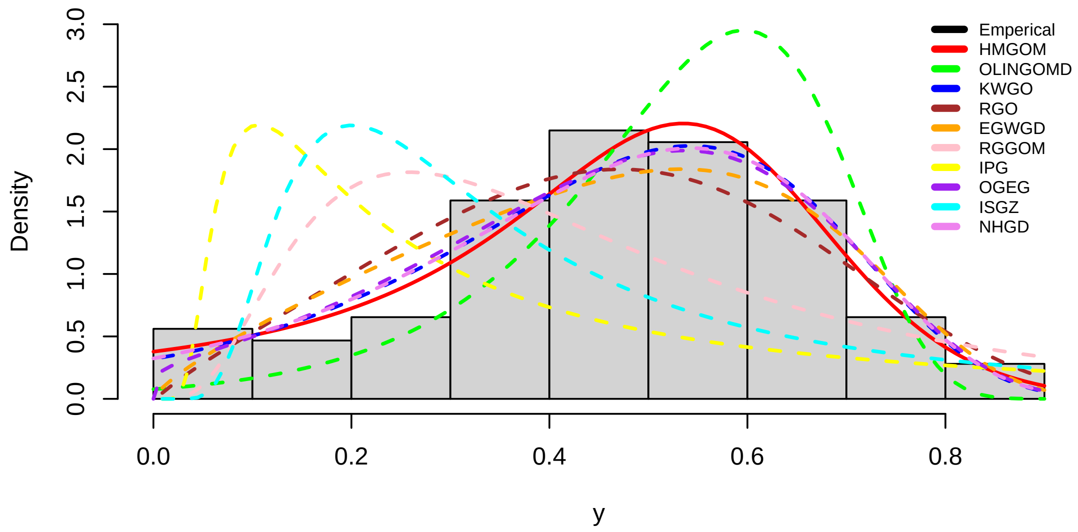

Figure 5.10: The fitted PDFs for transformed total milk production

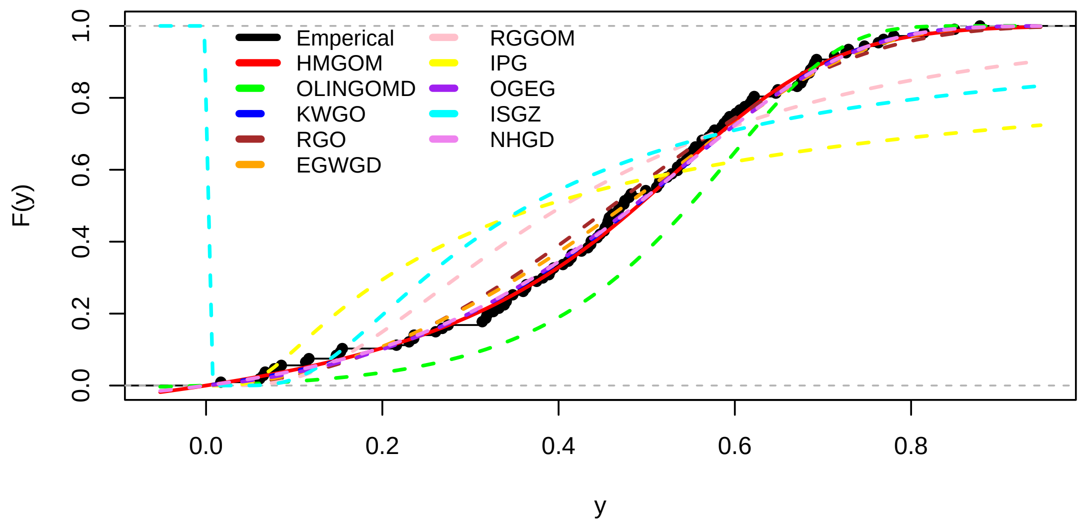

Figure 5.11: The fitted CDFs for transformed total milk production

The profile log-likelihood plots in Figure 5.12 provide visual evidence that the estimated parameter values of the HMGOM distribution correspond to the real maxima, validating the accuracy of the estimation process for analysing the transformed total milk production.

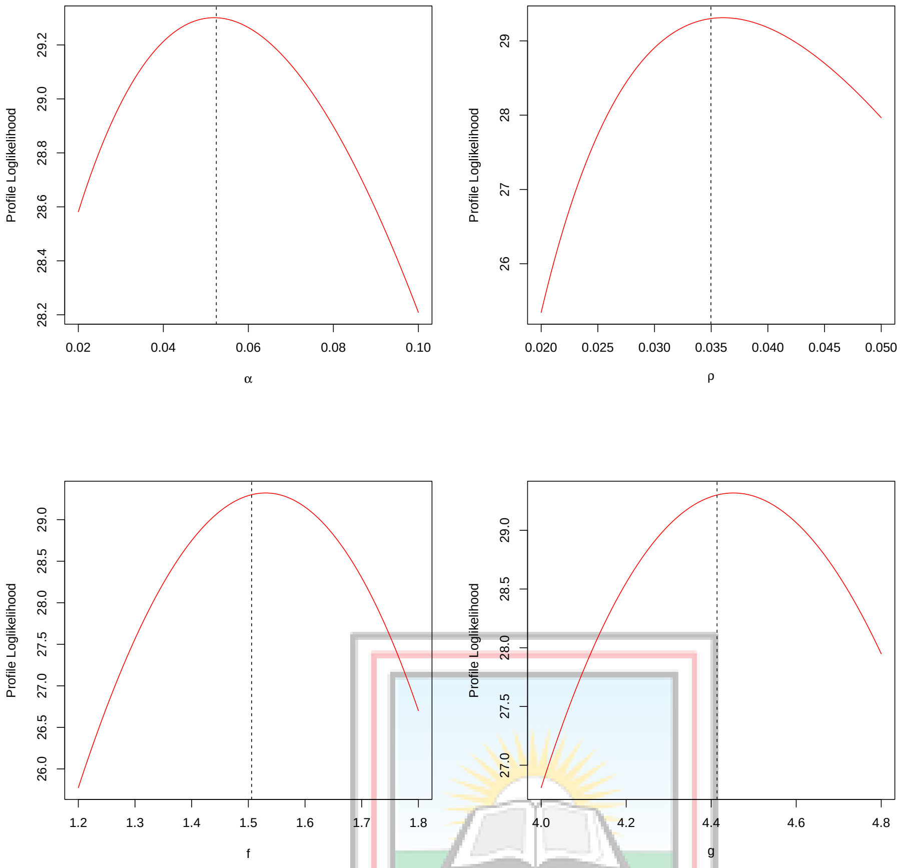

Figure 5.12: Profile log-likelihood plots of HMGOM for transformed total milk production

5.4 Application of the HMGOM Regression Model

The HMGOM regression model was applied to a real dataset and compared with the Gompertz regression model proposed by Azid *et al.* (2021). The selection of the most appropriate model was based on evaluating both the AIC and BIC, with the aim of choosing the model with the lowest values for both criteria. These criteria provide measures of model fit and complexity, allowing for a comprehensive assessment of the competing models. To evaluate the adequacy of the fitted model, residual analysis was performed. Cox Snell residuals, which are a type of standardised residuals, were generated and used as a diagnostic tool. The behaviour of these residuals should closely resemble that of a sample from a standard exponential distribution if the model is appropriate and captures the underlying data patterns effectively, as suggested by Nasiru *et al.* (2021). The fitted model was further assessed using the W and KS goodness-of-fit measures of the Cox Snell residuals. These measures provide insights into how well the model aligns with the observed data. A well-fitted model would exhibit the least W and KS values indicating a close correspondence between the expected and observed values of the residuals.

The relationship between Survival time (T) and duration of diabetes(DUR) in years of 40 male patients, was assessed using the HMGOM regression model. Table 5.11 shows the estimates of the HMGOM regression model and the Gompertz regression model and their corresponding goodness-of-fit. The coefficients for DUR were significant for the models fitted. However, the HMGOM regression model provides a better fit than the GZ regression model. The variable DUR in the HMGOM regression model, had a significant negative effect on the shape parameter f and scale parameter g. On the other hand, the variable Dur had a positive effect on the shape parameter α. By using the parameter estimates derived from the HMGOM regression model, we obtain the following results:

$$\log(f_a) = -0.4898 - 0.0763DUR_a$$

$$\log(g_a) = -8.2899 - 1.1961DUR_a$$

$$\log(\alpha_a) = 0.5695 + 1.5167DUR_a$$

Table 5.11: Comparison statistics

Models		Estimates	P-values	
HMGOM	ρ	0.6631(0.4168)	0.1116	
	a_0	-0.4898(0.2178)	0.0245	
	a_1	-0.0763(0.0179	1.983×10^{-5}	ℓ= -91.9595
	β_0	-8.2899(1.5124)	4.218×10^{-8}	AIC =197.9190
	$\beta 1$	-1.1961(0.2763)	1.497×10^{-5}	BIC=209.7411
	α_0	0.5695(0.2741)	0.7351	
	α_1	1.5167(0.2741)	3.1280×10^{-8}	
GZ	γ	0.3933(0.0581)	1.282×10^{-11}	ℓ=-101.2672
	λ_0	-6.3683(0.7022)	2.2×10^{-16}	AIC= 208.5345
	λ_1	0.0673(0.0339)	0.0471	BIC= 213.6011

To assess the suitability of the HMGOM regression model and GZ regression model, Cox-Snell residuals were obtained. The empirical probabilities of these residuals were compared to those of the standard exponential distribution using a probability-probability (P-P) plot, as depicted in Figure 5.13. Upon inspection of the P-P plot, it is evident that the residuals from the HMGOM regression model closely align with the diagonal line, indicating a better fit to the dataset. In contrast, the residuals from the GZ regression model deviate further from the diagonal line, suggesting a poorer fit.

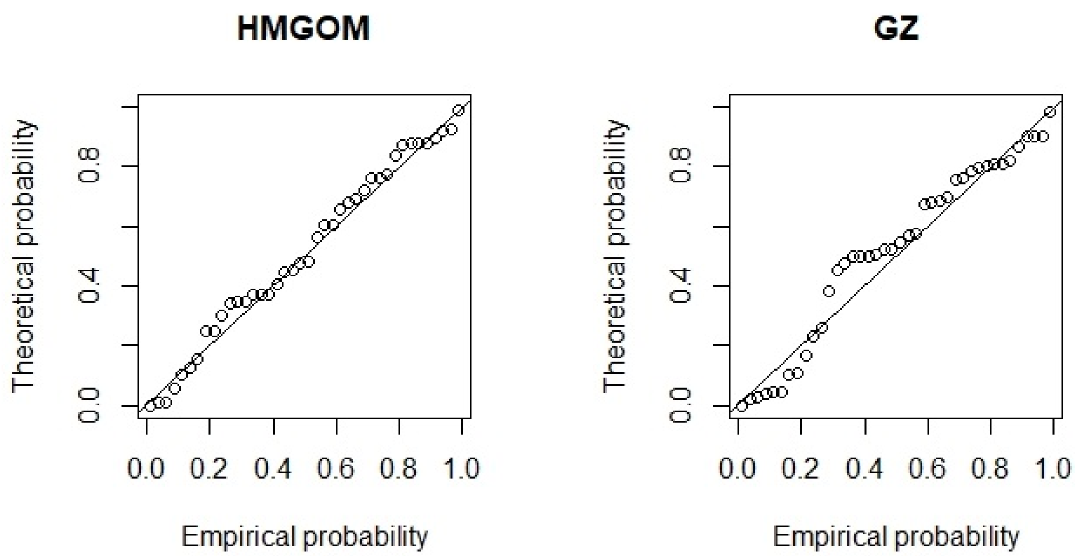

Figure 5.13: P-P plot of residuals

The diagnostic results of the fitted models are summarised in Table 5.12, revealing that the HMGOM regression model offers a better fit for the dataset.

Table 5.12: Goodness-of-fit statistics for residuals

Model	KS		W	
	Statistic	P-value	Statistic	P-value
HMGOM	0.0939	0.8719	0.0530	0.8607
GZ	0.1554	0.2889	0.1685	0.3389

5.5 Monte Carlo Simulations of the Harmonic Mixture Fréchet Distribution

In this section, we conduct simulation experiments to evaluate the accuracy of the estimated parameters in the HMFR distribution. The experiments are performed using three different parameter combinations: $(\alpha, \rho, d, g) = (0.1, 0.8, 2.5, 3.0)$, $(\alpha, \rho, d, g) = (0.3, 0.6, 1.9, 2.5)$ and $(\alpha, \rho, d, g) = (0.03, 0.42, 2.2, 2.6)$. We replicate the experiments 1000 times using various sample sizes: 30, 80, 200, 500, and 1000. The goal is to ascertain the precision of the estimated parameters in the HMFR distribution across these different sample sizes.

The results are shown in the Table 5.13, 5.14 and 5.15. As the sample sizes increase, we observe a general trend of decreasing ABs and MSEs for the estimators of various parameters. Although there may be deviations, the MLE consistently exhibit the least ABs and MSEs, indicating their superior performance as the best estimators.

Table 5.13: ABs and MSEs for $(\alpha, \rho, d, g) = (0.1, 0.8, 2.5, 3.0)$

Parameter	N	AB					MSE				
		MLE	OLSS	WLSS	CVM	AD	MLE	OLSS	WLSS	CVM	AD
α	30	0.0303	0.1292	0.1007	0.1780	0.1012	0.0029	0.0915	0.0623	0.1371	0.0711
	80	0.0176	0.0578	0.0747	0.0399	0.0839	0.0033	0.0432	0.0581	0.0269	0.0665
	200	0.0084	0.0244	0.0317	0.0196	0.0368	0.0020	0.0174	0.0237	0.0137	0.0285
	500	0.0051	0.0048	0.0139	0.0033	0.0102	0.0021	0.0027	0.0150	0.0015	0.0076
	1000	0.0021	0.0027	0.0065	0.0031	0.0041	0.0007	0.0015	0.0050	0.0020	0.0027
ρ	30	0.9495	0.6509	0.4967	0.4217	0.6104	8.6865	2.0680	1.0813	0.7608	2.6243
	80	0.1080	0.1548	0.2072	0.2570	0.2772	0.1111	0.5255	0.5853	0.8537	0.8980
	200	0.3186	0.0805	0.0500	0.0907	0.0774	17.0596	0.2452	0.0558	0.3699	0.1284
	500	0.0175	0.0207	0.0222	0.0184	0.0232	0.0663	0.0242	0.0274	0.0183	0.0285
	1000	0.0038	0.0094	0.0155	0.0088	0.0118	0.0027	0.0094	0.0364	0.0080	0.0147
d	30	0.4058	0.7828	0.7553	0.7914	0.7884	1.1336	1.8417	1.7393	1.8804	1.8697
	80	0.1866	0.2984	0.2801	0.2962	0.2937	0.3763	0.7129	0.6427	0.7023	0.6903
	200	0.0368	0.1171	0.1189	0.1195	0.1183	0.0388	0.2745	0.2831	0.2860	0.2800
	500	0.0074	0.0482	0.0475	0.0487	0.0482	0.0036	0.1163	0.1131	0.1185	0.1160
	1000	0.0026	0.0244	0.0224	0.0245	0.0243	0.0009	0.0595	0.0523	0.0594	0.05893
g	30	0.4053	0.4591	0.6006	0.4153	0.2776	0.7561	0.7929	1.5635	0.6343	0.4020
	80	0.0948	0.1731	0.2546	0.1889	0.2344	0.0784	0.3260	0.6412	0.3359	0.4829
	200	0.0993	0.0728	0.1101	0.0546	0.1141	1.2128	0.1384	0.2688	0.0759	0.2750
	500	0.0066	0.0312	0.0470	0.0225	0.0386	0.0034	0.0582	0.1182	0.0298	0.0859
	1000	0.0024	0.0135	0.0223	0.0112	0.0168	0.0008	0.0204	0.0569	0.0126	0.0352

Table 5.14: ABs and MSEs for $(\alpha, \rho, d, g) = (0.3, 0.6, 1.9, 2.5)$

Parameter	N	AB					MSE				
		MLE	OLSS	WLSS	CVM	AD	MLE	OLSS	WLSS	CVM	AD
α	30	0.0397	0.1725	0.1411	0.1804	0.1593	0.0052	0.0963	0.0716	0.1028	0.0862
	80	0.0252	0.0643	0.0547	0.0471	0.0605	0.0101	0.0356	0.0265	0.0216	0.0321
	200	0.0085	0.0226	0.0281	0.0170	0.0212	0.0022	0.0115	0.0166	0.0069	0.0102
	500	0.0033	0.0086	0.0108	0.0079	0.0104	0.0009	0.0043	0.0084	0.0036	0.0058
	1000	0.0021	0.0040	0.0054	0.0028	0.0031	0.0007	0.0019	0.0030	0.0012	0.0015
ρ	30	0.1962	0.7792	1.5758	1.8964	0.7341	0.1157	3.7316	14.0697	43.3902	2.5628
	80	0.1201	0.2833	0.4779	0.1195	0.1885	0.3647	1.5290	5.5306	0.1259	0.3187
	200	0.0137	0.0580	0.1401	0.0682	0.0713	0.0064	0.0713	1.1412	0.1221	0.1154
	500	0.0087	0.0293	0.0294	0.0234	0.0391	0.0049	0.0540	0.0633	0.0294	0.0847
	1000	0.0028	0.0147	0.0160	0.0135	0.0144	0.0011	0.0239	0.0349	0.0201	0.0226
d	30	0.9392	0.5772	0.5310	0.5936	0.6302	3.1812	1.0034	0.9115	1.0588	1.2182
	80	0.0835	0.2250	0.2071	0.2223	0.2251	0.0941	0.4054	0.3508	0.3960	0.4058
	200	0.0194	0.0911	0.0872	0.0922	0.0899	0.0175	0.1660	0.1527	0.1700	0.1619
	500	0.0060	0.0366	0.0366	0.0368	0.0364	0.0026	0.0671	0.0672	0.0678	0.0664
	1000	0.0016	0.0183	0.0179	0.0185	0.0185	0.0005	0.0335	0.0319	0.0342	0.0342
g	30	0.2714	0.5297	0.4047	0.7922	0.5353	0.2494	0.9186	0.6813	2.7916	1.0165
	80	0.0731	0.2240	0.3997	0.2248	0.1938	0.0841	0.4433	4.3132	0.4282	0.3957
	200	0.0155	0.1049	0.0778	0.0932	0.0554	0.0078	0.2259	0.1350	0.1807	0.1010
	500	0.0061	0.0353	0.0344	0.0312	0.0342	0.0022	0.0714	0.0876	0.0620	0.0740
	1000	0.0016	0.0120	0.0208	0.0108	0.0114	0.0004	0.0240	0.0439	0.0192	0.0192

Table 5.15: ABs and MSEs for $(\alpha, \rho, d, g) = (0.03, 0.42, 2.2, 2.6)$

Parameter	N	AB					MSE				
		MLE	OLSS	WLSS	CVM	AD	MLE	OLSS	WLSS	CVM	AD
α	30	0.0397	0.1725	0.1411	0.1804	0.1593	0.0052	0.0963	0.0716	0.1028	0.0862
	80	0.0252	0.0643	0.0547	0.0471	0.0605	0.0101	0.0356	0.0265	0.0216	0.0321
	200	0.0085	0.0226	0.0281	0.0170	0.0212	0.0022	0.0115	0.0166	0.0069	0.0102
	500	0.0033	0.0086	0.0108	0.0079	0.0104	0.0009	0.0043	0.0084	0.0036	0.0058
	1000	0.0021	0.0040	0.0054	0.0028	0.0031	0.0007	0.0019	0.0030	0.0012	0.0015
ρ	30	0.1962	0.7792	1.5758	1.8964	0.7341	0.1157	3.7316	14.0697	43.3902	2.5628
	80	0.1201	0.2833	0.4779	0.1195	0.1885	0.3647	1.5290	5.5306	0.1259	0.3187
	200	0.0137	0.0580	0.1401	0.0682	0.0713	0.0064	0.0713	1.1412	0.1221	0.1154
	500	0.0087	0.0293	0.0294	0.0234	0.0391	0.0049	0.0540	0.0633	0.0294	0.0847
	1000	0.0028	0.0147	0.0160	0.0135	0.0144	0.0011	0.0239	0.0349	0.0201	0.0226
d	30	0.9392	0.5772	0.5310	0.5936	0.6302	3.1812	1.0034	0.9115	1.0588	1.2182
	80	0.0835	0.2250	0.2071	0.2223	0.2251	0.0941	0.4054	0.3508	0.3960	0.4058
	200	0.0194	0.0911	0.0872	0.0922	0.0899	0.0175	0.1660	0.1527	0.1700	0.1619
	500	0.0060	0.0366	0.0366	0.0368	0.0364	0.0026	0.0671	0.0672	0.0678	0.0664
	1000	0.0016	0.0183	0.0179	0.0185	0.0185	0.0005	0.0335	0.0319	0.0342	0.0342
g	30	0.2714	0.5297	0.4047	0.7922	0.5353	0.2494	0.9186	0.6813	2.7916	1.0165
	80	0.0731	0.2240	0.3997	0.2248	0.1938	0.0841	0.4433	4.3132	0.4282	0.3957
	200	0.0155	0.1049	0.0778	0.0932	0.0554	0.0078	0.2259	0.1350	0.1807	0.1010
	500	0.0061	0.0353	0.0344	0.0312	0.0342	0.0022	0.0714	0.0876	0.0620	0.0740
	1000	0.0016	0.0120	0.0208	0.0108	0.0114	0.0004	0.0240	0.0439	0.0192	0.0192

5.6 Applications of the Harmonic Mixture Fréchet Distribution

In this section, we apply the HMFR distribution to three datasets to assess its empirical importance and evaluate its performance in modelling lifetime data. The HMFR distribution is compared with the Fréchet distribution and eight(8) other models. These eight(8) distributions can be seen in Table 5.16.

Table 5.16: Compared Models

Models	References
Burr X Fréchet (BRXFR)	Abouelmagd *et al.* (2018b)
Odd Lomax Fréchet (OLXF)	Hamed *et al.* (2020)
Type II Topp-Leone Fréchet Distribution (TIITLFD)	Shanker and Rahman (2021)
New exponential-X Fréchet (NEXF)	Alzeley *et al.* (2021)
Weibull Fréchet (WFR)	Afify *et al.* (2016)
Modified Fréchet-Rayleigh distribution (MFRD)	Ali *et al.* (2022)
Marshall-Olkin Fréchet distribution (MOF)	Krishna *et al.* (2013a)
Modified Fréchet (MF)	Tablada and Cordeiro (2017)

5.6.1 Annual Maximum Temperature

The range of annual maximum temperature values for the selected location was from the lowest value of 27.14 and the highest value of 29.15. The dataset exhibits a negative skewness of -0.72174, indicating a longer tail towards the left side of the distribution. Furthermore, it is characterised as platykurtic with a kurtosis of -0.13901, implying a flatter peak compared to a normal distribution.

The failure rate behaviour of the turbochargers failure time dataset was examined through a TTT plot. The TTT plot displayed an upward trend, indicating an increasing pattern. This observation is evident from the concave shape observed above the 45° line in Figure 5.14.

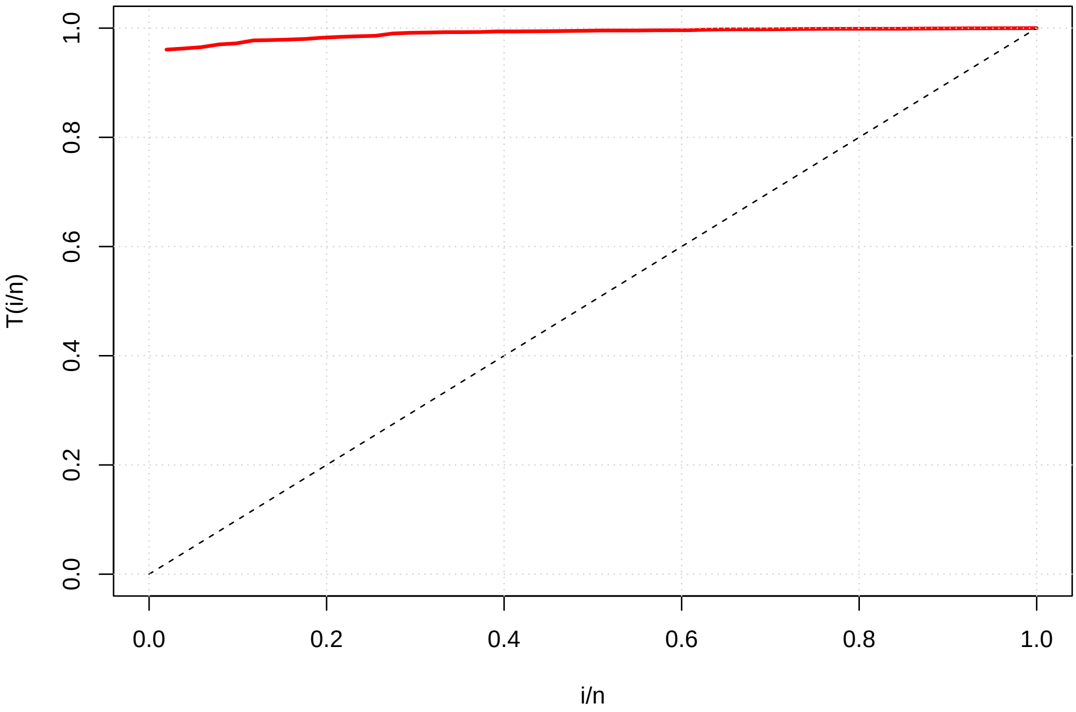

Figure 5.14: The TTT plot of the annual maximum temperature

Table 5.17 presents the MLEs for the fitted models, along with their respective SEs. Among the models, the parameters α and β for OLXF, θ for BRXFR, β for NEXF, θ for POF, a for WFR, and α for MOF were not found to be statistically significant at the 5% . However, all other parameters in their respective models exhibited statistical significance at the 5% level.

Table 5.17: MLEs for annual maximum temperature

Models		Estimates	SE	Z-value	P-Value
HMFR	α	40.0790	13.1322	3.0520	0.0023*
	ρ	0.9078	0.1543	5.8852	3.9750×10^{-9}*
	d	15.8698	3.0785	5.1551	2.5350×10^{-7}*
	g	30.2495	0.3419	88.4697	2.2000×10^{-16}*
FR	a	45.3511	4.8769	9.2992	2.2000×10^{-16}*
	b	28.0735	0.0894	314.0711	2.2000×10^{-16}*
OLXF	α	23.1059	37.9831	0.6083	0.5430
	β	0.5630	0.7048	0.7988	0.4244
	a	30.5067	0.9192	33.1895	2.2000×10^{-16}*
	b	18.3522	3.9236	4.6774	2.9050×10^{-16}*
BRXFR	θ	2.3847	2.6714	0.8927	0.3720
	a	27.4810	0.8143	33.7497	2.0000×10^{-16}*
	b	17.1136	8.2853	2.0655	0.0389 *
NEXF	λ	15.0636	3.1043	4.8525	1.2190×10^{-6}*
	α	31.4570	1.0673	29.4723	2.2000×10^{-16}*
	β	100.2569	97.1546	1.0319	0.3021
TIITLFD	λ	29.4032	8.7019	3.3789	0.0007*
	α	29.9191	6.6003	4.5330	5.8150×10^{-6}*
	β	0.8415	0.0680	12.3756	2.2000×10^{-16}*
WFR	α	19.9392	0.0962	207.3052	2.0000×10^{-16}*
	β	3.9803	0.4549	8.7500	2.0000×10^{-16}*
	a	0.0011	0.0011	1.0360	0.3002
	b	5.3437	0.6344	8.4235	2.0000×10^{-16} *
MFRD	α	2.1947×10^{2}	3.2926×10^{-8}	6.6655×10^{9}	2.2000×10^{-16} *
	λ	8.0889×10^{-2}	9.5331×10^{-4}	84.8500	2.2000×10^{-16} *
MF	α	100.7435	12.8332	7.8502	4.1530×10^{-15} *
	β	16.2220	1.9915	8.1454	3.7790×10^{-16}*
	λ	0.7396	0.1342	5.5096	3.5960×10^{-8} *
MOF	α	0.1000	0.1388	0.7206	0.4712
	a	31.0754	9.7647	3.1824	0.0015 *
	b	29.0203	0.7679	37.7920	2.0000×10^{-16}*

* means significant at 0.05 .

Based on multiple evaluation criteria shown in Table 5.18, the HMFR model demonstrates a better fit than the other models considered. It achieves the highest log-likelihood value, the lowest values for AIC, AICC, and BIC, and the lowest values for A, KS, and W. These results indicate that the HMFR model provides an improved fit to the dataset, making it a preferred choice for analysing the data.

Table 5.18: Comparison criteria for annual maximum temperature

Models	ℓ	AIC	AICC	BIC	KS	A	W
HMFR	-28.7909	65.5842	66.4537	73.3115	0.0645	0.3396	0.0470
FR	-42.5651	89.1302	89.4635	92.9938	0.2157	3.1804	0.5432
OLXF	-30.9246	69.8492	70.7188	77.5765	0.1355	0.9605	0.1814
BRXFR	-30.2993	66.5986	67.1092	74.3941	0.1247	0.7475	0.1410
NEXF	-30.9869	67.9738	68.4844	73.7692	0.1180	0.7227	0.1284
TIITLFD	-165.2245	336.4489	336.9596	342.2444	0.5138	18.4430	3.9403
WFR	-80.5159	169.0318	169.4529	176.7591	0.3604	12.0360	2.4098
MFRD	-95.5231	195.0461	195.2961	198.9098	0.4651	14.0050	2.9005
MF	-47.3878	100.7756	101.2862	106.5711	0.2596	4.4583	0.8034
MOF	-41.8305	89.6610	90.1716	95.4564	0.1770	2.5015	0.4127

The fitted PDFs and CDFs of the models are depicted in Figure 5.15 and 5.16, respectively. These plots visually demonstrate that the HMFR model exhibits a superior fit to the annual maximum temperature compared to the other models.

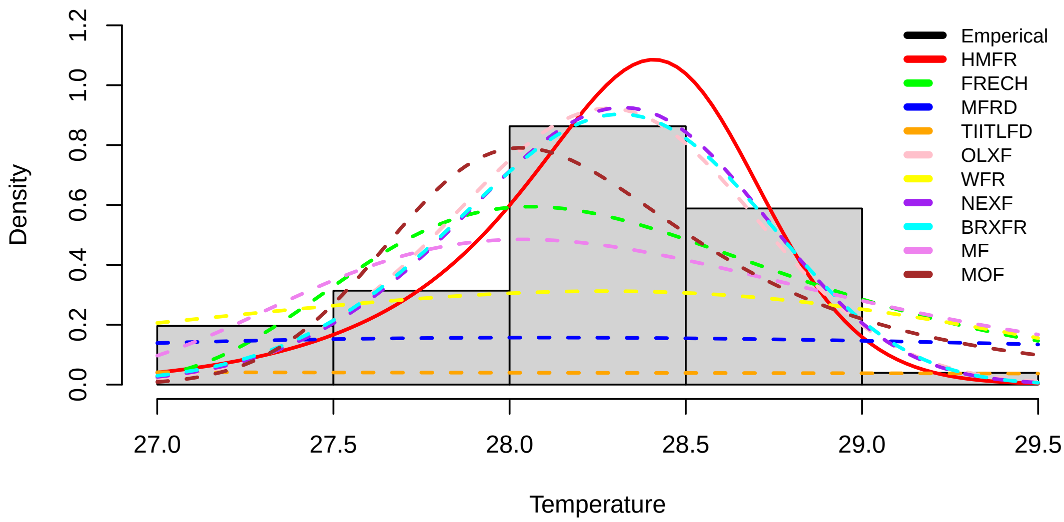

Figure 5.15: The fitted PDFs for annual maximum temperatures

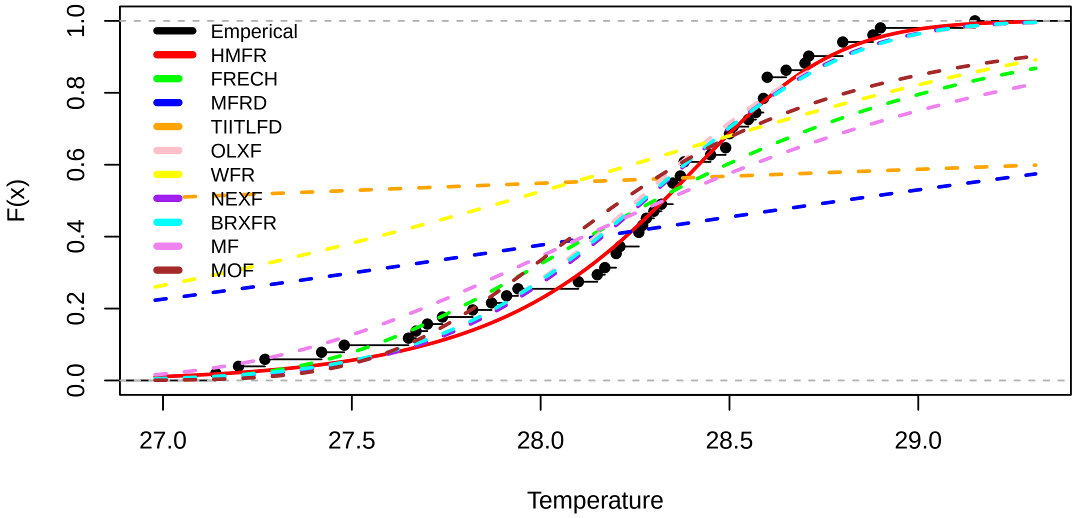

Figure 5.16: The fitted CDFs for annual maximum temperature

The profile log-likelihood plots in Figure 5.17 provide visual evidence that the estimated parameter values of the HMFR distribution correspond to the real maxima, validating the accuracy of the estimation process for analysing the annual maximum temperatures.

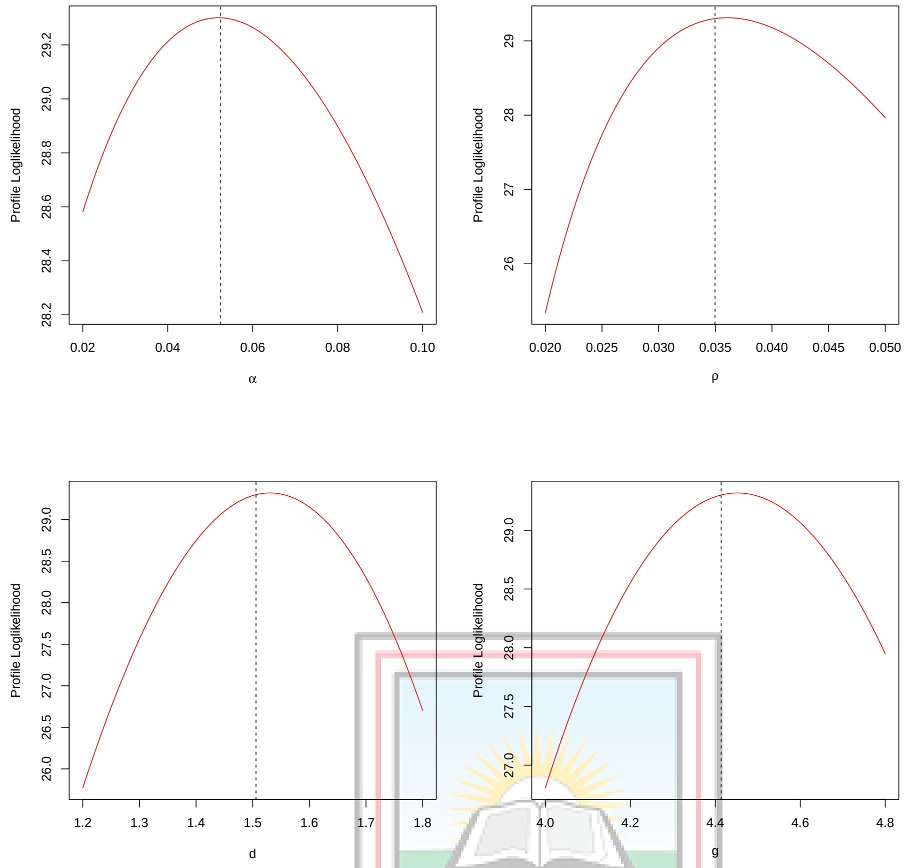

Figure 5.17: Profile log-likelihood plots of HMFR for annual maximum temperature

5.6.2 Annual Unemployment Rates Data

The unemployment rates in Ghana (1991-2021) ranged from a minimum value of 3.49 to a maximum value of 10.46. The distribution of the data set exhibited positive skewness with a value of 0.9636, indicating a longer tail on the right side of the distribution. Additionally, the data set was characterised by platykurtic behaviour with a value of 0.3614, indicating a flatter peak compared to a normal distribution. The failure rate behaviour of the turbochargers failure time dataset was examined through a TTT plot. The TTT plot displayed an upward trend, indicating an increasing pattern. This observation is evident from the concave shape observed above the 45° line in Figure 5.18.

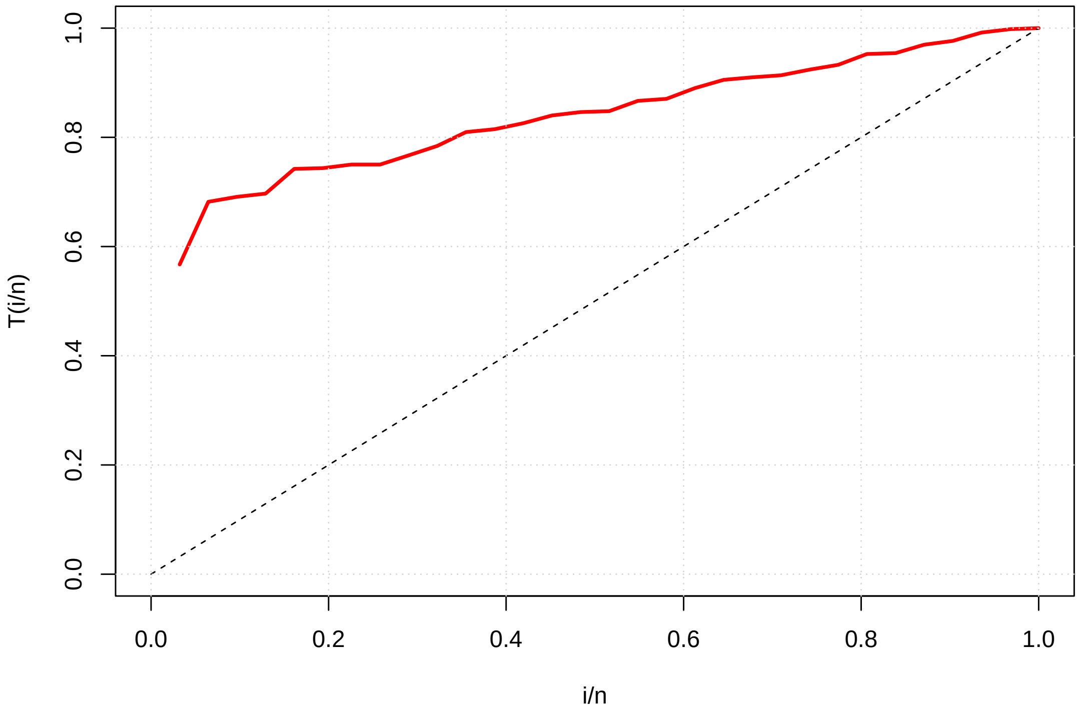

Figure 5.18: The TTT plot of the unemployment rates

Table 5.19 presents the MLEs for the fitted models along with their respective SEs. In the HMFR model, the parameters α, ρ, and d were not found to be statistically significant at 5%. Similarly, in the OLXF model, the parameters α, β, and b, in the BRXFR model, the parameters θ and a, in the NEXF model, the parameter β, in the POF model, the parameter θ, in the WFR model, the parameters α, a, and b, in the MFRD model, the parameter α, and in the MOF model, the parameter α, were not statistically significant at the 5% level. However, all other parameters in their respective models were found to be statistically significant at 5%.

Table 5.19: MLEs for unemployment rates

Models		Estimates	SE	Z-value	P-Value
HMFR	α	0.1154	0.8423	0.1370	0.8911
	ρ	0.2124	0.7075	0.3002	0.7641
	d	5.6793	3.3105	1.7156	0.0862
	g	4.4458	0.7415	5.9958	2.0250×10^{-9} *
FR	a	5.4461	0.6784	8.0280	9.9060×10^{-16} *
	b	5.0578	0.1832	27.6010	2.2000×10^{-16} *
OLXF	α	2.3256	2.9759	0.7815	0.4345
	β	2.0566	2.7620	0.7446	0.4565
	a	5.5703	1.6870	3.3020	0.0010*
	b	3.3100	1.7213	1.9229	0.0545
BRXFR	θ	10.6357	14.1366	0.7524	0.4518
	a	1.7521	1.3559	1.2922	0.1963
	b	0.6209	0.2418	2.5684	0.0102 *
NEXF	λ	1.9451	0.8683	2.2402	0.0251*
	α	8.9273	3.7989	2.3500	0.0188*
	β	5.8575	6.7416	0.8689	0.3849
TIITLFD	λ	9.7855	5.2663	1.8581	0.0632
	α	16.3877	8.2967	1.9752	0.0483 *
	β	1.3993	0.3549	3.9432	8.0410×10^{-5}*
WFR	α	13.7276	7.2129	1.9032	0.0570
	β	1.9702	0.6160	3.1981	0.0014 *
	a	6.5422	4.6380	1.4106	0.1584
	b	0.4098	0.2851	1.4376	0.1506
MFRD	α	14.5074	15.3008	0.9481	0.3431
	λ	0.2866	0.0616	4.6511	3.3020×10^{-6} *
MF	α	107.7300	3.0280×10^{-4}	3.5577×10^{5}	2.2000×10^{-16}*
	β	1.0345	0.1405	7.3647	1.7750×10^{-13}*
	λ	0.5833	8.6299×10^{-2}	6.7595	1.3850×10^{-11}*
MOF	α	6.3818	9.7604	0.6539	0.5132
	a	5.8467	1.2352	4.7336	2.2060×10^{-6}*
	b	4.1640	0.7496	5.5551	2.7740×10^{-8} *

* means significant at 0.05.

After evaluating multiple criteria shown in Table 5.20, it has been determined that the HMFR model outperforms the other models under consideration. The HMFR model achieves the highest log-likelihood value, indicating a better fit to the data compared to the alternative models. Additionally, it exhibits lower values for various model selection criteria such as AIC , AICC, and BIC . Furthermore, the HMFR model demonstrates lower values for statistical measures like A , KS , and W. These results collectively suggest that the HMFR model provides an improved fit to the dataset and is considered the preferred choice for analysing the data.

Table 5.20: Comparison criteria for unemployment rates

Models	ℓ	AIC	AICC	BIC	KS	A	W
HMFR	-56.3771	120.7541	122.2926	126.4901	0.0617	0.1603	0.0170
FR	-59.9664	123.9328	124.3614	126.8008	0.1518	1.1522	0.1766
OLXF	-57.7204	123.4408	124.9793	129.1767	0.0629	0.1706	0.0198
BRXFR	-58.1791	122.7959	122.3581	126.6601	0.0884	0.3128	0.0404
NEXF	-58.5243	123.0486	123.9375	127.3506	0.0706	0.1885	0.0247
TIITLFD	-58.5613	123.1226	123.6333	127.4246	0.0997	0.3643	0.0603
WFR	-57.8635	123.7270	125.2655	129.4629	0.0624	0.1750	0.0207
MFRD	-63.5791	131.1581	131.5867	134.0261	0.1485	2.2053	0.1855
MF	-58.1597	122.3194	123.2083	128.6214	0.0668	0.1854	0.0227
MOF	-58.4460	122.8920	123.7808	127.1940	0.0630	0.1942	0.0228

Figures 5.19 and 5.20 present the fitted PDFs and CDFs of the models, respectively, for the annual unemployment rates. From these figures, it is evident that the HMFR model provides a superior fit to the data set.

Figure 5.19: The fitted PDFs for annual unemployment rates

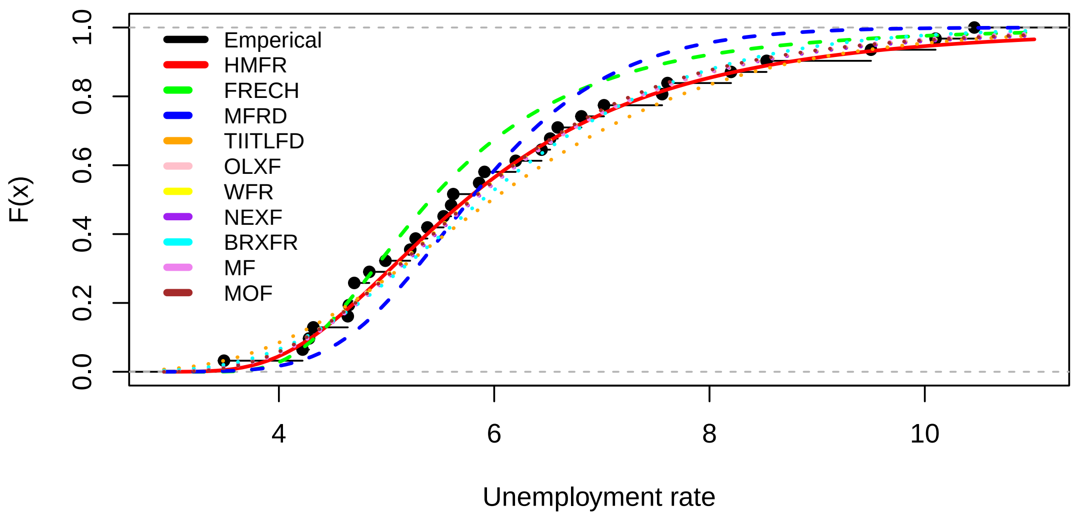

Figure 5.20: The fitted CDFs for annual unemployment rates

The profile log-likelihood plots in Figure 5.21 provide visual evidence that the estimated parameter values of the HMFR distribution correspond to the real maxima, validating the accuracy of the estimation process for analysing the annual unemployment rates.

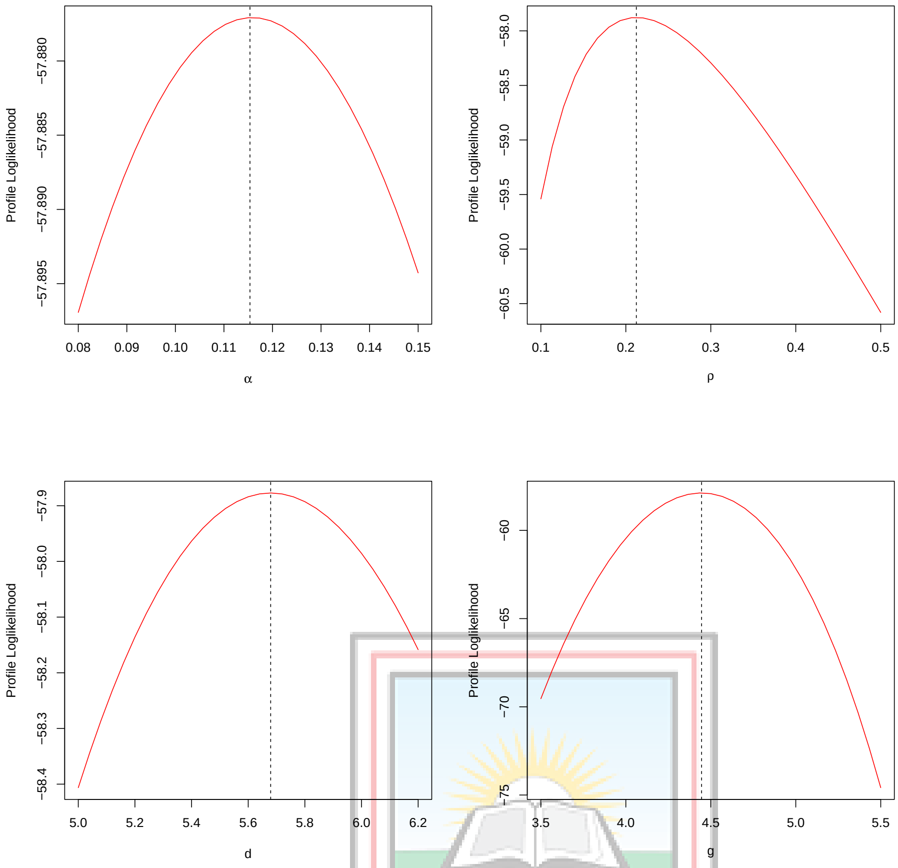

Figure 5.21: Profile log-likelihood plots of HMFR for annual unemployment rates

5.6.3 Bladder Cancer Remission Time

The range of remission time values for the given data set is a minimum value of 0.08 and a maximum value of 79.05. The data set exhibits a high level of positive skewness (3.3257) and a significant degree of kurtosis (16.1537), indicating a distribution that is heavily skewed and has a heavy tail.

The failure rate characteristics of the bladder cancer remission times were analysed using a TTT plot. The TTT plot revealed an inverted bathtub pattern, characterised by a concave shape above the 45° line and a convex shape below the 45° line. This pattern is visually depicted in Figure 5.22.

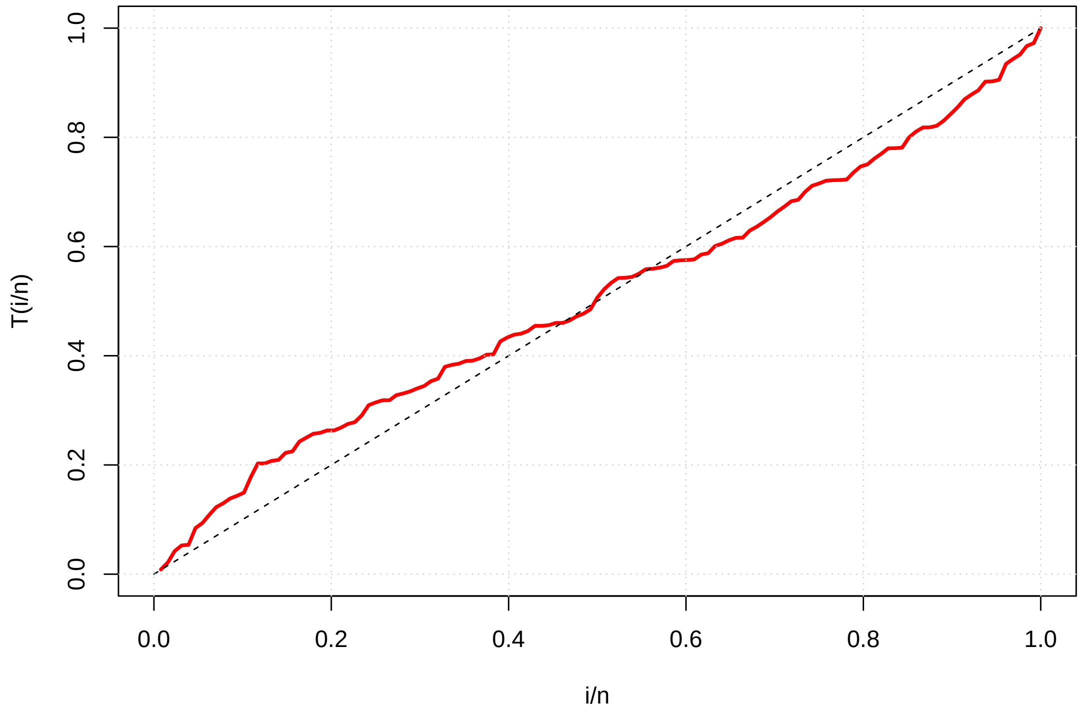

Figure 5.22: The TTT plot of the bladder cancer remission times

Table 5.21 presents the MLEs for the fitted models along with their standard errors. Among the models, the HMFR distribution had non-significant estimates for α and ρ, the OLXF distribution had non-significant estimates for α, β, and a, the BRXFR distribution had a non-significant estimate for a, and the WFR distribution had non-significant estimates for α and a, all at a significance level of 5%. However, the remaining models had significant estimates for their respective parameters at the same significance level.

Table 5.21: MLEs for bladder cancer remission times

Models		Estimates	SE	Z-value	P-Value
HMFR	α	0.0075	0.0059	1.2571	0.2087
	ρ	0.0011	0.0013	0.8759	0.3811
	d	1.7943	0.1688	10.6313	2.0000×10^{-16}*
	g	0.1438	0.0627	2.2948	0.0217 *
FR	a	0.7521	0.0424	17.7277	2.2000×10^{-16} *
	b	3.2582	0.4074	7.9968	1.2770×10^{-15}*
OLXF	α	10.9599	10.7136	1.0230	0.3063
	β	7.3718	6.7480	1.0924	0.2746
	a	6.3765	11.1471	0.5720	0.5673
	b	0.5934	0.2278	2.6048	0.00919*
BRXFR	θ	10.5872	3.4611	3.0589	0.0022 *
	a	0.0420	0.0319	1.3171	0.1878
	b	0.1537	0.0156	9.8552	2.2000×10^{-16}*
NEXF	λ	0.3706	0.0308	12.0272	2.2000×10^{-16} *
	α	105.1600	49.2872	2.1336	0.0329*
	β	12.5056	3.6673	3.4101	0.0006*
TIITLFD	λ	27.7208	13.1839	2.1026	0.0355*
	α	3.1026	0.2671	11.6141	2.2000×10^{-16}*
	β	0.2904	0.0367	7.9188	2.3980×10^{-15}*
WFR	α	9.7511	18.5793	0.5248	0.5997
	β	0.2546	0.0673	3.7826	0.0001*
	a	4.2136	0.9775	0.6039	0.5459
	b	2.5171	0.9359	2.6894	0.0072*
MFRD	α	0.4386	0.0398	11.0260	2.2000×10^{-16} *
	λ	0.0439	0.0039	11.3270	2.2000×10^{-16}*
MF	α	11.1133	3.8318	2.9003	0.0037 *
	β	0.4190	0.0563	7.4434	9.8150×10^{-15}*
	λ	0.0942	0.0145	6.5211	6.9800×10^{-11}*
MOF	α	23.3227	8.0536	2.8959	0.0038*
	a	1.2732	0.0805	15.8166	2.2000×10^{-16}*
	b	0.4479	0.0888	5.0422	4.6030×10^{-7}*

* means significant at 5%.

The HMFR model outperforms the other models in terms of multiple evaluation criteria in Table 5.22. It exhibits the highest log-likelihood value and demonstrates lower values for model selection criteria such as AIC, AICC, and BIC. Additionally, it achieves lower values for statistical measures like A, KS, and W. These findings collectively indicate that the HMFR model offers a superior fit to the dataset, making it the preferred choice for data analysis.

Table 5.22: Comparison criteria for bladder cancer remission times

Models	ℓ	AIC	AICC	BIC	KS	A	W
HMFR	-410.0725	828.1450	828.4702	839.5531	0.0331	0.1562	0.0171
FR	-444.0008	892.0015	890.0975	897.7056	0.1408	6.1182	0.9787
OLXF	-421.0557	850.1114	850.4366	861.5196	0.1108	2.4023	0.4409
BRXFR	-415.4706	836.9412	837.1347	845.4973	0.0680	0.9021	0.1446
NEXF	-417.0997	840.1993	840.3928	848.7554	0.0711	1.0378	0.1646
TIITLFD	-413.2888	832.5775	833.0882	841.1336	0.0540	0.5619	0.0818
WFR	-411.7882	831.5763	831.9015	842.9844	0.0608	0.5332	0.0840
MFRD	-422.7039	849.4077	849.5037	855.1118	0.1272	3.1031	0.5959
MF	-413.8641	833.7281	833.9216	842.2842	0.0753	0.8232	0.1275
MOF	-422.5995	851.1991	851.3926	859.7552	0.1062	2.7168	0.44012

Figure 5.23 displays the fitted PDFs of the models, while Figure 5.24 shows the corresponding CDFs for the bladder cancer remission times. As observed in these figures, the HMFR model provides the best fit to the data, as its PDF closely matches the observed distribution and its CDF follows the empirical distribution function. Among the alternative models, including BRXFR, NEXF, WFR, and MF, they also exhibit reasonably good fits to the data, with their PDFs and CDFs showing similarities to the observed distribution, albeit not as close as the HMFR model.

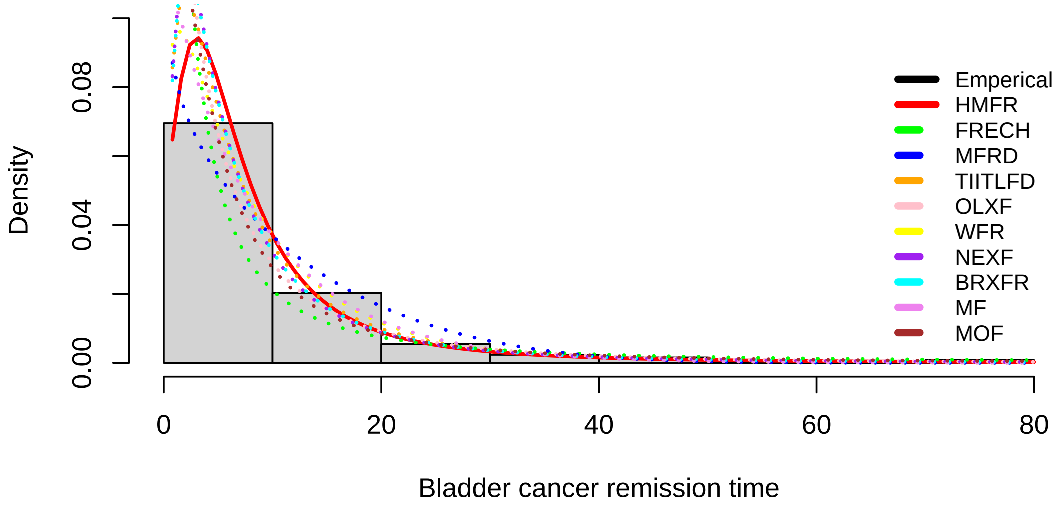

Figure 5.23: The fitted PDFs for bladder cancer remission times

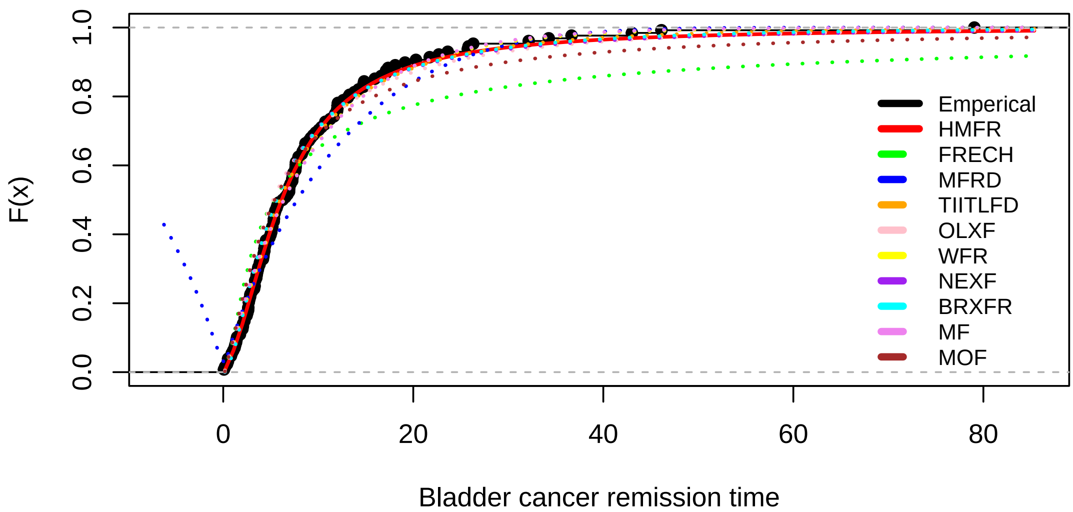

Figure 5.24: The fitted CDFs for bladder cancer remission times

Figure 5.25 presents the profile log-likelihood plots. These plots provide valuable insights into the behaviour of the estimated parameters and their impact on the likelihood function. From the figures, it is evident that the estimated parameter values align with the peaks of the log-likelihood function, indicating that they correspond to the true maxima of the distribution. This further supports the suitability of the HMFR model for describing the remission time data set.

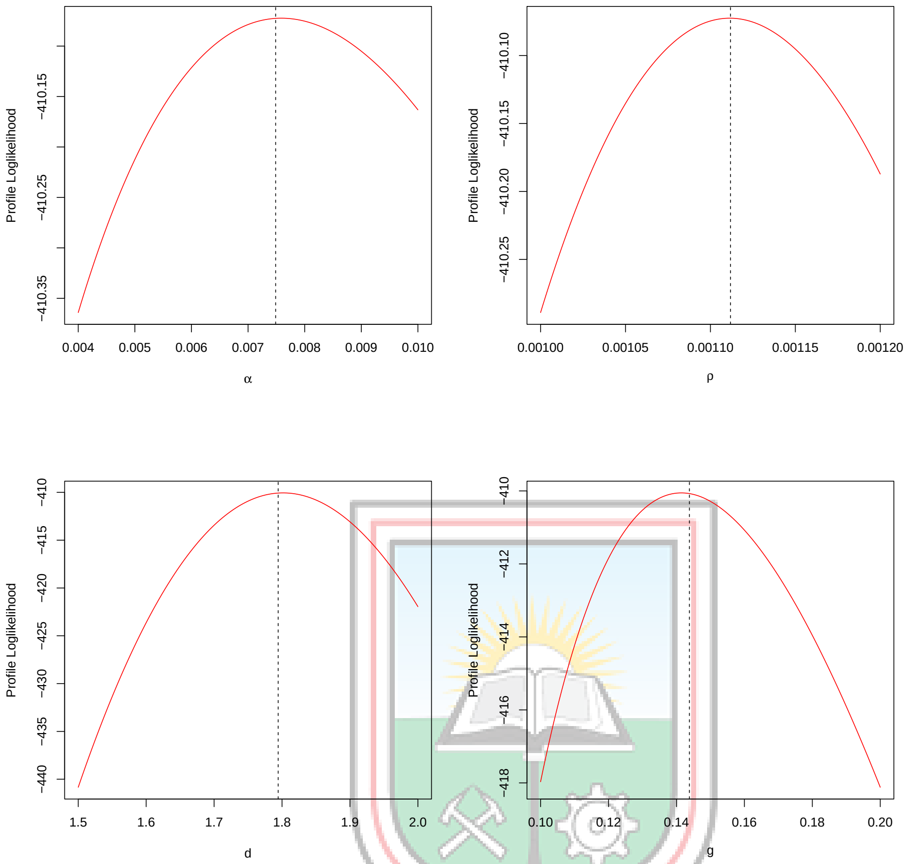

Figure 5.25: Profile log-likelihood plots of HMF for bladder cancer remission times

5.7 Monte Carlo Simulations of the Harmonic Mixture Burr XII Distribution

In this section, we conduct simulation experiments to evaluate the accuracy of the estimated parameters in the HMBRXII distribution. The experiments are performed using three different parameter combinations: $(\alpha, \rho, d, w) = (0.50, 0.20, 2.60, 1.20)$, $(\alpha, \rho, d, w) = (0.90, 0.50, 2.60, 1.02)$ and $(\alpha, \rho, d, w) = (0.45, 0.30, 2.05, 1.20)$. We replicate the experiments 1000 times using various sample sizes: 30, 80, 200, 500, and 1000. The goal is to assess the accuracy of the estimated parameters in the HMBRXII distribution across these different sample sizes.

The results are shown in Table 5.23, 5.24 and 5.25. As the sample sizes increase, we observe a general trend of decreasing ABs and MSEs for the estimators of various parameters. Although there may be deviations, the MLE consistently exhibit the least ABs and MSEs, indicating their superior performance as the best estimators.

Table 5.23: ABs and MSEs for $(\alpha, \rho, d, w) = (0.50, 0.20, 2.60, 1.20)$

Parameter	N	AB					MSE				
		MLE	OLSS	WLSS	CVM	AD	MLE	OLSS	WLSS	CVM	AD
α	30	0.2095	0.3210	0.1973	0.3039	0.2254	0.1193	0.3842	0.1157	0.3334	0.1568
	80	0.0837	0.1185	0.0970	0.0963	0.0720	0.1374	0.2800	0.1928	0.2141	0.1146
	200	0.0173	0.0354	0.0346	0.0387	0.0442	0.0562	0.1565	0.1487	0.1836	0.2660
	500	0.0058	0.0118	0.0145	0.0116	0.0213	0.0394	0.1129	0.1964	0.1435	0.3456
	1000	0.0031	0.0060	0.0071	0.0061	0.0114	0.0473	0.1279	0.1872	0.1408	0.3778
ρ	30	0.1049	0.1138	0.1917	0.1312	0.0982	0.0282	0.0327	0.1171	0.0538	0.0322
	80	0.0474	0.0407	0.0594	0.0387	0.0593	0.0446	0.0361	0.1100	0.0327	0.0977
	200	0.0192	0.0174	0.0140	0.0097	0.0274	0.0508	0.0392	0.0436	0.0163	0.1183
	500	0.0067	0.0068	0.0066	0.0070	0.0135	0.0351	0.0489	0.0579	0.0522	0.1461
	1000	0.0022	0.0031	0.0039	0.0038	0.0053	0.0280	0.0311	0.0775	0.0638	0.1117
d	30	0.6061	2.5971	2.5128	2.5805	2.5668	0.5243	6.7452	6.3828	6.6663	6.5950
	80	0.2929	2.5662	2.5650	2.5744	2.5588	0.1264	6.5958	6.6027	6.6398	6.5543
	200	0.2449	2.5906	2.5777	2.5942	2.5999	0.0800	6.7126	6.6533	6.7301	6.7592
	500	0.1202	2.5892	2.5664	2.5968	2.5911	0.0239	6.7054	6.6078	6.7435	6.7147
	1000	0.0975	2.5981	2.5398	2.5995	2.5968	0.0179	6.7502	6.4968	6.7572	6.7434
w	30	1.5589	0.3573	0.2025	0.3194	0.1875	1.5863	2.1662	2.0779	2.1360	2.0263
	80	0.7502	0.2424	0.1754	0.2555	0.1475	1.3973	2.3678	2.1691	2.1124	2.0728
	200	0.4360	0.2324	0.2308	0.1947	0.2007	1.3507	1.9656	2.0370	2.1451	2.3965
	500	0.3919	0.2024	0.2766	0.3416	0.2118	1.3666	1.7739	2.0492	1.5906	2.6104
	1000	0.1257	0.3361	0.2325	0.1993	0.2189	1.6405	1.7688	2.0521	1.9289	2.5952

Table 5.24: ABs and MSEs for $(\alpha, \rho, d, w) = (0.90, 0.50, 2.60, 1.02)$

Parameter	N	AB					MSE				
		MLE	OLSS	WLSS	CVM	AD	MLE	OLSS	WLSS	CVM	AD
α	30	0.3864	0.1206	0.1146	0.2967	0.2300	0.4450	0.0599	0.0471	1.3988	0.2195
	80	0.1226	0.0441	0.0470	0.0622	0.0340	0.3550	0.0456	0.0531	0.1649	0.0343
	200	0.0468	0.0206	0.0427	0.0246	0.0271	0.3151	0.0922	0.6318	0.1157	0.2055
	500	0.0160	0.0203	0.0133	0.0158	0.0167	0.1979	0.6006	0.2604	0.7425	0.3018
	1000	0.0037	0.0049	0.0047	0.0084	0.0056	0.0970	0.1725	0.1007	0.6187	0.2482
ρ	30	0.1827	0.1280	0.0969	0.1391	0.1454	0.1199	0.0608	0.0311	0.0697	0.0634
	80	0.0440	0.0396	0.0525	0.0506	0.0563	0.0653	0.0405	0.0616	0.0581	0.0715
	200	0.0165	0.0196	0.0205	0.0220	0.0221	0.0573	0.0469	0.0631	0.0615	0.0713
	500	0.0137	0.0089	0.0096	0.0092	0.0083	0.1579	0.0643	0.0792	0.0728	0.0652
	1000	0.0038	0.0039	0.0052	0.0044	0.0047	0.0625	0.0658	0.0870	0.0740	0.0815
d	30	0.6399	2.5304	2.3095	2.5051	2.5391	0.7009	6.4324	5.6597	6.3179	6.4772
	80	0.3121	2.6000	2.5844	2.5993	2.5745	0.1874	6.7600	6.6838	6.7562	6.6340
	200	0.1854	2.5987	2.5359	2.6000	2.6000	0.0619	6.7531	6.4688	6.7600	6.7600
	500	0.0866	2.5875	2.5461	2.5999	2.5938	0.0103	6.6959	6.5373	6.7593	6.7281
	1000	0.1151	2.5985	2.6000	2.5988	2.5955	0.0200	6.7524	6.7600	6.7535	6.7365
w	30	2.1154	0.4273	0.0746	0.0546	0.1623	6.0270	4.1687	2.4208	2.6104	2.4577
	80	0.8363	0.0510	0.0433	0.1000	0.0574	1.6054	2.5507	2.6102	2.4850	2.5018
	200	0.5378	0.0705	0.0799	0.0909	0.0793	1.6920	2.5944	2.4326	2.5093	2.5998
	500	0.7724	0.1394	0.0815	0.0801	0.1187	1.1552	2.9596	2.5572	2.6029	2.3718
	1000	0.2979	0.0628	0.0541	0.1396	0.1190	2.0218	2.5780	2.4886	2.6408	2.3721

Table 5.25: ABs and MSEs for $(\alpha, \rho, d, w) = (0.45, 0.30, 2.05, 1.20)$

Parameter	N	AB					MSE				
		MLE	OLSS	WLSS	CVM	AD	MLE	OLSS	WLSS	CVM	AD
α	30	0.1885	0.4023	0.3328	0.4181	0.3547	0.0941	0.4076	0.3696	0.4413	0.3635
	80	0.0595	0.1333	0.1310	0.1393	0.1087	0.0768	0.3305	0.3364	0.3501	0.2230
	200	0.0168	0.0548	0.0513	0.0522	0.0508	0.0454	0.3529	0.2987	0.3146	0.3082
	500	0.0059	0.0229	0.0196	0.0215	0.0262	0.0408	0.4820	0.2846	0.3351	0.4547
	1000	0.0031	0.0125	0.0122	0.0102	0.0136	0.0530	0.4306	0.4547	0.3176	0.4642
ρ	30	0.1609	0.1187	0.1387	0.1241	0.1233	0.0629	0.0502	0.0751	0.0456	0.0563
	80	0.0677	0.0426	0.0465	0.0475	0.0582	0.0775	0.0410	0.0549	0.0451	0.0929
	200	0.0216	0.0225	0.0181	0.0120	0.0190	0.0602	0.0610	0.0547	0.0485	0.0713
	500	0.0092	0.0085	0.0084	0.0072	0.0048	0.0635	0.0682	0.0652	0.0601	0.0308
	1000	0.0026	0.0040	0.0038	0.0046	0.0029	0.0421	0.0677	0.0525	0.0821	0.0363
d	30	0.5270	2.0274	1.9810	2.0220	2.0053	0.4315	4.1201	3.9772	4.0987	4.0438
	80	0.2356	2.0500	1.9693	2.0490	2.0466	0.1053	4.2025	3.9146	4.1984	4.1889
	200	0.1421	2.0433	2.0161	2.0497	2.0322	0.0346	4.1759	4.0736	4.2011	4.1324
	500	0.1162	2.0453	2.0088	2.0500	2.0480	0.0238	4.1835	4.0508	4.2024	4.1943
	1000	0.1013	2.0465	2.0153	2.0495	2.0457	0.0143	4.1883	4.0714	4.2006	4.1850
w	30	2.3595	0.2819	0.2415	0.2515	0.2697	6.7571	1.1769	0.9350	1.2204	1.0038
	80	1.0508	0.2318	0.2163	0.2175	0.1544	0.8475	1.052	1.0525	1.1285	1.0085
	200	0.4050	0.2138	0.1908	0.2273	0.2068	0.3997	1.1003	1.0776	1.0416	1.1099
	500	0.4281	0.3246	0.2487	0.2577	0.2714	0.3679	1.1316	1.0712	1.0932	1.2624
	1000	0.2975	0.3252	0.2545	0.2458	0.2824	0.5682	1.2391	1.2135	1.1125	1.2843

5.8 Applications of the Harmonic Mixture Burr XII Distribution

In this section, we apply the HMBRXII distribution to three datasets to assess its empirical importance and evaluate its performance in modelling lifetime data. The HMBRXII distribution is compared with nine(9) other models. These nine(9) distributions can be seen in Table 5.26.

Table 5.26: Compared Models

Models	References
Marshall-Olkin exponentiated Burr XII (MOEBRXII)	(Cordeiro *et al.*, 2017)
Exponentiated Burr XII Poisson distribution (EBRXIIP)	(Nasir *et al.*, 2019)
Marshall-Olkin Generalized Burr XII distribution (MOGBRXII)	(Afify and Abdellatif, 2020)
Weibull Burr XII distribution (WBRXII)	(Afify *et al.*, 2018)
Kumaraswamy exponentiated Burr XII distribution (KEBRXII)	(Afify and Mead, 2017)
Kumaraswamy Burr XII distribution (KWBRXII)	(Paranaíba *et al.*, 2013)
exponentiated Exponential Burr XII distribution (EEBRXII)	(Badr and Ijaz, 2021)
Gompertz-modified Burr XII distribution (GMBRXII)	(Abubakari *et al.*, 2021)
odd exponentiated half-logistic Burr XII distribution (OEHLBRXII)	(Aldahlan and Afify, 2018)

5.8.1 Taxes Revenues

The minimum value of the tax revenues was 0.3900, while the maximum value was 5.5600. The CS for the data set is 0.3985, indicating a positive skewness. Additionally, the CK is 0.2492, suggesting that the data set is platykurtic and has a flatter peak compared to a normal distribution curve.

The failure rate behaviour of the taxes revenues was examined through a TTT plot. The TTT plot displayed an upward trend, indicating an increasing pattern. This observation is evident from the concave shape observed above the 45° line in Figure 5.26.

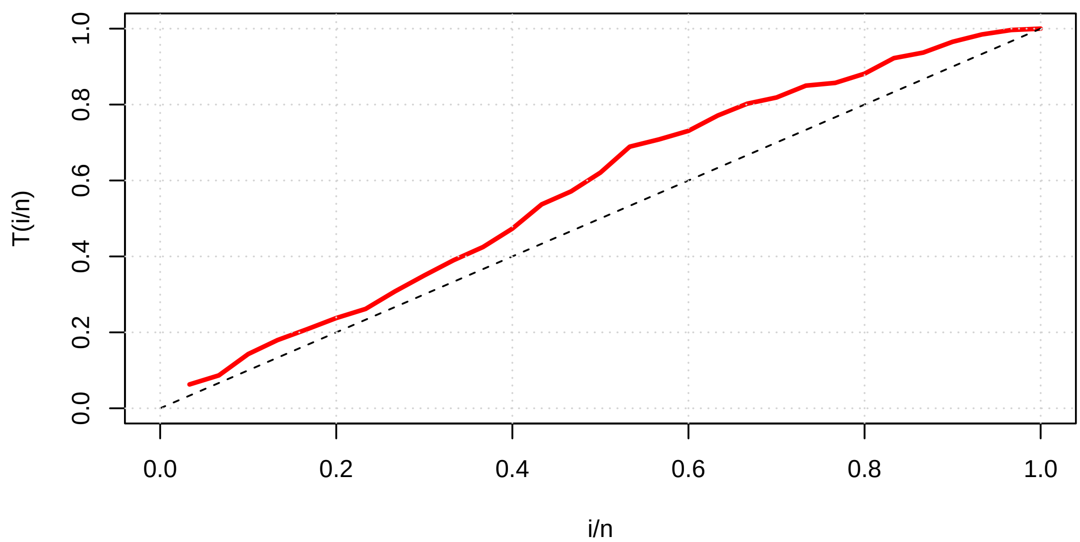

Figure 5.26: The TTT plot of the taxes revenues

Table 5.27 presents the MLEs for the fitted models and their respective SEs. Among the models, the parameters ρ for HMBRXII, α, λ, and k for MOEBRXII, α for EBRXIIP, δ for MOGBRXII, α and a for WBRXII, k for KEBRXII, k for KWBRXII, a for EEBRXII, λ for GMBRXII, and λ and a for OEHLBRXII were found to be not statistically significant at a significance level of 5%.

Table 5.27: MLEs for taxes revenues

Models		Estimates	SE	Z-value	P-Value
HMBRXII	α	0.048	0.016	3.031	0.002*
	ρ	0.002	0.002	0.664	0.507
	d	4.125	1.224	3.369	0.001*
	w	1.522	0.424	3.588	3.0×10^{-4}*
MOEBRXII	α	60.086	46.704	1.287	0.198
	λ	4.228	5.779	0.732	0.464
	c	1.518	0.693	2.191	0.028 *
	k	3.436	1.980	1.736	0.083
EBRXIIP	α	7.176	6.368	1.127	0.260
	θ	-4.806	1.489	-3.228	0.001 *
	c	1.402	0.487	2.881	0.004 *
	k	2.595	1.140	2.276	0.023 *
MOGBRXII	α	2.137	0.697	3.068	0.002 *
	β	0.373	0.159	2.351	0.019 *
	δ	114.463	97.270	1.177	0.239
	a	6.063	2.579	2.351	0.019 *
WBRXII	α	1.500	0.791	1.897	0.058
	β	0.642	0.238	2.698	0.007 *
	a	0.166	0.175	0.945	0.345
	b	2.351	0.987	2.383	0.017 *
KEBRXII	a	1.407	0.310	4.543	5.5×10^{-6}*
	β	10.322	2.272	4.543	5.5×10^{-6}*
	b	24.338	10.918	2.229	0.026 *
	c	0.726	0.264	2.755	0.006 *
	k	1.415	0.756	1.873	0.061
KWBRXII	a	0.533	0.234	2.277	0.023 *
	b	0.821	0.627	1.309	0.191
	c	4.867	1.551	3.138	0.002 *
	k	2.254	1.710	1.318	0.187
	s	3.532	0.691	5.110	3.2×10^{-7}*
EEBRXII	a	19.705	11.021	1.788	0.074
	b	178.164	0.032	5.62×10^{3}	2.2×10^{-16}*
	c	0.479	0.152	3.160	0.002 *
	k	1.502	0.650	2.310	0.021 *
GMBRXII	λ	0.153	0.361	0.425	0.671
	θ	0.842	0.265	3.178	0.002 *
	c	2.822	0.761	3.710	2.0×10^{-4}*
	d	0.043	0.011	4.007	6.1×10^{-5}*
OEHLBRXII	a	6.086	3.618	1.682	0.093
	α	0.776	0.256	3.034	0.002*
	b	0.399	0.186	2.147	0.032*
	λ	0.099	0.094	1.057	0.291

* means significant at 5%.

Table 5.28 demonstrates that the proposed HMBRXII model outperforms the other competing models. It achieves the highest log-likelihood value, the lowest values for AIC, AICC, and BIC, and the lowest values for A, KS, and W. Additionally, the HMBRXII model exhibited the lowest A, KS, and W values, further supporting its superior goodness-of-fit compared to the other models.

Table 5.28: Metrics for evaluation for taxes revenues

Models	ℓ	AIC	AICC	BIC	KS	A	W
HMBRXII	-140.724	289.448	289.869	299.869	0.049	0.304	0.047
MOEBRXII	-143.086	294.172	294.593	304.592	0.082	0.765	0.134
EBRXIIP	-149.778	307.556	307.977	317.977	0.119	1.773	0.299
MOGBRXII	-143.251	294.502	294.923	304.922	0.077	0.781	0.130
WBRXII	-140.791	289.583	290.004	300.004	0.062	0.446	0.075
KEBRXII	-143.341	296.682	297.320	309.708	0.090	0.795	0.145
KWBRXII	-140.535	291.070	291.708	304.095	0.057	0.358	0.061
EEBRXII	-141.600	291.200	291.621	301.621	0.088	0.636	0.129
GMBRXII	-141.446	290.892	291.313	301.312	0.084	0.691	0.109
OEHLBRXII	-141.325	290.649	291.070	301.070	0.064	0.493	0.078

Figure 5.27 and 5.28 present the fitted PDFs and CDFs of the models, respectively, for the taxes revenues. Upon examining these figures in detail, it is apparent that the HMBRXII model exhibits a significantly better fit to the data compared to the other models. The PDF curve of the HMBRXII model closely follows the distribution of the observed data points, indicating a high degree of accuracy in capturing the underlying patterns and characteristics of the data. Similarly, the CDF curve of the HMBRXII model accurately represents the cumulative probabilities of the data set, further confirming its superior fit.

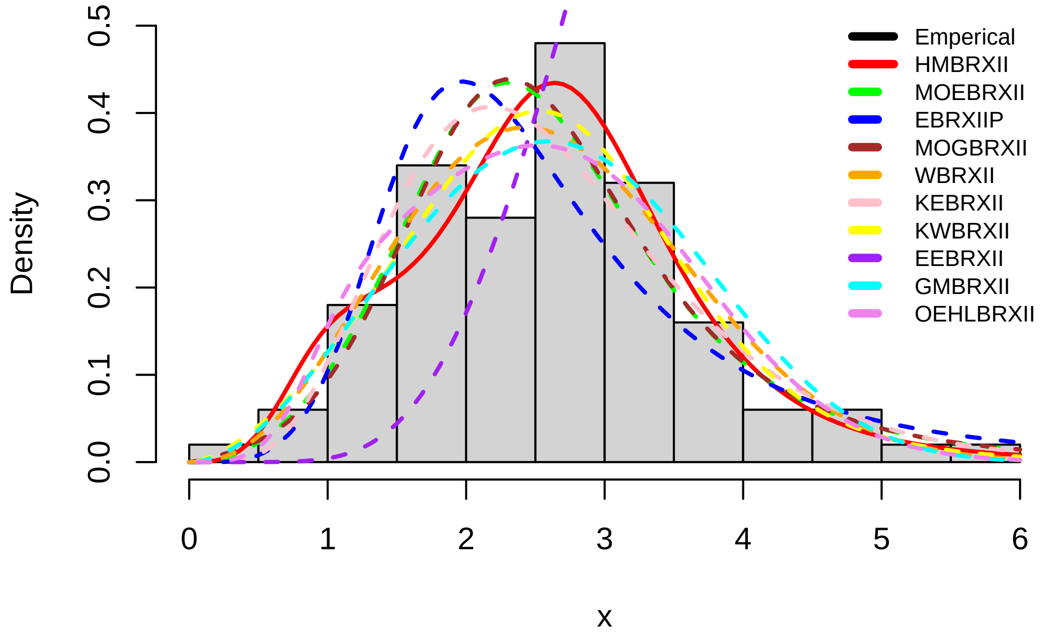

Figure 5.27: The fitted PDFs for taxes revenues

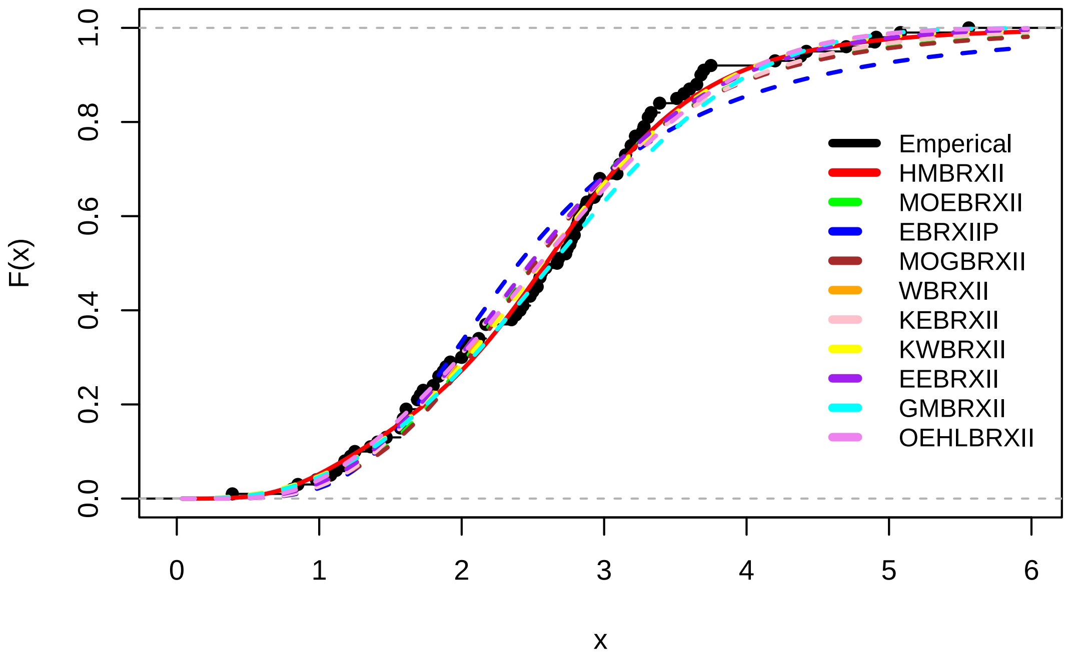

Figure 5.28: The fitted CDFs for taxes revenues

The profile log-likelihood plots of the HMBRXII distribution, applied to the tax revenues, are depicted in Figure 5.29. These plots serve as a visual assessment of the estimated values and their correspondence to the actual maxima of the data. Upon careful examination of the figures, it is evident that the estimated parameter values closely align with the observed maxima. The profile log-likelihood plots exhibit distinct peaks or plateaus around the estimated values, indicating that these values accurately capture the essential characteristics of the tax revenues.

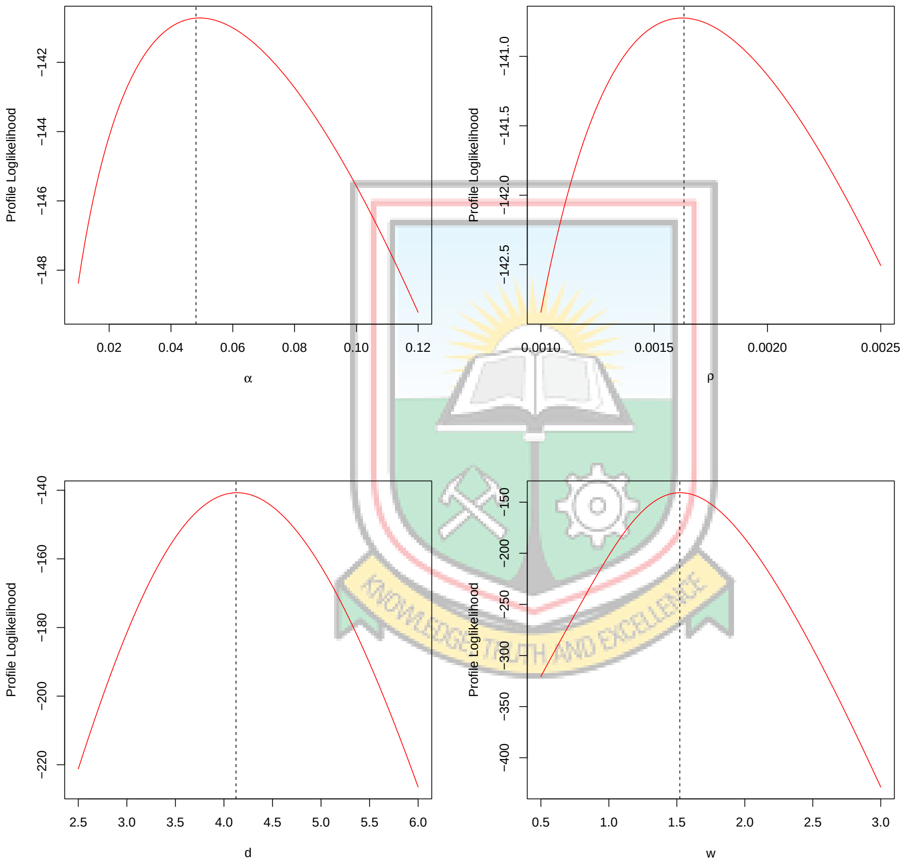

Figure 5.29: Profile log-likelihood plots of HMBRXII for taxes revenues

5.8.2 Precipitation in Minneapolis

The minimum value in the precipitation in Minneapolis is 0.3200, while the maximum value is 4.7500. The CS for the data set is 1.1447, indicating a positive skew. The CK is 1.6653, suggesting that the data set is platykurtic, meaning it has fewer extreme values and a flatter peak compared to a normal distribution curve.

The failure rate behaviour of the precipitation in Minneapolis was examined through a TTT plot. The TTT plot displayed an upward trend, indicating an increasing pattern. This observation is evident from the concave shape observed above the 45° line in Figure 5.30.

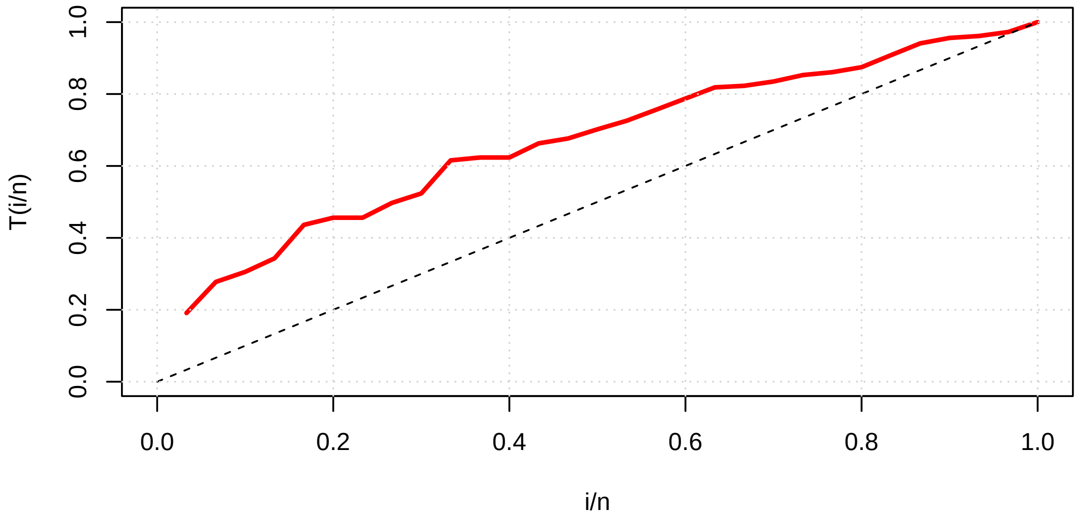

Figure 5.30: The TTT plot of the precipitation in Minneapolis

In Table 5.29, the MLEs and their corresponding standard errors are presented for the fitted models. Among the models, the parameters ρ for HMBRXII, α, λ, and k for MOEBRXII, α, θ, and k for EBRXIIP, δ and a for MOGBRXII, α and b for WBRXII, b, c, and k for KEBRXII, a and s for KWBRXII, a, b, and k for EEBRXII, λ, θ, and d for GMBRXII, and λ for OEHLBRXII were found to be statistically non-significant at the 5% significance level.

Table 5.29: MLEs for precipitation in Minneapolis

Models		Estimates	SE	Z-value	P-Value
HMBRXII	α	0.2153	0.0932	2.3104	0.0209 *
	ρ	0.0138	0.0492	0.2803	0.7792
	d	2.7434	0.8156	3.3637	0.0008*
	w	2.0127	0.9895	2.0341	0.0419 *
MOEBRXII	α	8.4755	10.7738	0.7867	0.4315
	λ	11.8805	20.3697	0.5832	0.5597
	c	0.8339	0.4231	1.9708	0.0487 *
	k	5.4476	3.3016	1.6500	0.0989
EBRXIIP	α	3.2341	2.8006	1.1548	0.2482
	θ	-2.2210	2.4519	-0.9058	0.3650
	c	1.3024	0.6100	2.1351	0.0328 *
	k	2.5781	1.5266	1.6887	0.09127
MOGBRXII	α	2.1205	1.0414	2.0362	0.0417 *
	β	2.9777	0.0793	37.5387	2×10^{-16}*
	δ	6.2105	8.6193	0.7205	0.4712
	a	0.5598	0.4209	1.3302	0.1835
WBRXII	α	7.3965	6.6295	1.1157	0.2645
	β	0.6732	0.2726	2.4697	0.0135 *
	a	0.3856	0.1464	2.6346	0.0084 *
	b	0.3221	0.2919	1.1036	0.2698
KEBRXII	a	1.3161	0.4666	2.8209	0.0048 *
	β	8.8604	3.1410	2.8209	0.0048 *
	b	10.3081	11.0407	0.9336	0.3505
	c	0.5475	0.5605	0.9768	0.3287
	k	1.9585	2.6041	0.7521	0.4520
KWBRXII	a	3.0600	2.3867	1.2821	0.1998
	b	4.6300	1.4464	3.2010	0.0014 *
	c	0.9600	0.3687	2.6034	0.0092 *
	k	4.7500	0.8365	5.6784	1.36×10^{-8}*
	s	9.2800	8.7099	1.0655	0.2867
EEBRXII	a	6.5384	5.1732	0.2063	0.2063
	b	3.8550	3.0890	1.2480	0.2120
	c	0.8343	0.3642	2.2909	0.0220 *
	k	1.6775	0.9982	1.6806	0.0928
GMBRXII	λ	0.2538	0.7446	0.3409	0.7332
	θ	0.2980	0.2587	1.1518	0.2494
	c	2.5256	0.7829	3.2258	0.0013 *
	d	0.3509	0.1949	1.8004	0.0718
OEHLBRXII	a	11.6035	5.7152	2.0303	0.0423 *
	α	0.2672	0.1145	2.3338	0.0196 *
	b	0.1684	0.0599	2.8123	0.0049 *
	λ	0.1932	0.2563	0.7538	0.4510

* means significant at 5%.

According to the results presented in Table 5.30, the HMBRXII model demonstrates a superior fit compared to the other competing models. This conclusion is supported by several criteria: the HMBRXII model achieved the highest log-likelihood value and the lowest values for AIC, AICC, and BIC. Additionally, the HMBRXII model obtained the smallest values for A, KS, and W, indicating a better overall goodness of fit compared to the alternative models.

Table 5.30: Metrics for evaluation for precipitation in Minneapolis

Model	ℓ	AIC	AICC	BIC	K-S	AD	CVM
HMBRXII	-38.1548	84.3095	85.9095	89.9143	0.0664	0.1024	0.0140
MOEBRXII	-38.34203	84.6841	86.2841	90.2889	0.0769	0.1490	0.0222
EBRXIIP	-38.7648	85.5295	87.1295	91.1343	0.0932	0.2183	0.0381
MOGBRXII	-38.6445	85.2891	86.8891	90.8938	0.0686	0.1355	0.0188
WBRXII	-38.2047	84.4094	86.0095	90.0143	0.0678	0.1111	0.0151
KEBRXII	-38.2047	86.4095	88.9094	93.4155	0.0712	0.1278	0.0182
KWBRXII	-38.1967	86.3934	88.8934	93.3994	0.0700	0.1442	0.0196
EEBRXII	-38.5193	85.0386	86.6386	90.6434	0.0880	0.1703	0.0262
GMBRXII	-38.1606	84.3212	85.9212	89.9260	0.0701	0.1529	0.0200
OEHLBRXII	-39.3450	86.6900	88.2900	92.2948	0.1230	0.3444	0.0576

Figure 5.31 displays the fitted PDFs of the compared distributions, while Figure 5.32 shows the fitted CDFs. Upon examining these figures in detail, it is apparent that the HMBRXII model exhibits a significantly better fit to the data compared to the other models. The curves of the HMBRXII distribution closely align with the observed data points, indicating a strong agreement between the model and the empirical data.

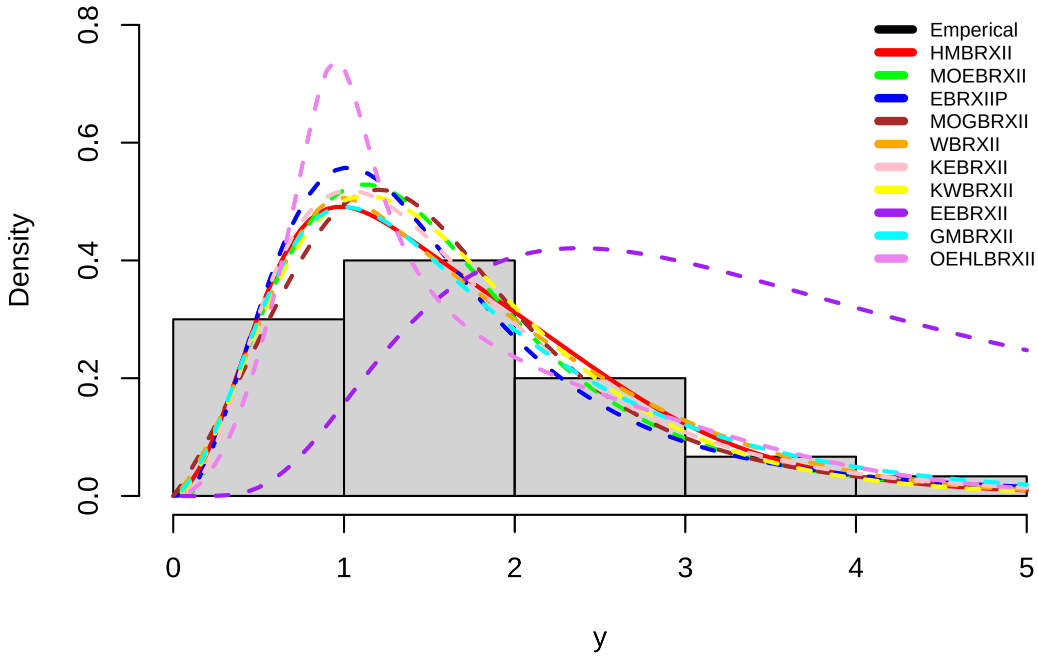

Figure 5.31: The fitted PDFs for precipitation in Minneapolis

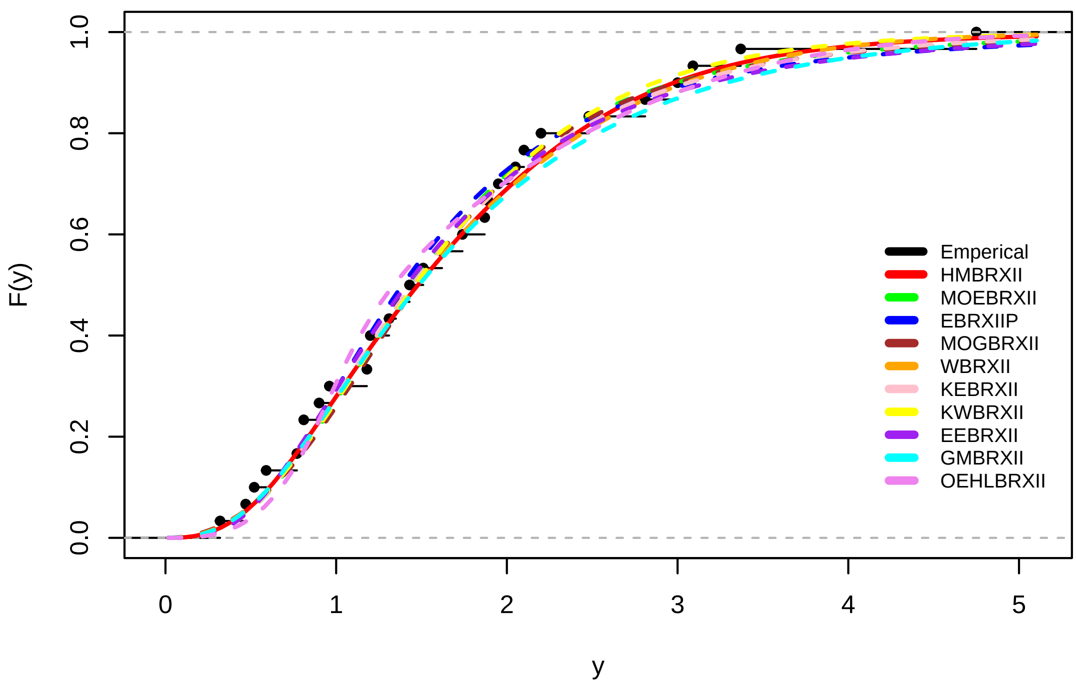

Figure 5.32: The fitted CDFs for precipitation in Minneapolis

The profile log-likelihood plots in Figure 5.33 provide visual evidence that the estimated parameter values of the HMBRXII distribution correspond to the real maxima, validating the accuracy of the estimation process for analysing the precipitation data set.

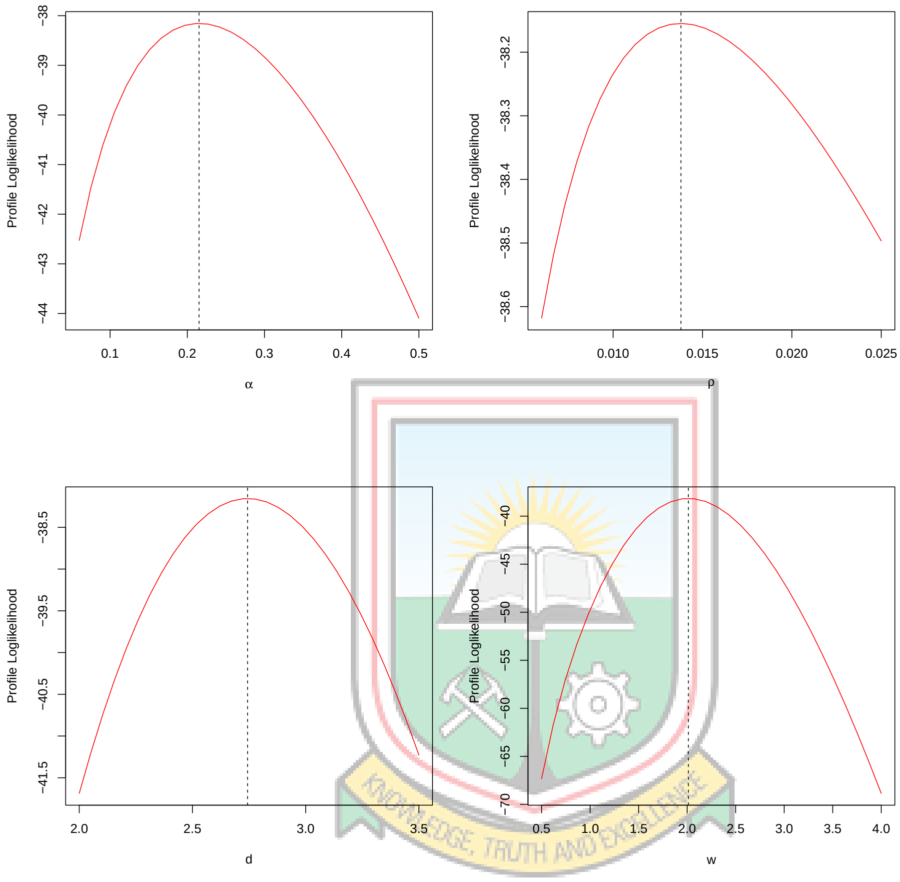

Figure 5.33: Profile log-likelihood plots of HMBRXII for precipitation in Minneapolis

5.8.3 Failure Time of epoxy Strands

The minimum failure time in the dataset is 0.0100, and the maximum failure time is 7.8900. The data set exhibits a positive skewness, as indicated by a CS of 3.0471. This means that the distribution of failure times is skewed towards higher values. Additionally, the data set is leptokurtic, with a CK of 14.4745. This implies that the distribution has more peak and heavier tails compared to a normal distribution.

The behaviour of the failure rate in the epoxy strands was examined using a TTT plot. The TTT plot exhibited a distinct convex-concave-convex pattern, as illustrated in Figure 5.34. This pattern indicates fluctuations in the failure rate over time, characterised by an initial increase, followed by a decrease, and then another increase.

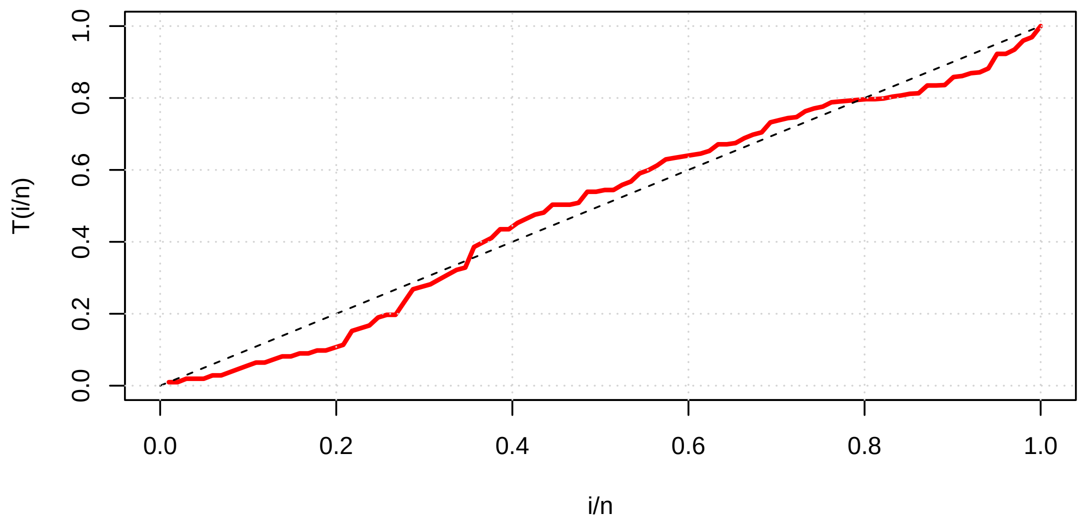

Figure 5.34: The TTT plot of the failure rate in the epoxy strands

The MLEs for the fitted models and their respective SEs are presented in Table 5.31. Among the estimated parameters, the values of ρ for HMBRXII, α, λ, and k for MOEBRXII, θ for EBRXIIP, δ for MOGBRXII, k for KEBRXII, b, c, and k for KWBRXII, a and k for EEBRXII, θ and c for GMBRXII, and λ for OEHLBRXII were not found to be statistically significant at the 5% significance level.

Table 5.31: MLEs for failure time of epoxy strands

Models		Estimate	SE	Z-value	P-Value
HMBRXII	α	0.1055	0.0386	2.7360	0.0062 *
	ρ	0.0061	0.0081	0.7502	0.4531
	d	0.7341	0.1234	5.9469	2.73×10^{-9} *
	w	7.0748	1.7098	4.1378	3.51×10^{-5} *
MOEBRXII	α	3.3778	1.7764	1.9016	0.0572
	λ	0.2064	0.1113	1.8541	0.0637
	c	2.5851	1.0257	2.5204	0.0117 *
	k	0.8750	0.5031	1.7391	0.0820
EBRXIIP	α	0.2129	0.0845	2.5106	0.0121 *
	θ	-1.5830	0.8542	-1.8533	0.0638
	c	2.9162	0.9253	3.1516	0.0016 *
	k	0.6235	0.3028	2.0588	0.0395 *
MOGBRXII	α	0.7905	0.1671	4.7300	2.25×10^{-6}*
	β	8.4341	0.0068	1235.0971	2.00×10^{-16}*
	δ	7.5801	6.1041	1.2418	0.2143
	a	0.4541	0.1245	3.6457	0.0003 *
WBRXII	α	3.6599	1.6549	2.2115	0.0270 *
	β	1.2229	0.2756	4.4367	9.14×10^{-6}*
	a	0.9114	0.1480	6.1594	7.30×10^{-10}*
	b	0.2299	0.1064	2.1608	3.07×10^{-2} *
KEBRXII	a	0.5289	0.0589	8.9870	2.00×10^{-16}*
	β	5.3352	0.5937	8.9870	2.00×10^{-16}*
	b	9.3028	4.2286	2.2000	2.78×10^{-2} *
	c	0.5175	0.2396	2.1598	3.08×10^{-2} *
	k	0.8782	0.5629	1.5602	1.19×10^{-1}
KWBRXII	a	0.1000	0.0378	2.6444	8.20×10^{-3} *
	b	0.7000	0.4937	1.4177	1.56×10^{-1}
	c	5.8000	0.9572	6.0595	1.37×10^{-9}
	k	0.5600	0.5033	1.1126	2.66×10^{-1}
	s	1.5000	0.3766	3.9831	6.80×10^{-5}*
EEBRXII	a	0.1146	0.0615	1.8636	6.24×10^{-2}
	b	0.3255	0.0981	3.3194	0.0009 *
	c	4.5666	2.0305	2.2490	0.0245 *
	k	1.4252	1.0232	1.3929	0.1636
GMBRXII	λ	49.2480	3.79×10^{-5}	1.30×10^{6}	2.20×10^{-16}*
	θ	8.14×10^{-4}	1.47×10^{-3}	0.5547	0.5791
	c	0.1877	0.1580	1.1883	0.2347
	d	0.0177	2.27×10^{-3}	7.8041	5.99×10^{-15}*
OEHLBRXII	a	2.9958	1.3454	2.2267	0.0260 *
	α	0.2603	0.1192	2.1834	0.0290 *
	b	0.2156	0.0900	2.3941	0.0167 *
	λ	2.0530	1.2029	1.7067	0.0879

* means significant at 5% significance level.

The comparison results presented in Table 5.32 confirm that the proposed HMBRXII model outperforms the other fitted models. The HMBRXII model exhibits the highest log-likelihood value, indicating a better fit to the failure time of epoxy strands. Additionally, the HMBRXII model shows the lowest values for the AIC, AICC, and BIC criteria, further supporting its superior goodness of fit. Moreover, the HMBRXII model demonstrates the lowest A, KS, and W values, indicating a closer match between the observed and predicted values.

Table 5.32: Metrics for evaluation for failure time of epoxy strands

Models	ℓ	AIC	AICC	BIC	KS	A	W
HMBRXII	-99.3723	206.7446	207.6537	217.2051	0.0547	0.3671	0.0450
MOEBRXII	-102.2690	212.5380	214.1380	222.9984	0.0820	0.8305	0.1220
EBRXIIP	-103.5217	215.0434	216.6434	225.5039	0.0902	1.2939	0.2317
MOGBRXII	-103.7589	215.5178	217.1178	225.9782	0.0908	1.3305	0.1920
WBRXII	102.6317	213.2634	214.8634	223.7239	0.0876	0.9187	0.1629
KEBRXII	-107.9973	225.9946	228.4946	239.0703	0.1249	2.2530	0.3895
KWBRXII	-99.2130	208.4261	210.9261	221.5017	0.0559	0.3873	0.0584
EEBRXII	-101.1276	210.2552	211.8552	220.7157	0.0736	0.6479	0.0943
GMBRXII	-106.5181	221.0363	222.6363	231.4967	0.1065	1.9254	0.2023
OEHLBRXII	-101.8226	211.6453	213.2453	222.1058	0.0704	0.8439	0.1335

The fitted PDFs and CDFs of the compared models are displayed in Figures 5.35 and 5.36. From these figures, it is evident that the HMBRXII model provides a better fit to the failure time of epoxy strands compared to the other models. The PDF and CDF curves of the HMBRXII model closely align with the observed data, indicating a more accurate representation of the underlying distribution.

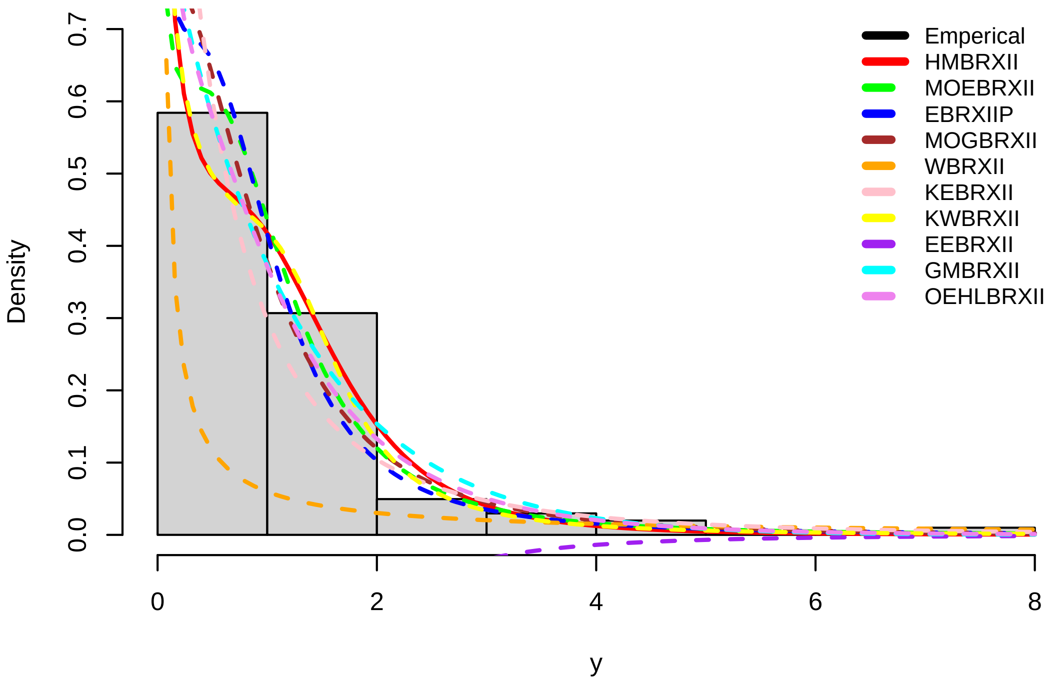

Figure 5.35: The fitted PDFs for failure time of epoxy strands

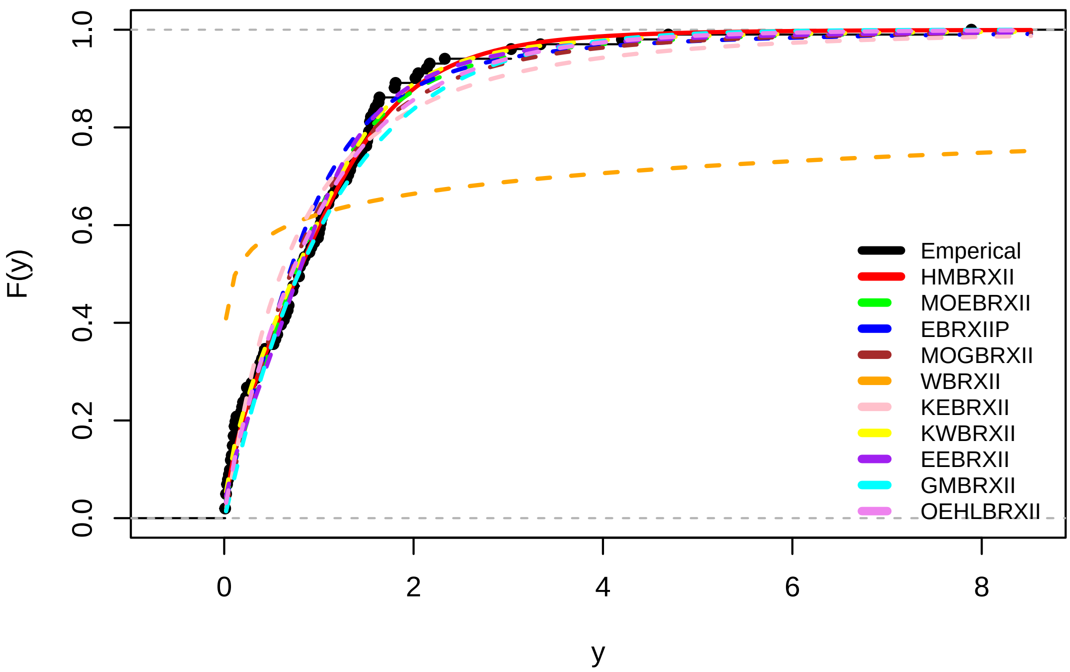

Figure 5.36: The fitted CDFs for failure time of epoxy strands

The profile log-likelihood plots depicted in Figure 5.37 showcase the estimated parameter values of the HMBRXII distribution based on the failure time of the epoxy strands. These plots offer a visual representation of the log-likelihood function as it varies with each individual parameter, while keeping the other parameters fixed at their estimated values.

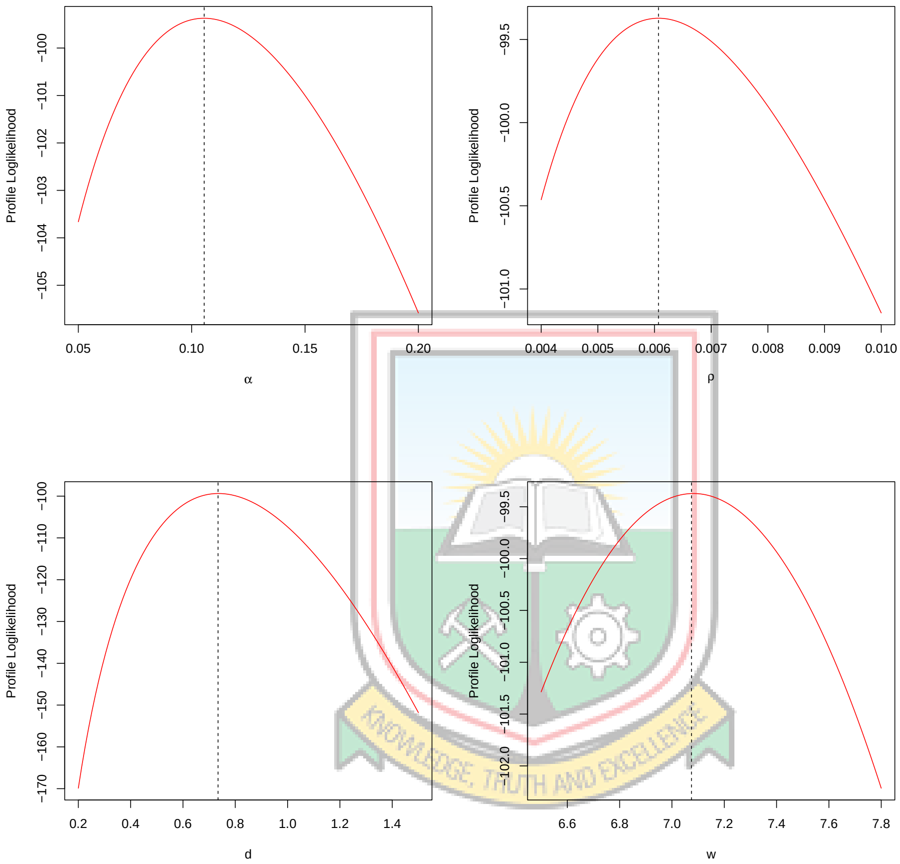

Figure 5.37: Profile log-likelihood plots of HMBRXII for failure time of epoxy strands

5.9 Assessment of the Log-Harmonic Mixture Burr XII Distribution

The LHMBRXII distribution is assessed using a real data set previously analysed by (Nasiru *et al.*, 2022). The model is compared with the log-Weibull Burr XII (LWBRXII) distribution proposed by (Afify *et al.*, 2018) and the log-Gumbel Burr XII (LGBRXII) distribution introduced by (Al-Aqtash *et al.*, 2021).

The fitted distribution is given by

$$y_a = \beta_0 + \beta_1 z_{a1} + \beta_2 z_{a2} + \beta_3 z_{a3} + \epsilon_a,$$

where:

- y_a being the proportion of fat in the arms for the a-th observation.
- β_0 is the intercept term, representing the expected proportion of fat in the arms when all covariates are zero.
- $\beta_1, \beta_2, \beta_3$ are the regression coefficients associated with age, body mass index, and sex, respectively. They represent the expected change in the proportion of body fat in the arms for a one-unit change in the corresponding covariate, holding other covariates constant.
- z_{a1}, z_{a2}, z_{a3} are the values of the covariates (age, body mass index, and sex) for the a-th observation.
- ϵ_a is the error term, representing the random variation or unexplained part of the distribution.

Table 5.33 displays the MLEs, SEs, and corresponding p-values of the fitted distributions. In this context, when comparing the LHMBRXII distribution to the other models under consideration, it consistently demonstrates lower AIC and BIC values. This suggests that the LHMBRXII distribution provides a better fit to the data. With the parameter estimates obtained from the LHMBRXII distribution, we can obtain

$$y_a = -0.1021 + 0.0011 z_{a1} + 0.0156 z_{a2} - 0.1714 z_{a3} + \epsilon_a.$$

Based on the findings of the analysis, it can be inferred that age and body mass index exhibit a statistically significant and positive correlation with the proportion of body fat in the arms, while gender, using female as the reference category, displays a statistically significant and negative association.

Table 5.33: Evaluation of the quality of fit for regression models

Distributions		Estimates	P-values	Goodness-of-fit
	β_0	-0.1021 (0.024)	2.5×10^{-5}	
	β_1	0.0011 (0.0002)	7.8×10^{-11}	
LHMBRXII	β_2	0.0156 (0.0011)	2.2×10^{-16}	ℓ= 456.840
	β_3	-0.1714 (0.0061)	2.2×10^{-16}	AIC = -897.680
	ρ	0.4084 (0.0365)	2.2×10^{-16}	BIC= -868.104
	α	0.4323 (0.0423)	2.2×10^{-16}	
	w	0.9954 (0.1762)	1.6×10^{-8}	
	σ	0.0275 (0.0027)	2.2×10^{-16}	
	β_0	-0.1980 (0.0262)	4.6×10^{-14}	
LWBRXII	β_1	0.0013 (0.0002)	4.6×10^{-13}	
	β_2	0.0163 (0.0011)	2.2×10^{-16}	ℓ=453.053
	β_3	-0.1681 (0.0063)	2.2×10^{-16}	AIC= -890.107
	β	0.1359 (0.0325)	2.9×10^{-5}	BIC= -860.530
	a	4.6862 (0.0005)	2.2×10^{-16}	
	b	1.8952 (0.0027)	2.2×10^{-16}	
	σ	0.0399 (0.0071)	2.4×10^{-8}	
	β_0	-0.0880 (0.0247)	4.0×10^{-3}	
LGBRXII	β_1	0.0013 (0.0002)	7.8×10^{-13}	
	β_2	0.0158 (0.0011)	2.2×10^{-16}	ℓ=453.031
	β_3	-0.1705 (0.0063)	2.2×10^{-16}	AIC= -890.062
	β	3.2727 (0.0003)	2.2×10^{-16}	BIC= -860.485
	k	6.0574 (0.0003)	2.2×10^{-16}	
	σ	2.2967 (0.0009)	2.2×10^{-16}	
	τ	0.0537 (0.0024)	2.2×10^{-16}	

To assess the appropriateness of the LHMBRXII, LWBRXII, and LGBRXII models, Cox-Snell residuals were generated. When comparing the residuals of the three models, it is observed that the residuals of the LHMBRXII model exhibit closer alignment with the diagonal line on the probability-probability (P-P) plot depicted in Figure 5.38. This indicates that the LHMBRXII model provides a superior fit to the dataset in comparison to the LWBRXII and LGBRXII models.

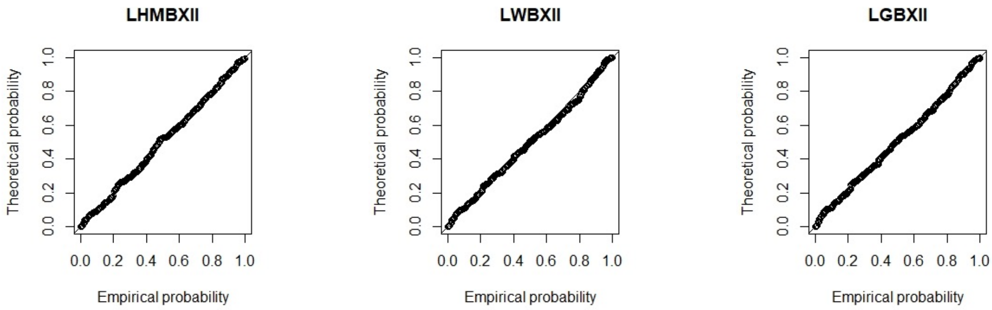

Figure 5.38: P-P plot of residuals

The diagnostic results presented in Table 5.34 indicate that the LHMBRXII model provides a better fit for the data set.

Table 5.34: Residual analysis results

Models	KS	W	A
LHMBRXII	0.034	0.032	0.229
LWBRXII	0.050	0.098	0.738
LGBRXII	0.038	0.070	0.652

CHAPTER 6

CONCLUSIONS AND RECOMMENDATIONS

6.1 Introduction

In this chapter, we bring together the key findings, implications, and practical suggestions derived from our research. This is aimed at providing a comprehensive understanding of the topic and contribute to the existing knowledge in the field. The conclusions and recommendations presented herein serve as a culmination of the efforts made and pave the way for further exploration and application of the research outcomes.

6.2 Conclusion

Addressing weaknesses in classical distributions have been of interest in recent times. When these classical distributions are modified they are made much more adaptive to modelling various types of data sets.

The study proposed three special distributions from the harmonic mixture-G family of distributions thus the harmonic mixture Gompertz, harmonic mixture Fréchet and harmonic mixture Burr XII distributions. These distributions are heavy-tailed as the family they were developed from was heavy-tailed. Assessing the density plots and plots of the failure rate functions of the proposed distributions indicate that the new distributions addressed either the weaknesses in skewness, kurtosis or ability to model non-monotonic failure rates.

Some statistical properties of the proposed distributions such as moments, incomplete moments, quantile functions, entropy, mean deviation, median deviation, mean residual life, inequality measures, moment generating function (MGF), stress-strength reliability and order statistics were obtained.

The study as well adopted some estimators thus the maximum likelihood estimation, the ordinary least squares estimation, the weighted least squares estimation, the Cramér-von Mises estimation and the Anderson-Darling estimation to estimate the parameters of the proposed distributions. A simulations study was performed to assess these estimators and the maximum likelihood estimation method adjudged the best estimator of the proposed distribution.

In the final step of the analysis, each of the proposed probability distributions was applied to three distinct lifetime data sets. The goal was to assess how well these distributions suited the data. Moreover, these distributions were compared against nine other modified models derived from the baseline distribution from which they originated. The results indicated that the three unique distributions proposed in the study were highly competitive and displayed a better fit when compared to the other distributions. This was evident through the lowest values of selection criteria such as the Akaike information criterion, Corrected Akaike information criteria, and Bayesian information criterion. Additionally, these special distributions exhibited the best fit according to goodness-of-fit test statistics, including the Kolmogorov-Smirnov test, Anderson-Darling test, and Cramér-von Mises test. Apart from the distribution analysis, the study also involved the development and application of two regression models on the lifetime data sets. The assessment of the Cox-Snell residuals from these models revealed that they provided a superior fit compared to the alternative models that were considered.

6.3 Contributions to Knowledge

This thesis makes several significant contributions to the field of probability distributions by modifying and enriching the Gompertz, Fréchet, and Burr XII distributions using the HMG family. The research outcomes provide valuable insights and advancements that contribute to the existing knowledge in the following ways:

i. Flexibility and Versatility: The modifications achieved through the integration of the HMG family add a new level of flexibility and versatility to the Gompertz, Fréchet, and Burr XII distributions. The modified distributions exhibit improved abilities to accommodate a wide range of data characteristics, including skewed and heavy-tailed data. This enhanced flexibility opens doors for researchers and practitioners to apply these modified distributions in diverse domains and empowers them to more effectively model and analyse complex data sets.

ii. Framework for Further Research: The modifications made to the Gompertz, Fréchet, and Burr XII distributions using the HMG family provide a foundation for further research in distribution theory. The success of this thesis in modifying these distributions prompts further exploration of other probability distributions and the integration of the HMG family into additional models. This research opens avenues for investigating the performance, applicability, and advantages of modified distributions in diverse contexts, encouraging future researchers to build upon these findings and expand the knowledge base in this area.

6.4 Recommendations

Based on the findings and outcomes of this research, the following recommendations are proposed for further exploration and utilisation of the modified distributions incorporating the HMG family:

i. Practical Applications: It is recommended that researchers and practitioners in fields such as finance, economics, environmental sciences, and engineering consider adopting these modified distributions in their respective domains. Further studies and practical applications can be pursued to evaluate the effectiveness and benefits of the modified distributions in specific applications, thereby enabling more accurate and precise modelling of data that exhibits skewness and heavy tails.

ii. Estimation Methods: As the modified distributions are introduced, it is crucial to develop robust and efficient estimation methods specific to these distributions. Researchers should focus on exploring other estimation methodologies, such as Bayesian approaches which can intend contribute to the practical adoption of these modified distributions, making them accessible to a wider range of researchers and practitioners.

iii. Extension to Other Distributions: The success achieved in modifying the Gompertz, Fréchet, and Burr XII distributions with the HMG family suggests the potential for similar enhancements to other probability distributions. Researchers are encouraged to explore the applicability of the HMG family in modifying other commonly used distributions.

REFERENCES

Abdelhady, D. H. and Amer, Y. M. (2021), "On the inverse power Gompertz distribution", *Annals of Data Science*, Vol. 8, No. 3, pp. 451-473.

Abonongo, A. (2021), *"New lifetime statistical distribution for systems connected in series"*, PhD thesis, University for Development Studies,Ghana.

Abouelmagd, T., Al-mualim, S., Afify, A. Z., Ahmad, M., and Al-Mofleh, H. (2018a), "The odd Lindley Burr XII distribution with applications", *Pakistan Journal of Statistics*, Vol. 34, No. 1, pp. 15-32.

Abouelmagd, T., Hamed, M., Afify, A. Z., Al-Mofleh, H., and Iqbal, Z. (2018b), "The Burr X Fréchet distribution with its properties and applications", *Journal of Applied Probability and Statistics*, Vol. 13, No. 1, pp. 23-51.

Abu-Zinadah, H. H. and Aloufi, A. S. (2014), "Some characterisations of the exponentiated Gompertz distribution", *International Mathematics Forum*, Vol. 9, No. 30, pp. 1427-1439.

Abubakari, A. G., Nasiru, S., and Abonongo, J. (2021), "Gompertz-modified Burr XII distribution: properties and applications", *Life Cycle Reliability and Safety Engineering*, Vol. 10, No. 3, pp. 199-215.

Afify, A. and Abdellatif, A. (2020), "The extended Burr XII distribution: properties and applications", *Journal of Nonlinear Sciences and Applications*, Vol. 13, No. 3, pp. 133-146.

Afify, A. Z., Cordeiro, G. M., Ortega, E. M., Yousof, H. M., and Butt, N. S. (2018), "The four-parameter Burr XII distribution: Properties, regression model, and applications", *Communications in Statistics-Theory and Methods*, Vol. 47, No. 11, pp. 2605-2624.

Afify, A. Z. and Mead, M. (2017), "On five-parameter Burr XII distribution: properties and applications", *South African Statistical Journal*, Vol. 51, No. 1, pp. 67-80.

Afify, A. Z., Yousof, H. M., Cordeiro, G. M., M. Ortega, E. M., and Nofal, Z. M. (2016), "The Weibull Fréchet distribution and its applications", *Journal of Applied Statistics*, Vol. 43, No. 14, pp. 2608-2626.

Ahmad, Z., Hamedani, G. G., and Butt, N. S. (2019), "Recent developments in distribution theory: A brief survey and some new generalised classes of distributions", *Pakistan Journal of Statistics and Operation Research*, Vol. 15, No. 1, pp. 87-110.

Ahmed, A. D., Abdulwahhab, B. I., and Abdulah, E. K. (2021), "Estimation of the parameters of mixed Fréchet distribution and its employment in simple linear regression", *Turkish Journal of Computer and Mathematics Education*, Vol. 12, No. 10, pp. 5077-5081.

Al-Aqtash, R., Mallick, A., Hamedani, G., and Aldeni, M. (2021), "On the Gumbel-Burr XII Distribution: regression and application", *International Journal of Statistics and Probability*, Vol. 10, No.2, pp. 1-16.

Al-Khedhairi, A. and El-Gohary, A. (2008), "A new class of bivariate Gompertz distributions and its mixture", *International Journal of Mathematical Analysis*, Vol. 2, No. 5, pp. 235-253.

Al-Moisheer, A. (2021), "Mixture of Lindley and lognormal distributions: Properties, estimation, and application", *Journal of Function Spaces*, Vol. 2021.

Al-Noor, N. H. and Assi, N. K. (2021), "Rayleigh gamma gompertz distribution: Properties and applications", In *AIP Conference Proceedings*, volume Vol. 2334, pp. 090003. AIP Publishing LLC.

Al-Noor, N. H., Khaleel, M. A., and Assi, N. K. (2022), "The Rayleigh Gompertz distribution: Theory and real applications", *International Journal of Nonlinear Analysis and Applications*, Vol. 13, No. 1, pp. 3505-3516.

Al Sobhi, M. M. (2021), "The modified Kies–Fréchet distribution: properties, inference and application", *AIMS Mathematics*, Vol. 6, No. 5, pp. 4691-4714.

Alamri, O. A., Abd El-Raouf, M., Ismail, E. A., Almaspoor, Z., Alsaedi, B. S., Khosa, S. K., and Yusuf, M. (2021), "Estimate stress-strength reliability model using Rayleigh and half-normal distribution", *Computational Intelligence and Neuroscience*, Vol. 2021.

Aldahlan, M. and Afify, A. Z. (2018), "The odd exponentiated half-logistic Burr XII distribution", *Pakistan Journal of Statistics and Operation Research*, Vol. 14, No. 2, pp. 305-317.

Ali, M., Khalil, A., Mashwani, W. K., Alrajhi, S., Al-Marzouki, S., and Shah, K. (2022), "A Novel Fréchet-Type Probability Distribution: Its Properties and Applications", *Mathematical Problems in Engineering*, Vol. 2022.

Almetwally, E. M. and Muhammed, H. Z. (2020), "On a bivariate Fréchet distribution", *Journal of Statistics Applications and Probability*, Vol. 9, No. 1, pp. 1-21.

Alotaibi, R., Khalifa, M., Baharith, L. A., Dey, S., and Rezk, H. (2021), "The mixture of the Marshall–Olkin extended Weibull distribution under type-II censoring and different loss functions", *Mathematical Problems in Engineering*, Vol. 2021.

Alzeley, O., Almetwally, E. M., Gemeay, A. M., Alshanbari, H. M., Hafez, E., and Abu-Moussa, M. (2021), "Statistical inference under censored data for the new exponential-X Fréchet distribution: Simulation and application to leukemia data", *Computational Intelligence and Neuroscience*, Vol. 2021.

Anafo, A. Y., Brew, L., and Nasiru, S. (2021), "The Equilibrium Renewal Burr XII Distribution: Properties and Applications", *Asian Journal of Probability and Statistics*, Vol. 15, No. 2, pp. 18-40.

Anderson, T. W. and Darling, D. A. (1952), "Asymptotic theory of certain" goodness of fit" criteria based on stochastic processes", *The annals of mathematical statistics*, Vol. 23, N0. 2, pp. 193-212.

Atanda, O., Mabur, T., and Onwuka, G. (2020), "A New Odd Lindley-Gompertz Distribution: Its Properties and Applications", *Asian Journal of Probability and Statistics*, pages 29–47.

Azid, N. N. N., Arasan, J., Zulkafli, H. S., Adam, M. B., *et al.* (2021), "Assessing the adequacy of the Gompertz regression model in the presence of right censored data", In *Journal of Physics: Conference Series*. IOP Publishing.

Badr, M. and Ijaz, M. (2021), "The exponentiated exponential Burr XII distribution: theory and application to lifetime and simulated data", *Plos one*, Vol. 16, No. 3, pp. e0248873.

Badr, M. and Shawky, A. (2014), "Mixture of Exponentiated Fréchet Distribution", *Life Science Journal*, Vol. 11, No. 3, pp. 392-404.

Badr, M. M. (2019), "Beta generalised exponentiated Fréchet distribution with applications", *Open Physics*, Vol. 17, No. 1, pp. 687-697.

Badr, M. M., Elbatal, I., Jamal, F., Chesneau, C., and Elgarhy, M. (2020), "The transmuted odd Fréchet-G family of distributions: Theory and applications", *Mathematics*, Vol. 8, No. 6, pp. 958.

Bakouch, H. S., El-Bar, A., and Ahmed, M. (2017), "A new weighted Gompertz distribution with applications to reliability data", *Applications of Mathematics*, Vol. 62, No. 3, pp. 269-296.

Behboodian, J. (1972), "On the distribution of a symmetric statistic from a mixed population", *Technometrics*, Vol. 14, No. 4, pp. 919-923.

Bello, O. A., Doguwa, S. I., Yahaya, A., and Jibril, H. M. (2021), "A type II half logistic exponentiated-G family of distributions with applications to survival analysis", *FUDMA Journal of Sciences*, Vol. 5, No. 3, pp. 177-190.

Bercher, J. (2012), "A simple probabilistic construction yielding generalized entropies and divergences, escort distributions and q-Gaussians", *Physica A: Statistical Mechanics and its Applications*, Vol. 391, No. 19, pp. 4460-4469.

Bhat, A., Mudasir, S., and Ahmad, S. (2018), "Mixture of Exponential and Weighted Exponential Distribution: Properties and Applications", *International Journal of Scientific Research in Mathematical and Statistical Sciences*, Vol. 5,No. 6, pp. 38-46.

Bhatti, F. A., Ali, A., Hamedani, G., and Ahmad, M. (2018a), "On generalized log Burr XII distribution", *Pakistan Journal of Statistics and Operation Research*, Vol. 14, No. 2, pp. 615-643.

Bhatti, F. A., Cordeiro, G. M., Korkmaz, M. Ç., Hamedani, G., *et al.* (2021), "On the Burr XII-gamma distribution: development, properties, characterisations and applications", *Pakistan Journal of Statistics and Operation Research*, Vol. 17, No. 4, pp.771-789.

Bhatti, F. A., Hamedani, G., Yousof, H. M., Ali, A., and Ahmad, M. (2018b), "On modified Burr XII-inverse exponential distribution: properties, characterisations and applications", *Journal of Biostatistics and Biometrics*, Vol. 2018, No. 1, pp. 1-17.

Bhatti, F. A., Hamedani, G., Yousof, H. M., Ali, A., and Ahmad, M. (2020), "On Modified Burr XII-Inverse Weibull Distribution: Development, Properties, Characterizations and Applications", *Pakistan Journal of Statistics and Operation Research*, Vol. 16, No. 4, pp. 721-735.

Burr, I. W. (1942), "Cumulative frequency functions", *The annals of mathematical statistics*, Vol. 13, No. 2, pp. 215-232.

Chaubey, Y. P. and Zhang, R. (2013), "Survival distributions with bathtub shaped hazard: A new distribution family", Technical report, Concordia University, Department of Mathematics & Statistics.

Chaudhary, A. K., Sapkota, L. P., and Kumar, V. (2020), "Inverted shifted Gompertz distribution with theory and applications", *Pravaha*, Vol. 26, No. 1, pp. 1-10.

Cordeiro, G., Mead, M., Afify, A. Z., Suzuki, A., and Abd El-Gaied, A. (2017), "An extended Burr XII distribution: properties, inference and applications", *Pakistan Journal of Statistics and Operation Research*, pages 809–828.

Cordeiro, G. M., Alizadeh, M., and Diniz Marinho, P. R. (2016), "The type I half-logistic family of distributions", *Journal of Statistical Computation and Simulation*, Vol. 86, No. 4, pp. 707-728.

Cordeiro, G. M., Ortega, E. M., and da Cunha, D. C. (2013), "The exponentiated generalized class of distributions", *Journal of data science*, Vol. 11, No. 1, pp. 1-27.

Creedy, J. (2001), "Measuring income inequality", *Taxation and Economic Behaviour: Introductory surveys in economics*, Vol. 1, pp. 3.

da Silva, R. V., de Andrade, T. A., Maciel, D. B., Campos, R. P., and Cordeiro, G. M. (2013), "A new lifetime model: the gamma extended Fréchet distribution.", *Journal of Statistical Theory and Applications*, Vol. 12, No. 1, pp. 39-54.

da Silva, R. V., Gomes-Silva, F., Ramos, M. W. A., and Cordeiro, G. M. (2015), "The exponentiated Burr XII Poisson distribution with application to lifetime data", *International Journal of Statistics and Probability*, Vol. 4, No. 4, pp. 112.

Daniyal, M. and Aleem, M. (2014), "On the mixture of Burr XII and Weibull distributions", *Journal of Statistics Applications and Probability*, Vol. 3, No. 2, pp. 251.

Deka, D., Das, B., Baruah, B. K., and Baruah, B. (2021), "Some properties on Fréchet-Weibull distribution with application to real life data", *Mathematics and Statistics*, Vol. 9, No. 1, pp. 8-15.

Eghwerido, J. (2020), "The alpha power Weibull Fréchet distribution: properties and applications", *Turkish Journal of Science*, Vol. 5, No. 3, pp. 170-185.

Eghwerido, J. T., Nzei, L. C., and Agu, F. I. (2021a), "The alpha power Gompertz distribution: Characterisation, properties, and applications", *Sankhya A*, Vol. 83, No. 1, pp. 449-475.

Eghwerido, J. T., Ogbo, J. O., and Omotoye, A. E. (2021b), "The Marshall-Olkin Gompertz distribution: Properties and applications", *Statistica*, Vol. 81, No. 2, pp. 183-215.

El-Bassiouny, A., El-Damcese, M., Mustafa, A., and Eliwa, M. (2016a), "Bi-variate exponentiated generalised Weibull-Gompertz distribution", *Journal of Applied Probability and Statistics*, Vol. 11, No. 1, pp. 25-46.

El-Bassiouny, A., El-Damcese, M., Mustafa, A., and Eliwa, M. (2016b), "Mixture of exponentiated generalised Weibull-Gompertz distribution and its applications in reliability", *Journal of Statistics Applications and Probability*, Vol. 5, No. 3, pp. 455-468.

El-Bassiouny, A., El-Damcese, M., Mustafa, A., and Eliwa, M. (2017), "Exponentiated generalised Weibull-Gompertz distribution with application in survival analysis", *Journal of Statistics Applications and Probability*, Vol. 6, No. 1, pp. 7-16.

El-Damcese, M., Mustafa, A., El-Desouky, B., and Mustafa, M. (2015), "The odd generalized exponential Gompertz", *Applied Mathematics*, Vol. 6, No. 14, pp. 2340-2353.

El-Gohary, A., Alshamrani, A., and Al-Otaibi, A. N. (2013), "The generalized Gompertz distribution", *Applied mathematical modelling*, Vol. 37, No. 1-2, pp. 13-24.

Elbatal, I., Altun, E., Afify, A. Z., and Ozel, G. (2019a), "The generalized Burr XII power series distributions with properties and applications", *Annals of Data Science*, Vol. 6, No. 3, pp. 571-597.

Elbatal, I., Jamal, F., Chesneau, C., Elgarhy, M., and Alrajhi, S. (2019b), "The modified beta Gompertz distribution: Theory and applications", *Mathematics*, Vol. 7, No. 1, pp. 3.

Eliwa, M., El-Morshedy, M., and Ibrahim, M. (2019), "Inverse Gompertz distribution: properties and different estimation methods with application to complete and censored data", *Annals of data science*, Vol. 6, No. 2, pp. 321-339.

Eraikhuemen, I. B., Ieren, T. G., Asongo, A. I., Yakubu, B. S., Bala, A. H., *et al.* (2021), "A transmuted power Gompertz distribution: Properties and applications", *Theory and Practice of Mathematics and Computer Science*, Vol. 9, pp. 127-'45.

Ghosh, I. and Bourguinon, M. (2017), "A new extended Burr XII distribution", *Austrian Journal of Statistics*, Vol. 46, No. 1, pp. 33-39.

Granzotto, D., Louzada, F., and Balakrishnan, N. (2017), "Cubic rank transmuted distributions: inferential issues and applications", *Journal of statistical Computation and Simulation*, Vol. 87, No. 14, pp. 2760-2778.

Guerra, R. R., Peña-Ramírez, F. A., and Cordeiro, G. M. (2021), "The Weibull Burr XII distribution in lifetime and income analysis", *Anais da Academia Brasileira de Ciências*, Vol. 93, No. 3, pp. 1-28.

Gupta, R. C. and Bradley, D. M. (2003), "Representing the mean residual life in terms of the failure rate", *Mathematical and Computer Modelling*, Vol. 37, No. 12-13, pp. 1271-1280.

Hamed, M., Aldossary, F., and Afify, A. Z. (2020), "The four-parameter Fréchet distribution: Properties and applications", *Pakistan Journal of Statistics and Operation Research*, Vol. 16, No. 2, pp. 249-264.

Hassan, A. S., Abd-Elfattah, A., and Hassan, M. M. (2018), "Bayesian analysis for mixture of Burr XII and Burr X distributions", *Far East Journal of Mathematical Sciences*, Vol. 103, No. 6, pp. 1031-1041.

Hassan, A. S., Elgarhy, M., Nassr, S. G., Ahmad, Z., and Alrajhi, S. (2019), "Truncated Weibull Frèchet distribution: statistical inference and applications", *Journal of Computational and Theoretical Nanoscience*, Vol. 16, No. 1, pp. 52-60.

Hussein, E. A., Aljohani, H. M., and Afify, A. Z. (2021a), "The extended Weibull–Fréchet distribution: properties, inference, and applications in medicine and engineering", *AIMS Mathematics*, Vol. 7, No. 1, pp. 225-246.

Hussein, E. A., Aljohani, H. M., and Afify, A. Z. (2021b), "The extended Weibull-Fréchet distribution: properties, inference, and applications in medicine and engineering", *AIMS Mathematics*, Vol. 7, No.1, pp. 225-246.

Ibrahim, M. (2019), "A new extended Fréchet distribution: properties and estimation", *Pakistan Journal of Statistics and Operation Research*, Vol. 15, No. 3, pp. 773-796.

Iqbal, M. Z., Arshad, M. Z., Ahmad, M., Ahmad, I., Iqbal, T., and Bhatti, M. A. (2019), "Double truncated transmuted Fréchet distribution: properties and applications", *Mathematical Theory and Modelling*, Vol. 9, No. 3, pp. 11-34.

Jahanshahi, S., Yousof, H. M., and Sharma, V. K. (2019), "The Burr X Fréchet model for extreme values: mathematical properties, classical inference and Bayesian analysis", *Pakistan Journal of Statistics and Operation Research*, Vol. 15, No. 3, pp. 797-818.

Karim, R., Hossain, P., Begum, S., and Hossain, F. (2011), "Rayleigh mixture distribution", *Journal of Applied Mathematics*, Vol. 2011.

Kazemi, M. R., Jafari, A. A., and Tahmasebi, S. (2021), "A modification of the Gompertz distribution based on the class of extended-Weibull distributions", *Journal of Statistical Theory and Applications*, Vol. 19, No. 4, pp. 472-480.

Khaleel, M. A., Al-Noor, N. H., and Abdal-Hameed, M. K. (2020), "Marshall Olkin exponential Gompertz distribution: Properties and applications", *Periodicals of Engineering and Natural Sciences*, Vol. 8, No. 1, pp. 298-312.

Khalil, M. G. and Rezk, H. (2019), "Extended Poisson Fréchet distribution and its applications", *Pakistan Journal of Statistics and Operation Research*, Vol. 15, No. 4, pp. 905-919.

Khan, M. S., King, R., and Hudson, I. L. (2017), "Transmuted generalised Gompertz distribution with application", *Journal of Statistical Theory and Applications*, Vol. 16, No. 1, pp. 65-80.

Kharazmi, O., Nik, A. S., Hamedani, G., and Altun, E. (2022), "Harmonic mixture-G family of distributions: Survival regression, simulation by likelihood, bootstrap and Bayesian discussion with MCMC algorithm", *Austrian Journal of Statistics*, Vol. 51, No. 2, pp. 1-27.

Korkmaz, M. Ç. and Erisoglu, M. (2014), "The Burr XII-geometric distribution", *Journal of Selcuk University Natural and Applied Science*, Vol. 3, No. 4, pp. 75-87.

Krishna, E., Jose, K., Alice, T., and Ristić, M. M. (2013a), "The Marshall-Olkin Fréchet distribution", *Communications in Statistics-Theory and Methods*, Vol. 42, No. 22, pp. 4091-4107.

Krishna, E., Jose, K., and Ristić, M. M. (2013b), "Applications of Marshall–Olkin Fréchet distribution", *Communications in Statistics-Simulation and Computation*, Vol. 42, No. 1, pp. 76-89.

Kuje, S., Abubakar, M. A., Alhaji, I. S., and KE, L. (2020), "Theoritical analysis of the generalised odd Lindley-Gompertz distribution", *Asian Journal of Science and Technology*, Vol. 11, No. 03, pp. 10792-10803.

Kuje, S., Lasisi, K., Nwaosu, S., and Alkafawi, A. M. A. (2019), "On the properties and applications of the Odd-Lindley Gompertz distribution", *Asian Journal of Science and Technology*, Vol. 10, No. 10, pp. 10364-10370.

Lee, E. T. and Wang, J. (2003), *"Statistical methods for survival data analysis"*, volume Vol. 476, John Wiley and Sons.

Louzada, F., Ramos, P. L., and Perdoná, G. S. (2016), "Different estimation procedures for the parameters of the extended exponential geometric distribution for medical data", *Computational and mathematical methods in medicine*, Vol. 2016.

Macdonald, P. D. M. (1971), "Comment on "An Estimation Procedure for Mixtures of Distributions" by Choi and Bulgren", *Journal of the Royal Statistical Society: Series B (Methodological)*, Vol. 33, No. 2, pp. 326-329.

Mahdy, M., abdelfattah, A., and Ismail, G. (2021), "Length Biased Burr-XII Distribution: Properties and Application", *International Journal of Sciences: Basic and Applied Research*, Vol. 65, No. 1, pp. 222-244.

Mahmoud, M. and Mandouh, R. (2013), "On the transmuted Fréchet distribution", *Journal of Applied Sciences Research*, Vol. 9, No. 10, pp. 5553-5561.

Makubate, B., Gabanakgosi, M., Chipepa, F., and Oluyede, B. (2021), "A new Lindley-Burr XII power series distribution: model, properties and applications", *Heliyon*, Vol. 7, No. 6, pp. e07146.

Mansour, M., Aryal, G., Afify, A., and Ahmad, M. (2018), "The Kumaraswamy exponentiated Fréchet distribution", *Pakistan Journal of Statistics*, Vol. 34, No. 3, pp. 177-193.

Marganpoor, S., Ranjbar, V., Alizadeh, M., and Abdollahnezhad, K. (2020), "Generalised odd Fréchet family of distributions: Properties and applications", *Statistics in Transition New Series*, Vol. 21, No. 3, pp. 109-128.

Mazucheli, J., Menezes, A. F., and Dey, S. (2019), "Unit-Gompertz distribution with applications", *Statistica*, Vol. 79, No. 1, pp. 25-43.

Missov, T. I. and Lenart, A. (2011), "Linking period and cohort life-expectancy linear increases in Gompertz proportional hazards models", *Demographic Research*, Vol.24,pp. 455-468.

Miura, K. (2011), "An introduction to maximum likelihood estimation and information geometry", *Interdisciplinary Information Sciences*, Vol. 17, No. 3, pp. 155-174.

Moolath, G. B. and Jayakumar, K. (2017), "T-transmuted X family of distributions", *Statistica*, Vol. 77, No. 3, pp. 251-276.

Nadarajah, S. and Kotz, S. (2003), "The exponentiated Fréchet distribution", *Interstat Electronic Journal*, Vol. 14, pp. 1-7.

Nadarajah, S. and Pogány, T. K. (2013), "On the characteristic functions for extreme value distributions", *Extremes*, Vol. 16, No. 1, pp. 27-38.

Nadarajah, S., Teimouri, M., and Shih, S. H. (2014), "Modified beta distributions", *Sankhya B*, Vol. 76, No. 1, pp. 19-48.

Nasir, A., Yousof, H. M., Jamal, F., and Korkmaz, M. Ç. (2019), "The exponentiated Burr XII power series distribution: properties and applications", *Stats*, Vol. 2, No. 1, pp. 15-31.

Nasir, M. A., Özel, G., and Jamal, F. (2018), "The Burr XII uniform distribution: theory and applications", *Journal of Reliability and Statistical Studies*, Vol. 11, No. 2, pp.143-158.

Nasiru, S. (2018), *"A new generalization of transformed-transformer family of distributions"*, PhD thesis, JKUAT.

Nasiru, S. and Abubakari, A. G. (2022), "Marshall-Olkin Zubair-G family of distributions", *Pakistan Journal of Statistics and Operation Research*, Vol. 18, No.1, pp. 195-210.

Nasiru, S., Abubakari, A. G., and Angbing, I. D. (2021), "Bounded odd inverse pareto exponential distribution: Properties, estimation, and regression", *International Journal of Mathematics and Mathematical Sciences*, Vol. 2021.

Nasiru, S., Abubakari, A. G., and Chesneau, C. (2022), "New lifetime distribution for modeling data on the unit interval: properties, applications and quantile regression", *Mathematical and Computational Applications*, Vol. 27, No. 6, pp. 105.

Nzei, L. C., Eghwerido, J. T., and Ekhosuehi, N. (2020), "Topp-Leone Gompertz Distribution: Properties and Applications", *Journal of Data Science*, Vol. 18, No. 4, pp. 782-794.

Ogunde, A., Fatoki, O., and Audu, J. (2020a), "Cubic transmuted Gompertz distribution: As a life time distribution", *Journal of Advances in Mathematics and Computer Science*, Vol. 35, No. 1, pp. 105-116.

Ogunde, A. A., Ajao, I. O., and Olalude, G. A. (2020b), "On the application of Nadarajah Haghighi Gompertz distribution as a life time distribution", *Open Journal of Statistics*, Vol. 10, No. 5, pp. 850-862.

Ogunde, A. A., Olalude, G. A., Adeniji, O. E., and Balogun, K. (2021), "Lehmann type II Fréchet Poisson distribution: properties, inference and applications as a life time distribution", *International Journal of Statistics and Probability*, Vol. 10, No. 3, pp. 1-8.

Okasha, H. M. and Shrahili, M. (2017), "A New Extended Burr XII Distribution with Applications", *Journal of Computational and Theoretical Nanoscience*, Vol. 14, No. 11, pp. 5261-5269.

Paranaíba, P. F., Ortega, E. M., Cordeiro, G. M., and Pascoa, M. A. d. (2013), "The Kumaraswamy Burr XII distribution: theory and practice", *Journal of Statistical Computation and Simulation*, Vol. 83, No. 11, pp. 2117-2143.

Pillai, J. K. and Moolath, G. B. (2019), "A new generalisation of the Fréchet distribution: properties and application", *Statistica*, Vol. 79, No. 3, pp. 267-289.

Pollard, J. H. and Valkovics, E. J. (1992), "The Gompertz distribution and its applications", *Genus*, Vol. 48, No.3, pp. 15-28.

Rahman, M. M., Al-Zahrani, B., and Shahbaz, M. Q. (2018), "New general transmuted family of distributions with applications", *Pakistan Journal of Statistics and Operation Research*, Vol. 14, No.4, pp. 807-829.

Ramos, P. L., Louzada, F., Ramos, E., and Dey, S. (2020), "The Fréchet distribution: Estimation and application-An overview", *Journal of Statistics and Management Systems*, Vol. 23, No. 3, pp. 549-578.

Raya, M. A. and Butt, N. S. (2019), "Extended Weibull Burr XII Distribution: Properties and Applications", *Pakistan Journal of Statistics and Operation Research*, Vol. 15, No. 4, pp.891-903.

Reyad, H., Korkmaz, M. Ç., Afify, A. Z., Hamedani, G., and Othman, S. (2021), "The Fréchet Topp Leone-G family of distributions: Properties, characterizations and applications", *Annals of Data Science*, Vol. 8, No. 2, pp. 345-366.

Reyad, H. M. and Othman, S. A. (2017), "The Topp-Leone Burr-XII distribution: properties and applications", *British Journal of Mathematics and Computer Science*, Vol. 21, No. 5, pp. 1-15.

Roy, S. and Adnan, M. (2012), "Wrapped generalized Gompertz distribution: An application to Ornithology", *Journal of Biometrics and Biostatistics*, Vol. 3, No. 6, pp. 153-156.

Roy, T. D. and Rahman, U. H. (2021), "The Poisson-Fréchet distribution: an overview with respect to Rainfall data", *Journal of Mathematics and Computer Science*, Vol. 11, No. 1, pp. 1063-1075.

Shalabi, R. M. (2020), "Cubic Transmuted Fréchet Distribution", *Journal of Applied Sciences Research*, Vol. 16, No. 1, pp. 9-19.

Shama, M., Dey, S., Altun, E., and Afify, A. Z. (2022), "The gamma–Gompertz distribution: Theory and applications", *Mathematics and Computers in Simulation*, Vol. 193, pp. 689-712.

Shanker, R. and Rahman, U. H. (2021), "Type II Topp-Leone Fréchet distribution: Properties and applications", *Statistics in Transition New Series*, Vol. 22, No. 4, pp. 139-152.

Shaw, W. T. and Buckley, I. R. (2007), "The alchemy of probability distributions : Beyond Gram-Charlier and Cornish-Fisher expansions , and skew-normal or kurtotic-normal distributions", In *2007 IMA First Conference on Computational Finance*.

Silva, R. C. d., Sanchez, J. J., Lima, F. P., and Cordeiro, G. M. (2021), "The Kumaraswamy Gompertz distribution", *Journal of Data Science*, Vol. 13, No. 2, pp. 241-260.

Swain, J. J., Venkatraman, S., and Wilson, J. R. (1988), "Least-squares estimation of distribution functions in Johnson's translation system", *Journal of Statistical Computation and Simulation*, Vol. 29, No. 4, pp. 271-297.

Tablada, C. J. and Cordeiro, G. M. (2017), "The modified Fréchet distribution and its properties", *Communications in Statistics-Theory and Methods*, Vol. 46, No. 21, pp. 10617-10639.

Taniş, C. and Saraçoğlu, B. (2022), "Cubic rank transmuted generalised Gompertz distribution: properties and applications", *Journal of Applied Statistics*, Vol. 50, No. 1, pp. 1-19.

Teamah, A., Elbanna, A. A., and Gemeay, A. M. (2020a), "Fréchet-Weibull mixture distribution: properties and applications", *Applied Mathematical Sciences*, Vol. 14, No. 2, pp. 75-86.

Teamah, A.-E. A., Elbanna, A. A., and Gemeay, A. M. (2020b), "Fréchet-Weibull distribution with applications to earthquakes data sets", *Pakistan Journal of Statistics*, Vol. 36, No. 2, pp.135-147.

Teamah, A. E.-m. A., Elbanna, A. A., and Gemeay, A. M. (2020c), "Right truncated Fréchet-Weibull distribution: statistical properties and application", *Delta Journal of Science*, Vol. 41, No. 1, pp. 20-29.

Trapeznikova, I. (2019), "Measuring income inequality", *IZA World of Labour.*

Ul Haq, M. A., Yousof, H. M., and Hashmi, S. (2017), "A new five-parameter Fréchet model for extreme values", *Pakistan Journal of Statistics and Operation Research*, Vol. 13, No. 3, pp. 617-632.

Van Erven, T. and Harremos, P. (2014), "Rényi divergence and Kullback-Leibler divergence", *IEEE Transactions on Information Theory*, Vol. 60, No. 7, pp. 3797-3820.

Yamaguchi, Y., Okamura, H., and Dohi, T. (2010), "A variational Bayesian approach for estimating parameters of a mixture of Erlang distribution", *Communications in Statistics—Theory and Methods*, Vol. 39, No. 13, pp. 2333-2350.

Yousof, H. M., Altun, E., and Hamedani, G. (2018), "A new extension of Fréchet distribution with regression models, residual analysis and characterisations", *Journal of Data Science*, Vol. 16, No. 4, pp. 743-770.

Yousof, H. M., Hamedani, G. G., and Ibrahim, M. (2020), "The two-parameter X gamma Fréchet distribution: characterizations, copulas, mathematical properties and different classical estimation methods", *Contributions to Mathematics*, Vol. 2, pp. 32-41.

Zhang, Z. (1997), "Parameter estimation techniques: A tutorial with application to conic fitting", *Image and vision Computing*, Vol. 15, No. 1, pp. 59-76.

APPENDICES

Appendix A List of Publications

i. Ocloo, S.K., Brew, L., Nasiru, S. and Odoi, B., 2022. "Harmonic Mixture Fréchet Distribution: Properties and Applications to Lifetime Data". *International Journal of Mathematics and Mathematical Sciences*, Vol. 2022, pp. 1-20. `https://doi.org/10.1155/2022/6460362`

Hindawi
International Journal of Mathematics and Mathematical Sciences
Volume 2022, Article ID 6460362, 20 pages
https://doi.org/10.1155/2022/6460362

Hindawi

Research Article

Harmonic Mixture Fréchet Distribution: Properties and Applications to Lifetime Data

Selasi Kwaku Ocloo,[1] **Lewis Brew**,[1] **Suleman Nasiru**,[2] **and Benjamin Odoi**[1]

[1]*Department of Mathematical Sciences, University of Mines and Technology, Tarkwa, Ghana*
[2]*Department of Statistics, C.K. Tedam University of Technology and Applied Sciences, Navrongo, Ghana*

Correspondence should be addressed to Selasi Kwaku Ocloo; ma-skocloo4645@st.umat.edu.gh

Received 13 June 2022; Revised 6 August 2022; Accepted 16 August 2022; Published 28 September 2022

ii. Ocloo, S.K., Brew, L., Nasiru, S. and Odoi, B., 2023. "On the Extension of the Burr XII Distribution: Applications and Regression". *Computational Journal of Mathematical and Statistical Sciences*, Vol.2, No. 1, pp. 1-30.

Computational Journal of Mathematical and Statistical Sciences
2(1), 1–30
DOI:10.21608/cjmss.2023.181739.1000
https://cjmss.journals.ekb.eg/

Research article

On the Extension of the Burr XII Distribution: Applications and Regression

Selasi Kwaku Ocloo[1*], **Lewis Brew**[1], **Suleman Nasiru**[2], **Benjamin Odoi**[1]

[1] Department of Mathematical Sciences, University of Mines and Technology, Ghana.
[2] Department of Statistics, C.K. Tedam University of Technology and Applied Sciences, Ghana.

* **Correspondence:** slsocloo@gmail.com.

iii. Ocloo, S.K., Brew, L., Nasiru, S. and Odoi, B., 2023. "Another Extension of the Gompertz Distribution: Properties, Applications and Regression". *Journal of Statistics and Management System*, (Under Review).

Index